SYNTHESIS OF

DIAMINOPURINES

By

David Michel Adrien Taddei

A Thesis submitted

In partial fulfilment for the award of

Doctor of Philosophy of the University of St Andrews

School of Chemistry

University of St Andrews

Purdie Building, North Haugh

St Andrews, Fife

KY16 9ST

29 September 2004

DECLARATION

I, David Michel Adrien Taddei, herby certify that this thesis, which is approximately 43,000 words in length, has been written by me, that it is the record of work carried out by me and that it has not been submitted in any previous application for a higher degree.

Date: 02/05/2005 Signature of candidate:

I was admitted as a research student in September, 2001 and as a candidate for the degree of Doctor of Philosophy in September, 2004; the higher study for which this is a record was carried out at the University of St Andrews between 2001 and 2004.

Date: 02/05/2005 Signature of candidate:

I hereby certify that the candidate has fulfilled the conditions of the Resolution and Regulations appropriate for the degree of Doctor of Philosophy in the University of St Andrews and that the candidate is qualified to submit the thesis in application for that degree.

Date: 02/05/2005 Signature of supervisor:

(Professor J.D. Woollins)

COPYRIGHT DECLARATION

Unrestricted access

In submitting this thesis to the University of St Andrews I understand that I am giving permission for it to be made available for use in accordance with the regulations of the University Library for the time being in force, subject to any copyright vested in the work not being affected thereby. I also understand that the title and abstract will be published, and that a copy of the work may be made and supplied to any *bona fide* library or research worker.

Date: 02/05/2005 Signature of candidate:

ABSTRACT

Dihalogenopurines are the traditional precursors of diaminopurines, which represent an important family of antineoplastic agents as very potent CDK inhibitors. Here we report that 6-chloro-2-iodopurine can be prepared from the functionalisation of *tris*-*O*-acetylguanosine and consequent acidic cleavage of the ribose moiety. Alternatively, we have synthesised this particular dihalogenopurine from hypoxanthine using a highly efficient and regioselective lithiation/quenching sequence with Harpoon's base then tributyltin chloride. The 6-chloride was found very difficult to displace with anilines, although the base catalysed conditions are well documented in the literature. Our results demonstrate that oxidative cleavage of a 6-benzylsulfanyl moiety offers an alternative when the introduction of weak nucleophiles like anilines is required. Purvalanol A, a known potent CDK inhibitor has been prepared using this strategy.

Few 6-purin-yl-methanesulfonic esters are known in the literature but the 6-mesyl leaving group of these compounds is known to react with amines. We implemented the Traube synthesis to prepare 2-benzylsulfanylhypoxanthine from thiourea and ethyl cyanoacetate. This compound can be protected selectively at the *N*-9 position but fails to yield the corresponding 6-*O*-methanesulfonic ester. However, we will describe how chlorination and a regioselective Mitsunobu

alkylation allow the easy preparation of the novel 6-chloro-2-benzylsulfanyl-9-isopropylpurine. We have discovered that treating this compound with anilines and catalytic amounts of hydrochloric acid affords the desired 6-anilinopurines almost quantitatively without the forcing conditions experienced for dihalogenopurines. Finally, we successfully implemented the oxidative cleavage of the 2-benzylsulfanyl moiety to give access to diaminopurine analogues in a high-yielding sequence. Our novel strategy represents an interesting solution to the low reactivity of dihalogenopurines.

We found that functionalisation of the alcohol function of *N*-protected *R*-valinols as their phosphoryloxy analogues is a surprisingly difficult reaction and that complex mixtures are obtained, either by reaction with the triethylphosphite/iodine or the diethyl phosphochloridate/triethylamine systems. Although previously reported, the metallation of diethyl phosphite followed by reaction with a *O*-tosyl valinol failed to afford the desired phosphonic ester. We have synthesised the more reactive *N*-tosylaziridine analogue and proven that it reacts with lithium diethyl phosphate. We finally accomplished the synthesis of 4-aminobenzene sulfonamides and their reaction with 6-chloro-2-benzysulfanyl-9-isopropylpurine successfully afforded novel sulfonamide containing diaminopurines with potential potency as CDK inhibitors.

ACKNOWLEDGEMENTS

First of all, I would like to express my deepest gratitude to my family for their love and support, especially to my parents and brothers who have always encouraged me to work hard. I have always trusted your advice and am so glad I listened to you all these years, thank you so much for the time and effort you have put in my education and in helping me to become a better person.

After three years working in the Woollins group, all my past and present colleagues deserve a massive praise for creating such an enjoyable working environment and for the memorable moments of friendship we have shared. I wish you much happiness and success in your lives, guys! Huge thank you to the postdocs Steve (Doc Bloater), Petr (Chubby Czech) and Prav (the one and only Handbook of Chemistry) for all your help, Quing and Hua (the Smileys), Matt and Jo Wheatley (Monsieur and Madame Bloaties), Ian (Grunty Lover), Monkey Stu, Colin Burchellinho (a kind of Ronaldinho, without the bad teeth and dodgy hair), Rehan (Sugar Reh), Mirea and Heather.

Eternal thanks go to my supervisor Prof. Woollins for his moral support and advice but more importantly for trusting my hidden abilities as a chemist and providing the necessary funding for this project and to Dr Alex Slawin for her kindness and amazing expertise in turning my crystals into structures of all sorts. Thanks also to the technical and academic staff of the Department for their

crucial help, especially Mrs Smith (NMR) and Drs Alan Aitken and Nick Westwood for the much appreciated problem solving sessions. My final thoughts are for all my friends from St Andrews who have always been here for me (merci Pierrot), you have all made this possible, and also to my mates from Knoll Pharmaceutical, Mark Weston and Dr Gerard Thomas, hope to work with you again at some stage in my career!

CONTENTS

LIST OF FIGURES

LIST OF SCHEMES

LIST OF TABLES

ABBREVIATIONS AND SYMBOLS

The following abbreviations and symbols are used throughout this thesis:

Å	angstrom, length unit (10^{-10} m)
ATP	adenosine triphosphate
Bn	benzyl radical, $C_6H_5CH_2$-
CDK	cyclin dependent kinase, enzyme, generic term used to describe this particular type of kinase
Cdk	catalytic kinase subunit of an activated Cdk-Cyclin enzymatic complex
CI	chemical ionisation
D-	dextrogyre
DCM	dichloromethane
DDO	dimethydioxirane
DEAD	diethyl azodicarboxylate
DIAD	diisopropyl azodicarboxylate
DMA	*N,N*-dimethylaniline
DMF	*N,N*-dimethylformamide
DNA	deoxyribonucleic acid

EI	electron impact, ionisation technique
ESI	electrospray ionisation
Ether	diethyl ether
EtOAc	ethyl acetate
FT	Fourier transform, mathematical process
Gln	glutamine, amino acid
GSK	GlaxoSmithKline
HMBC	heteronuclear multiple bond connectivity, NMR technique
Hunig'base	Diisopropylethylamine
Hz	Hertz, frequency unit
IC_{50}	Inhibitory concentration at 50%
Ile	isoleucine, amino acid
IR	infrared
J	coupling constant, Hz
K	Kelvin, temperature unit
kDa	kilo Dalton, mass unit for proteins
Leu	leucine, amino acid
LiTMP	lithium 2,2,6,6-tetramethylpiperidide (Harpoon's base)
M	concentration, $mol.L^{-1}$
m/z	mass over charge ratio

m-CPBA	*m*-chloroperbenzoic acid
Me	methyl radical, CH_3-
MeCN	acetonitrile
MeOH	methanol
MS	mass spectrometry
NMR	nuclear magnetic resonance
°	degrees, temperature unit
°C	degrees centigrade, temperature unit
PDB	protein databank
Ph	phenyl radical, C_6H_5-
Phe	phenylalanine, amino acid
ppm	part per million
R_f	retention factor, chromatography
RNA	ribonucleic acid
SAR	structure activity relationship
Ser	serine, amino acid
TEBAC	triethylbenzylammonium chloride
THF	tetrahydrofuran
THP	tetrahydropyran
Thre	threonine, amino acid

TLC	thin layer chromatography
Ts	*p*-toluenesulfonyl, tosyl $MeC_6H_4SO_2$-
Val	valine, amino acid
XRD	X-ray diffraction
δ	chemical shift, ppm
ν	wavenumber, cm^{-1}

GENERAL EXPERIMENTAL CONDITIONS

Unless otherwise stated, all reactions were performed under an atmosphere of oxygen free nitrogen using standard Schlenk glassware and procedures. All glassware was dried at 120°C prior to use. Solvents and reagents were purchased from BDH, Aldrich, Lancaster, Acros, or Fluka and used as received. In addition, toluene, and hexane were distilled from sodium wire, while THF and ether were distilled from sodium-benzophenone; DMA, DCM and acetonitrile from CaH_2 under nitrogen. Deuteriated solvents were dried over molecular sieves when appropriate and used as supplied. Water was distilled and degassed prior to use.

TLC was performed on aluminium sheets of silica 60_{254} from Aldrich, and visualised under UV light at 254nm or after exposure to aqueous potassium permanganate or to a 5% solution of ninhydrin in butanol. Column chromatography was performed using silica gel 35-70μ 60A from FluorochemLtd. Melting points were recorded on a Gallenkamp melting point apparatus and are uncorrected. ^{1}H, ^{13}C, and ^{31}P NMR experiments were either recorded on a Jeol 270 or on Bruker Avance 300 instruments. Chemical shifts are referred to in ppm. ^{1}H and ^{13}C NMR shifts were referenced to tetramethylsilane (Me_4Si) while ^{31}P NMR shifts were referenced to 85% phosphoric acid (H_3PO_4). Infrared spectra were recorded either as potassium bromide discs for solids or on

cesium iodide plates for oils on a Perkin Elmer 2000 FT-IR instrument. Mass spectrometry was performed either by the EPSRC MS service centre (University of Wales, Swansea, UK) or the MS service at the University of St Andrews. Microanalyses were carried out in the Centre for Solid Characterisation at the University of St Andrews.

CHAPTER 1: INTRODUCTION

1.1 *Cancer, a major disease in the XXIst century?*

Cancer, also named neoplastic disease, can be defined as the uncontrolled growth of an abnormal mass of tissue, called a tumour[1]. Its cells divide and reproduce autonomously, without being subject to the usual homeostatic control of the host. Besides, neoplastic cells have a tendency to invade normal tissues, but are not attacked by the traditional immune mechanisms which kill bacterial infection[1,2]. This can be explained by the fact that differences between normal and cancer human cells are merely quantitative and thus neoplastic cells are not eliminated as easily as other infectious agents[3].

Moreover, the function of the infected cells is so altered that the chronical consequences are often lethal to the host, the degree of damage being directly related to both the rate of cell division and the anatomic location of the tumour. Death can result for example via haemorrhage, miscellaneous infections, restricted oxygenation or mass effect. It must be highlighted that tumours are divided into malignant, *i.e.* cancerous, or non-malignant, *i.e.* benign, depending on their relative lethality, but a benign tumour can eventually become lethal depending on its location and rate of growth[1]. The pain associated with the final

stages of the disease is so important that the most potent analgesics (morphine based opiates) have to be administered, regardless of being seriously addictive and of their other side-effects[2]. Finally, cancer is difficult to treat because of its invading properties: metastasis occurs when cancer cells escape from their original location and move to another tissue or organ via the blood or the lymphatic tissues, where secondary tumour masses usually grow so rapidly those treatments are unsuccessful, so that death of the patient is the only end result.

Consequently, there have been considerable efforts to develop medical treatments to eradicate this fatal disease since the 1940. When the tumour can be easily accessed and is well defined, surgery is preferred and often efficient, but the irreversible loss of the damaged tissue or organ can be highly detrimental for the patient's life. Radiotherapy has also proved to be successful in curing skin cancers and certain localised tumours. However, because of the variety of neoplastic diseases, cancer chemotherapy has been providing over the years an important number of drugs, but none of them has been widely recognised as crucial as the discovery of penicillin for antibacterial therapy for instance. The main problem lies in the fact that all potent drugs are unfortunately not able to eradicate every single malignant cell of the tumour but only a constant fraction of them, so that the remaining cancer cells often increase their resistance to the chemical agent. Hence, retreatment with the same prescription would not be as efficient and the chances of metastasis would increase significantly. Anticancer

drugs are often highly toxic to healthy cells and thus have to be administered to patients with extreme caution.

At present, about a dozen different neoplasms[2] can be cured by chemotherapy in a majority of patients. For example, significant progress is being made in the treatment of breast cancer by combination of several drugs[3-4]. Leukaemia can be treated with no less than 4 different drugs, usually with different modes of action. A medical speciality, oncology, is responsible for the design of various medical protocols based on single or combination cancer chemotherapy. There are several molecular approaches to tackle cancer, which determine the mode of action of the drug, but the ultimate aim is to induce apoptosis (cell "suicide") of the malignant cells with high selectivity towards healthy cells. A classification of a few antineoplastic agents is given below according to their mode of action and few examples of drugs are given page 4.

- **Alkylating agents and other DNA-interacting substances:** these act by alkylating nucleophilic atoms of nucleic acids or proteins. The effects of this alkylation are complex but it is clear that non-functional DNA can lead to the death of the cell[2].
- **Antimetabolites:** these are compounds able to prevent either the biosynthesis or the utilisation of normal cellular metabolites, closely related in structure to the metabolite they antagonise and are often enzyme inhibitors. The cells lacking these essential metabolites simply

cannot biosynthesise the essential nucleic acids required for DNA replication[2].

- **Antibiotics, natural products and hormones:** there are several different families, whose mode(s) of action have not always been established, such as actinomycins, anthracyclins, bleomycins, or the Vinca alkaloids. Even steroid hormones such as oestrogens or androgens have been found active against some specific tumours[2].

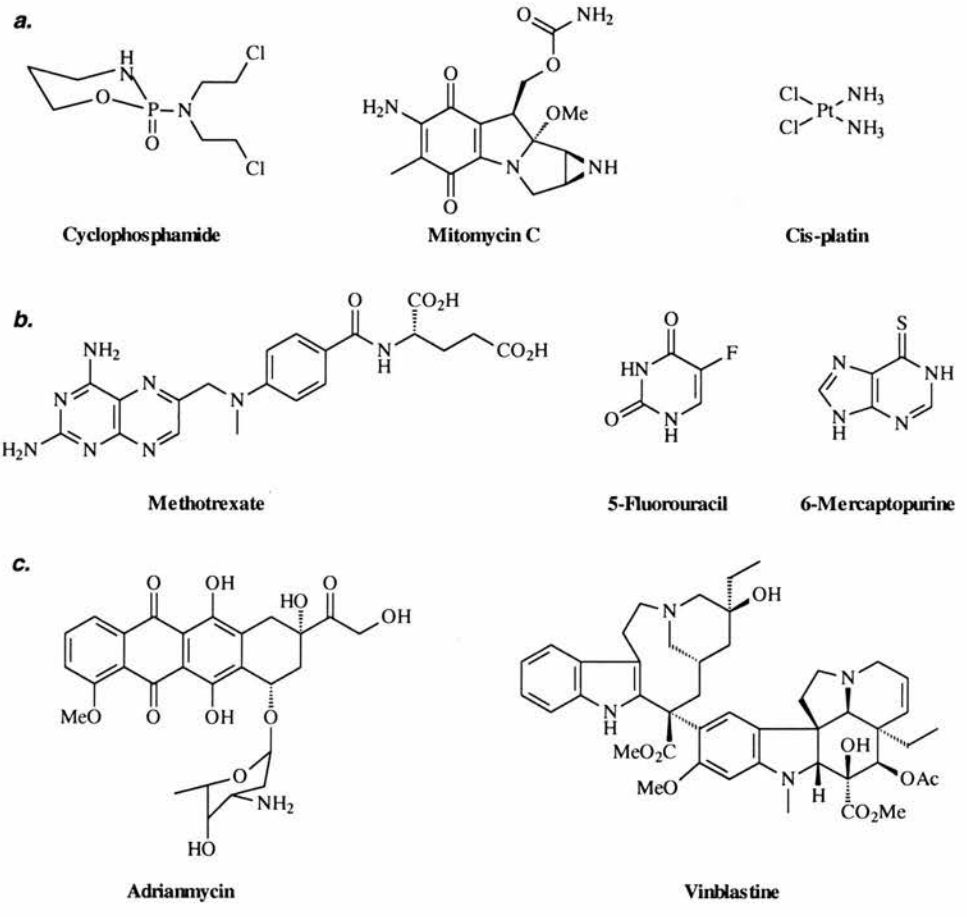

Figure 1.1 Some important antineoplastic agents: ***a.*** Alkylating agents, ***b.*** Antimetabolites, ***c.*** Antibiotics and natural products

Although it is almost impossible to produce exact figures as for the mortality due to all forms of cancers, the World Health Organisation has created several databases[5] which provide rough but striking estimates of the cancer incidence and mortality worldwide. The figures provided below are those of the year 2000:

- More than **5.3 million cases** of cancer worldwide, excluding the skin neoplasms
- About **3.5 million people killed** worldwide by cancer, excluding skin related neoplasms
- **30% less victims** in the more developed countries even if the number of cancer cases are similar to those of the less developed countries, due to the high cost and sophistication of the available antineoplastic chemotherapy
- **Asia** and **Europe** heavily affected by the disease as shown below on figure 1.2.

However, these estimates, like any statistical data have to be analysed carefully. For instance, the American Cancer Society provided much more pessimistic figures[6], since it also included estimates for skin related neoplasms, with more than 530,000 American people killed by all types of cancer. It is anticipated that cancer will become the main killer in the US and in many other countries this century and that the number of cases is more than likely to increase. Besides, various aspects of the modern life, also called the environmental factors, which include a much more sedentary life, unhealthy food habits, a higher

exposure to chemical pollution and various carcinogenic chemicals, etc... are favourable for the generalisation of the disease in our populations.

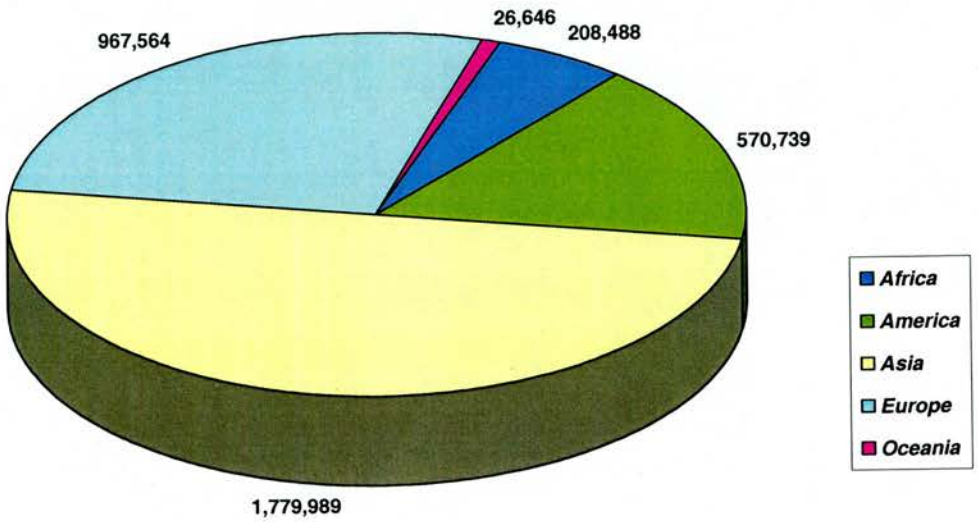

Figure 1.2 Cancer death estimates in year 2000 per continent, excluding skin related cancers[5]

Therefore, there is a clear medical need for improved chemotherapy to treat neoplastic diseases and a formidable challenge for drug discovery chemists. Not only current treatments are more palliative than curative, but their mode of action involve damaging DNA or preventing its synthesis indirectly by inhibiting the biosynthesis of nucleic acid precursors or finally by disrupting the hormonal stimulation of cell growth[1-6]. Consequently, the shift towards novel mechanistic targets lead to the identification of tumour suppressing genes and oncogenes, the former being lost or inactivated while the latter being activated in tumours.

Besides, recent advances in the molecular biology of cancer[7], especially in the field of cell cycle regulators, have created several biomolecular pathways and targets for cancer drug discovery. The importance of these cellular proteins in cell cycle progression and their pharmacological potential have promoted the molecular biology of cancer to one of the most rapidly evolving areas in pharmaceutical research. Therefore, the 2001 Nobel prize for Medicine was awarded to P.Nurse and T.Hunt, from the Imperial Cancer Research Fund and to L.Hartwell from the Fred Hutchinson Cancer Research Centre, for their discovery of those crucial cell cycle regulators, the **Cyclin Dependent Kinases (CDKs)**.

1.2 *Cyclin dependent kinases as novel molecular targets in cancer therapy*

Although life is still the most difficult biomolecular process to rationalise, the growth and reproduction of living organisms has been associated with the growth and division of their cells since the middle of the 19thcentury[8]. Following the discovery of DNA in 1953 by Watson and Crick as the chemical memory for genetic information and of its conservative function of the biochemical engine, the next revolution was the recent characterisation of key regulators of the cell cycle, the Cyclin Dependent Kinases (referred either as CDKs, Cdk-Cyclin or Cyclin/Cdk complexes)[7-10].

1.2.1 Structure, function and regulation of Cyclin Dependent Kinases

The Cyclin Dependent Kinases represent a family of heterodimeric Serine/Threonine Protein Kinases[11] and have been shown to be essential in all eukaryotes for determining the timing of crucial events of the cell cycle and for driving this latter from one phase to another. The active dimeric proteins are composed of two components[8]:

- a catalytic **cyclin dependent kinase** (**Cdk**) subunit
- a **cyclin** subunit which regulates the activity of the Cdk subunit

The inactive monomeric Cdks are minimal protein kinase catalytic subunits and their sequence includes approximately 300 amino acids[12]. Their structure has a similar overall fold as other eukaryotic protein kinases[11-13]: it consists of a N-terminal lobe rich in β-sheet, referred as the N-lobe[13], a larger C-terminal lobe rich in α-helix, thus named C-lobe and finally a deep hydrophobic cleft at the junction of the two lobes, where the site of catalysis is located. However, while the Cdk subunits are characterised by a high level of structural similarity, the cyclin subunits constitute a highly diverse protein family, with sizes ranging from 35 to 90kDa[12]. The only structural homology seems to be a sequence of roughly 100 residues, the cyclin box[14], which is crucial for binding and activation of the Cdk subunit[14-15].

The active Cdk-cyclin complexes are in fact responsible for the phosphorylation[8-15] of various proteins which are absolutely crucial to the cell-cycle progression. Effectively, they transfer a γ-phosphate from their natural substrate, **Adenosine TriPhosphate (ATP),** to a serine or threonine residue of their host protein[8-15]. Phosphate transfers are in fact common regulatory events in the monitoring of the cell cycle[14]. In practice, CDKs act as cell cycle checkpoints which order the biomolecular machine to enter each next phase at the required timing[9]. No less than 9 cyclin dependent kinases[16] have been identified in vertebrates and thus named CDK 1,2,3, etc..., while more than 12 cyclins have been called cyclins A,B,C, etc..., but it must be mentioned that subtypes in the cyclin classification do exist, such as cyclins D1, D2 and D3. Nevertheless, not all Cdk-cyclin complexes act as previously described but some can serve to integrate external growth signals[17]. Thus, they are not central to the arsenal that drives the dividing cell and they have a secondary function, coupling the cell division motor with extracellular signals. Finally, other Cdks can also regulate the transcription process[18] by association with RNA polymerase II.

About four major mechanisms of Cdk activation have been recognised by experimental studies of Cdks implicated in cell cycle control[12].Whether all these pathways are actually utilised by all Cdks remain unknown but there are some common features. The primary mechanism involves binding of the cyclin subunit: this key step has been shown *in vitro* to enhance the catalytic activity by more than 10,000-fold compared to that of the monomeric Cdk[11]. The activity of

monomeric Cdk2, as shown on Figure 1.3, is prevented first by the T-loop (residues 146-170), represented in yellow, which effectively hinders the entrance of the active site cleft to the incoming protein substrate[13]. Besides, a number of key residues promoting the transfer of the ATP phosphate are not aligned correctly because of the disruptive position of a small helix near the binding site, the helix L12. However, upon binding of the cyclin subunit (see figure 1.4), the induced conformation changes, such as the melting of the helix L12 or the flattening of the T-loop[13], lead not only to the opening of the catalytic cleft, thus enabling the approach of the protein substrate, but also to the correct positioning of the side-chains compulsory for the orientation of ATP. Nonetheless, all Cdks do not bind to all cyclins due to the specificity of particular cyclin-Cdk interactions.

Different active Cdk-Cyclin complexes have been shown to intervene at different moments of the cell cycle: as shown on Figure 1.5 page 16, a periodical and ordered activation each Cdk-cyclin complex forces the cell-cycle to continue[10-16]. Experiments have demonstrated that the level of CDKs is invariant but that their activities are modulated by interaction with their cyclin regulatory partners, whose level fluctuates at the exact moments when CDK activity needs to be altered[9]. It must be noted however that a specific type of cyclin is generally associated with the same transition(s) in each round of cell division. Hence, cyclins levels have to be controlled by gene transcription and protein degradation: the regulatory importance of cyclin gene transcription was shown by the linearity

observed between levels of cyclin mRNA, and the protein itself[19]. Besides, a cyclin needs to be degraded at the exit of a particular transition to deactivate its Cdk partner.

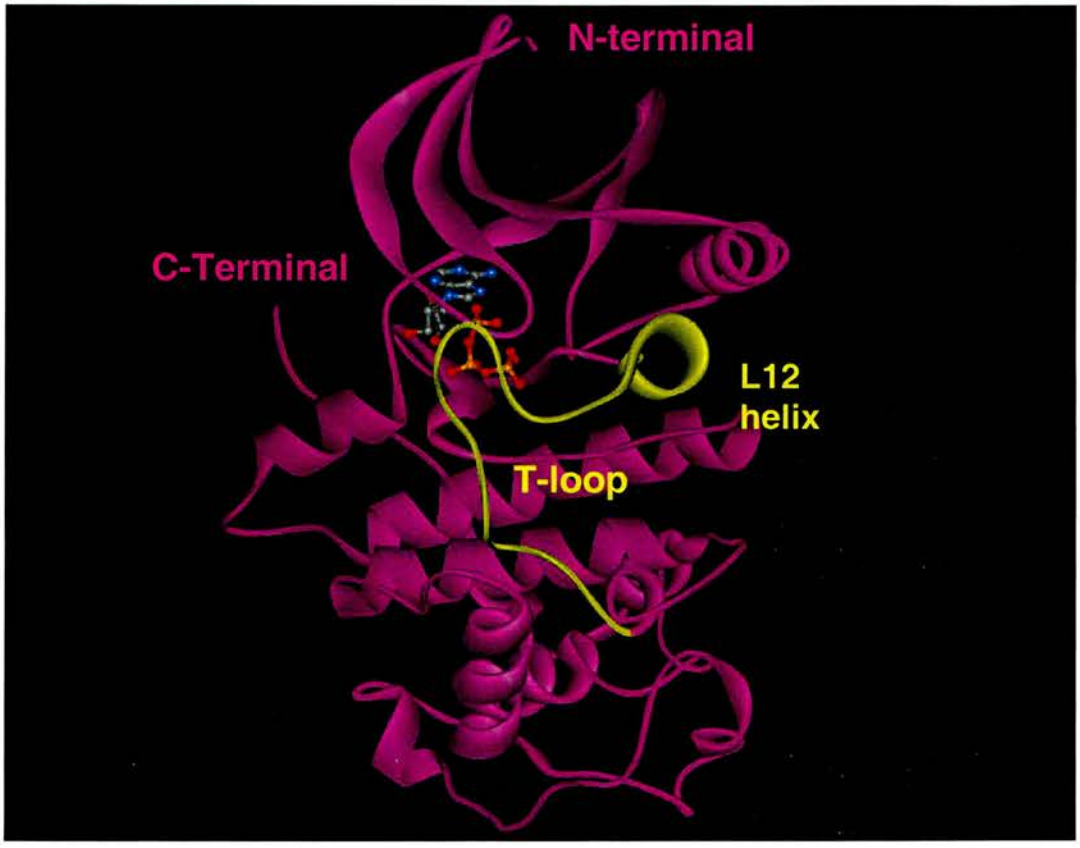

Figure 1.3 Phosphorylated monomeric Cdk2 with its ATP substrate[13]. The large C-terminal lobe rich in α-helix and the smaller N-terminal lobe rich in β-sheet constitute the major structural domains of the Cdk catalytic subunit. The **T-loop**, highlighted in yellow, prevents protein binding by criss-crossing the binding site and hindering its access to ATP, represented in ball and stick. Besides, the small helix **L12** restrains the

positioning of key residues involved in ATP orientation. (PDB[20] structure 1B39 processed with the WebLabViewer software)

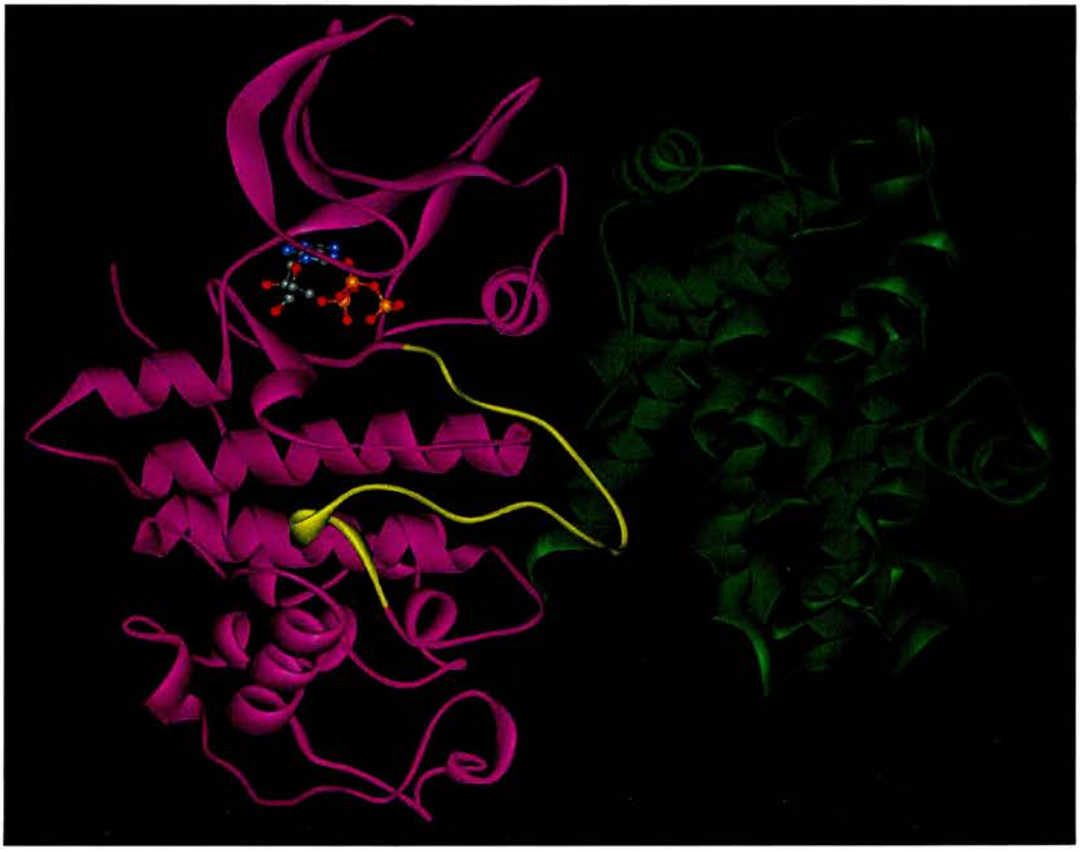

Figure 1.4 Phosphorylated Cdk2-CyclinA complex with its ATP substrate[13]. Compared to the previous figure, major conformational changes induced by binding to cyclin A (coloured in green) have affected the folding of the Cdk2 subunit, highlighted in purple: the yellow T-loop has been flattened and does not hinder the access to the catalytic cleft any more while the L12 helix has been melted through binding with the cyclin. The phosphates, due to favourable interactions with Cdk residues,

have adopted a conformation orthogonal to that in the previous monomeric structure, which will enable correct positioning of the γ-phosphate to face the hydroxylated side-chain of the protein substrate. (PDB[20] structure 1JST processed with the WebLabViewer software, ATP in ball and stick representation)

In order to achieve full catalytic activity[11], most CDKs require phosphorylation in addition to cyclin binding, on a conserved residue, namely Threonine160. This second modification usually increases the activity by an additional 80- to 300- fold compared to the Cdk-Cyclin complex. The structural effects on the binding site are only minor[12], but the phosphate acts as the centroid of a network of hydrogen bonding that stabilises the neighbouring Cdk-Cyclin interactions. The enzyme responsible for phosphorylating Cdks is known as CAK (Cdk-Activating Kinase) and the major candidate for higher organisms is the Cdk7-cyclinH-Mat1 complex[12].

The third mechanism for the control of CDK activity is achieved thanks to binding with the Cdk-Inhibitory subunits (CKIs)[9-12]. In mammalian organisms, two classes of CKIs, the Cip/Kip and INK4 protein families provide a specific pathway by which the cell cycle progression can be stopped through inactivation of its main engine, and clock, the CDKs. Both families do not inhibit the same complexes[11-12] and their mode of action is also different: the INK4 inhibitors bind to the inactive monomeric Cdk subunit, preventing binding of the cyclin subunit,

while the Cip/Kip class prevents phosphorylation of the active Cdk-Cyclin complex by the CAK enzyme through binding to the complex and has a broader preference.

Finally, the fourth mechanism involves inhibiting CDKs by phosphorylation[12] of conserved tyrosine residues (Threonine 14 or 15) present on the Cdk subunit, the effect being an inhibitory alteration of the orientation of the ATP phosphates or of crucial catalytic residues[21]. The importance of this regulatory pathway can be demonstrated: inhibitory phosphorylation of Cdk4 is necessary for G1 arrest after DNA damage in certain cells and the expression of a nonphosphorylatable mutant Cdk2 is lethal to human cells. In conclusion, the activity of CDKs can be regulated through a number of processes at the molecular levels that rely on conformational changes, due to the intrinsic flexibility of monomeric Cdk. Consequently, their ability to be activated/inactivated just like on/off switches explains why CDKs are widely involved in the regulation of the cell division cycle, the apoptosis, transcription and differentiation processes but more surprisingly, of several functions of the nervous system[22].

1.2.2 Role of Cyclin Dependent Kinases in the cell cycle

Cells from higher eukaryotic organisms spend a vast amount of their time and energy to ascertain that cell growth and division, commonly called the **cell cycle**, completes successfully[10]. Failures involve for instance a possible

corruption of the genome and loss of cell viability[16]. This is why the cell cycle is very closely controlled by multiple complex mechanisms involving hundreds of proteins. Much of these biological pathways occur through regulation of one single family, the CDKs, which can be represented as the engines that drive the events of cell division[12] but also as the clocks that time them. Finally, some specific CDKs behave as information processors that can integrate intra or extracellular signals in order to co-ordinate smoothly each crucial step of the cell cycle[11]. As it was mentioned previously, their ability to trigger cell cycle events is entirely dependent on the association of their cyclin partners, whose precisely oscillating concentrations enable CDKs to act as on/off switches. This finely tuned molecular network ensures a precise timing of the several biochemical events that duplicate the DNA of one cell, then distribute the genetic material into two newly identical daughter cells.

The cell cycle starts by a **first gap phase (G1)** where the cell ascertains it can enter a new division process and prepares for DNA replication. Thus, its proteins are often mutated in human cancers and are considered as some of the most promising molecular targets[9]. Effectively, the Cdk-cyclin complexes involved in this G1 phase allow it to progress to the next phase, the **DNA synthesis (S)**. When a second exact copy of the genome has been generated, progression to the **second gap phase (G2),** where numerous proteins are synthesised in preparation for the separation of the 2 daughter cells, **mitosis (M)**. There are various biomolecular sensors or checkpoints able to detect an anomaly

in the process, to direct the cellular arsenal to rectify the abnormalities (e.g. DNA damage) or even to arrest cell division, thanks to CDK inhibitors or other types of natural products[9]. There is finally an **inactive G0 state** where many cell functions are disabled and the cell re-enters the division cycle only when stimulated by complex cascade transduction signals. (see figure 1.5 below)

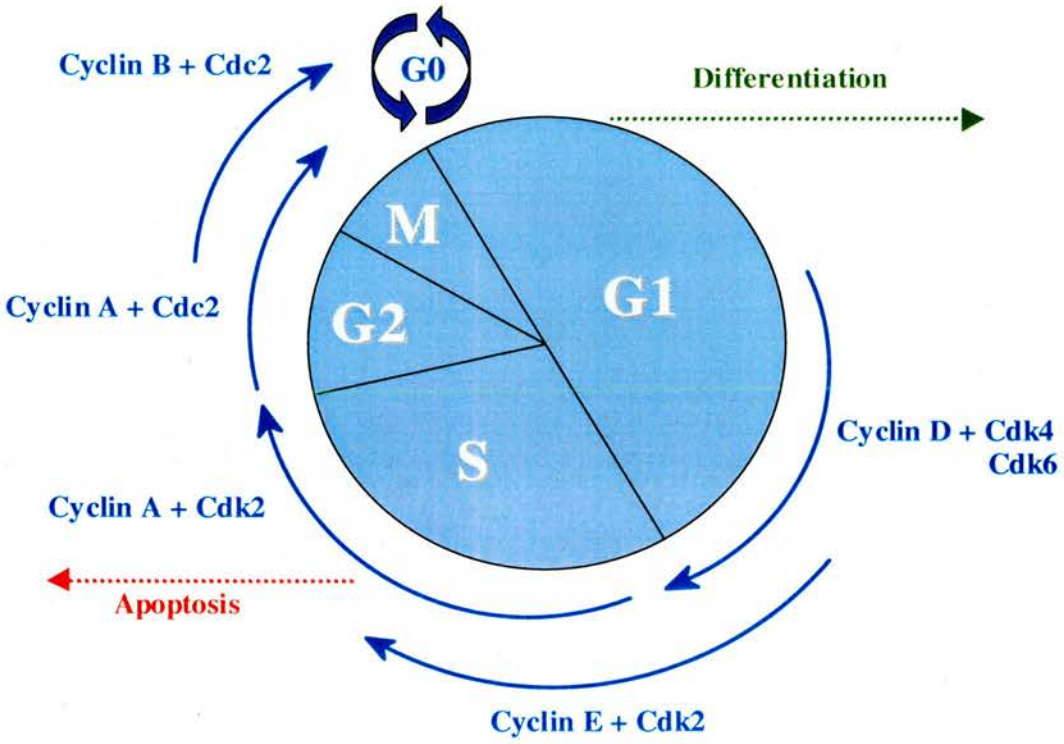

Figure 1.5 Some of the Cdk-Cyclin complexes involved in the cell cycle

As seen in the previous Figure 1.5, relatively few Cyclin-Cdk complexes are directly implicated in the cell cycle. The G1 phase involves a general preparation of the biomolecular machine to DNA synthesis. Thus, following this

general check-up, this transition of the cell cycle is characterised by a number of positive growth factor stimulations that are converted by CyclinD/CDK 4 and 6 as signals to enter the second phase, the S phase[16]. Following production of cyclin E and phosphorylation of CDK2 by CyclinH/CDK7 (the CAK enzyme), DNA synthesis can begin and is also monitored by the CyclinA/CDK2 complex. The precise function of the two CDK complexes during this phase is still unclear, but what is sure is that their presence is absolutely critical[12]. The cell then enters the G2 phase and begins preparations for the mitosis phase (M). CDK1, also referred as Cdc2 in the literature, was shown to play a major role in these latter stages in association with CyclinsA/B: full activation of the catalytic complexes also requires phosphorylation of Thr160/161 by the CAK enzyme as for CyclinE/CDK2[12].

There is a negative feedback control possible through phosphorylation of Thr14/15 and this control pathway can halt the cell cycle if DNA replication has been found to be incomplete, or DNA damage has been detected. Clearly, the benefits of suddenly inactivating the various CDK complexes crucially involved in cell cycle progression thanks to phosphorylation of Thr14/15 enables the regulatory apparatus to use these kinases as checkpoint controls. As a matter of fact, cells constantly assess both external and internal signals and environment to ensure that all phases of the division cycle are correctly completed and CDKs can be best described as its engines, clocks and information processors[11-16].

1.2.3 Pharmacology of Cyclin Dependent Kinase Inhibitors

More importantly, in a number of different neoplastic diseases, CDKs were found to be more or less **mutated** in malignant cells or their natural inhibitors were at least strongly deregulated[16]. Consequently, these protein kinases appear to represent a promising family of novel molecular targets[7] for antineoplastic chemotherapy. Since these enzymes contribute crucially to the control of specifically timed events compulsory to the cell cycle, it is not so surprising that their malfunction can lead to proliferative disorders like cancers, where the tumour cells are not subject to the homeostatic control of the host and reproduce independently.

A definite proof-of-concept concerning the involvement of CDKs in cancer was obtained when small molecular inhibitors of cyclin dependent kinases were indeed found to arrest cell proliferation of many tumour cell lines and also to induce apoptosis in the tumour cells *in vitro* but more importantly *in vivo* as well[1-2] Hence, there has been a considerable interest over the past five years in the design and synthesis of more potent and selective CDK inhibitors for use in anticancer therapy[16]. Since they act as non-DNA-interactive anti-proliferative agents, thus preventing any carcinogenic risk, this new class of antineoplastic substances could well be administered in the future in combination with other cytotoxic drugs with different modes of action to increase the overall efficacy of the current treatments. The potential of these CDK inhibitors is such that

competition is already fierce with numerous academic groups as well as the majority of the main pharmaceutical and biotech companies involved in CDK research: the increasing number of agreements and collaborations, along with recent patents[10] covering either the CDK or cyclin targets, their screening or even families of their inhibitors are signs that cell cycle research is entering a new age.

1.2.4 Structural diversity and similarity of action of CDK inhibitors

Several families of CDK inhibitors[16] have been discovered over the past few years and most efforts have been devoted to improve the potency and selectivity of these compounds by traditional lead optimisation, generation of compound libraries by combinatorial chemistry[24], molecular modelling[25-26] as well as QSAR[27] (Quantitative Structure-Activity Relationships) studies. The results of these different approaches show that a wide range of chemical structures can interact with the ATP binding site in various CDKs[16]. However, optimisation of the selectivity towards one specific CDK is difficult[28-30] simply because of the high degree of sequence similarity for a large number of protein kinases[12,28,29] and since most kinases use ATP as their substrate. Designing ATP-competitive inhibitors selective towards CDKs was indeed found to be extremely challenging. Despite the apparent structural differences, all families of CDK inhibitors share the same properties[22]:

- they are small molecules, with a molecular weight below 600
- most are flat, highly hydrophobic heterocycles

- they act by binding in the kinase ATP-binding cleft and compete with the CDK natural substrate, ATP
- most interactions are hydrophobic and involve H-bonds with the kinase
- the backbone carbonyl and amino side-chains of Leu83 act respectively as H-bond acceptor and donor to the inhibitors, whereas the backbone carbonyl of Glu81 acts exclusively as a H-bond acceptor.

The first approaches involved optimising similar structures to some of the more advanced tyrosine kinase inhibitors, such as SU 5416 **1**, a 3-substituted indolinone, which was entering phase II clinical trials for cancer indications in 2000[31]. The main features of this family are its flat conformation as well as the high degree of conjugation. Another family, namely substituted quinazolines like compound **2**, originally developed as tyrosine kinase inhibitors[32,33], was shown to be active in the submicromolar region for CDK2/CyclinE (IC_{50} = 0.65μM) due to the strong recognition of the quinazoline core in the ATP binding cavity.

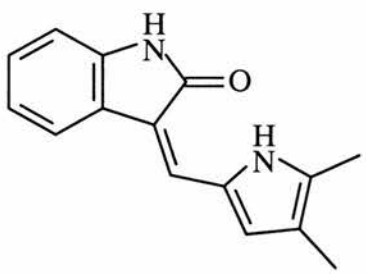

SU 5416 **1**

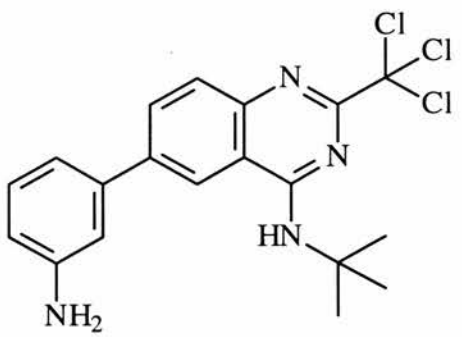

Quinazoline **2**

Another ATP-competitive kinase inhibitor, staurosporine **3**, is a natural product, which was isolated from *Streptomyces staurosporeus*[34], and showed significant CDK inhibition[35], with a high potency for CDK2/CyclinA (IC_{50} = 7nM). Co-crystallisation with CDK2 showed key interactions within the ATP binding pocket, hydrogen bonding with Glu81, Leu83, Gln131 and the side-chain of Asp86. The direct hydroxy analogue of compound **3**, UCN-01 **4**, entered phase I clinical trials in 2000 to evaluate its pharmacokinetics and tolerability[36]. It must be emphasised that compounds **3** and **4** are nonspecific kinase inhibitors and have thus exhibited numerous non-mechanism-dependent side effects in the trials.

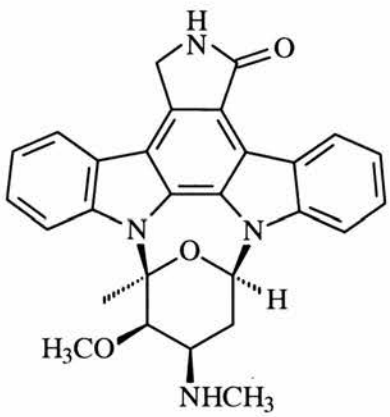

Staurosporine **3**

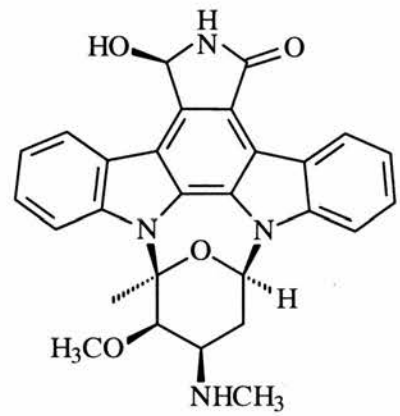

UCN-01 **4**

Another important class of CDK inhibitors is the well-documented flavonoid family, including quercetin **5**, flavopiridol **6** and 2-thioflavopiridol **7**. Quercetin **5** is a naturally occurring compound which has exhibited cardiovascular and analgesic properties on top of its anticancer effects[37] and it presented the flavone core as a structural template for lead optimisation and lead

to the discovery of its synthesised analogues **6** and **7**, which both include an additional 8-piperidine substituent and modification of the 2-aryl moiety. Flavone **6** is the most advanced CDK inhibitor in this series, with submicromolar potencies towards a range of CDKs and was in phase II clinical trials for treatment of several neoplasms in 2000[38,39]. The scope of variation allowed around the flavone core certainly afforded numerous CDK inhibitors that showed lack of selectivity and moderate potencies with regard to CDKs, but was one of the most studied pharmacophore. The 2-thiol ether analogue **7** retains CDK inhibitory activity and has potential application in the treatment of cancer, inflammation and arthritis. Similarly to the staurosporine derivatives, X-ray crystallography of flavopiridol analogues showed the same key hydrogen bonds formed with Glu31 and Leu83[40].

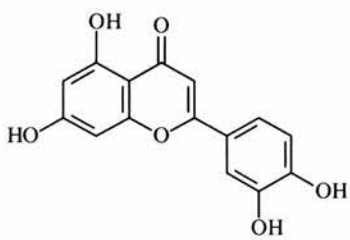

Quercetin **5**

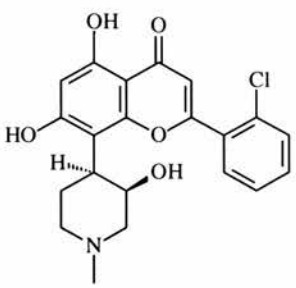

Flavopiridol **6**

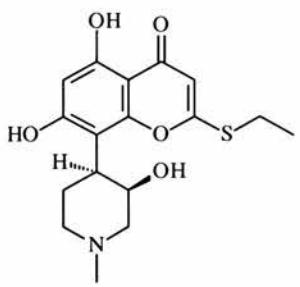

2-Thioflavopiridol **7**

A series of benzazepines, the paullones[41], presented submicromolar potency for CDK1/CyclinB. Its 9-bromo lead derivative **8** showed moderate potency towards CDK1/CyclinB (IC_{50} = 0.4 μM) while being selective to some extent with respect to CDK2/CyclinE and CDK4/CyclinD1. Attempts to optimise its potency lead to the paullone analogue **9,** with greater potency but data from its

cellular activity suggested an alternative mechanism for its antiproliferative properties[42]. Automatic docking by computer modelling[41]of the paullone inhibitors into the active site of CDK1 suggested the importance of an hydrogen-bond with Leu83, which seems to be crucial for binding of a relatively broad range of molecular structures.

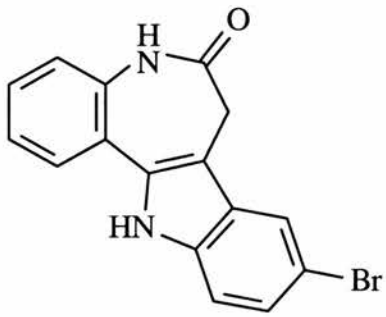

Paullone **8**

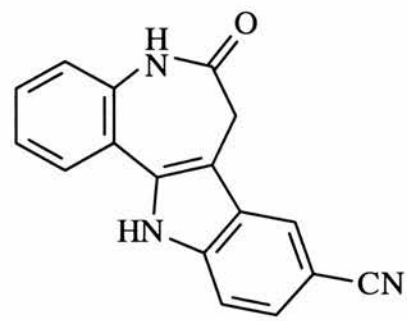

9-cyano analogue **9**

The discovery of a naturally occurring cytokinin, olomoucine **10,** by Czech researchers resulted in the design of a large number of CDK inhibitors based on the purine ring system, due mainly to its scope of variation[43]. Olomoucine was only a modest hit, with potencies for CDK1/cyclinB, CDK2/CyclinA and CDK2/cyclinE of 7μM. Roscovitine **11** was an interesting result from the molecule variation strategy[44] and exhibited a 10-fold improved potency for CDK1, CDK2 and CDK5 (IC_{50} = 650nM) while retaining selectivity towards other kinases. A combinatorial chemistry approach resulted in CVT 313 **12**, a specific and ATP-competitive inhibitor of CDK2/CyclinA (IC_{50} = 500nM) that was found to inhibit reversibly cell proliferation at the G1/S and G2/M transitions[45].

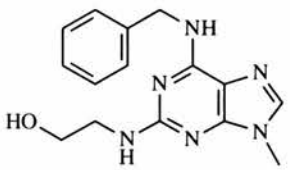

Olomoucine **10**

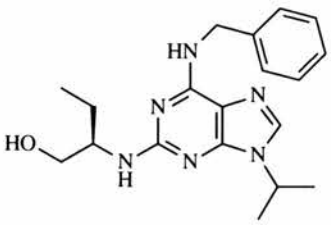

Roscovitine **11**

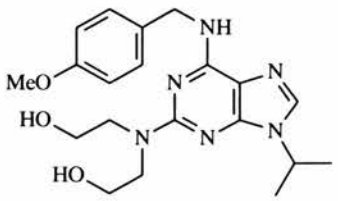

CVT 313 **12**

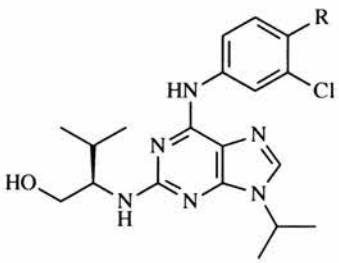

Purvalanol A, R=H **13a**
Purvalanol B, R=CO_2H **13b**

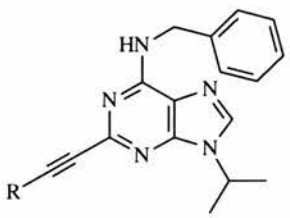

2-alkynylated purines,
R=alkyl alcohols **14**

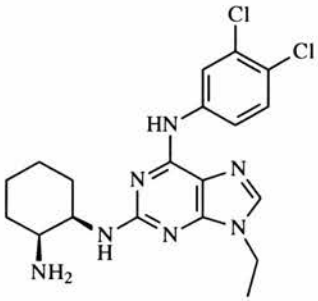

CGP 74514 **15**

Another chemical library[24] led to the identification amongst several hundreds of active compounds of the most potent CDK inhibitors in this purine series, the Purvalanols **(13a,b)**. Purvalanol B **13b** presents an extra carboxylic acid in the *para*-position of the *meta*-bromoaniline of purvanalol A **13a** and has potencies for CDK2/CyclinA of 6nM and for CDK2/cyclinE of 9nM. Crystallographic studies of olomoucine co-crystallised with CDK2 indicated key hydrogen bonds with Leu83, Glu81 and Gln131[46]. The importance of the residues Leu83 and Glu81 was once more demonstrated. Furthermore, in order to explore the SAR of this series, other groups have prepared 2-alkynylated purines such as compound **14** with improved CDK1/CyclinB IC_{50}'s from 1.2 to 0.18 μM[47]. Finally, Novartis researchers have reported CGP 74514 **15** as a selective and potent CDK1 and CDK2 inhibitor[48], with IC_{50} of 16 and 9nM respectively.

Research groups at GlaxoWellcome chose the indolinone from compound **1** as their template and synthesised a variety of hydrazone analogues[49] with traditional substituent variations around the positions 4,5,6,7 of the indolinone scaffold. Hydrazone **16** showed not only good potency (IC_{50} = 6.2nM) but also a 10-fold selectivity to CDK2 with respect to other CDKs[50]. Replacement of the fused pyridine core by a thiazole ring and variation of the amine side-chain on the sulphonate moiety afforded compound **17** with an improved potency (CDK2 IC_{50} = 0.54nM)[30]. Nevertheless, little decrease in tumour growth was observed when dosed daily after 20 days in the *in vivo* testing.

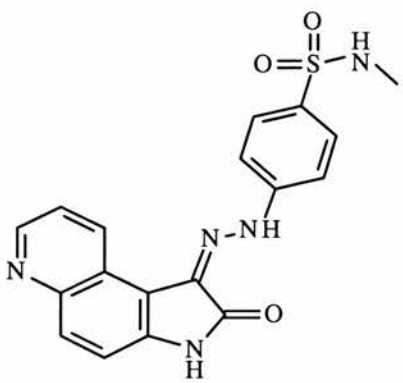

GW5181 **16**

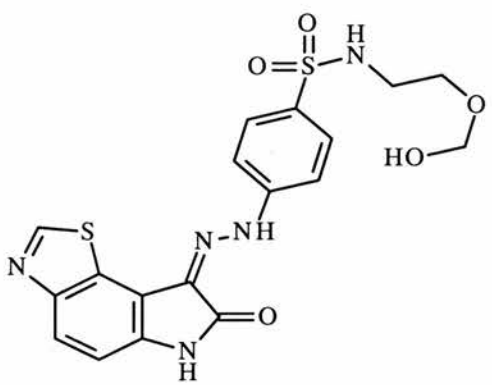

Thiazole analogue **17**

A completely novel approach was implemented successfully by Japanese researchers at the Banyu Tsukuba Research Institute in collaboration with Merck to prepare a new class of potent and selective CDK4 inhibitors[28]: they performed first a *de novo* structural computer design of new scaffold candidates by input of

the specific structural requirements for ATP-competitive inhibition of CDK4, then confirmed the predicted binding mode of the hit structures by synthesising some analogues of the diarylurea compound **18** and obtaining their crystal structure when bound to CDK4. If the 7-hydroxynaphtyl lead **18** was only weakly active (CDK4 IC_{50} = 4μM), by combined molecule variation, combinatorial chemistry and molecular modelling strategies, they eventually discovered compound **19**, a highly potent and selective CDK inhibitor, with an IC_{50} = 1.6nM and selectivity of 190-fold with respect to CDK1 and greater to other kinases[29].

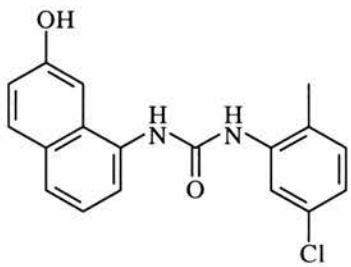

Diarylurea lead **18**

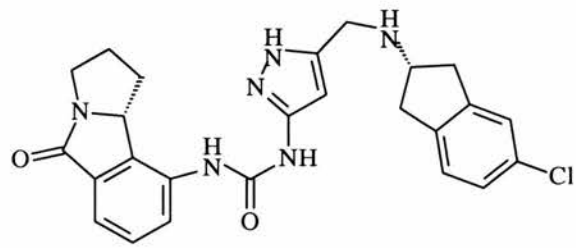

5-Alkylaminomethyl-pyrazole-3-yl urea **19**

Finally, groups at DuPont Pharmaceuticals and Novartis are independently developing two very similar series based on the same indenepyrazole scaffold. Following some positive results from High-Throughput Screening (HTS), the hit structure A3915 **20** was optimised following its decent inhibitory activity[51]

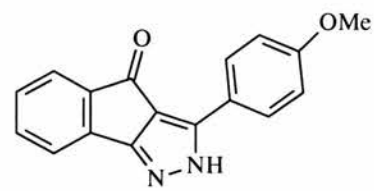

A3915 **20**

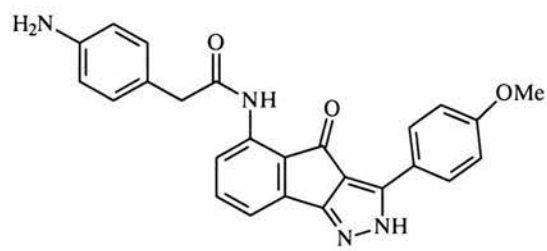

Acetamide analogue **21**

against CDK2 and CDK4 (26 and 43μM respectively) to result in the acetamide analogue **21** which displays a CDK2 potency of 38 nM and a 12-fold selectivity with respect to CDK4.

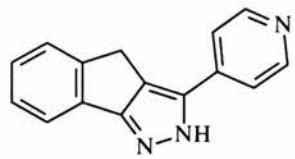

4-pyridinylindenepyrazole **22**

In contrast, the more recent Novartis series (compound **22**) which was discovered through Virtual Screening, does not bear any substitution on the phenyl, and is only weakly active against CDK2 and CDK1 (1.6 and 1.3μM respectively)[52].

More recent families of CDK inhibitors have appeared in the literature but will not be discussed here[53-55]. First of all, they only display moderate activity and selectivity as most of those are only in the optimisation process of the hit compound. Secondly, they are all based on the similar features that were highlighted before:

- a multi-substituted flat core structure featuring fused aromatic rings and 5- and/or 6-membered nitrogen heterocycle such as the purine core of the olomoucine family, the flavone of flavopiridols, the benzazepine of the paullones, the indenopyrazole of the Dupont/Merck series
- some aromatic amine substituents like the anilines of the 2,6,9-purines, the phneylhydrazones of the Glaxo oxindoles and the pyrazole of the Merck diarylureas

Although the most recent improvements in the purine family only resulted in Olomoucine II[56], bearing a methoxy group in the *para*-position of the 6-anilino substituent and comparable activity/selectivity to Roscovitine, a careful analysis of the current Structure-Activity-Relationships of this particular family and other additions from predictive docking by molecular modelling showed that there was still scope for further work on the synthetic and medicinal aspects and will be discussed in the next section.

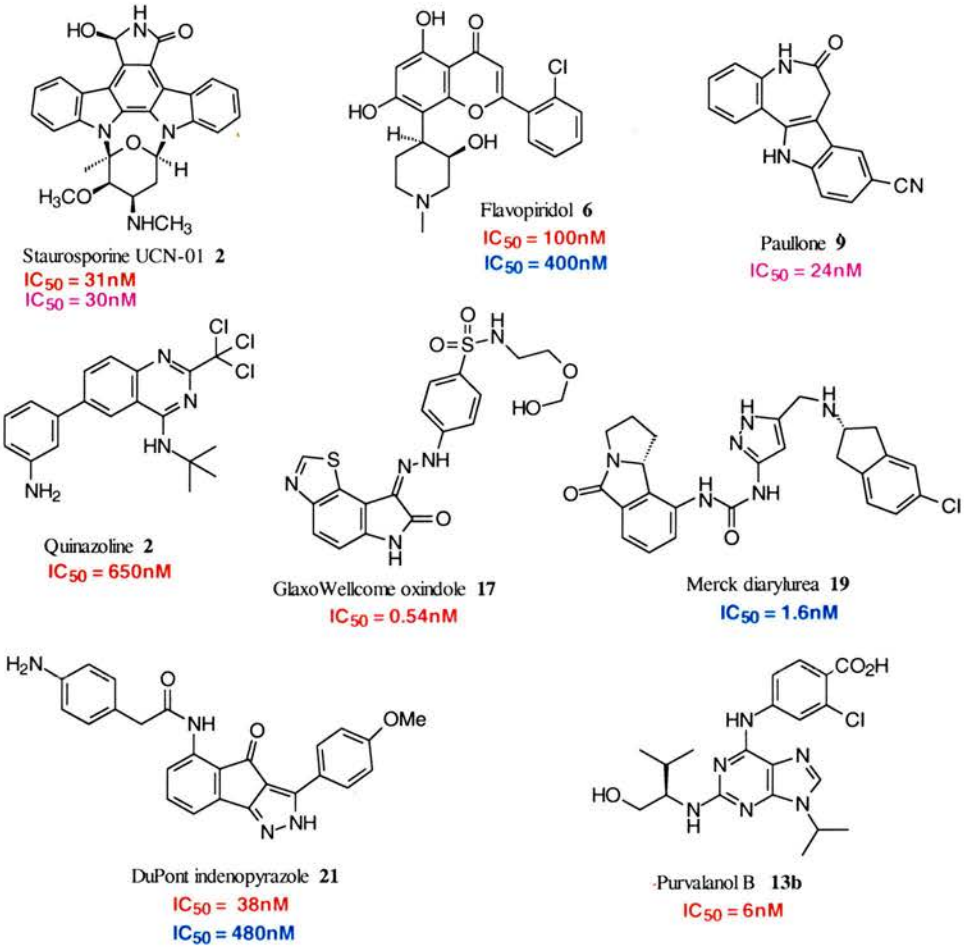

Figure 1.6 Most potent compounds from important CDKI families (inhibition relative to Cdk1, Cdk2 or Cdk4)

1.3 *Structure Activity Relationship analysis of the 2,6-diaminopurine pharmacophore and molecular modelling conclusions*

1.3.1 Rational drug design on 2,6,9-trisubstituted purines as CDK inhibitors

The **original lead** of this extensively studied family of CDK inhibitors, olomoucine **10**, was isolated by researchers at Palackeho University, Olomouc, Czech Republic[43] and is based like ATP **24** on a substituted purine scaffold. From a medicinal chemist's point of view, the most rational and successful method for improving the biological activity of known compounds still relies on the so-called **molecule variation** technique[57]. It has been shown empirically that even minor structural changes for a given molecule in chain lengths, polarity, stereochemistry, hydrophobicity, chemical functionality, and so on can induce the most dramatic leaps in potency towards given molecular targets[58].

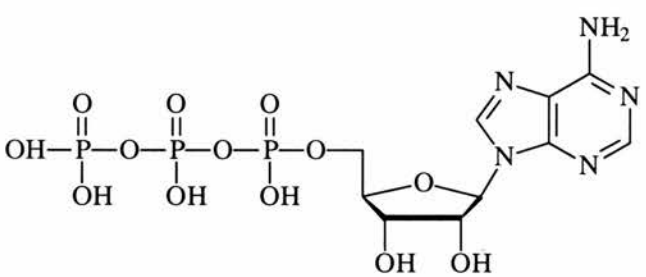

Adenosine TriPhosphate (ATP) **24**

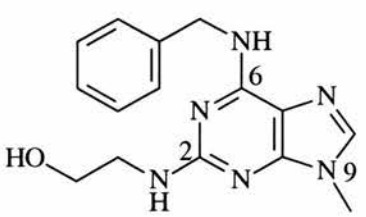

Olomoucine **10**

Therefore, a great deal of information on how the compounds are interacting with the active site of the enzyme can be gained by designing efficient syntheses that allow a defined number of variations around the hit structure. Structure Activity Relationships, often referred as **SAR** in the pharmaceutical industry, compile all results from compound screening into a logical set of conclusions relating the chemical structure of the lead family to the biological activity they exhibit[57-59]. In the case of substituted aromatic heterocycles like the purine ring of the olomoucine class, it has to be checked whether substitution is definitely required, *i.e.* crucial to maintain similar activity, and also if substituting different positions on the rings could improve the potency. Then, by varying the hydrophobicity and steric bulk of the substituents, it is generally noticed that the important enzyme ⇔ inhibitor interactions can be deducted by analysing the most significant gaps in affinity.

1.3.2 Previous lead optimisation studies on 2,6,9-purines

At first, the N-9 methyl (atom numbering on structure **10** on page 23) was replaced by various linear (methyl, ethyl, propyl), non-linear (isopropyl, tertbutyl) or cyclic (cyclopentyl, cyclohexyl, 2-tetrahydropyranyl) alkyl radicals and it was concluded that isopropyl was the best N-9 substituent but that cyclopentyl also produced satisfactory results[60]. More importantly, small polar groups such as 2-hydroxyethyl seemed to be tolerated well, which indicated a potential place for improving the water solubility of a future drug candidate if required[61].

In parallel, the importance of the 6-benzylamino group[43] was demonstrated when it was replaced with success with various substituted anilines and it appeared that the aromatic moiety is compulsory for CDK inhibition[61]. Besides, its substitution seemed to increase potency even more[45]. Results between the anilino and benzylamino series were effectively comparable, although slightly better with the anilines[43]. With purvalanols A **13a** and B **13b** (see both structures page 24), a major leap in potency was achieved[24], and it was suggested that the *para*-carboxylic acid on the aniline, a very polar group, contributed to this effect. Consequently, it is interesting to establish whether other polar groups could be tolerated as well. Nevertheless, it must be added that polar groups might decrease cell permeability since some inhibitors like purvalanol B with polar groups were effectively found **inactive *in vivo***, although extremely potent in the *in vitro* kinase assay. A classical solution to this problem relies on the **prodrug approach**[62], analogous to the protecting groups used in organic chemistry: by converting the polar group into a non-polar functional group that will be "deprotected" by enzymes *in vivo* (for the specific example of purvalanol B, converting the carboxylic acid into an ester that will be hydrolysed by esterases in the target cell). Moreover, classical **bioisosteres** for carboxylic acids include phosphonic acids, esters or amides[62] and so the direct purvalanol analogues would be worth preparing and screening. These hypotheses have been confirmed so far by recent additions from the Legraverend group, University of Paris Orsay, who demonstrated first with molecular modelling[25,26]then by QSAR[27]calculations

that polar groups in *meta* or *para* positions of the 6-anilino or 6-benzylamino substituent would increase CDK inhibition, so more analogues need to be prepared in this purvalanol B subseries to verify this hypothesis.

Furthermore, the importance of the non-substituted positions 1,3 and 7 was confirmed by X-ray crystallography of several inhibitors bound to CDKs since the nitrogens were found to interact by hydrogen bonding with some aminoacid residues[63]. Consequently, since H-bonds are important molecular interactions in reversible enzyme inhibition, this result clearly indicated that these positions have to remain unsubstituted.

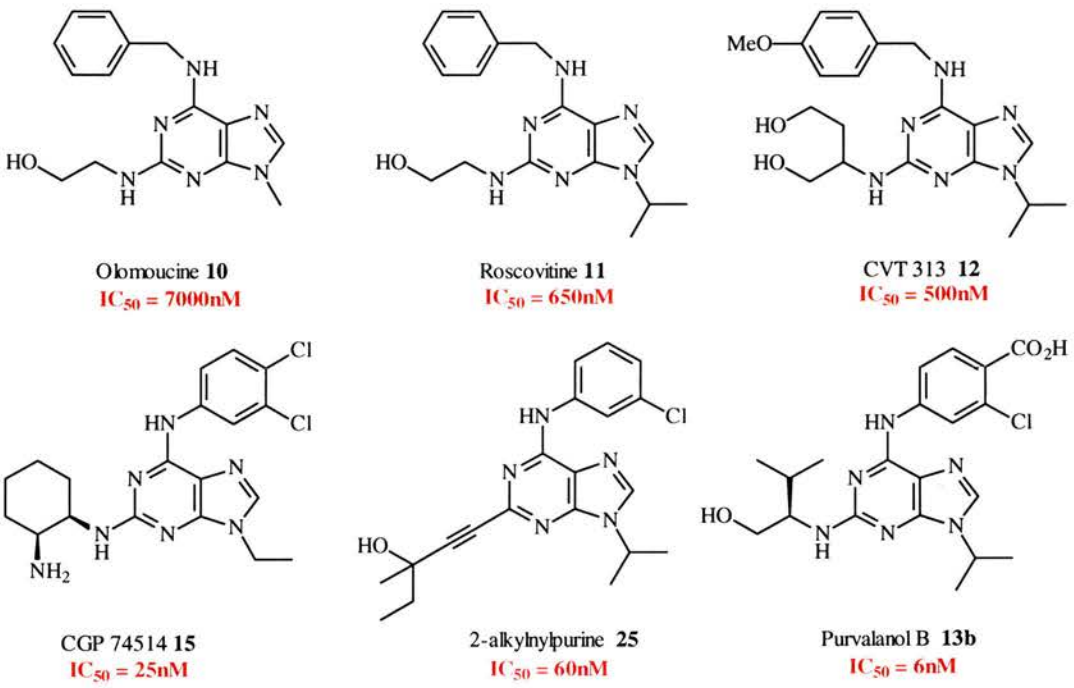

Figure 1.7 Important CDK2 inhibitors of the olomoucine family

Similarly, several research groups extensively investigated the 2-amino substituent with traditional medicinal chemistry techniques, such as further substitution of the secondary 2-amino, extension then isomerisation of the linear alkyl side chain, the best side-chain being that of purvalanols A and B, a *R*-valinol linked to the α-amino group[24]. On top of that, some decent results were obtained with aliphatic heterocycles like thiamorpholine for instance[60], but no phosphorus or sulfur containing groups were tested. The Legraverend research group also discovered that a new class of substituents for the 2-position of the purine ring, namely hydroxyalkyl-1-ynes[47], was also producing satisfactory results, and concluded that the 2-nitrogen directly linked to the purine ring was probably not crucial for CDK inhibition[25]. Therefore, more analogues with altered 2-substituents need to be prepared and tested: not only is the SAR still unclear about the functionalities that the catalytic cleft can accommodate in this region but more recent conclusions from molecular modelling studies also tend to indicate that the neighbouring phosphate pocket pointing towards the outside of the cleft could be beneficial for binding affinity. Figure 1.8 below summarises the main ideas described here above and highlights some of the important CDK inhibitors in the olomoucine series.

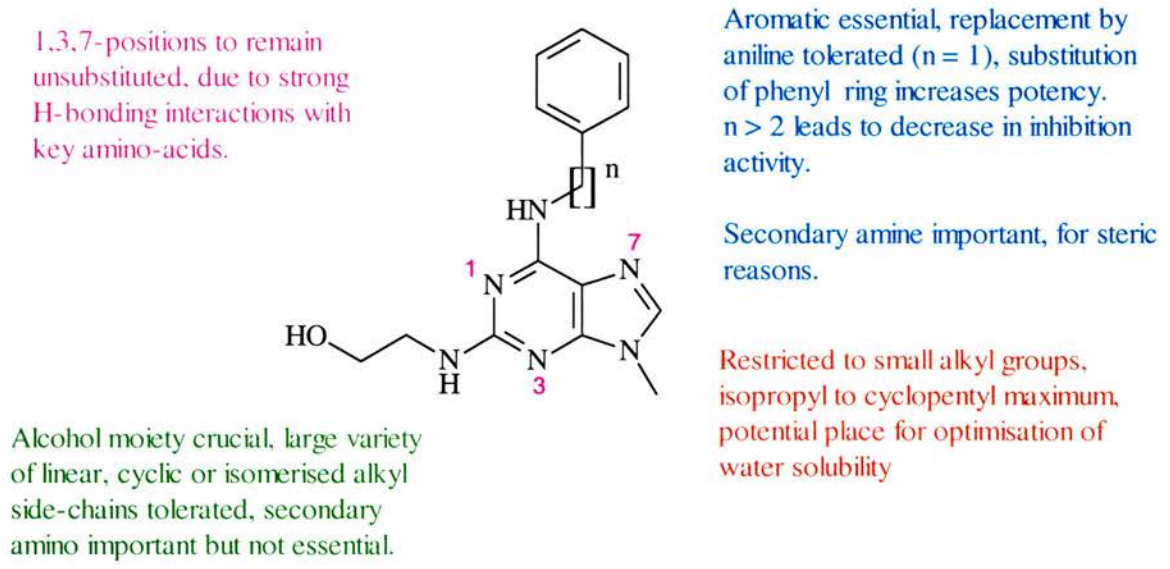

Figure 1.8 SAR of the 2,6-diaminopurine pharmacophore shown on olomoucine **10**

To conclude, it seems that further investigation of the 6-substituent could lead to an improvement of the potency: polar moieties such as the carboxylic group of purvalanol B have not been tested so far, and classical bioisosteres include sulphonamides, sulphonic acids. As shown by the GlaxoWellcome oxindole series[49-50], substituted sulphonamides were exhibiting excellent potency as well as selectivity towards CDK2, so it is important to establish whether this could improve the testing profile of the olomoucine series. Finally, due to the scope of variation tolerated around the 2-amino substituent, other polar groups could well be introduced to replace the hydroxy group and the new side-chains linked to the purine with the best 6-substituent.

1.3.3 Recent additions from molecular modelling studies

Several crystal structures of CDK2 complexed with some inhibitors (Olomoucine and roscovitine[46], purvalanol A and B[24], staurosporine[36], and deschloroflavopiridol) have been obtained. However, the structure of CDK1 has not been reported to my knowledge. As shown before, this illustrates how CDKs are able to accommodate very diverse classes of molecular entities in their binding site. Since the primary sequence is very closely related from one CDK to another first, and also to other kinases[12], it is extremely important to understand what key structural features generate selectivity and how they can be used for the design of more selective CDK inhibitors.

A recent structural classification of protein kinases has been performed by molecular modellers from Aventis Pharma Deutschland[64] and demonstrates what structural features of CDK inhibitors can increase their **CDK selectivity** with respect to other protein kinase families. They used the crystallographic data from the CDK2-purvalanol B complex[24] along with various computational techniques, including GRID Molecular Interaction Fields (MIFs)[65,66], Comparative Molecular Field Analysis (CoMFA)[67,68], and Comparative Molecular Similarities Indices Analysis (CoMSIA)[69-70] to generate an alignment rule for Three-Dimensional Quantitative Activity Relationship (3D-QSAR)[71] of purine-based CDK inhibitors.

The main conclusions confirm the previous deductions from the SAR studies and explain why purvalanol B is a more potent and selective CDK2 inhibitor. First of all, the hydrophobic interactions close to N9 and C2' with the two isopropyl groups (see atom numbering in Figure 1.9 next page) seems highly favourable for the selectivity to the CDK family with respect to other kinases. The N9 isopropyl, rather than other alkyl substituents, appears to be better accommodated by the residues Val64, Phe80, Ala144. As for the C2' isopropyl, this group looks to be closely enfolded by the hydrophobic area close to Ile10 and Val18.

Moreover, there are some favourable interactions in this zone close to the C3' primary hydroxy moiety close to polar amino acid side-chains, this area also being solvent-exposed. Finally, introduction of particular substituents on the *meta-* and *para-* positions of the C-6 N-phenyl ring will certainly increase the selectivity: Gln85 and Ile10 appear to accommodate this aromatic ring, while there are favourable interactions between the aromatic *meta*-chloro and Asp86 and between the *para*-carboxylic acid and Lys89. Consequently, they propose a novel model for 2,6,9-trisubstituted purine binding:

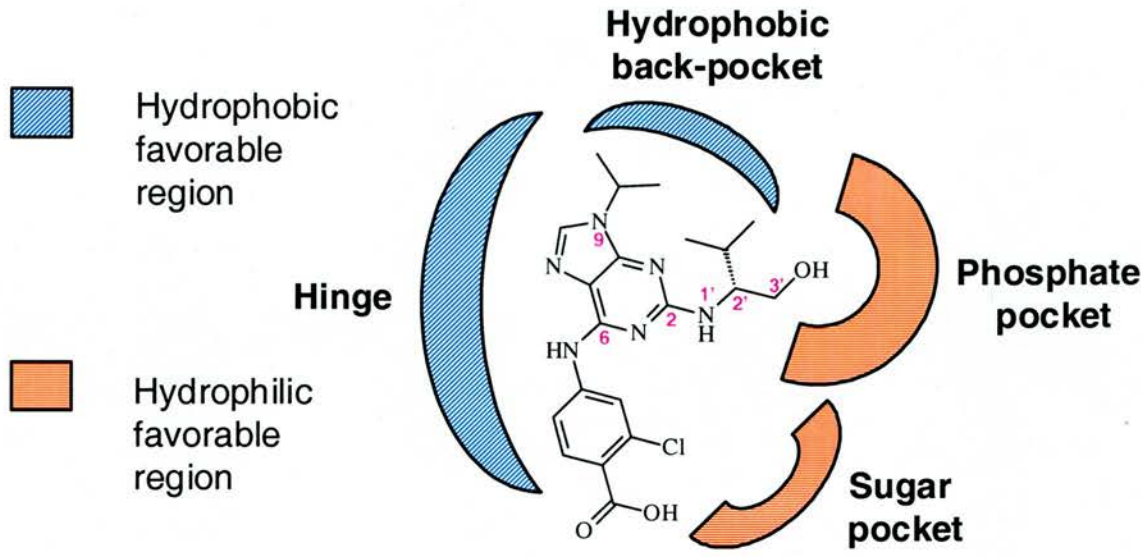

Figure 1.9 Adventis model for CDK2 binding of 2,6,9-purines shown on purvalanol B **13b**

Their results from the CoMFA and CoMSIA studies also confirm that the two isopropyl groups at positions N9 and C2' lie in sterically favoured regions and that these steric bulky interactions are important to retain selectivity with respect to other kinase families. Besides, both the polar hydroxy and carboxylic groups are orientated towards hydrophilic favoured regions. Finally, more positive charged moieties at the phosphate-binding pocket, next to the cleft entrance, would have another beneficial effect on the selectivity profile of future compounds.

Another novel approach worth being mentioned that was reported by Japanese and Merck scientists is the identification of altered amino acid residues around the ATP binding pocket[29]. Since the primary structure of most CDKs looks very similar, they formulated the hypothesis that the **most frequently altered residues** for one particular CDK could have an effect on the selectivity (see figure 1.10 page 39). Thus, they compared the amino acid sequence of CDK4 to that of other CDKs and protein kinases and identified the most altered residues. Then, using Virtual High-Throughput Screening (VHTS) of their compound library, they discovered a lead structure that was interacting with these specific residues and tried to optimise the substitution and steric bulk of the inhibitors to eventually prepare compound **19** of this diarylurea class, not only highly potent (IC_{50} = 1.6nM) but very selective with respect to other kinases and CDKs.

Molecular modelling from the X-ray structures of CDK2 cocrystallized with various inhibitors (A. *des*-chloroflavopiridol, B. staurosporine, C. Roscovitine on Figure 1.11 page 40) also enabled them to identify the key aminoacids as well as the structural requirements for binding in the ATP cavity[28]. First of all, this model fits perfectly with all three different classes of Cdk inhibitors, but is limited: for instance, it fails to rationalise for instance why flavopiridol inhibitors are much less potent than those of the olomoucine class, as the important structural requirements (H-bonding with Leu83 and Glu81) indeed feature for both classes of compounds. Nevertheless, it is very similar to the

Adventis model of Figure 1.9. Thus, both are often used as starting points for the design of novel hydrophobic cores.

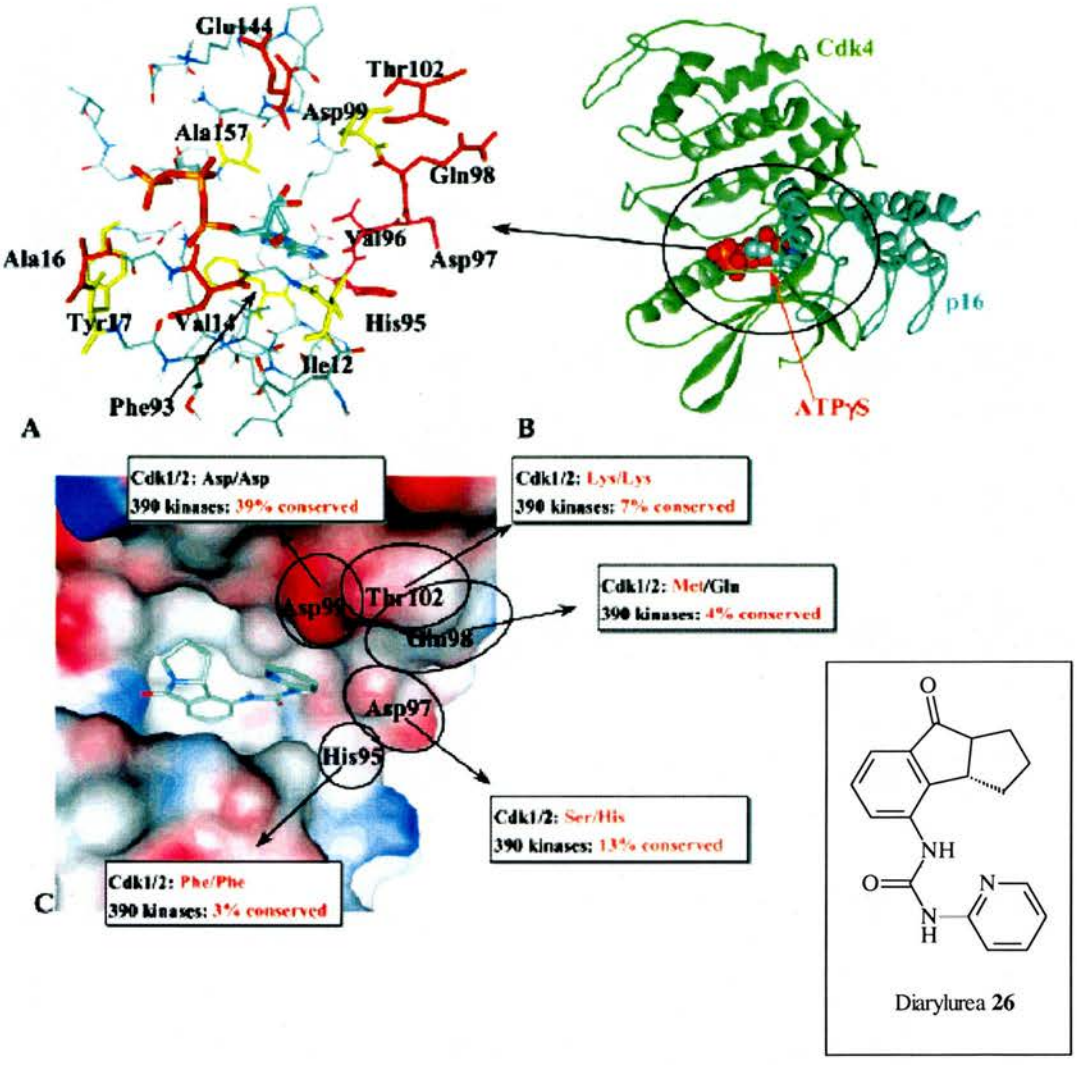

Figure 1.10 Altered CDK4 residues[29]. **A.** Yellow residues <40% conserved in 390 kinases, and in contact with (26) or ATPγS, Red residues replaced in CDK1/2 <40% conserved in 390 kinases and in contact with (26) or ATPγS. **B.** Superimposed model of CDK4-ATPγS-p16. **C.** Binding mode of (26) in CDK4 homology model with frequently altered residues. (Solvent accessible surface, probe=1.4Å, coloured by partial charge)

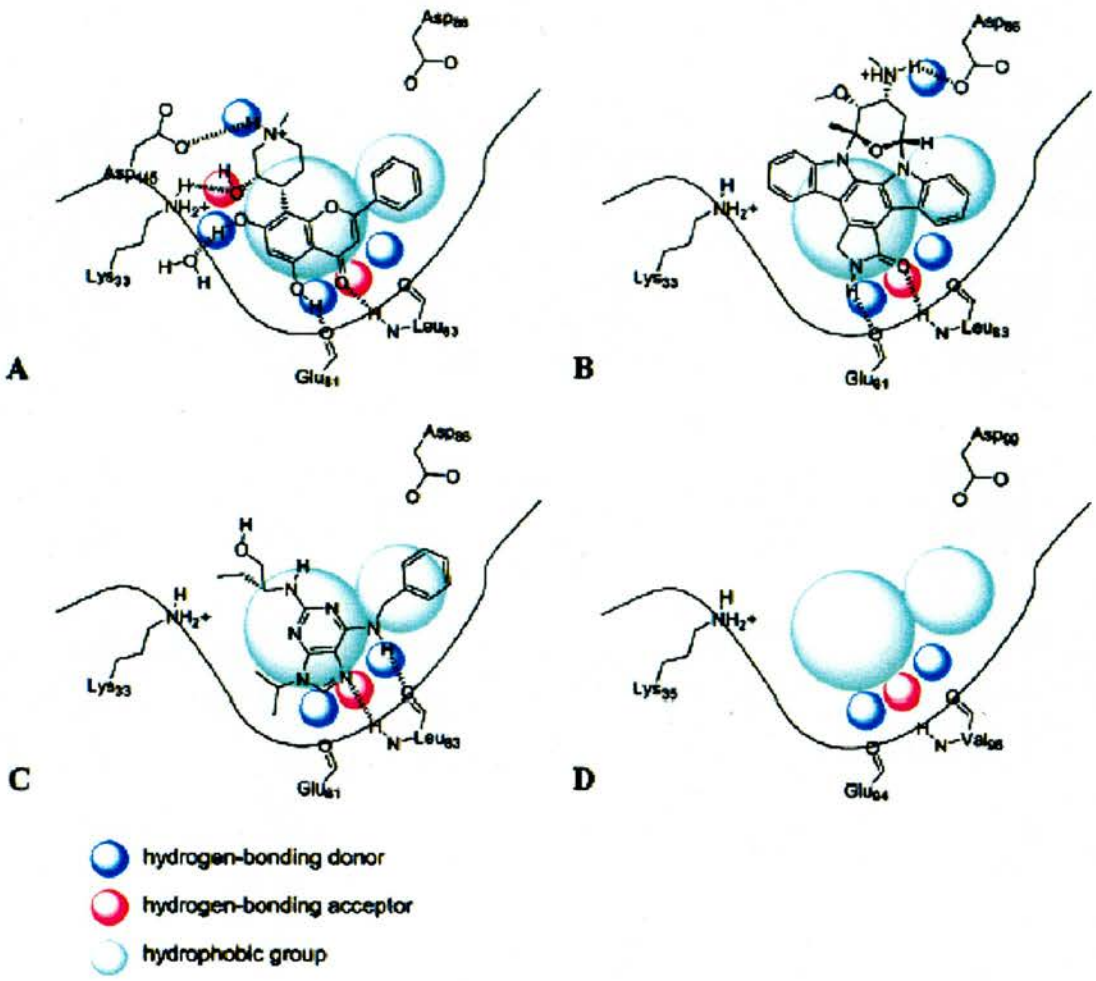

Figure 1.11 Model for CDK4 inhibitor structural requirements[28] **A.** deschloro flavopiridol-CDK2 complex. **B.** Staurosporine-CDK2 complex. **C.** Predicted structural requirements in CDK4 homology model

Some of the GSK oxindole CDK inhibitors have been successfully co-crystallised with CDK2 and the corresponding structures (1FVT and 1FVV) are available on the Protein DataBank[20]. GSK compound **27** of Figure 1.13 page 42 features an oxindole core fused with a thiazole ring at the 4- and 5-positions and also substituted with an phenylhydrazine at the 3-position bearing a sulfonamide in the *para*-position.

As shown in Figure 1.12 below, the crystal structure shows that the flat thiazolo-oxindole ring is orientated towards the hydrophobic pockets deep inside the CDK binding cavity. The phenyl hydrazine points towards the outside of the cavity and it is striking that the 2-aminopyridine group of the sulphonamide seems to interact with amino-acid residues located outside the binding pocket. Apart from the Merck diaryl ureas, this had never been reported before and the selectivity profile of both classes of compounds tends to indicate that the crucial amino-acids for CDK selectivity might not be located inside the binding cavity but on its periphery.

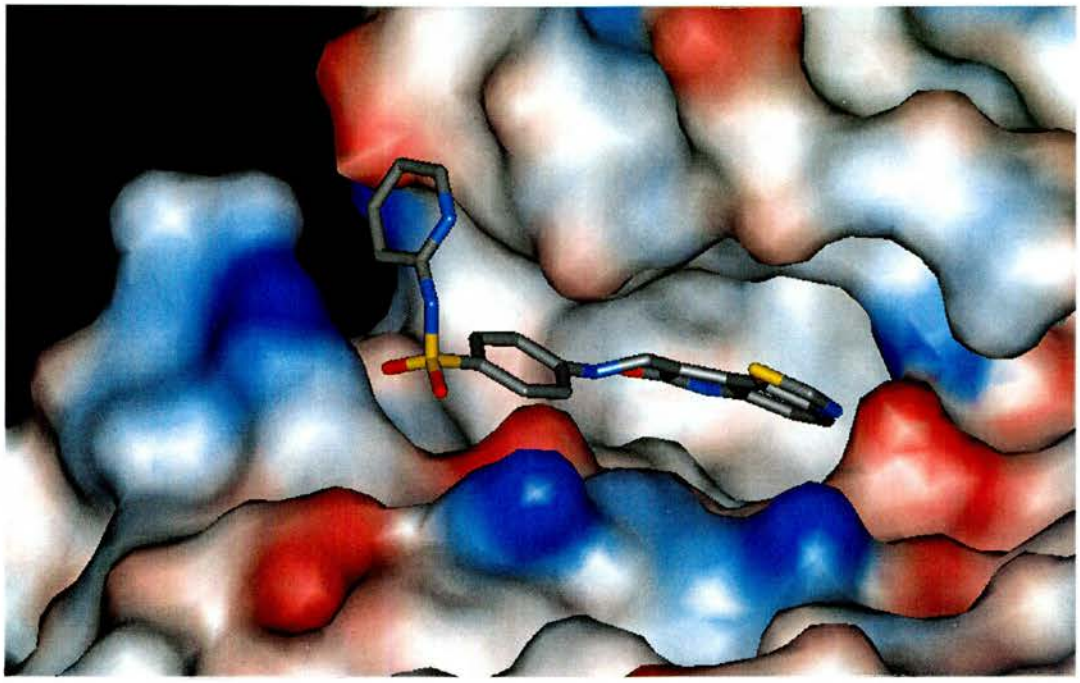

Figure 1.12 Docking of oxindole **27** (stick representation) in CDK2 (solvent accessible surface, probe 1.4Å, coloured by partial charge)

Endicott *et al.*[72] showed how similar the binding mode of most CDK inhibitors was with the important features being the 2 or 3 H-bonding interactions between the amino-acid Glu81 and Leu83 of the protein backbone and the inhibitor. It can be noticed that both Purvalanol **13b** and GSK oxindole **27** both possess one hydrogen bond heteroatom donor (nitrogen for the purine, oxygen for the oxindole) and two hydrogen bond acceptors. Figure 1.13 below highlights this common property of both inhibitors as well as the overlapping orientation of the aminophenyl substituent, diplayed in cyan. The crystal structures of both inhibitors (PDB 1FVV and 1CKP) confirms this hypothesis, both phenyl rings are similarly orientated.

Therefore, introducing sulphonamide moieties on Purvalanol B at the *para*-position represented an interesting prospect: would the introduction of these sulphonamide substituents induce a leap in selectivity as observed for the GSK oxindoles?

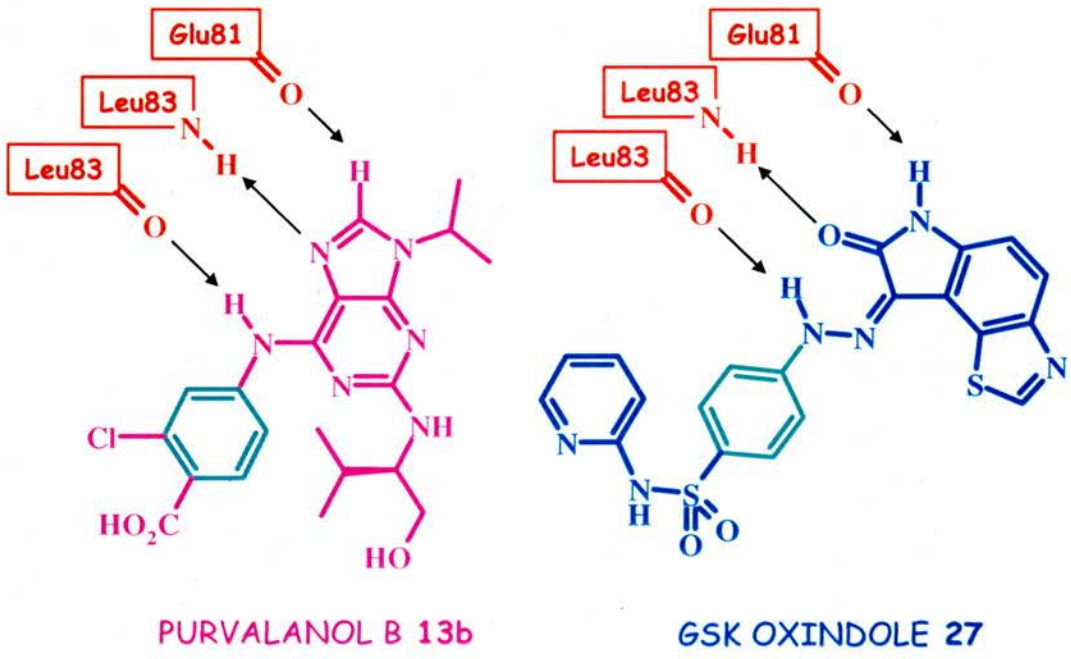

Figure 1.13 Binding mode comparison of Purvalanol B **13b** and GSK oxindole **27** (hydrogen bonds represented as black arrows)

As mentioned previously, the current CDK inhibitors do not seem to interact with the secondary neighbouring phosphate pocket. The triphosphate group of ATP is closely folded by this hydrophilic pocket (see Figure 1.14) but inhibitors of the Olomoucine family do not exploit this feature of ATP binding[64].

Since CDK inhibition is based on competing with ATP for binding, it seemed a logical approach to prepare Purvalanol analogues bearing substituents that would interact with this binding pocket. Some of the possible groups included sulfonic acids and phosphonic acids and esters. Would the introduction of substituents binding in the phosphate sub-pocket increase the binding affinity of novel Purvalanol based CDK inhibitors?

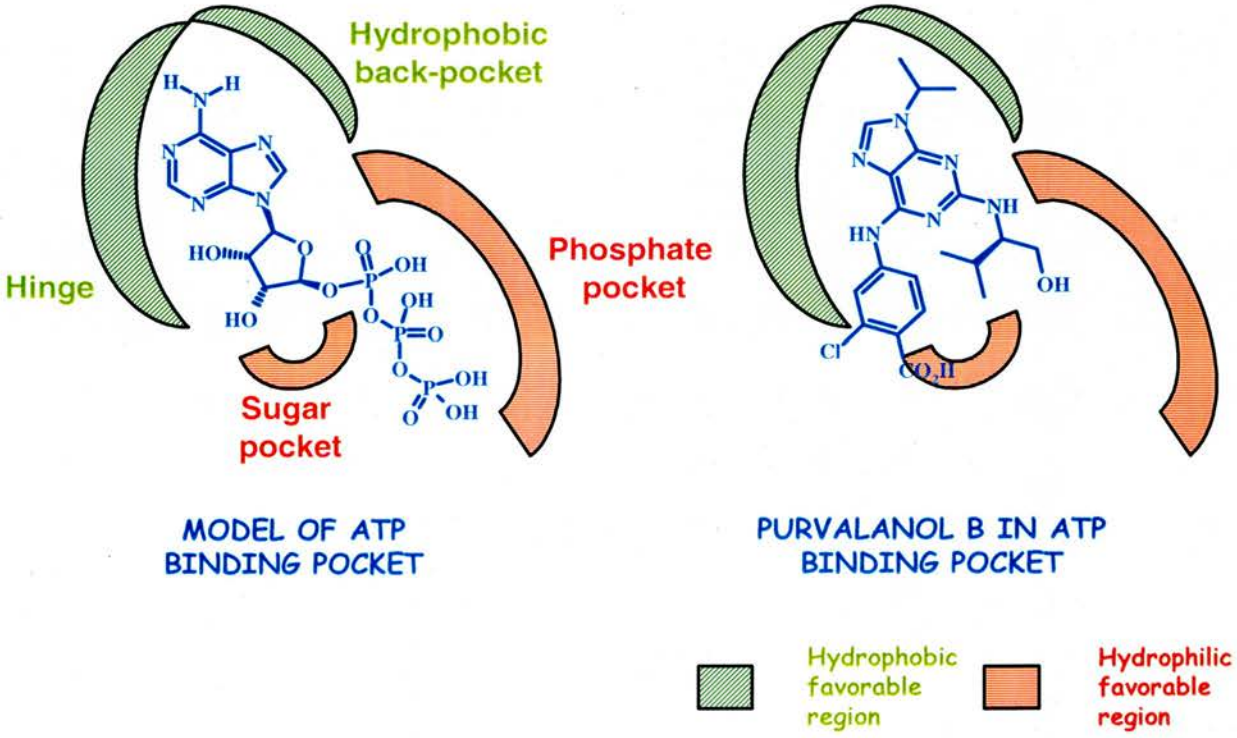

Figure 1.14 Binding mode of ATP and Purvalanol B

1.4 *Initial chemical strategy*

1.4.1 Molecular targets

Following the excellent results obtained in the GSK oxindole series (compounds **17** page 22 and **27** pages 32-33) which include substituted sulphonamide containing anilines, it seemed appealing to synthesise the direct purvalanol B analogues **28** with the best side-chains in this series (aliphatic and aromatic amines). Not only do the general orientation of the purine and oxindole compounds overlap well as demonstrated in the previous section but the key interactions are remarkably similar as well: heteroaromatic core closely enfolded deep inside the binding cavity, and aniline ring with its polar substituents pointing towards the sugar-binding pocket of ATP.

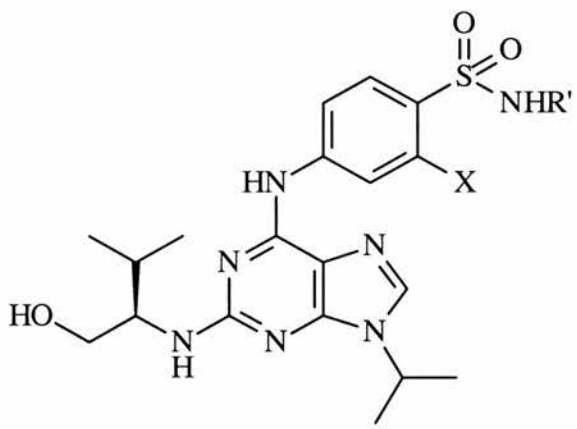

X = -Cl, H

28

Figure 1.15 Some of the anticipated sulphonamide containing 2,6,9-trisubstituted purine analogues of Purvalanols **13a**, **13b**.

It was particularly surprising that no research group had reported these analogies before. Investigating whether the introduction of the sulphonamide moiety on the aniline of Purvalanols could lead to an improvement in the selectivity profile of the 2,6,9-trisubstituted purines was the primary goal of this project.

We showed that the 2-substituents were also prone to optimisation, possibly with the introduction of polar groups in order to create additional interactions with the phosphate-binding cavity of figure 1.14 page 34. However, it seemed reasonable to limit the project objectives to the secondary molecular targets below.

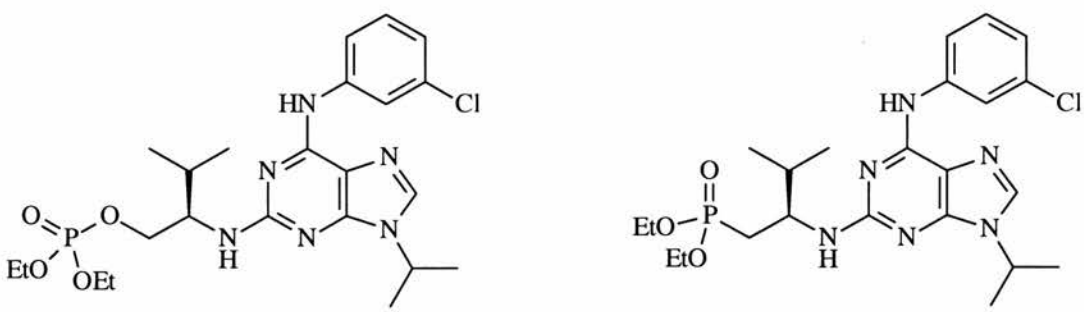

29 **29**

Figure 1.16 Some of the anticipated phosphorus containing analogues of Purvalanol A **13a**.

1.4.2 Retrosynthetic approach

The synthesis of 2,6,9-trisubstituted purine CDK inhibitors has been extensively described in the literature[60,61] and relies on the displacement of halogenopurines by anilines for C6-substitution and by primary amines for C2-substitution. Thus, the obvious synthetic methodology is to prepare 2,6-dihalogenopurines first, then to react these starting materials with various amino-containing C6 and C2 side-chains. There is a slight variation in the retrosynthetic sequence whether 6-chloro-2-iodo-9-isopropylpurine **30** or 2,6-dichloropurine **31** is chosen as the purine starting material.

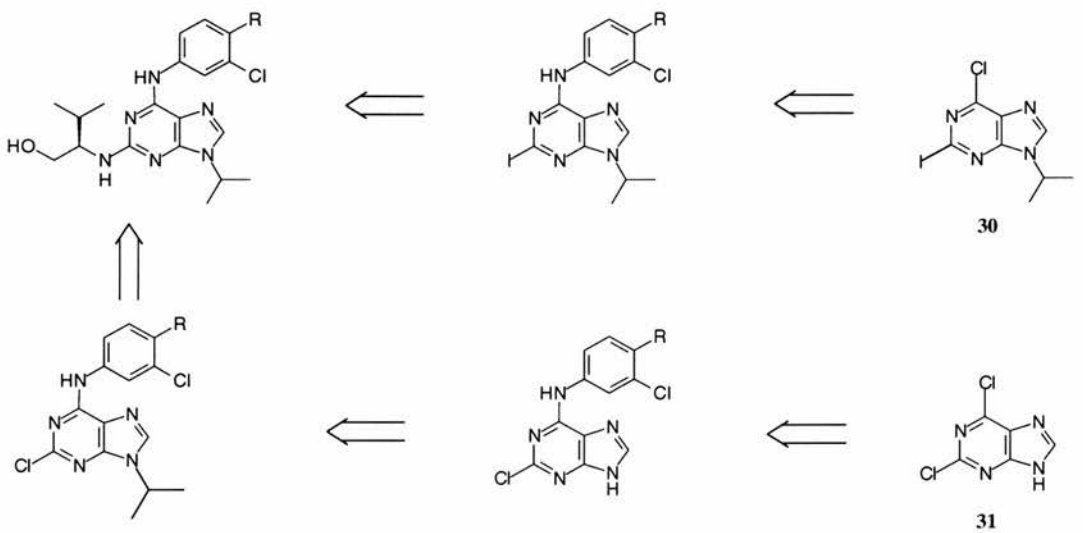

Figure 1.17 Retrosynthetic pathways towards 2,6,9-trisubstituted purines

As a matter of fact, the commercially available, albeit quite expensive, 2,6-dichloropurine can be alkylated on positions 7- and 9-, thus producing a mixture of isomers. This problem is avoided when the 6-chloro is displaced first by the substituted aniline, then follows the regioselective alkylation on N9 due to the presence of the bulky C6 substituent. The C6 chlorine is known to be much more reactive towards displacement by primary amines[45]. Another reported starting material is 6-chloro-2-fluoropurine[73].

1.4.3 Synthesis of purine intermediates

The general chemical strategy relied on the commercially available 2,6-dichloropurine or more ideally 6-chloro-2-iodo-9-isopropylpurine, whose synthesis had been published and did not seem problematic[61,74]. Scheme 1.1 highlights the multistep synthetic route required for the 6-chloro-2-iodo-9-isopropylpurine starting material: the first step involves cyclisation to form the dihydroxypyrimidine ring **32**, then follows the chlorination of both hydroxyls to yield the symmetrical 2,4-diamino-4,6-dichloropyrimidine **33**. Then, after displacement of one chlorine with isopropylamine, ring closure using triethoxymethane, the diazotation step finally affords the desired trisubstituted purine **39** in acceptable yields.

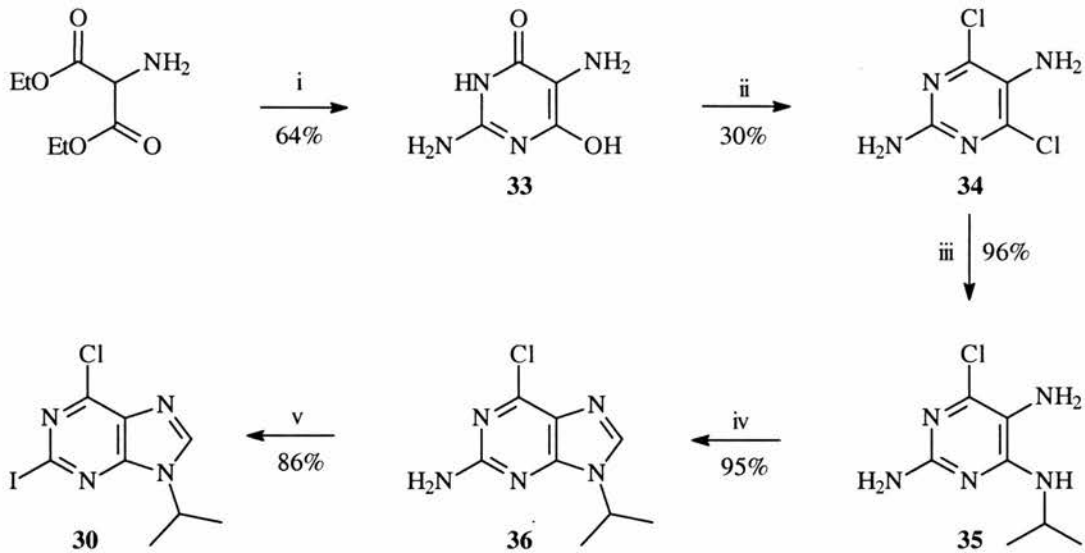

Conditions: i) guanidine, NaOEt, EtOH ii) $POCl_3$, PCl_5, TEBAC, MeCN iii) *i*-$PrNH_2$, Et_3N, BuOH iv) $CH(OEt)_3$, H^+, Me_2NCOMe v) *i*-$Pr(CH_2)_2NO_2$ then CuI, I_2, DCM

Scheme 1.1 Synthesis of 6-chloro-2-iodo-9-isopropylpurine **30**

The synthesis of 2,6-dichloropurine is significantly shorter[60] than that of the previous purine starting material: following oxidation with aqueous hydrogen peroxide of adenine to result in the N-1-purine oxide **37**, and diazotisation to afford the 6-hydroxy-1N-purine-oxide intermediate **38**, the final chlorination reaction gave 2,6-dichloropurine **31** in moderate yields. Even if the synthesis of 2,6-dichloropurine could be achieved in three steps, compared to six for that of 6-chloro-2-iodo-9-isopropylpurine, several papers reported that the incorporation of the 2-aminosubstituent was sometimes difficult or even failed with some secondary amines[23,45]. Consequently, it was decided to focus at first on the preparation of the purine starting material **30** only, which did not seem to present

any major drawbacks, apart from being time-consuming. Besides, its reactivity towards amines to displace the halogens is reported to be higher than that of 2,6-dichloropurine, since it is not necessary to use sealed vessels for the displacement reaction with amines[23]. Finally, the 9-isopropyl group would be already present and this would prevent the difficult separation of 7- and 9-alkylated mixtures obtained when N-alkylating purines[75].

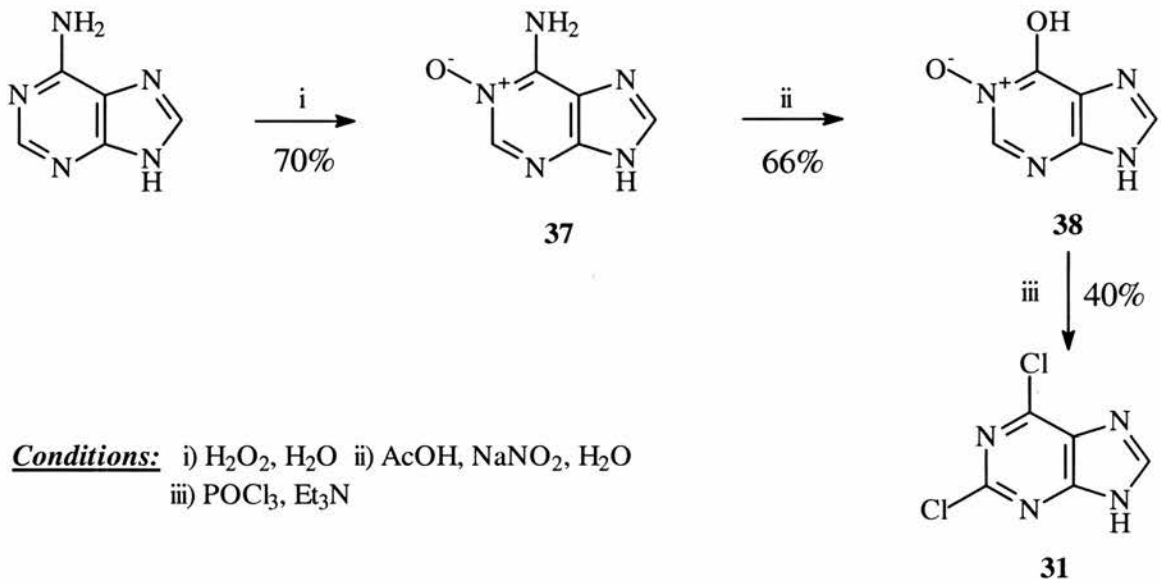

Scheme 1.2 Synthesis of 2,6-dichloropurine **31**

CHAPTER 2: SYNTHESIS AND REACTIVITY OF 2,6-DIHALOGENOPURINES

2.1 *Introduction*

The synthesis of 2,6-diaminopurine CDK inhibitors was discussed earlier in chapter 1 (see section 1.4.3). Lee *et al* synthesised 2,6-dichloropurine from adenine in three steps[60], the most important reaction being the chlorination with phosphorus oxychloride $POCl_3$ of the purine N-1 oxide intermediate. It must be emphasised that this expensive starting material is available from most chemical manufacturers. However, some research groups reported that the 2-chloride of this dihalogenopurine can be difficult to displace with aliphatic amines and highlighted the forcing conditions necessary for the reaction to proceed in decent yields[23,45]. A major conclusion to their studies was the beneficial replacement of the 2-chloride by iodide or fluoride to enhance the reactivity of the heterocycle towards nucleophiles.

In this chapter, we will discuss at first the results obtained in the synthesis of an alternative dihalogenopurine intermediate, 6-chloro-2-iodopurine, from literature procedures[61,74] (see Scheme 1.1 page 49) and from our synthetic strategies. Then, the reactivity of this compound with aromatic and aliphatic amines will be presented. Finally, we will report the substitution of the 6-chloride

by the benzylsulfonyl leaving group[76-78] and the synthesis of Purvalanol A from 6-benzylsulfonyl-2-iodo-9-isopropylpurine.

2.2 *Results and discussion*

2.2.1 Attempted synthesis of 6-chloro-2-iodo-9-isopropyl from guanidine

Legraverend *et al* reported the synthesis of 6-chloro-2-iodo-9-isopropyl purine in a synthetic route involving a Traube reaction with guanidine, a ring-closure of the 5,6-diaminopyrimidine and a non-aqueous diazotisation-iodine substitution[79] as seen in Scheme 2.1. We first tried to reproduce those results in order to obtain a significant amount of diaminopurine precursor. The Traube reaction with diethyl aminomalonate and guanidine in refluxing ethanol in the presence of stoiechiometric sodium ethanoate yielded the desired pyrimidine **1** as its hydrochloride salt in only 32% yield. The product was characterised by MS, IR spectroscopy and elemental analysis and the results fitted perfectly with the published data: the ESI mass spectrum displays the parent ion at m/z = 143 for $[M+H]^+$ while the IR data was in good agreement with the published compound[74].

However, the chlorination of both hydroxyl groups of pyrimidine **1** with a mixture of phosphorus oxychloride ($POCl_3$) and phosphorus pentachloride (PCl_5) was not as successful as reported. Indeed, the reaction failed to give the formation of the required dichloropyrimidine **3** in good yields despite the completely

anhydrous conditions as mentioned in the literature. Instead the starting material **1** was retrieved and characterised.

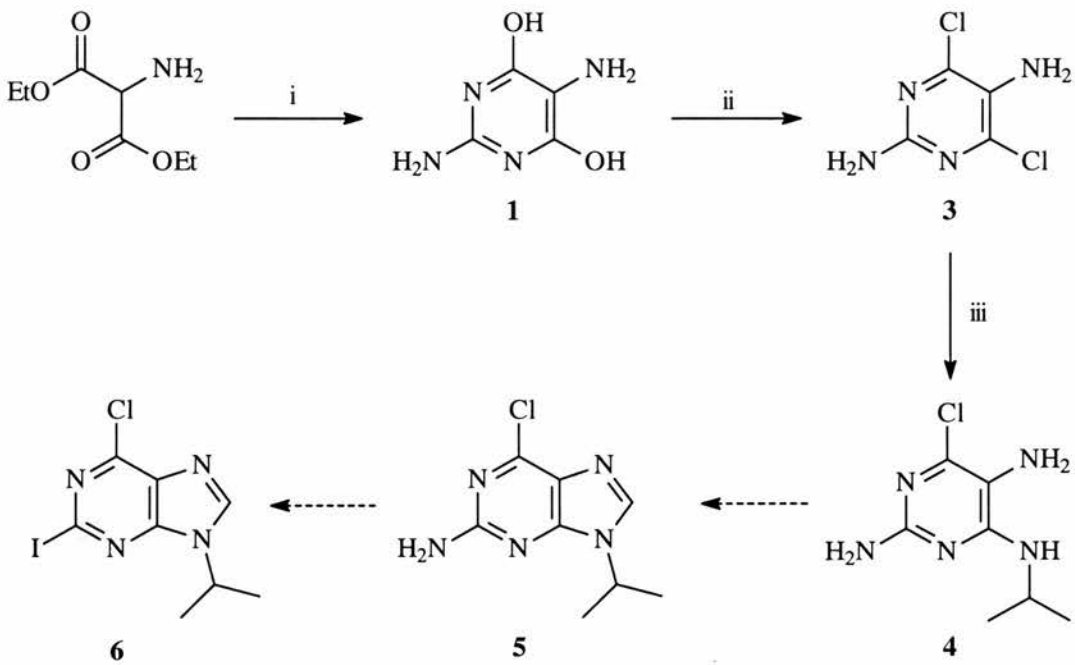

Conditions: i) guanidine, EtONa, EtOH, Δ, 34% ii) $POCl_3$, PCl_5, TEBAC, MeCN, Δ, 16% iii) *i*-$PrNH_2$, Et_3N, *n*-butanol. Δ, 30%

Scheme 2.1 Attempted synthesis of 2-amino-6-chloro-9-isopropylpurine

As the purity of all reagents had been checked and flame-dried Schlenk glassware used on a vacuum line under a nitrogen atmosphere, another explanation of this failure could be the harsh work-up procedure that involves neutralising the acidic reaction mixture with a solution of sodium hydroxide and refluxing the mixture for a few minutes. It is possible that hydrolysis could have occurred at that stage and that the starting material is regenerated during this

work-up. As aromatic amines are known to react with phosphorus pentachloride[80], the conditions could in theory generate the *N*-pyrimidinyl diphosphorimidic trichloride **2a** in anhydrous conditions then the *N*-pyrimidinyl diphosphoramidic dichloride **2b** following hydrolysis, it is thus believed that this work-up is necessary to regenerate the diamino functionalities of pyrimidine **3** (see Scheme 2.2). None of the intermediates **2a** and **2b** have been isolated and characterised. Nevertheless, when the basic mixture was not refluxed, the desired dichloropyrimidine **3** was only obtained in 2-16% yield as a colourless solid. The identity of the product was confirmed by MS and IR spectroscopy: the EI mass spectrum displays only the molecular ion at m/z = 179 for $[M]^+$.

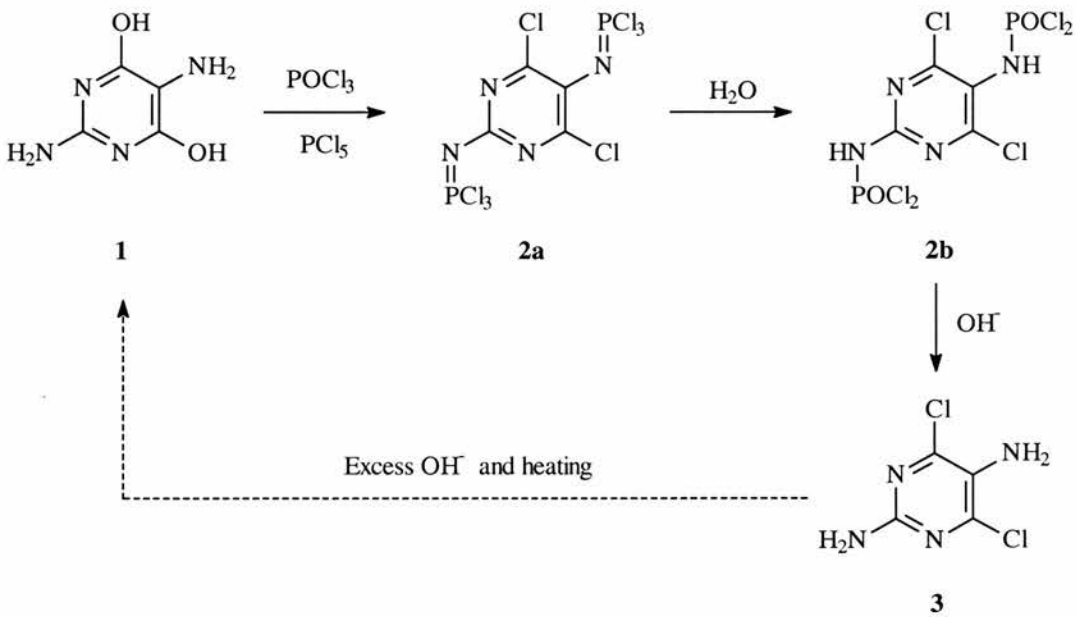

Scheme 2.2 Hypothetical side-reactions occurring during the work-up of the chlorination of **1**

The next step involved the displacement of one chloride of compound **3** by isopropylamine in refluxing *n*-butanol with triethylamine. Although the paper indicated that the reaction was complete in 3 days, it took more than 10 days at ambient pressure to notice any changes by TLC. The product was isolated in only 30% yield using the reported conditions. No improvement over several attempts was achieved. Thus, there was a clear need to design an improved synthesis for 6-chloro-2-iodo-9-isopropylpurine **6**.

2.2.2 Synthesis and hydrolysis of 6-chloro-2-iodopurine nucleosides

The chemistry of purine nucleosides has been extensively studied over the last 40 years because of the central importance of these compounds in biological systems[75,81] and of their implication in various diseases[82-85] and numerous methodologies are available towards the synthesis of 2,6-dihalogenopurine nucleosides[86-89]. Our chosen synthetic strategy relied on the preparation of 6-chloro-2-iodopurine from guanosine, using a *tris*-acetylated ribosyl as the protecting group for the 9-position during the functionalisation of the 2- and 6-positions of the purine, as seen on scheme 2.3. It was anticipated that cleavage of the sugar moiety[90] of the 6-chloro-2-iodopurine nucleoside **10** would occur in mild aqueous acidic conditions to generate the desired dihalogenopurine **11**.

The three hydroxyls of guanosine were protected as their acetyl esters with acetyl chloride in refluxing DMF in the presence of pyridine[86] in 92% yield and analytically pure *tris*-*O*-acetyl guanosine **4** was obtained as colourless needles

suitable for XRD studies following several recrystallisations of the crude product from methanol. The ^{13}C NMR spectrum clearly shows 3 resonances at δ 169.6, δ 169.8 and δ 170.4 ppm, consistent for the three acetyl C=O groups as well as three methyl resonances at δ 20.5, δ 20.7 and δ 20.8 ppm. The ESI^+ mass spectrum displays the parent ion $[M+1]^+$ at *m/z* 410 while the IR showed a very strong C=O at 1748 cm^{-1} characteristic of saturated esters[91] (1750-1735 cm^{-1}) in the IR spectrum. The solid state structure shown in Figure 2.1 confirmed the identity of the desired product. It can be noted that the ribofuranosyl has adopted the *anti*-glycosidic conformation[92] due to the absence of a substituent *ortho* to the glycosyl bond (see figure 2.2 page 7) and that the pyrimidinol tautomer[93] is preferred in the solid state.

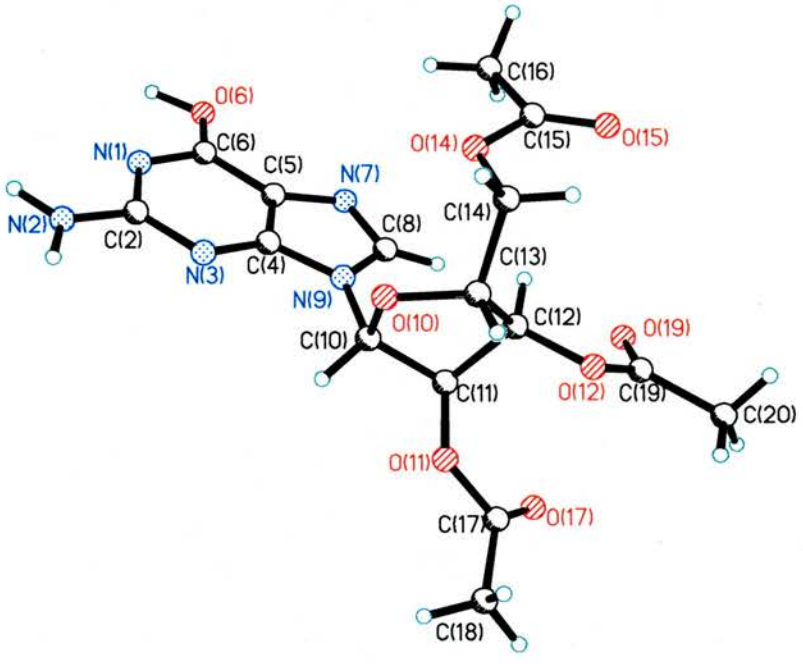

Figure 2.1 Crystal structure of *tris-O*-acetylated nucleoside **8**

	8
Bond length	
N(1)-C(6)	1.365(12)
N(1)-C(2)	1.404(9)
N(7)-C(8)	1.302(10)
N(9)-C(10)	1.480(9)
C(11)-O(11)	1.438(8)
C(17)-O(17)	1.152(12)
C(15)-O(15)	1.196(14)
Bond angle	
C(6)-N(1)-C(2)	124.7(8)
N(9)-C(4)-C(5)	105.3(9)
N(7)-C(5)-C(4)	110.9(8)
C(4)-N(9)-C(8)	106.2(7)
C(10)-O(10)-C(13)	109.3(8)
O(12)-C(12)-C(11)	114.4(6)
O(17)-C(17)-C(18)	129.7(11)

Table 2.1 Selected bond lengths (Å) and angles (º) for nucleoside **8**

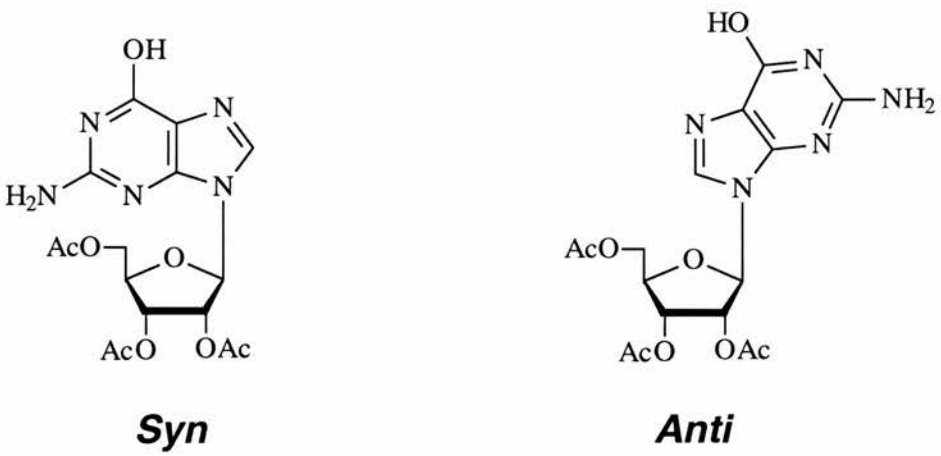

Syn ***Anti***

Figure 2.2 Possible *Syn* and *Anti*-glycosidic conformations for *tris-O*-acetylated nucleoside **8**

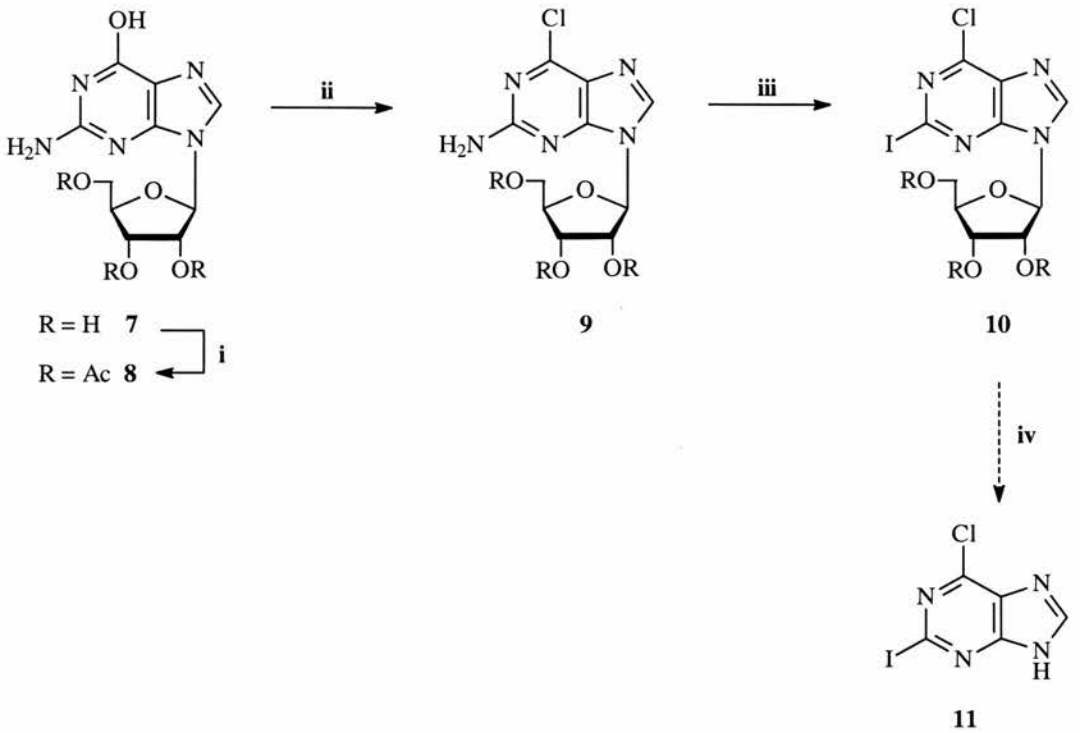

Conditions: i) Ac_2O, pyridine, DMF, Δ, 92% ii) $POCl_3$, DMA, TEBAC, MeCN, Δ, 72%
iii) $CH_3CH(CH_3)CH_2CH_2ONO$, CuI, I_2, CH_2I_2, THF, Δ, 80%
iv) $HCl_{(aq)}$, dioxane, Δ, 25%

Scheme 2.3 Synthesis of 6-chloro-2-iodopurine **11** from guanosine **7**

Chlorination at the 6-position was successfully implemented using the strictly anhydrous conditions described by Morris and Uznanski[86], using the common chlorinating agent $POCl_3$ in the presence of a base, DMA, and a chloride donor, triethylbenzylammonium chloride, TEBAC. The reaction was complete within 30 minutes of reflux under a nitrogen atmosphere at 120°C, and the solvent and excess phosphorus chloride were flash evaporated on the vacuum line. The resulting dark oil was partitioned between water and DCM prior to flash chromatography on silica gel using 2-4% MeOH in DCM to retrieve crystalline

6-chloroguanosine **9**. Crystals suitable for X-ray crystallography were obtained by layering a deuterated chloroform solution of **9** with hexane and the following crystal structure displays a *syn*-glycosidic conformation unlike its precursor **8** in Figure 2.3 while selected bond lengths and angles are displayed below in Table 2.2.

	9
Bond length	
N(1)-C(6)	1.305(4)
N(1)-C(2)	1.369(3)
N(7)-C(8)	1.304(3)
N(9)-C(10)	1.446(3)
C(11)-O(11)	1.427(3)
C(15)-O(15)	1.206(3)
C(17)-O(17)	1.200(3)
Bond angle	
C(6)-N(1)-C(2)	117.2(2)
N(9)-C(4)-C(5)	104.9(2)
N(7)-C(5)-C(4)	111.2(2)
C(4)-N(9)-C(8)	106.1(2)
C(10)-O(10)-C(13)	109.11(17)
O(12)-C(12)-C(11)	108.15(19)
O(17)-C(17)-C(18)	126.0(2)

Table 2.2 Selected bond lengths (Å) and angles (º) for nucleoside **9**

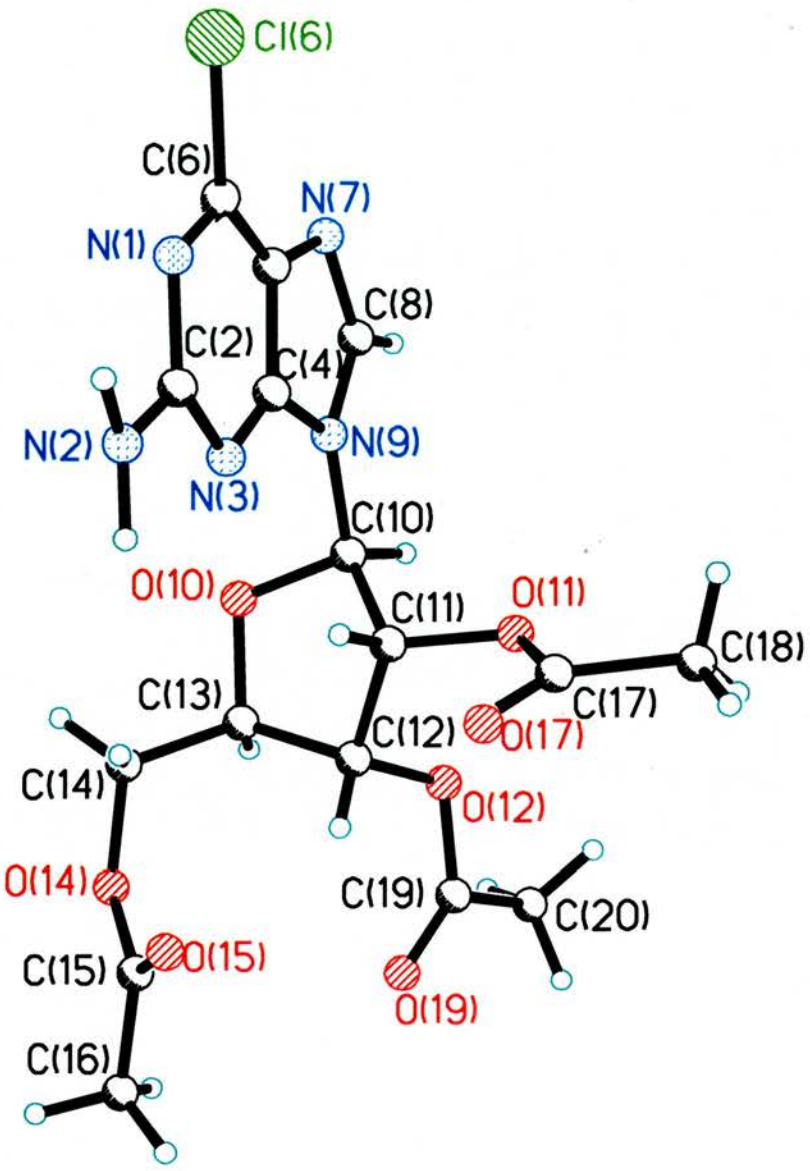

Figure 2.3 Crystal structure of *tris-O*-acetylated 6-chloroguanosine **9**

The diazotisation/iodine substitution enabled us to convert the 2-amino moiety of nucleoside **9** into a 2-iodide in good yield using the conditions

described previously by Matsuda *et al.*[94] This reaction is thought to occur from a purin-2-yl radical[95,96] arising from the thermal decomposition of the diazonium salt formed when the 2-amino of nucleoside **9** reacts with isoamyl nitrite. This radical then generates the 2-iodo product **10** by abstracting an iodine atom from the halogen source, diiodomethane. No side-reaction with THF occurred as the hypothetical 2-hydro analogue of **10** was neither noticed on TLC nor isolated by chromatography although it was mentioned by Matsuda. Crystals suitable for XRD studies were obtained by layering a deuterated chloroform solution of **10** with hexane and the crystal structure displayed a *anti*-glycosidic conformation unlike the nucleoside precursor 9, possibly due to the introduction of the bulky 2-iodide.

	10
Bond length	
N(1)-C(6)	1.305(4)
N(1)-C(2)	1.369(3)
N(7)-C(8)	1.304(3)
N(9)-C(10)	1.446(3)
C(11)-O(11)	1.427(3)
C(17)-O(17)	1.200(3)
Bond angle	
C(6)-N(1)-C(2)	117.2(2)
N(9)-C(4)-C(5)	104.9(2)
N(7)-C(5)-C(4)	111.2(2)
C(4)-N(9)-C(8)	106.1(2)
C(10)-O(10)-C(13)	109.11(17)
O(12)-C(12)-C(11)	108.15(19)
O(17)-C(17)-C(18)	126.0(2)

Table 2.3 Selected bond lengths (Å) and angles (º) for nucleoside **10**

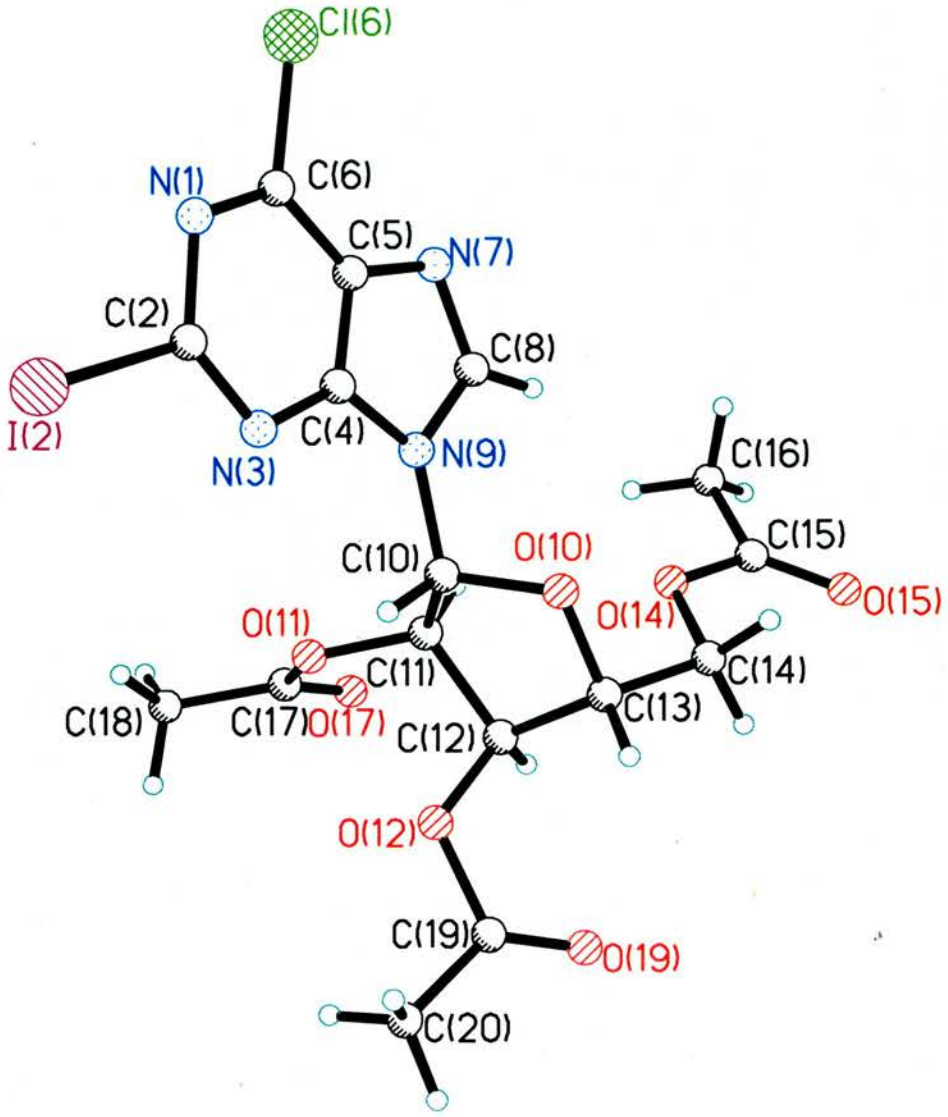

Figure 2.4 Crystal structure of 6-chloro-2-iodo purine nucleoside **10**

Hydrolysis under acidic conditions of the 6-chloro-2-iodopurine nucleoside **9** was more problematic than anticipated[90]. The very first attempts involved refluxing the nucleoside in aqueous 2M hydrochloric or sulphuric acid and were both unsuccessful. Although no starting material was left after 24 hours at reflux, no product was present in the reaction mixture after careful adjustment to pH 10 with concentrated ammonia. The resulting mixture was composed of highly polar compounds as there was a single spot on the TLC baseline following elution with 20% MeOH in DCM.

We believed that decomposition had occurred due to the strong acidic conditions as 6-chloropurines can be prone to decomposition in acidic conditions[97]. We speculate that cleavage of the ribofuranosyl occurred followed by decomposition of the generated 6-chloro-2-iodopurine product in these conditions. It was thus attempted to use milder conditions for this step and a good compromise was obtained with 0.2M HCl in water/dioxane at 80°C for 7 hours. TLC indicated that the reaction was not complete but that a more polar product was present (R_f = 0.43 for the starting material, R_f = 0.12 for the purine product **11** with EtOAc/hexane 1:1). Chromatography on silica gel with EtOAc/hexane 1:1 to 2:1 yielded the desired product in only 25% yield, while 30% of the starting material was retrieved. Longer reactions times (12-24 hours) at the same temperature resulted in more decomposition of the desired product, while the starting material appeared untouched (by TLC) at room temperature over 5 days.

This new and simple synthetic sequence allowed us to prepare a required dihalogenopurine, 6-chloro-2-iodopurine **11**, in 13% over 4 steps from the commercially available guanosine hydrate. According to kinetic studies on the hydrolysis of various purine nucleosides[97], 6-aminopurine nucleosides are less prone to decomposition with respect to their 6-chloropurine analogues. Therefore, reaction of nucleoside **10** with anilines then acidic cleavage of the ribose moiety might represent a solution to the decomposition issue and a new strategy to generate 6-amino-2-halogenopurines. Unfortunately, this hypothesis has not been verified due to the following results in the next section.

2.2.3 Synthesis of 6-chloro-2-iodopurine from hypoxanthine

When hypoxanthine **12** was treated with excess phosphorus oxychloride in the presence of DMA at 120°C for 2 hours under a nitrogen atmosphere[98], 6-chloropurine **13** was isolated as monohydrated crystals in 86% yield, after two recrystallisations of the crude solid from boiling water (see Scheme 2.4). The crystal structure shown below was obtained. It displays intermolecular hydrogen bonds from the nitrogen atom N(7A) to the N(19) hydrogen of an adjacent molecule with a distance of 1.953(7) Å. The recrystallisation solvent also favoured the formation of two further H-bond interactions, between the hydrogens of water H(10A) and H(10B) and the nitrogen atoms of two purines (N11A) and N(3) at distances of 1.993(10) Å and 1.915(8) Å respectively.

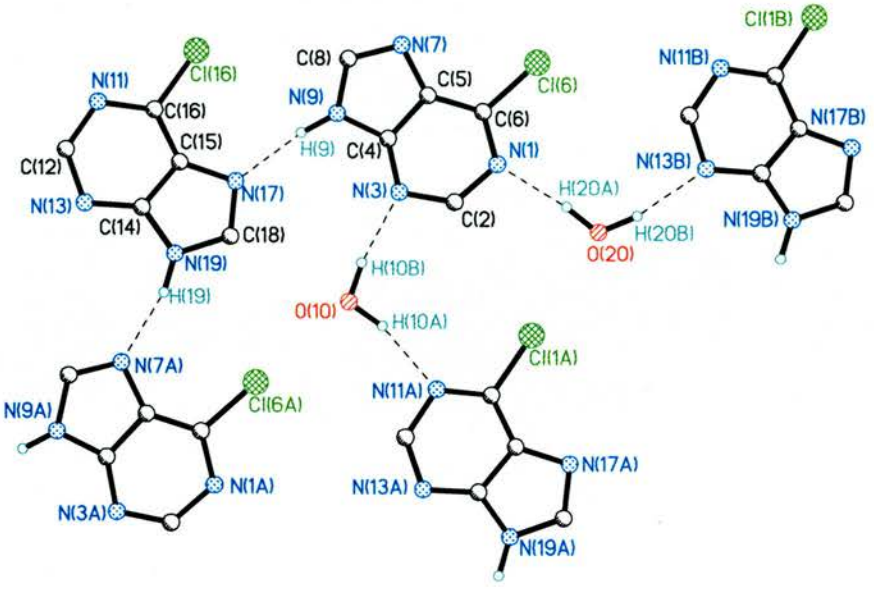

Figure 2.5 Crystal structure of 6-chloropurine **13**

	13
Bond length	
N(1)-C(2)	1.349(4)
C(4)-N(9)	1.370(4)
C(5)-C(6)	1.374(4)
C(6)-Cl(6)	1.727(3)
N(7)-C(8)	1.310(4)
C(8)-N(9)	1.368(4)
Bond angle	
C(6)-N(1)-C(2)	116.6(2)
N(3)-C(4)-N(9)	128.7(3)
N(9)-C(4)-C(5)	105.6(2)
N(1)-C(6)-Cl(6)	117.4(2)
C(8)-N(9)-C(4)	105.8(2)

Table 2.4 Selected bond lengths (Å) and angles (º) for purine **13**

The purine *N*-9 was protected as the tetrahydropyran-2-yl (THP) derivative **14** by reacting **13** with the carbocation formed *in situ* from 2,3-dihydropyran and catalytic amounts of *p*-toluenesulfonic acid in refluxing THF. The regioselectivity of this reaction had been extensively investigated in previous reported work by UV-VIS spectroscopy[99] and similar studies have also shown that reactions of 6-chloropurine with carbocations are selective for *N*-9[100]. We found from NMR and X-Ray diffraction studies of crystals of **14** that the *N*-7 isomer was not present in the recrystallised product. It must be noticed that the THP carbon C1' is stereogenic thus purine **14** was obtained as a mixture of enantiomers. Further Pendant and ^{1}H-^{13}C HMBC (Heteronuclear Multiple Bond Connectivity) experiments enabled the complete regiochemical assignment of the 9-THP product **14**. According to the structure of **14** shown below, the purine carbon atoms are all bound to two electronegative atoms, apart from C-5, thus the highest field ^{13}C resonance in the aromatic region (δ 131.3) was assigned to C-5. In theory, $^{3}J(^{1}H$-$^{13}C)$ long-range couplings would be observed between H-8 and the purine carbons C-5 and C-4, even possibly with the THP carbon C-1'. Indeed, such couplings were seen by HMBC NMR between a purine proton (δ 8.79), C-5 (δ 131.3) and another aromatic carbon, which is assignable to the purine C-4 (δ 151.6). More crucially, the regiospecificity of the N-9 protection was definitely confirmed as $^{3}J(^{1}H$-$^{13}C)$ couplings were observed between the lowest field aliphatic

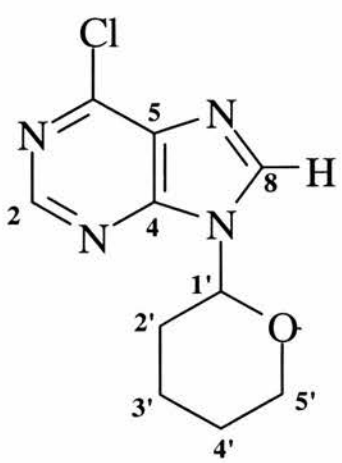

14

THP proton H-1' (δ 5.76) and the purine carbons C-8 (δ 145.1) and C-4 (δ 151.6). The crystal structure of purine **13** shown below displays an *anti*-glycosidic conformation as for the nucleosides **8** and **10**, while the tetrahydropyranyl ring is as expected in the *chair* form. The THP ring is slightly twisted as the interplanar angle between the purine and the tetrahydropyranyl ring was found to be 13.4° with respect to the purine ring.

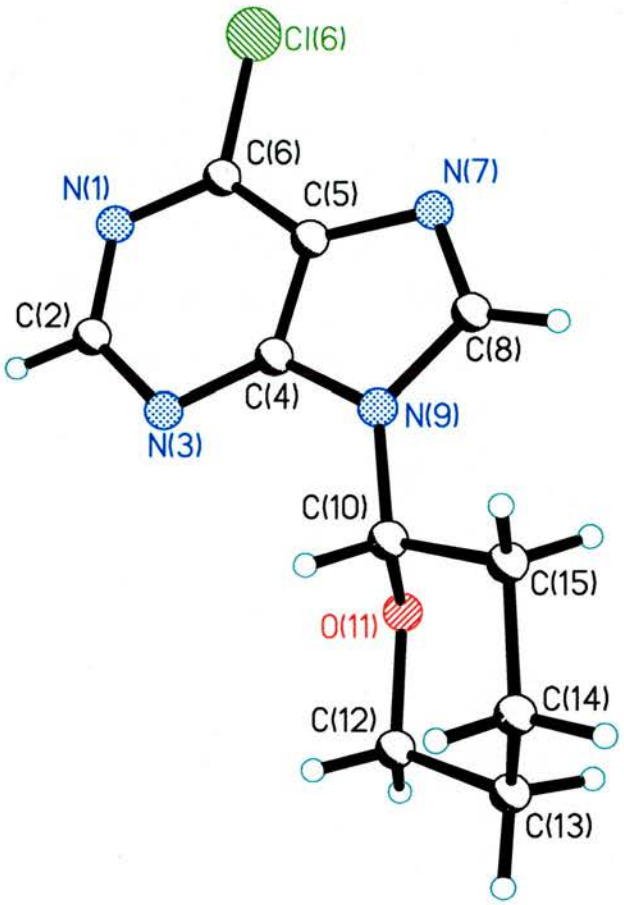

Figure 2.6 Crystal structure of 9-THP protected purine **14**

	14
Bond length	
N(1)-C(2)	1.349(4)
C(4)-N(9)	1.370(4)
C(5)-C(6)	1.374(4)
C(6)-Cl(6)	1.727(3)
N(7)-C(8)	1.310(4)
C(8)-N(9)	1.368(4)
Bond angle	
C(6)-N(1)-C(2)	116.6(2)
N(3)-C(4)-N(9)	128.7(3)
N(9)-C(4)-C(5)	105.6(2)
N(1)-C(6)-Cl(6)	117.4(2)
C(8)-N(9)-C(4)	105.8(2)

Table 2.5 Selected bond lengths (Å) and angles (º) for purine **14**

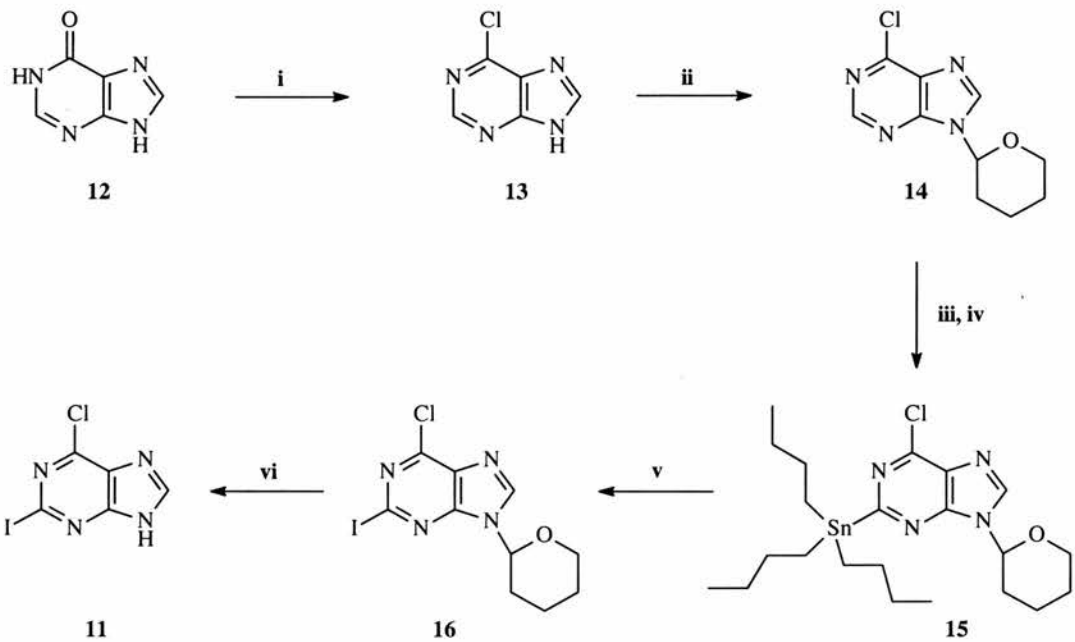

Conditions: i) $POCl_3$, DMA, Δ, 86% ii) TsOH, 2,3-dihydropyran, THF, Δ, 68%
iii) LiTMP, THF, −78°C iv) Bu_3SnCl, THF, −78°C, 95+% (over two steps)
v) I_2, THF, 95% vi) $CuCl_2$, $EtOH_{(aq)}$, 98%

Scheme 2.4 Synthesis of 6-chloro-2-iodopurine **11** from hypoxanthine **12**

Due to the presence of two acidic protons, H-2 and H-8, treating the 9-THP purine **14** with a strong deprotonating base could produce complex mixtures of mono and dilithiated species. However, according to the work of Tanaka et *al.*[101-102], then of the Legraverend group[76], a regioselective 2-lithiation of 6-chloropurine derivatives is achievable at low temperature in THF with 5 equivalents of Harpoon's base (lithium 2,2,6,6-tetramethylpiperidide). Quenching the lithiated species with 5 equivalents of tributyltin chloride affords, after chromatography on silica gel, the 2-stannylated product exclusively in very high yields (95-100%). Using these conditions, we managed to prepare quantitatively the 2-stannylated purine **15**.

Full characterisation by NMR, IR, low and high resolution MS and elemental analysis was obtained after purification of the crude oil by flash chromatography on silica gel with hexane/ethyl acetate (4:1). ^{1}H NMR showed only one purine proton (δ 8.15), assignable to either H-8 or H-2, as a result of a 2- or 8-substitution respectively. The ^{1}J, ^{2}J, and $^{3}J(^{13}C\text{-}^{119}Sn)$ couplings between the tin atom and the corresponding *n*-butyl aliphatic carbons were observed in ^{13}C NMR. As for its precursor **14**, $^{1}H\text{-}^{13}C$ correlation by long-range coupling enabled us to verify the regioselectivity of this lithiation-quenching strategy and full assignment of the 2-tributylstannylated purine **15** was thus possible. As previously, $^{3}J(^{1}H\text{-}^{13}C)$ correlations were detected between H-8 (δ 8.15) and the purine carbons C-5 (δ 129.2) and C-4 (δ 149.1). Furthermore, another couple of

^{1}H-^{13}C correlations of the THP proton H-1' (δ 5.71), the lowest field aliphatic proton resonance due to the electronegative atoms N-9 and the THP oxygen, was seen with C-8 (δ 140.6) and C-4 (δ 149.1). The result confirmed the regioselectivity of this reaction for the 2-position.

While often highly toxic, organotin compounds such as the purine derivative **15** undergo a range of useful substitution reactions with various electrophiles under mild conditions. Access to 2-halogenopurines (iodo, bromo, chloro[101,102] and even fluoro[103]) is possible. The Stille reaction enables C-C bond formation to synthesise the 2-benzyl, -phenyl, -alkenyl, and –alkynyl analogues of **15**[101,102].

Reacting **15** with excess iodine at room temperature in THF afforded the 2-iodopurine **16** in 95% yield, after trituration in *n*-hexane to separate the product from the very soluble purine **15** and the tributyltin iodide by-product. Flash chromatography on silica gel with ethyl acetate/*n*-hexane (1:1) was used when the product required further purification. The HMBC studies showed the same $^{3}J(^{1}H$-$^{13}C)$ correlations that were observed for the precursors **14** and **15.** Crystallographic studies by X-Ray Diffraction (XRD) of a single crystal of the 2-iodopurine **16** revealed the structure in Figure 2.7 and confirmed the HMBC correlations regarding the regioselectivity of this reaction. Table 2.6 shows selected bond lengths and angles.

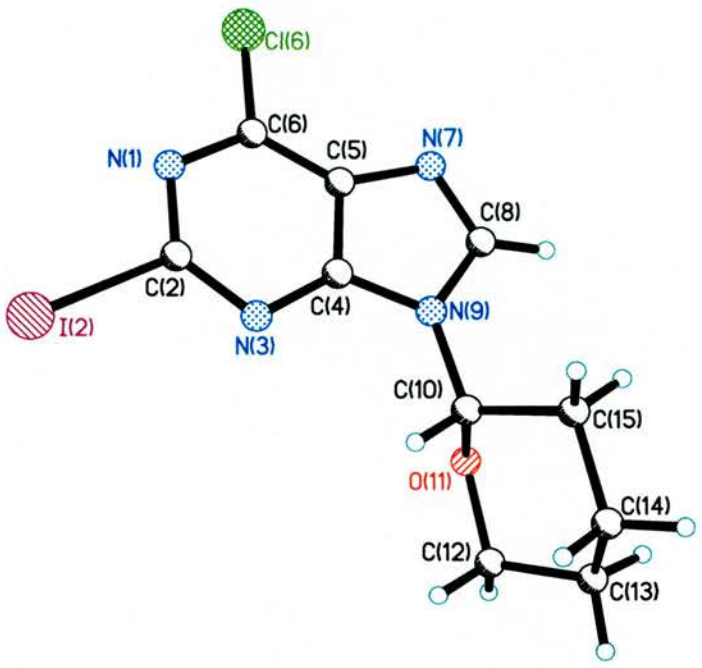

Figure 2.7 Crystal structure of 9-THP protected purine **16**

	16
Bond length	
N(3)-C(4)	1.345(5)
C(2)-I(2)	2.108(4)
C(6)-Cl(6)	1.730(4)
N(9)-C(10)	1.454(6)
C(8)-N(7)	1.299(6)
C(14)-C(15)	1.526(6)
Bond angle	
N(3)-C(2)-I(2)	115.2(3)
C(6)-C(5)-N(7)	135.5(4)
C(4)-N(9)- C(8)	105.3(2)
O(11)-C(10)-N(9)	106.1(3)
N(9)-C(10)-C(15)	113.0(4)

Table 2.6 Selected bond lengths (Å) and angles (º) for purine **16**

Hydrolysis in acidic conditions has been used predominantly to cleave a tetrahydropyran-2-yl group from a protected amine, while neutralisation of the aqueous solution with ammonia or sodium hydroxide afforded the free base[103]. Preliminary attempts with 2.5M aqueous hydrochloric acid then water/trifluoroacetic acid (1:1), followed by neutralisation by dropwise addition of concentrated ammonia to precipitate the free base of purine **11** proved to be unsatisfactory: TLC indicated that no starting material was left but very little product seemed present in the reaction mixture after adjustment to pH 12.

Refluxing the 9-THP purine **10** with 10 mol% of copper(II) chloride in ethanol/water (95:5)[105] was however a highly efficient deprotection (98% yield). The isolation of analytically pure 6-chloro-2-iodopurine **11** product was achieved by flash column chromatography on silica gel using ethyl acetate/*n*-hexane (1:1). Single crystal structure determination confirmed the identity of **11**. It appears that the recrystallisation solvent favoured the π-stacking of the heterocyclic rings as several hydrogen-bonds are found between the I(2), Cl(6) and N(7) atoms of the purine and the hydrogen atoms of water. Finally, a fourth type of hydrogen-bond within the structure was observed between the N(9)-hydrogen of the purine and the oxygen atom of water. The hydrogen bond distances range from 1.90(2) Å between H(9A) and O(10) to 2.99(7) Å between H(10B) and I(2C).

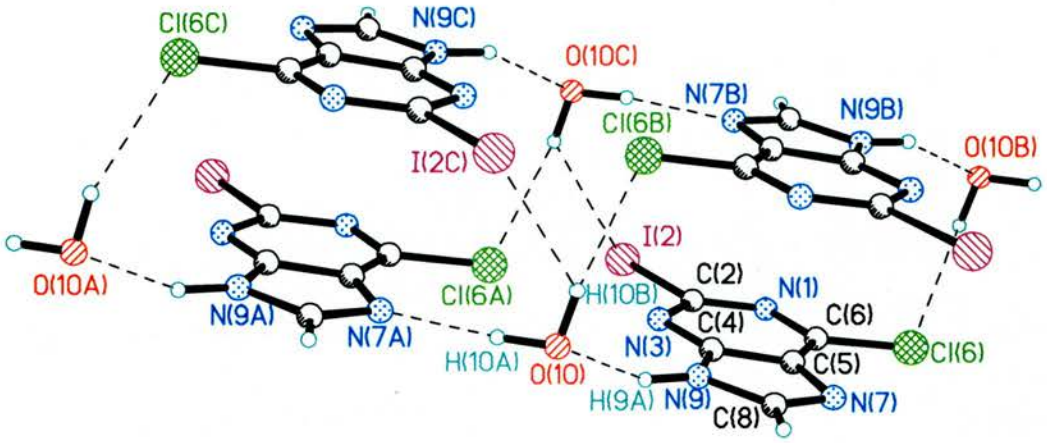

Figure 2.8 Crystal structure of dihalogenopurine **11**

(H-bonds displayed as black-dotted lines)

	11
Bond length	
N(1)-C(2)	1.348(6)
N(3)-C(4)	1.344(6)
C(4)-C(5)	1.396(7)
C(5)-N(7)	1.394(6)
C(6)-Cl(6)	1.718(5)
C(8)-N(9)	1.370(7)
Bond angle	
N(3)-C(2)-N(1)	128.2(4)
C(6)-C(5)-N(7)	134.0(4)
C(4)-N(9)- C(8)	105.7(4)
N(7)-C(8)-N(9)	114.6(4)
N(1)-C(6)-Cl(6)	117.9(3)

Table 2.7 Selected bond lengths (Å) and angles (º) for purine **11**

2.2.4 Reactivity of 6-chloro-2-iodopurine 11

Introduction of an aliphatic group at the *N*-9 position of 6-chloropurines can be accomplished by nucleophilic displacement of alkyl bromides or iodides in the presence of a base[23], generally cesium or potassium carbonate. Alternatively, it was reported that alkylations with primary and secondary alcohols under Mitsunobu conditions[106] are successful with purines bearing a chloride in the 6-position. However, as purines are known to exist in approximately equal proportions as their 7*H*- and 9*H*-tautomers in solution, while the 1*H*- and 3*H*-forms are negligible[75], both nucleophilic substitutions of alkyl halides[75] and the Mitsunobu reaction[107] can produce mixtures of 7- and 9-monoalkylated purines as shown on scheme 2.5 below.

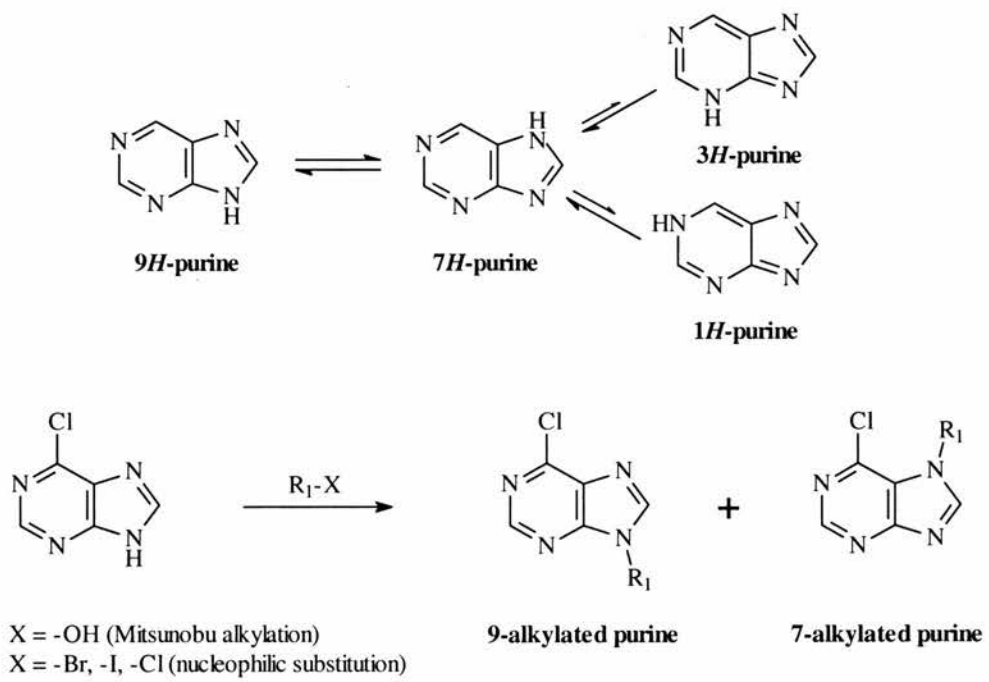

Scheme 2.5 Purine tautomerism and *N*-alkylation regioselectivity

Schultz *et al* reported that the Mitsunobu reaction could lead to the exclusive formation of *N*-9 alkylated 6-chloropurines at lower temperatures[24], while the proportion of the *N*-7 isomer increases significantly when the alkylation is carried out at room temperature[107]. A Mitsunobu alkylation of 6-chloro-2-iodopurine **11** was attempted at -15°C with isopropanol and the commonly used triphenylphosphine/diethyl azodicarboxylate system in anhydrous THF. According to TLC, the reaction was close to completion but purification by chromatography on silica gel with ethyl acetate/ hexane 1:1 afforded a 1:1 mixture of the desired 9-isopropylpurine **17** and of the hydrazine by-product **18** (ratio determined by comparison of the integrals on the ^{1}H NMR spectrum) in 20% yield as shown below:

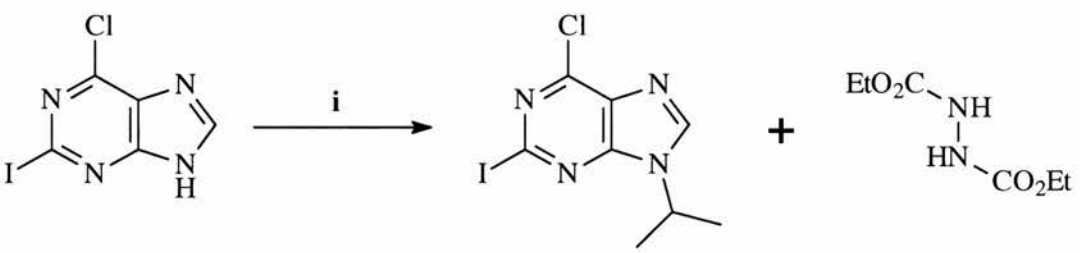

11 **17** **18**

Conditions: i) Ph_3P, *i*-PrOH, THF, -15°C then DEAD, 2 days, 20%

Scheme 2.6 Mitsunobu reaction of purine **11** with isopropanol

Further attempts to separate the desired purine **17** and the hydrazine side-product **18** by recrystallisation or Soxhlet extraction with hexane were unsuccessful and analytically pure 6-chloro-2-iodo-9-isopropylpurine **17** could not be obtained at this stage.

It was decided to introduce the 9-isopropylpurine at a later stage. As the introduction of anilines at the 6-position of the purine **11** would surely induce a significant leap in polarity and thus in the retention factors R_f, it was anticipated that the separation of the 6-anilino-9-isopropylpurine analogues of **11** and the hydrazine side-product of the Mitsunobu reaction would be easier. A first attempt to displace the 6-chloride of **11** with *m*-chloroaniline was totally unsuccessful in refluxing ethanol in the presence of 4 equivalents of triethylamine, *i.e.* the conditions described by Legraverend *et al*[61].

No improvement was obtained when increasing the reaction temperature (120°C in n-butanol, 150°C in DMF) or the amounts of *m*-chloroaniline: TLC showed only unreacted starting material **11** and *m*-chloroaniline. It was disappointing that the reaction did not proceed at all even in a sealed glass tube at 140°C, thus we found that purine **11** was unreactive with this aniline under those commonly used conditions. No reaction was observed with aniline or even the more nucleophilic benzylamine. These results had not been expected as the nucleophilic substitution of 6-chloropurines by anilines or benzylamine

derivatives have been used extensively by several research groups involved with the synthesis of 2,6-diaminopurine CDK inhibitors[60,61].

More recently, the use of the benzylsulfonyl leaving group has been described by Legraverend as a potential replacement for the 6-chloride of dihalogenopurines[76-78]. They found that nucleophilic substitution of this group occurs at room temperature with aliphatic amines and at 80°C with aromatic amines like anilines in ethanol. As shown on scheme 2.7, the direct precursor, 6-benzylsulfanyl-2-iodopurine **19,** was easily accessible in 96% yield by adding the sodium salt of benzyl mercaptan, formed *in situ* by treating the thiol with sodium hydride in DMF, to purine **11** at room temperature. Evaporation to dryness and partition of the crude residue between DCM and dilute brine then water afforded the crude 6-benzylsulfanylpurine **19** in almost quantitative yield and good purity. An analytically pure sample was obtained by flash column chromatography on silica gel using ethyl acetate/petroleum ether 40-60° 3:2 as eluant.

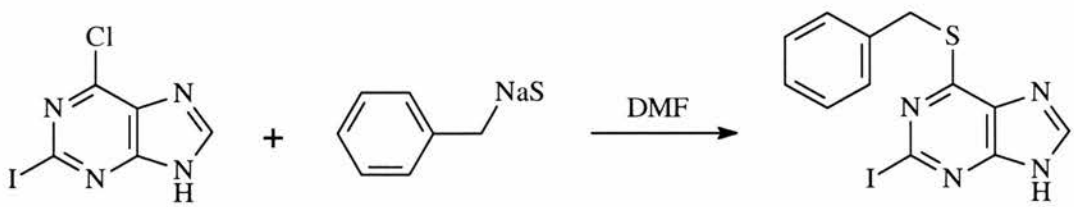

11 **19**

Scheme 2.7 Synthesis of 6-benzylsulfanylpurine **19**

We successfully conducted a Mitsunobu reaction with a recently developed system, DIAD-Ph_3P (diisopropyl azodicarboxylate-triphenylphosphine), at -50°C under a nitrogen atmosphere[108-110]. Previously, the azodicarboxylate reagent had been added last to a cooled solution of the purine, the phosphine and the isopropanol in THF. However much better results were obtained this time when the alcohol was added last. It is known that DIAD reacts instantly at low temperatures with triphenylphosphine as a precipitate formed upon addition of the reagent to a solution of the purine and the phosphine in THF at -50°C. TLC indicated that no starting material was left in the solution following gradual warming to room temperature and stirring under nitrogen for 2 days. More importantly, the *N*-9-isopropylpurine **20** was not contaminated with the hydrazine side-product as previously and was pure after flash column chromatography with ethyl acetate/petroleum ether 40-60° 1:2. The results from elemental analysis and IR spectroscopy agreed with the proposed formula and chemical functionalities respectively as a strong $\nu_{C\text{-}I}$ was seen at 558cm^{-1} while more aliphatic $\nu_{C\text{-}H}$ were observed in the characteristic 3000-2800cm^{-1} region. The EI mass spectrum displays the molecular ion $[M]^+$ at *m/z* 410.0052.

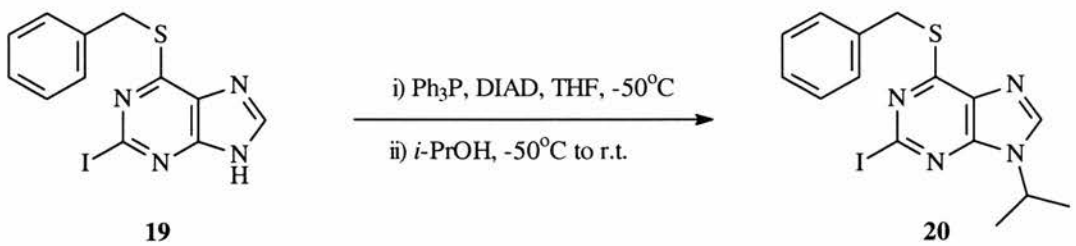

19 **20**

Scheme 2.8 Regioselective Mitsunobu alkylation on purine **19**

This highly efficient reaction (81 % yield) was found to be regioselective by NMR spectroscopy. First of all, in the ^{1}H experiment, only one set of isopropyl signals (doublet at δ 1.49 and septet at δ 4.71ppm) could be detected. Secondly, HMBC studies confirmed this observation as $^{3}J(^{1}H\text{-}^{13}C)$ correlations were observed between the purine proton H8 (δ 8.19) and the purine carbons C5 (δ 132.1) and C4 (δ 150.5) and with the tertiary isopropyl carbon (δ 49.9). Similarly, another set of couplings were found between the tertiary isopropyl hydrogen (δ 4.71) and the purine carbons C4 (δ 150.5) and C8 (δ 143.7). Crystals suitable for crystallography were obtained from deuterated methanol and the corresponding crystal structure shown in Figure 2.9 confirmed the results from the HMBC experiment.

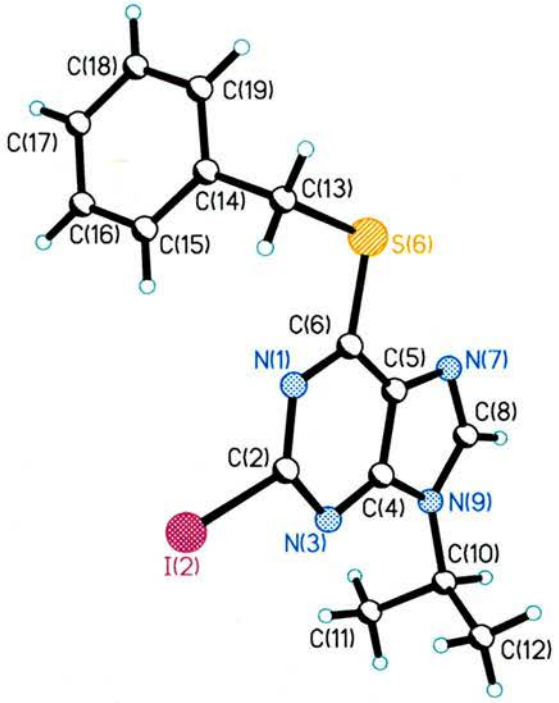

Figure 2.9 Crystal structure of 9-isopropylpurine **20**

	20
Bond length	
N(1)-C(2)	1.341(3)
C(2)-I(2)	2.110(2)
C(4)-N(9)	1.376(3)
C(4)-C(5)	1.401(3)
C(6)-S(6)	1.754(2)
S(6)-C(13)	1.825(2)
N(9)-C(10)	1.481(3)
C(10)-C(12)	1.507(4)
Bond angle	
N(3)-C(2)-N(1)	129.3(2)
N(9)-C(4)-C(5)	105.0(2)
C(6)-S(6)-C(13)	102.29(11)
C(8)-N(9)-C(10)	125.4(2)
C(4)-N(9)- C(10)	128.9(2)
C(14)-C(13)-S(6)	110.69(17)
S(6)-C(13)-H(13A)	109.5

Table 2.8 Selected bond lengths (Å) and angles (º) for purine **20**

The oxidation of 6-benzylsulfanylpurine **20** to the sulfone **21** with 3 equivalents of *m*-chloroperbenzoic acid appeared complete after 24 hours in dichloromethane in the presence of magnesium sulphate (see Scheme 2.9 below). Filtration of the dessicant and thorough washing with dichloromethane afforded after evaporation to full dryness a crude foamy residue that contained mostly the desired sulfone **21** and the *m*-chlorobenzoic acid by-product, other impurities were not characterised. Chromatography on silica gel using EtOAc/petroleum ether 1:1 to elute first the benzoic acid then neat EtOAc to retrieve the sulfone

was successful although significant amount of material was lost during the purification. It is possible that a fraction of the product had decomposed on the acidic silica support, as benzylsulfanyl have been known to decompose in the presence of water or acid. Nevertheless, analytically pure **21** was successfully obtained in 20% yield and up to 90% when the chromatography was replaced by a simple reprecipitation of the product with hexane from a DCM solution. The CI MS spectrum only displays the parent ion $[M+1]^+$ at *m/z* 443.0043 while the IR spectrum shows two very strong S=O stretching bands at 1339 and 1211cm^{-1} which are characteristic of the sulfone functionality.

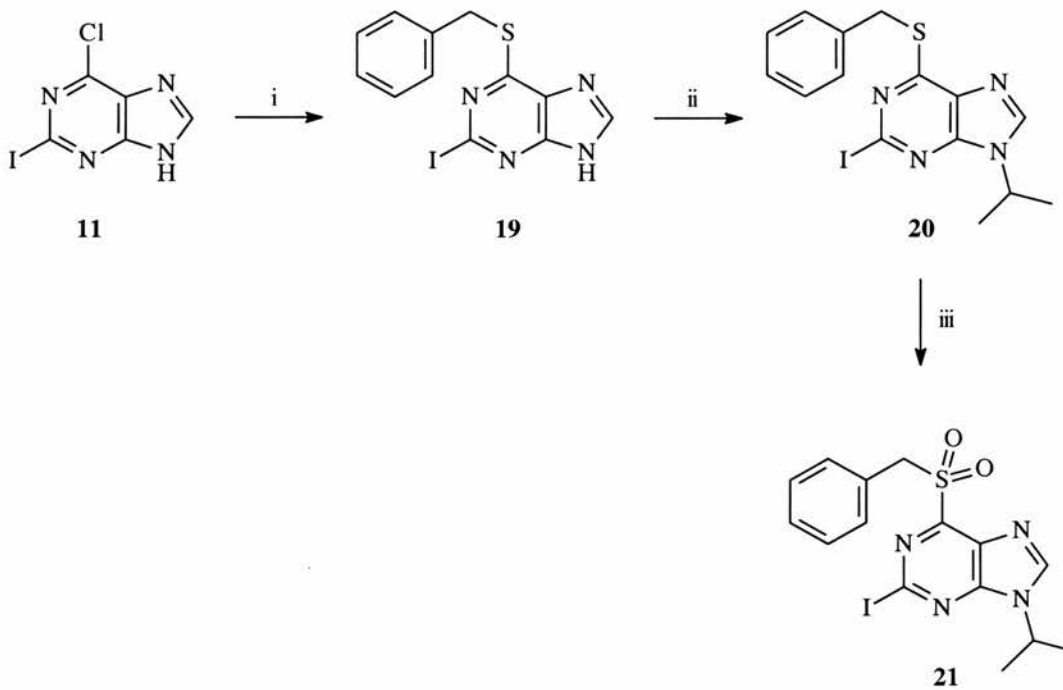

11 **19** **20** **21**

Conditions: i) $PhCH_2SNa$, DMF, 96% ii) Ph_3P, DIAD, THF, -50°C then *i*-PrOH, -50°C then room temperature, 2 days, 81% iii) $MgSO_4$, *m*-CPBA, DCM, 24 hours, 90%

Scheme 2.9 Synthesis of 6-benzylsulfonylpurine **21** from 6-chloro-2-iodopurine **11**

The reaction between sulfone **21** and 5 equivalents of *m*-chloroaniline in *n*-butanol was incomplete after 2 days at 120°C at ambient pressure as only unreacted starting material and aniline were detected on TLC. This was surprising as Legraverend *et al.* reported that purine **21** could be coupled with aliphatic and aromatic amines at room temperature and 80°C respectively[111]. However the reaction proceeded to near completion in a sealed Parr bomb at 160°C in an oven overnight, very little starting material could be detected by TLC. Evaporation to full dryness of the reaction mixture and purification by flash column chromatography on silica gel successfully afforded the 6-anilinopurine **22** as an oily foam in 32% yield (see scheme 2.10). The CI^+ MS spectrum displays only the parent ion $[M+1]^+$ at *m/z* 413.9966 while the IR spectrum shows a sharp and intense NH stretching at 3312cm^{-1} characteristic of the secondary amine.

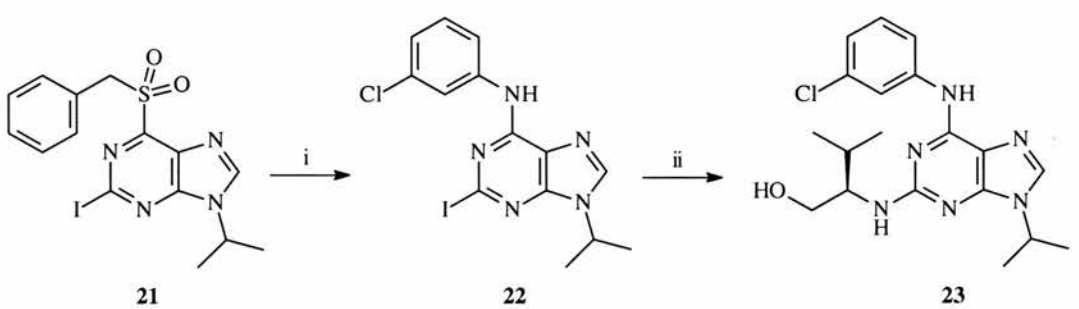

21 **22** **23**

Conditions: i) *m*-chloroaniline, *n*-butanol, 160°C in a sealed Parr bomb, 32% ii) (R)-valinol, *n*-butanol, 160°C in a sealed Parr bomb, 37%

Scheme 2.10 Synthesis of Purvalanol A **23**

Finally, the displacement of the 2-iodide of **22** by 10 equivalents of *R*-valinol occurred in *n*-butanol in the presence of Hunig's base (*N,N,N*-diisopropylethylamine) in a Parr bomb after 48 hours in an oven at 160°C and afforded Puvalanol A **23** in 37% yield following purification by flash column chromatography on silica gel using 1-5% MeOH in DCM and recrystallisation from isopropanol. The spectroscopic data were in good agreement with the literature[24].

2.3 *Conclusion*

A required dihalogenopurine, 6-chloro-2-iodopurine **11**, has been synthesised from guanosine hydrate in 13% yield and from hypoxanthine in 54% yield. Both strategies have been successfully scaled up to 50g of starting material and allow the preparation of this dihalogenopurine in multi-gram quantities. The compound and intermediates have been fully characterised by modern spectroscopic techniques and X-ray crystallography.

However, this traditional diaminopurine precursor was found completely unreactive with *m*-chloroaniline under the conditions reported by Legraverend et *al.* even under pressure in a Parr Bomb. It was reported that 6-chloropurines can fail to react with anilines and that alternative leaving groups are the benzylsulfonyl and mesylate moeities.

A more recently developed diaminopurine precursor, 6-benzylsulfonyl-2-iodo-9-isopropylpurine **21** has been synthesised from 6-chloro-2-iodopurine **11** and successfully afforded a known CDK inhibitor, Purvalanol A **23**, by reaction with *m*-chloroaniline first and *R*-valinol. It was however disappointing that very forcing conditions (160°C in a Parr Bomb) were still required to displace the 6-benzylsulfonyl and 2-iodo leaving groups as there was no sign of reaction after several days at reflux under ambient pressure. Nucleophilic displacements by amines at the 2- and 6-positions have been found to be very slow and incomplete, hence not as straightforward as reported by previous research groups. To conclude, the synthesis of a novel and more reactive diaminopurine precursor was necessary to prepare novel diaminopurines under milder conditions.

2.4 *Experimental*

2,5-Diamino-4,6-dichloropyrimidine hydrochloride **1**

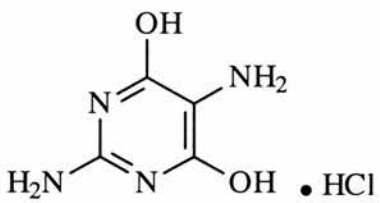

To a solution of sodium ethoxide (116.44g, 1.7mol) in ethanol (500ml) was added powdered guanidine hydrochloride (54.51g, 0.6mol) at room temperature under a nitrogen atmosphere. Stirring was continued for 1 h under nitrogen prior to dropwise addition of a solution of diethyl aminomalonate hydrochloride (100g, 0.6mol) in ethanol (500ml). After 24 h of stirring at room temperature, with a gradual colour change from pale brown to pale yellow, the mixture was refluxed for 3 hours then cooled to room temperature overnight. The solvent volume was reduced to approximately 300ml, the residue was diluted in water (1.5L), then concentrated hydrochloric acid (1L) was carefully added to precipitate a yellow solid. After filtration, the yellow solid was recrystallised from hydrochloric acid 2N/ethanol 4:1 to afford after drying on the vacuum line dihydroxypyrimidine **1** as colourless needles (34g, 34%); mp=280°C (lit.[61], mp >260°C); IR (KBr disc, cm^{-1}): 3315m, 3296m, 3271m, 2962m, 1662s, 1565m, 1490m, 1452m, 1398s, 1195m, 1007w, 762m, 675m, 657m, 610w, 548m; MS (ESI^+) *m/z* 143 $[M+H]^+$, $C_4H_6N_4O_2$ requires 142.116; Microanalytical data found: C: 27.12 H: 3.82 N: 31.45, expected for $C_4H_6N_4O_2$.HCl C: 26.89 H: 3.92 N: 31.37.

2,5-Diamino-4,6-chloropyrimidine **3**

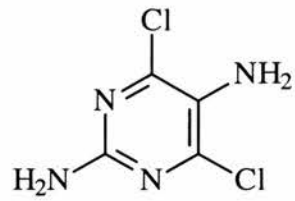

To a mixture of dihydroxypyrimidine **1** (2.00g, 11.2mmol) and triethylbenzylammonium chloride (9.27g, 4.8mmol) in anhydrous acetonitrile (45ml), stirred at room temperature under a nitrogen atmosphere, was injected phosphorus oxychloride (47ml, 560mmol), stirring under nitrogen was continued for 5 minutes prior to the addition of phosphorus pentachloride (2.12g, 11.2mmol). The reaction mixture was refluxed under nitrogen for 4 hours, then evaporated to dryness after cooling into a dark oil, on which icy water (50ml) was poured onto. The mixture was left to stir for 30 minutes (pH=1), then carefully neutralised with concentrated ammonium hydroxide (pH=9) with cooling in an ice-bath. After saturation of the solution with sodium chloride, the solution was extracted with ethyl acetate (3x100ml), the combined organic extracts were dried over anhydrous magnesium sulphate, and evaporated to dryness into a pale yellow solid. Recrystallisation from ethanol afforded dichloropyrimidine **3** as slightly tan needles (326mg, 16%); mp=190°C (lit.[61] mp=188-191°C); R_f 0.27 [DCM/MeOH 95:5]; ^{1}H NMR (270MHz, d_6-dmso) δ_H 4.71 (broad s, 2H, NH_2), 6.49 (broad s, 2H, NH_2); MS (EI) *m/z* 179 $[M]^+$, $C_4H_4Cl_2N_4$ requires 179.007; Microanalytical data found: C: 26.51 H: 2.64 N: 31.15, expected for $C_4H_4Cl_2N_4$ C: 26.84 H: 2.25 N: 31.30.

2,5-Diamino-6-chloro-4-*N*-isopropylaminopyrimidine **4**

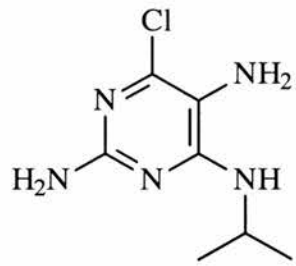

To a pale yellow mixture of dichloropyrimidine **3** (230mg, 1.3mmol) in *n*-butanol (25mL) was added triethylamine (2.5mL, 17.8mmol) and isopropylamine (0.16mL, 1.9mmol) and the resulting solution was heated at reflux under nitrogen for 10 days. Following evaporation to full dryness, the crude yellow solid was purified by column chromatography on silica gel using 5% MeOH in DMC then recrystallised from water to afford the 4-*N*-isopropylaminopyrimidine **4** as slightly tan needles (90mg, 30%); mp=190°C (lit.[61] mp=188-191°C); R_f 0.08 [DCM/MeOH 95:5] ^{1}H NMR (270MHz, d_6-dmso) δ_H 1.14 (d, $^3J_{H\text{-}H}$ = 6.45Hz, 6H, -CH(C*H*$_3$)$_2$), 3.91 (broad s, 2H, -N*H*$_2$), 4.15 (septet, $^3J_{H\text{-}H}$ = 6.43Hz, 1H, -C*H*(CH$_3$)$_2$), 5.67 (br s, 2H, -N*H*$_2$), 6.20 (d, 1H, N*H*CHMe$_2$); MS (ESI$^+$) *m/z* 202 [M+1]$^+$, $C_7H_{12}ClN_5$ requires 201.078; Microanalytical data found: C: 41.89 H: 5.70 N: 35.17, expected for $C_7H_{12}ClN_5$ C: 41.69 H: 6.00 N: 34.73.

2-Amino-6-hydroxy-9-(*tris-O*-acetyl-β,D-ribofuranosyl)purine **8**

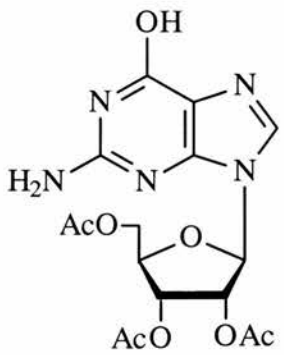

To a stirred mixture of pre-dried guanosine (15.05g, 0.05mol) in DMF (40mL) was added anhydrous pyridine (15mL) and acetic anhydride (30mL, 0.32mol) under nitrogen. The resulting mixture was heated at 75°C for 24 hours under nitrogen. The yellow solution was filtered while still hot, and concentrated into a colourless solid that was recrystallised twice from MeOH to retrieve *tris-O*-acetylguanosine **8** as colourless needles (14.72g, 92%); mp=232°C (lit.[86] mp=230-233°C); R_f 0.53 [DCM/MeOH 8:2] ^{1}H NMR (300MHz, d_6-dmso) δ_H 2.02 (s, 3H, COC*H*$_3$), 2.03 (s, 3H, COC*H*$_3$), 2.10 (s, 3H, COC*H*$_3$), 4.28 (d, $^3J_{H\text{-}H}$ = 5.94Hz, 2H, C*H*$_2$OAc), 4.35 (m, 1H, furanosyl H4'), 5.48 (dd, $^3J^1_{H\text{-}H}$ = 2.05Hz and $^3J^2_{H\text{-}H}$ = 3.84 Hz, 1H, furanosyl H3'), 5.79 (t, $^3J_{H\text{-}H}$ = 5.89Hz, 1H, furanosyl H2'), 5.98 (d, $^3J_{H\text{-}H}$ = 6.14Hz, 1H, furanosyl H1'), 6.53 (br s, 2H, N*H*$_2$), 7.93 (s, 1H, purine H8), 10.75(br s, 1H, O*H*); ^{13}C NMR (75.5MHz, d_6-dmso) δ_C 20.5 (s, COCH$_3$), 20.7 (s, COCH$_3$), 20.9 (s, COCH$_3$), 63.4 (s, -CH$_2$OAc), 70.6 (s, furanosyl C3'), 72.4 (s, furanosyl C2'), 79.9 (s, furanosyl C4'), 84.7 (s, furanosyl C1'), 117.1 (s, purine C5), 136.0 (s, purine C8), 151.5 (s, purine C6), 154.2 (s, purine C4), 157.0 (s, purine C2), 169.6 (s, COCH$_3$), 169.8 (s, COCH$_3$), 170.4 (s, COCH$_3$); MS (ESI$^+$) *m/z* 410 [M+1]$^+$, $C_{16}H_{19}N_5O_8$ requires 409.351; IR (KBr

disc, cm^{-1}): 3466m, 3310m, 3198m, 3061m, 2987m, 2852m, 2735m, 1748vs, 1701vs, 1631vs, 1608vs, 1572s, 1538vs, 1482s, 1416m, 1366s, 1220vs, 1171s, 1122s, 1092vs, 1072vs, 1018m, 958m, 911m, 891m, 858m, 834m, 811m, 784m, 748w, 709w, 694w, 678m, 638m, 614w, 589w, 576w, 543w; Microanalytical data found: C: 47.10 H: 4.75 N: 17.16, expected for $C_{16}H_{19}N_5O_8$ C: 41.69 H: 6.00 N: 34.73; Crystals suitable for X-Ray crystallography were obtained by recrystallisation from MeOH.

2-Amino-6-chloro-9-(*tris*-*O*-acetyl-β,D-ribofuranosyl)purine **9**

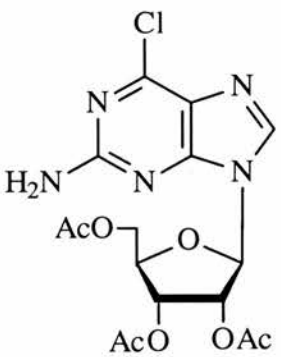

To thoroughly dried (8.4g, 20.5mmol) and TEBAC (8.32g, 36.5mmol) was added anhydrous acetonitrile (100mL) under a nitrogen atmosphere. Following cooling to 0°C, DMA (6.65mL, 36.48mmol) then phosphorus oxychloride (10.2mL, 121.5mmol) were added under nitrogen and stirring for 1 hour at room temperature then at 120°C for 15mn. The solvent and excess $POCl_3$ were removed under vacuum to recover an orangish oil that was partitioned between chloroform (100mL) and crushed ice (250g). The aqueous were further extracted with chloroform (2x100mL) and the combined organics were washed with saturated aqueous sodium bicarbonate (75mL), water (2x75mL) and dried over

magnesium sulphate. Following evaporation to dryness into a yellowish oil, purification by flash column chromatography on silica gel using 2-6% MeOH in DCM afforded the 6-chloropurine nucleoside **9** as a colourless solid (8.62g, 72%); mp=150°C (lit.[86] mp=147-153°C); R_f 0.39 [DCM/MeOH 96:4] ^{1}H NMR (300MHz, d_6-dmso) δ_H 2.02 (s, 3H, COC*H*$_3$), 2.03 (s, 3H, COC*H*$_3$), 2.08 (s, 3H, COC*H*$_3$), 4.36 (m, 1H, furanosyl H4'), 5.67 (t, $^3J_{H\text{-}H}$ = 4.86Hz, 1H, furanosyl H3'), 5.89 (t, $^3J_{H\text{-}H}$ = 5.12Hz, 1H, furanosyl H2'), 5.95 (d, $^3J_{H\text{-}H}$ = 4.86Hz, 1H, furanosyl furanosyl H1'), 7.22 (br s, 2H, -NH_2), 7.83 (s, 1H, purine H8); ^{13}C NMR (75.5MHz, d_6-dmso) δ_C 20.8 (s, CO*C*H$_3$), 20.9 (s, CO*C*H$_3$), 21.1 (s, CO*C*H$_3$), 63.3 (s, -*C*H$_2$OAc), 70.8 (s, furanosyl C3'), 73.1 (s, furanosyl C2'), 80.3 (s, furanosyl C4'), 87.0 (s, furanosyl C1'), 126.1 (s, purine C5), 141.1 (s, purine C8), 152.2 (s, purine C4), 153.5 (s, purine C2), 159.6 (s, purine C6), 169.8 (s, *C*OCH$_3$), 170.0 (s, *C*OCH$_3$), 170.9 (s, *C*OCH$_3$); MS (EI) *m/z* 427 $[M]^+$, $C_{16}H_{18}ClN_5O_7$ requires 427.796; IR (KBr disc, cm^{-1}): 3445m, 3313m, 3210m, 3123w, 2983w, 2967w, 2923w, 1765s, 1732s, 1636s, 1614s, 1558s, 1522m, 1485m, 1454m, 1410m, 1378m, 1323m, 1250s, 1215s, 1144m, 1125m, 1104m, 1047s, 997m, 983m, 939w, 907m, 854w, 840w, 805w, 784w, 740w, 730w, 693w, 596w, 572w, 550w, 531w, 513w; Microanalytical data found: C: 44.92 H: 4.24 N: 16.37, expected for $C_{16}H_{18}ClN_5O_7$ C: 44.62 H: 4.19 N: 16.01; Crystals suitable for X-Ray crystallography were obtained by crystallisation from $CDCl_3$.

6-Chloro-2-iodo-9-(*tris*-*O*-acetyl-β,D-ribofuranosyl)purine **10**

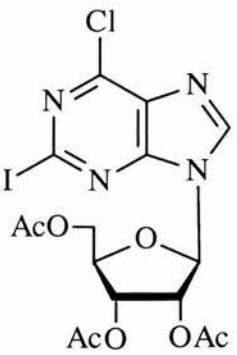

To pre-dried *tris*-*O*-acetyl-6-chloroguanosine **9** (2.88g, 6.75mmol), iodine (1.71g, 6.75mmol), and copper(I) iodide (1.35g, 7.07mmol) in anhydrous THF (35mL) was added under a nitrogen atmosphere diiodomethane (5.65mL, 6.98mmol) then isoamylnitrite (2.85mL, 20.81mmol) and the resulting deep purple mixture was heated at 105°C for 1 hour. Following cooling to room temperature, aqueous saturated sodium thiosulphate (50mL) was added and stirred for 1 hour to result in a yellow solution that was extracted with DCM (3x100mL). The combined organics were dried over magnesium sulphate and concentrated in vacuum into a yellow oil that was purified by flash column chromatography on silica gel using 0.5-3% MeOH in DCM and recrystallisation from isopropanol to finally afford the 6-chloro-2-iodopurine nucleoside **10** as pale yellow needles (2.92g, 80%); mp=183°C (lit.[94] mp=182-183°C); R_f 0.75 [DCM/MeOH 95:5] ^{1}H NMR (300MHz, d_6-dmso) δ_H 2.04 (s, 3H, COC*H*$_3$), 2.07 (s, 3H, COC*H*$_3$), 2.11 (s, 3H, COC*H*$_3$), 4.35 (m, 1H, furanosyl H4'), 5.52 (t, $^3J_{H\text{-}H}$ = 5.63Hz and $^3J_{H\text{-}H}$ = 4.35Hz 1H, furanosyl H3'), 5.72 (t, $^3J_{H\text{-}H}$ = 5.38Hz, 1H, furanosyl H2'), 6.14 (d, $^3J_{H\text{-}H}$ = 5.38Hz, 1H, furanosyl furanosyl H1'), 7.21 (br s, 2H, -NH_2), 8.15 (s, 1H, purine

H8); ^{13}C NMR (75.5MHz, d_6-dmso) δ_C 20.8 (s, $COCH_3$), 21.0 (s, $COCH_3$), 21.3 (s, $COCH_3$), 63.3 (s, -CH_2OAc), 71.0 (s, furanosyl C3'), 73.7 (s, furanosyl C2'), 81.2 (s, furanosyl C4'), 87.0 (s, furanosyl C1'), 117.4 (s, purine C2), 132.6 (s, purine C5), 143.5 (s, purine C8), 151.4 (s, purine C4), 152.3 (s, purine C6), 169.8 (s, $COCH_3$), 170.0 (s, $COCH_3$), 170.6 (s, $COCH_3$); MS (ESI^+) *m/z* 561 $[M+Na]^+$, $C_{16}H_{16}ClIN_4O_7$ requires 538.678; IR (KBr disc, cm^{-1}): 3470w, 3111w, 2960w, 1745vs, 1585vs, 1552vs, 1494s, 1433s, 1410m, 1383s, 1345s, 1222vs, 1163m, 1141vs, 1113s, 1100s, 1078s, 1049m, 975s, 952m, 941m, 909s, 880m, 865s, 818s, 785w, 739w, 724m, 705w, 671w, 659w, 649w, 627m, 607m; Microanalytical data found: C: 35.96 H: 3.11 N: 10.01, expected for $C_{16}H_{16}ClIN_4O_7$ C: 35.68 H: 2.99 N: 10.40; Crystals suitable for X-Ray crystallography were obtained by recrystallisation from EtOH.

6-Chloro-2-iodo-9*H*-purine **11** (Method A)

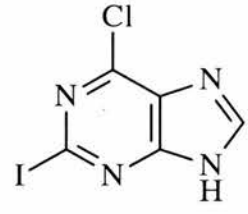

To 6-chloro-2-iodopurine nucleoside **10** (573mg, 1.07mmol) stirred in 1,4-dioxane (10mL) was added hydrochloric acid (2mL, 1N, 2mmol) portionwise and the resulting solution was stirred at 80°C for 7 hours. Following cooling to 0°C and neutralisation to pH 10 by dropwise addition of concentrated ammonia, the resulting mixture was evaporated to full dryness and partitioned between ethyl acetate(50mL) and water (2x25mL). The organics were dried over magnesium

sulphate and concentrated into a colourless solid that was purified by flash column chromatography on silica gel using 2:1 EtOAc/hexane to afford the dihalogenopurine **11** as a colourless solid (75mg, 25%); decomposition at 200°C; R_f 0.12 [hexane/ethyl acetate 1:1]; ^{1}H NMR (300 MHz, d_6-dmso) δ_H 8.62 (s, 1H, H8); ^{13}C NMR (75.4 MHz, d_6-dmso) δ_C 117.4 (C5), 129.5 (C2), 146.9 (C8), 147.3 (C6), 155.7 (C4); MS (EI): *m/z* 280 $[M]^+$, 153 $[M\text{-}I]^+$; High Resolution MS (EI): *m/z* 280.9019 $[M]^+$, $C_5H_2ClIN_4O$ requires 280.9013; IR (KBr disc, cm^{-1}): 3423m, 3098w, 3064w, 2922w, 2542w, 2347w, 1803w, 1686m, 1649w, 1604m, 1559s, 1492w, 1475w, 1400w, 1373w, 1344s, 1292m, 1239m, 1216s, 1149s, 1004w, 952m, 899w, 855s, 788w, 731m, 659w, 642m, 609m, 542m, 525w; Microanalytical data found C: 21.59 H: 0.93 N: 19.53, expected for $C_5H_2ClIN_4O$ C: 21.41 H: 0.72 N: 19.98.

6-Chloro-9*H*-purine monohydrate **13**

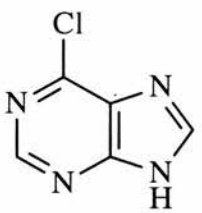

To a stirred mixture of hypoxanthine **12** (7.00 g, 11.2 mmol) in dry DMA (18 mL, 140 mmol) was added dropwise at 0°C phosphoryl oxychloride (175 mL, 1.9 mol) over a 30 minute periode. The pale green mixture was heated at reflux for 2 hours to give a red solution. Following evaporation to dryness into a reddish oil, icy water (200 mL) was slowly added and the green solution was carefully neutralised to pH 9 with concentrated ammonia. The solution was evaporated to

dryness into a yellow solid which was recrystallised twice from water to afford 6-chloropurine **13** (8.26 g, 86%) as a pale yellow crystalline solid, decomposition at 280°C (lit.[98], mp 250°C); ^{1}H NMR (300 MHz, d_6-dmso) δ_H 3.49 (s, 2H, H_2O), 8.67 (s, 1H, H8), 8.71 (s, 1H, H2); ^{13}C NMR (75.4 MHz, d_6-dmso) δ_C 129.4 (C5), 146.1 (C8), 147.7 (C6), 151.4 (C2) 154.2 (C4); MS (CI) *m/z* 155 $[M+H]^+$ $C_5H_3ClN_4$ requires 154.557; IR (KBr disc, cm^{-1}): 3478s, 3428s, 3121m, 3059m, 2974m, 2808m, 2710m, 2544m, 1655w, 1607s, 1574s, 1478w, 1449m, 1427w, 1397s, 1332s, 1285w, 1239s, 1157w, 1114w, 1002w, 940m, 922w, 861s, 730m, 678w, 639s, 603m, 556m, 508m. Microanalytical data found C: 35.02 H: 2.62 N: 32.39, expected for $C_5H_3ClN_4.H_2O$ C: 34.80 H: 2.92 N: 32.47. Crystals suitable for X-Ray crystallography were obtained by recrystallisation from water.

6-Chloro-9-(tetrahydro-pyran-2-yl)-9*H*-purine **14**

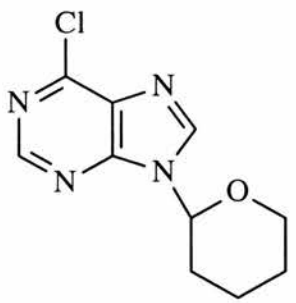

To a stirred mixture of 6-chloropurine **13** (4.35 g, 28.2 mmol) and *p*-toluenesulfonic acid (72 mg, 0.4 mmol) in dry THF (40 mL) was added at 80°C 2,3-dihydropyran (3 mL, 32.9 mmol). Reflux under a nitrogen atmosphere was continued overnight, concentrated ammonia (2.5 mL) was added dropwise following cooling to room temperature. After evaporation to dryness, the yellowish oil was dissolved in ethyl acetate (100 mL) and extracted with brine

(50 mL), water (2 x 50 mL) then dried over anhydrous sodium sulfate. The organic extracts were concentrated in vaccum into a yellow oil that was extracted with boiling petroleum ether 60-80°C. The ether extracts were cooled in a fridge overnight to precipitate a colourless powder that was recrystallised from petroleum ether 60-80°C to afford 6-chloro-9-THP-purine **14** (3.38 g, 68%) as colourless crystals (needles), mp 70°C (lit.[99] 69-71°C); ^{1}H NMR (300 MHz, d_6-dmso) δ_H 1.58 (m, 3H, THP), 1.74 (m, 2H, THP), 2.00 (m, 2H, THP), 2.30 (m, 1H, THP), 3.70 (m, 1H, THP H3'), 4.00 (dm, $^3J(^1H\text{-}^1H)$=10.8 Hz, 1H, THP H2'), 5.76 (dd, $^3J(^1H\text{-}^1H)$=2.3Hz & $^3J(^1H\text{-}^1H)$=11Hz, 1H, THP H1'), 8.79 (s, 1H, purine H8), 8.90 (s, 1H, purine H2); ^{13}C NMR (75.4 MHz, d_6-dmso) δ_C 22.5 (THP C3'), 24.8 (THP C4'), 30.0 (THP C2'), 68.1 (THP C6'), 82.0 (THP C1'), 131.3 (purine C5), 145.9 (purine C8), 149.6 (purine C6), 151.6 (purine C4), 152.1 (purine C2); MS (EI): *m/z* 238 $[M]^+$, 210 $[M\text{-}(CH_2)_2]^+$, 155 $[M\text{-}THP]^+$; IR (KBr disc, cm^{-1}): 3107m, 2959m, 2938m, 2873m, 1595s, 1568s, 1491m, 1467w, 1450m, 1396m, 1337s, 1300w, 1268w, 1218s, 1180m, 1145m, 1086s, 1045s, 951s, 907m, 878w, 856m, 822w, 794w, 783w, 648m, 636m, 596m. Microanalytical data found C: 50.32 H: 4.65 N: 23.47, expected for $C_{10}H_{11}ClN_4O$ C: 50.63 H: 4.51 N: 23.48. Crystals suitable for X-Ray crystallography were obtained by recrystallisation from petroleum ether 40-60°C.

6-Chloro-9-(tetrahydro-pyran-2-yl)-2-(tributylstannyl)purine **15**

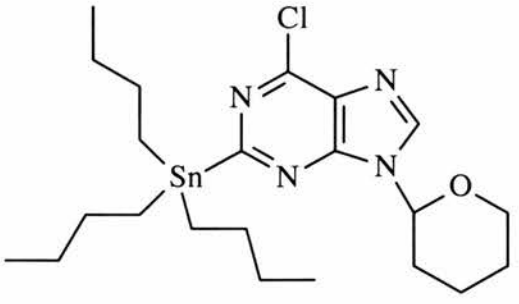

To a stirred solution of 2,2,6,6-tetramethylpiperidine (19.5 mL, 115.5 mmol) in dry hexane (15 mL) and dry THF (30 mL) was added dropwise at –78°C *n*-butyl lithium (48.5 mL, 2.6 M solution in hexanes, 121.3 mmol) over 30 minutes. Following stirring at the same temperature for 1 hour, was added dropwise a solution of 9-protected purine **14** (5.5 g, 23.1 mmol) in dry THF (30 mL). After 30 minutes of stirring at –78°C was added dropwise to the dark mixture tributyltin chloride (31.3 mL, 115.5 mmol) and stirring at the same temperature was continued for 1 hour. The resulting dark solution was quenched by dropwise addition of a saturated aqueous ammonium chloride solution (50 mL). Following overnight warming to room temperature with stirring, saturated aqueous sodium carbonate (50mL) was added. Extraction with ethyl acetate (2 x 50 mL) and drying of the combined organics over magnesium sulfate afforded after evaporation to full dryness ayellowish oil. Purification by flash column chromatography using hexane/ethyl acetate (4:1) afforded the 2-stannylated purine **15** (12.20 g, 100%) as a colourless oil; R_f 0.11 [hexane/ethyl acetate 4:1]; ^{1}H NMR (300 MHz, $CDCl_3$) δ_H 0.81 (t, $^3J(^1H\text{-}^1H)$=7.4Hz, 9H, $[CH_3(CH_2)_3]_3Sn$), 1.13 (t, $^3J(^1H\text{-}^1H)$=7.9 Hz, 6H, $[CH_3(CH_2)_2CH_2]_3Sn$), 1.27 (m, $^3J(^1H\text{-}^1H)$=7.7 Hz, 6H, $[CH_3CH_2(CH_2)_2]_3Sn$), 1.55 (m, $^3J(^1H\text{-}^1H)$=7.7 Hz, 9H $[CH_3\ CH_2CH_2CH_2]_3Sn$

and THP), 1.75 (m, 2H, THP) 2.10 (m, 2H, THP), 3.72 (td, $^{3}J(^{1}H\text{-}^{1}H)$=3.3Hz & $^{3}J(^{1}H\text{-}^{1}H)$=11.8Hz, 1H, THP H3'), 4.13 (dm, ^{3}J ($^{1}H\text{-}^{1}H$)= 11.5Hz, 1H, THP H3'), 5.71 (dd, $^{3}J(^{1}H\text{-}^{1}H)$=2.8Hz & $^{3}J(^{1}H\text{-}^{1}H)$=7.2Hz, 1H, THP H1'), 8.15 (s, 1H, purine H8); ^{13}C NMR (75.4 MHz,$CDCl_3$) δ_C 9.7 (t,$^{1}J(^{13}C\text{-}^{119}Sn)$=165.3Hz, $[CH_3(CH_2)_2CH_2]_3Sn$), 12.7 ($[CH_3(CH_2)_3]_3Sn$), 21.7 (THP C4'), 23.9 (THP C3'), 26.2 (t, $^{2}J(^{13}C\text{-}^{119}Sn)$=27.1Hz, $[CH_3CH_2CH_2CH_2]_3Sn$), 27.9 (t, $^{3}J(^{13}C\text{-}^{119}Sn)$=10.5Hz, $[CH_3CH_2CH_2CH_2]_3Sn$), 30.8 (THP C2'), 67.7 (THP C5'), 81.5 (THP C1'), 129.2 (purine C5), 140.6 (purine C8), 148.2 (purine C6), 149.1 (purine C4), 180.8 (purine C2); MS (ESI): *m/z* 529 $[M+H]^+$, 155 $[M\text{-}THP\text{-}Sn(Bu)_3]^+$; Found (ESI): *m/z* 529.1746 $[M+H]^+$; $C_{22}H_{37}ClN_4OSn$ requires 529.1751; IR (KBr disc, cm^{-1}): 3110m, 2955s, 2873s, 2731m, 2669m, 2637w, 2585w, 2419w, 2217w, 2050w, 1929w, 1743w, 1651m, 1582s, 1538s, 1486s, 1464s, 1414s, 1394s, 1377s, 1342s, 1309s, 1279s, 1225s, 1210s, 1180s, 1155s, 1138s, 1087s, 1059s, 1046s, 1023s, 1005s, 945s, 935m, 911s, 877s, 857s, 844m, 823m, 788s, 769w, 747w, 694s, 650s, 590m, 545w, 509m. Microanalytical data found C: 50.04 H: 7.07 N: 10.62, expected for $C_{22}H_{37}ClN_4OSn$ C: 50.04 H: 7.34 N: 10.82.

6-Chloro-2-iodo-9-(tetrahydro-pyran-2-yl)- 9H-purine **16**

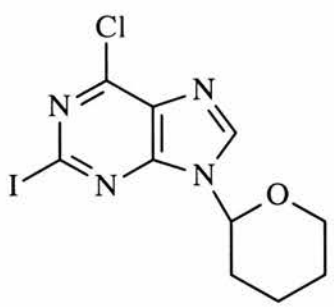

To a stirred solution of 2-stannylated purine **15** (12.20 g, 23.1 mmol) in dry THF (200 mL) was added iodine (9 g, 35.3 mmol) portionwise. Stirring was continued for 24 hours under a nitrogen atmosphere. Following the treatment of excess iodine with saturated sodium metabisulfite, and subsequent stirring for one hour, the solution was extracted with dichloromethane (3 x 100 mL). The combined organics were washed with brine (100 mL), water (100 mL), dried over magnesium sulfate, then evaporated to full dryness into a yellowish oil. Trituration with *n*-hexane (75 mL) precipitated the 2-iodopurine **16** (8.0 g, 95%) as a pale yellow solid, mp 114°C; R_f 0.28 [hexane/ethyl acetate 1:1]; ^{1}H NMR (300 MHz, $CDCl_3$) δ_H 1.46 (m, 3H, THP), 1.78 (m, 2H, THP), 2.01 (m, 1H, THP), 3.72 (td, $^3J(^1H\text{-}^1H)$=3.6 & $^3J(^1H\text{-}^1H)$=11.5Hz, 1H, THP H3'), 4.10 (dm, $^3J(^1H\text{-}^1H)$=1.8Hz & $^3J(^1H\text{-}^1H)$=11.8Hz, 1H, THP H2'), 5.70 (dd, $^3J(^1H\text{-}^1H)$=2.3Hz & $^3J(^1H\text{-}^1H)$=10.5Hz, 1H, THP H1'), 8.22 (s, 1H, purine H8); ^{13}C NMR (75.4 MHz, $CDCl_3$) δ_C 22.4 (THP C4'), 24.6 (THP C3'), 32.0 (THP C2'), 68.9 (THP C5'), 82.3 (THP C1'), 116.5 (purine C2), 131.5 (purine C5), 143.0 (purine C8), 150.3 (purine C6), 151.6 (purine C4); MS (ESI): *m/z* 365 $[M+H]^+$, 239 $[M-I]^+$; Found (ESI): *m/z* 364.9665 $[M+H]^+$; $C_{10}H_{22}ClIN_4O$ requires 364.9661; IR (KBr): 3111m, 2957m, 2684m, 1795w, 1589s, 1546s, 1485m, 1471m, 1454w, 1443m, 1418m, 1400w, 1371m, 1342s, 1309m, 1280w, 1260w, 1227s, 1205s, 1180s, 1148s, 1135s, 1105m, 1082s, 1057m, 1042s, 955s, 936m, 909s, 901m, 879m, 861s, 822m, 789m, 714w, 658w, 634w, 601s, 546w. Microanalytical data found C: 32.75 H: 2.62 N: 15.74, expected for

$C_{10}H_{10}ClIN_4O$ C: 32.95 H: 2.76 N: 15.37. Crystals suitable for X-Ray crystallography were obtained by crystallisation from $CDCl_3$/hexane.

6-Chloro-2-iodo-9*H*-purine **11** (Method B)

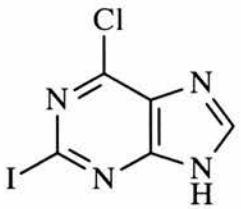

To a stirred solution of 9-protected purine **16** (34.58 g, 95 mmol) in 95:5 ethanol/water (250 mL) was added at room temperature copper(II) dichloride (1.345 g, 10 mmol). The resulting mixture was refluxed at 85°C for 5 hours with vigorous stirring. Following evaporation to dryness into a tan residue, purification by flash column chromatography using hexane/ethyl acetate (1:1) afforded 6-chloro-2-iodo-purine **11** (26 g, 98%) as a colourless solid, decomposition at 200°C; R_f 0.12 [hexane/ethyl acetate 1:1]; ^{1}H NMR (300 MHz, d_6-dmso) δ_H 8.68 (s, 1H, H8); ^{13}C NMR (75.4 MHz, d_6-dmso) δ_C 117.1 (C2), 129.3 (C5), 146.8 (C8), 147.1 (C6), 155.9 (C4); MS (EI): *m/z* 280 $[M]^+$, 153 $[M-I]^+$; Found (EI): *m/z* 280.9019 $[M]^+$; $C_5H_2ClIN_4O$ requires 280.9013; IR (KBr): 3423m, 3098w, 3064w, 2922w, 2542w, 2347w, 1803w, 1686m, 1649w, 1604m, 1559s, 1492w, 1475w, 1400w, 1373w, 1344s, 1292m, 1239m, 1216s, 1149s, 1004w, 952m, 899w, 855s, 788w, 731m, 659w, 642m, 609m, 542m, 525w. Microanalytical data found C: 21.59 H: 0.93 N: 19.53, expected for $C_5H_2ClIN_4O$ C: 21.41 H: 0.72 N: 19.98. Crystals suitable for X-Ray crystallography were obtained by recrystallisation from water.

6-Chloro-2-iodo-9-isopropyl-purine **17**

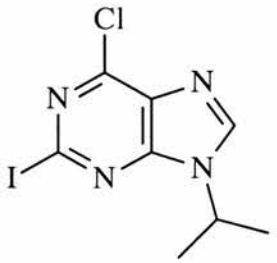

To a colourless solution of 6-chloro-2-iodopurine **11** (220mg, 0.78mmol) and triphenylphosphine (410mg, 1.57mmol) stirred in anhydrous THF (20mL) was added isopropanol (0.1mL, 1.57mmol) under a nitrogen atmosphere. Following cooling to -10 to -20°C, diethyl azodicarboxylate (0.26mL, 1.57mmol) was added dropwise under nitrogen. Stirring under nitrogen was continued for 1 hour at the same temperature. More diethyl azodicarboxylate (0.26mL, 1.57mmol) was added dropwise and the reaction mixture was stirred under nitrogen for 1 day at room temperature. Following quenching with isopropanol (2.5mL), the resulting yellow solution was evaporated to full dryness into a yellow oil that was purified by flash column chromatography to recover purine **17** as a colourless foam (78 mg, 20% based on the molecular weights of the **17**/diethyl ester hydrazine 1:1 mixture); R_f 0.40 [hexane/ethyl acetate 1:2]; mp 118°C (lit.[102] 108-109°C); ^{1}H NMR (300 MHz, $CDCl_3$) δ_H 1.21 (t, $^3J(^1H\text{-}^1H)$=6.91Hz, 6H, hydrazine CH_3CH_2OCO-), 1.57 (d, $^3J(^1H\text{-}^1H)$=6.66Hz, 1H, purine –$CH(CH_3)_2$), 4.14 (q, $^3J(^1H\text{-}^1H)$=7.17 Hz, 4H, hydrazine CH_3CH_2OCO-), 4.85 (septet, $^3J(^1H\text{-}^1H)$=6.91 Hz, 1H, purine –$CH(CH_3)_2$), 6.58 (br s, 2H, 2 hydrazine –NH), 8.04 (s, 1H, purine H8); ^{13}C NMR (75.4 MHz, $CDCl_3$) δ_C 14.8 (s, purine $CH(CH_3)_2$) 22.9 (s, hydrazine CH_3CH_2OCO-), 48.6 (s, purine $CH(CH_3)_2$), 62.6 (s, hydrazine

CH_3CH_2OCO-), 116.6 (s, purine C2), 132.4 (s, purine C5), 143.3 (s, purine C8), 150.7 (s, purine C6), 152.6 (s, purine C4), 157.20 (s, hydrazine CH_3CH_2O*C*O-); MS (ESI^+): *m/z* 322 $[M+1]^+$, Found (ESI^+): *m/z* 322.9558 $[M+1]^+$; $C_8H_8ClIN_4$ requires 322.9555; Microanalytical data found C: 34.49 H: 3.72 N: 17.36, expected for $C_8H_8ClIN_4.C_6H_{12}N_2O_4$ C: 33.72 H: 4.04 N: 16.85.

6-Benzylsulfanyl-2-iodo-9*H*-purine **19**

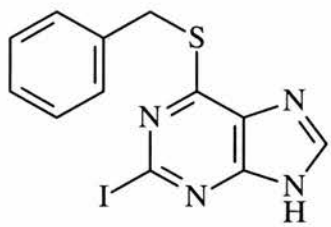

To a solution of benzyl mercaptan (0.5mL, 3.93mmol) in DMF (5mL) was added sodium hydride (164mg, 4.1mmol) portionwise under a nitrogen atmosphere, stirring was continued overnight under nitrogen. The resulting solution was added under nitrogen to a solution of purine **11** (1g, 3.6mmol) in DMF (5mL) and stirring under nitrogen was continued for 2 days. Following evaportation to full dryness and partition of the resulting yellow foam between DCM (3x15mL) and water (25mL), the organics were dried over magnesium sulphate and evaporated into a pale yellow residue. Purification by flash column chromatography on silica gel using petroleum ether 40-60° then 3:2 EtOAc/petroleum ether afforded the 6-benzylsulfanylpurine 19 as a pale yellow solid (1.26g, 96%); mp 86-88°C; R_f 0.32 [hexane/ethyl acetate 1:2]; ^1H NMR (300 MHz, d_6-dmso) δ_H 4.54 (s, 2H, PhC*H*$_2$S-), 7.20-7.33 (m, 3H, aromatics *Ph*CH_2S-), 7.46-7.48 (m, 2H, aromatics *Ph*CH_2S-), 8.36 (s, 1H, purine H8); ^{13}C NMR (75.4 MHz, d_6-dmso) δ_C 32.2 (s,

PhCH$_2$S-), 118.9 (s, purine C2), 127.2 (s, Ph C4'), 128.3 (s, Ph C3'), 129.2 (s, purine C5), 129.3 (s, Ph C2'), 137.7 (s, Ph C1'), 143.9 (s, purine C8), 151.9 (s, purine C4), 158.4 (s, purine C6); MS (ESI$^+$): *m/z* 368.9670 $[M+1]^+$; $C_{12}H_{10}IN_4S$ requires 368.9665; IR (KBr disc, cm^{-1}): 3099m, 3050m, 3025m, 2924m, 2854m, 2648m, 1656w, 1558vs, 1495m, 1453m, 1392m, 1366m, 1329vs, 1296m, 1274m, 1227vs, 1139s, 1069m, 1030w, 1007m, 947s, 927m, 853s, 785w, 762w, 728m, 697s, 653m, 641s, 619s, 562w, 539m, 523m; Microanalytical data found C: 39.29 H: 2.59 N: 15.68 S: 8.96, expected for $C_{12}H_9IN_4S$ C: 39.14 H: 2.46 N: 15.22 s: 8.71.

6-Benzylsulfanyl-2-iodo-9-isopropylpurine **20**

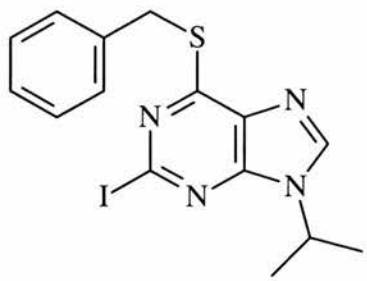

To thoroughly dried 6-benzylsulfanylpurine (534mg, 1.45mmol) and triphenylphosphine (420mg, 1.6mmol) in a flame-dried round-bottomed Schlenk flask was added anhydrous THF (10mL) under a nitrogen atmosphere and the resulting yellow solution was cooled to -50°C. Diisopropyl azodicarboxylate (0.3mL, 1.6mmol) was added dropwise under nitrogen and stirring was continued for 30 minutes at this temperature prior to the dropwise addition of anhydrous isopropanol (0.12mL, 1.6mmol). The resulting solution was stirred at -50°C for 30 minutes then gradually warmed to room temperature, stirred under nitrogen for

3 days, then evaporated to full dryness into a pale yellow oil that was purified by flash column chromatography on silica gel using petroleum ether 40-60°C then EtOAc/petroleum ether 1:1 as eluants to afford 9-isopropylpurine **20** as pale yellow needles (486mg, 81%). R_f 0.62 [hexane/ethyl acetate 1:2]; mp 115-117°C; ^{1}H NMR (300 MHz, MeOD) δ_H 1.49 (d, $^3J(^1H\text{-}^1H)$=6.66 Hz, 6H, purine CH(CH_3)$_2$), 4.42 (s, 2H, PhCH_2S-), 4.71 (s, $^3J(^1H\text{-}^1H)$=6.66 Hz, 1H, purine CH(CH$_3$)$_2$), 7.06-7.19 (m, 3H, aromatics *Ph*CH$_2$S-), 7.36 (m, 2H, aromatics *Ph*CH$_2$S-), 8.19 (s, 1H, purine H8); ^{13}C NMR (75.4 MHz, MeOD) δ_C 22.9 (s, purine CH(CH_3)$_2$), 34.4 (s, PhCH$_2$-), 49.9 (s, purine CH(CH$_3$)$_2$), 119.2 (s, purine C2), 128.8 (s, Ph C4'), 129.9 (s, Ph C3'), 130.9 (s, Ph C2'), 132.1 (s, purine C5), 139.3 (s, Ph C1'), 143.7 (s, purine C8), 150.5 (s, purine C4), 162.6 (s, purine C6); MS (EI$^+$): *m/z* 410.0052 [M]$^+$; $C_{15}H_{15}IN_4S$ requires 410.0062; IR (KBr disc, cm^{-1}): 3286m, 3248m, 3093m, 3023m, 2978m, 2941m, 2875m, 1736s, 1715s, 1564vs, 1542vs, 1493m, 1429m, 1454m, 1416m, 1388m, 1374s, 1331vs, 1260m, 1205vs, 1177s, 1140s, 1108s, 1051m, 941s, 885w, 856w, 776w, 776m, 736m, 702w, 678m, 650w, 620m, 558m, 509w; Microanalytical data found C: 45.10 H: 3.89 N: 13.69 S: 7.49, expected for $C_{15}H_{15}IN_4S$ C: 43.90 H: 3.69 N: 13.66 s: 7.80. Crystals suitable for X-Ray crystallography were obtained by crystallisation from MeOD.

6-Benzylsulfonyl-2-iodo-9-isopropylpurine **21**

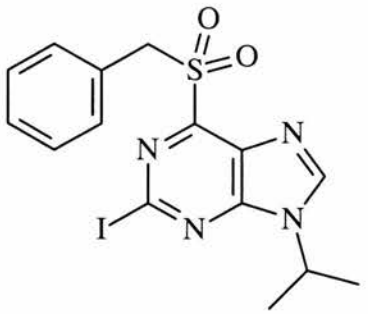

To a solution of *m*-chloroperbenzoic acid (3.99g, 70% w/w with water, 15.8mmol) stirred in anhydrous DCM (100mL) under a nitrogen atmosphere was added magnesium sulphate (5.96g, 49.5mmol). Following overnight stirring under nitrogen of the resulting mixture, a solution of purine **20** (2.16g, 5.27mmol) in DCM (100mL) was then added dropwise and stirring was continued for 24 hours at ambient temperature. The colourless precipitate was filtered off and washed thoroughly with DCM (3x100mL) and the filtrate was evaporated to full dryness into a yellow solid. Flash column chromatography on silica gel with 2:1 EtOAc/petroleum ether 40-60°C then EtOAc provided a sample of analytically pure purine **21**. Reprecipitation with hexane from a saturated solution of DCM afforded the purine **21** as a colourless solid. (2.09g, 90%); R_f 0.16 [hexane/ethyl acetate 1:2]; decomposition at 160-170°C; ^{1}H NMR (300 MHz, $CDCl_3$) δ_H 1.54 (d, $^3J(^1H\text{-}^1H)$=6.66 Hz, 6H, purine $CH(CH_3)_2$), 4.82 (s, 2H, $PhCH_2SO_2$-), 4.85 (s, $^3J(^1H\text{-}^1H)$=6.66 Hz, 1H, purine $CH(CH_3)_2$), 7.20-7.24 (m, 3H, aromatics $PhCH_2SO_2$-), 7.34-7.37 (m, 2H, aromatics $PhCH_2SO_2$-), 8.21 (s, 1H, purine H8); ^{13}C NMR (75.4 MHz, $CDCl_3$) δ_C 22.8 (s, purine $CH(CH_3)_2$), 48.9 (s, purine $CH(CH_3)_2$), 59.1 (s, $PhCH_2SO_2$-), 116.5 (s, purine C2), 126.8 (s, Ph C1'), 129.1 (s, Ph C3'), 129.3 (s, Ph C2'), 130.3 (s, purine C5), 132.0 (s, Ph C4'), 146.5 (s,

purine C8), 154.0 (s, purine C4), 155.6 (s, purine C6); MS (CI^+): *m/z* 443.0043 $[M+1]^+$; $C_{15}H_{16}N_4O_2SI$ requires 443.0039; IR (KBr disc, cm^{-1}): 3107m, 3057w, 3025w, 2978w, 2918w, 2931w, 1582s, 1550s, 1488s, 1556s, 1403m, 1388m, 1374m, 1339vs, 1261m, 1237m, 1211vs, 1150vs, 1134vs, 1032m, 943m, 908m, 884w, 860m, 827w, 808w, 774s, 719s, 697s, 662m, 640s, 622m, 606s, 594m, 519s; Microanalytical data found C: 40.85 H: 3.28 N: 12.94 S: 7.39, expected for $C_{15}H_{15}N_4SO_2I$ C: 40.74 H: 3.42 N: 12.67 S: 7.25.

6-(3-Chlorophenylamino)-2-iodo-9-isopropylpurine **22**

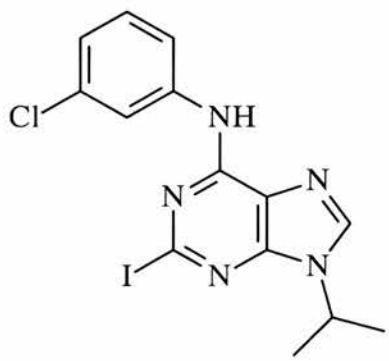

To a solution of 6-benzylsulfonylpurine **21** (217mg, 0.49mmol) in ethanol stirred at room temperature under a nitrogen atmosphere was added *m*-chloroaniline (0.10mL, 0.94mmol) and the resulting dark solution was refluxed at 90°C under nitrogen for 24 hours, cooled and evaporated to full dryness into a dark oil. Purification by flash chromatography on silica gel using EtOAc/petroleum ether 40-60°C 2:1 then EtOAc afforded the 6-anilinopurine **22** as a yellowish foam (65mg, 32%); R_f 0.10 [hexane/ethyl acetate 1:2]; ^1H NMR (300 MHz, $CDCl_3$) δ_H 1.53 (d, $^3J(^1H\text{-}^1H)$=6.66 Hz, 6H, purine $CH(CH_3)_2$), 4.80 (s, $^3J(^1H\text{-}^1H)$=6.66 Hz, 1H, purine $CH(CH_3)_2$), 7.01 (dd, $^3J(^1H\text{-}^1H)$=7.94 Hz and $^3J(^1H\text{-}^1H)$=2.05 Hz, 1H,

aniline C_d), 7.22 (t, $^3J(^1H\text{-}^1H)$=8.19 Hz, 1H, aniline C_c), 7.58 (dd, $^3J(^1H\text{-}^1H)$=8.19 Hz and $^3J(^1H\text{-}^1H)$=2.05 Hz, 1H, aniline C_b), 7.74 (s, 1H, aniline NH), 7.79 (t, $^3J(^1H\text{-}^1H)$=2.05 Hz, 1H, aniline C_f), 7.98 (s, 1H, purine H8); ^{13}C NMR (75.4 MHz, $CDCl_3$) δ_C 23.2 (s, purine $CH(CH_3)_2$), 47.6 (s, purine $CH(CH_3)_2$), 116.0 (s, purine C2), 118.1 (s, aniline C_b), 120.1 (s, aniline C_f), 120.7 (s, purine C5), 124.0 (s, aniline C_d), 130.4 (s, aniline C_c), 135.0 (s, aniline C_e), 138.5 (s, purine C8), 139.9 (s, aniline C_a), 150.0 (s, purine C4), 151.1 (s, purine C6); MS (CI^+): *m/z* 413.9966 $[M+1]^+$ and *m/z* 286.0072 $[M\text{-}I]^+$; $C_{14}H_{14}ClIN_5$ requires 413.9964; IR (KBr disc, cm^{-1}): 3312m, 3206m, 3113m, 2978m, 2929m, 1699m, 1615s, 1575s, 1480s, 1440s, 1404vs, 1330s, 1314s, 1273m, 1220m, 1188m, 1151m, 1077m, 1022m, 995w, 920w, 883w, 775w, 698w, 681w, 6654w, 631w, 599w, 571w, 528w; Microanalytical data found C: 40.10 H: 3.98 N: 18.02, expected for $C_{14}H_{13}ClIN_5$ C: 40.68 H: 3.17 N: 16.95.

2-(1*R*-Isopropyl-2-hydroxyethylamino)-6-(3-chlorophenylamino)-9-isopropylpurine **23** (Purvalanol A)

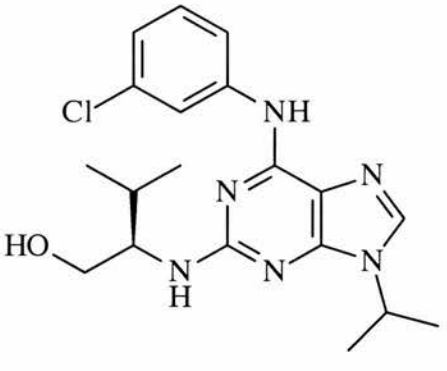

To a solution of 2-iodopurine **22** (170mg, 0.41mmol) in *n*-butanol (10mL) was added Hunig'base (0.5mL, 90mmol) and *R*-valinol (500mg, 4.9mmol). The resulting solution was heated at 160C in a Parr bomb for 24 hours. Following

cooling down and evaporation to full dryness, the resulting oil was purified by flash chromatography on silica gel using 1-5% MeOH in DCM to afford Purvalanol A as a colourless solid (59mg, 37%); R_f 0.20 [DCM/MeOH 95:5]; ^{1}H NMR (270 MHz, $CDCl_3$) δ_H 1.01 (d, $^3J(^1H\text{-}^1H)$=6.68 Hz, 6H, valinol $CH(CH_3)_2$), 1.47 (d, $^3J(^1H\text{-}^1H)$=6.70 Hz, 6H, purine $CH(CH_3)_2$), 1.97 (m, $^3J(^1H\text{-}^1H)$=6.70 Hz, 1H, valinol $CH(CH_3)_2$), 3.60-3.71 (m, 1H, valinol $NHCHCH_2OH$), 3.80-4.01 (m, 2H, valinol $NHCHCH_2OH$), 4.50 (sept, $^3J(^1H\text{-}^1H)$=6.70 Hz, 1H, purine $CH(CH_3)_2$), 5.16 (d, $^3J(^1H\text{-}^1H)$=7.94 Hz, 1H, valinol $NHCHCH_2OH$), 6.92 (d, $^3J(^1H\text{-}^1H)$=7.92 Hz, 1H, aniline C_d), 7.13 (t, $^3J(^1H\text{-}^1H)$=8.16 Hz, 1H, aniline C_c), 7.41 (d, $^3J(^1H\text{-}^1H)$=8.16 Hz, 1H, aniline C_b), 7.70 (t, $^3J(^1H\text{-}^1H)$=1.76 Hz, 1H, aniline C_f), 7.97 (s, 1H, purine H8), 8.47 (broad s, 1H, aniline NH); ^{13}C NMR (67. 9 MHz, $CDCl_3$) δ_C 19.1 (s, valinol $CH(CH_3)_2$), 19.5 (s, valinol $CH(CH_3)_2$, 23.2 (s, purine $CH(CH_3)_2$), 46.6 (s, purine $CH(CH_3)_2$), 30.0 (s, valinol $Me_2CHCHNH$), 59.5 (s, valinol $NHCHCH_2OH$), 64.7 (s, valinol $HOCH_2CHNH$), 114.5 (s, purine C5), 117.8 (s, aniline C_b), 119.8 (s, aniline C_f), 122.5 (s, aniline C_d), 131.3 (s, aniline C_c), 134.3 (s, aniline C_e), 135.1 (s, purine C8), 140.8 (s, aniline C_a), 150.9 (s, purine C4), 152.0 (s, purine C6), 159.8 (s, purine C2); MS (ESI^+): *m/z* 389.1863 $[M+1]^+$, $C_{19}H_{26}ClN_6O$ requires 389.1857; IR (KBr disc, cm^{-1}): 3326m, 3232m, 3114m, 2960s, 2930s, 2873m, 1634s, 1575vs, 1480s, 1422m, 1362m, 1336m, 1031m, 1248m, 1172w, 1132m, 1080m, 1028m, 871w, 777m, 698w, 640m, 529w; α_D^{25}(MeOH) -34 (2.34mg in 2mL) Microanalytical data found C: 58.92 H: 6.32 N: 22.30, expected for $C_{19}H_{25}ClN_6O$ C: 58.54 H: 6.61 N: 21.58.

CHAPTER 3: SYNTHESIS AND REACTIVITY OF 2-BENZYLSULFANYLPURINES

3.1 *Introduction*

We have shown in the previous chapter that the traditional 2,6-diaminopurine precursors, the 2,6-dihalogenopurines, exhibit poor reactivity with amines and that these particular nucleophilic substitutions require forcing conditions including high temperatures up to 160°C in a sealed Parr bomb. More reactive leaving groups would allow an easier preparation of a wider range of 2,6-diaminopurine CDK inhibitors. As demonstrated before, the oxidative cleavage of the benzylsulfanyl by nucleophiles including deactivated anilines is more successful than the chloride leaving group and has attracted some interest in the literature for the functionalisation of purines at the 2- and 6-positions[112,113]. Furthermore, this thioether has been used as a traceless linker[113] for the solid phase synthesis of pteridine and related purine heterocycles by Suckling *et al.* An interesting alternative is the displacement of the mesylate leaving group with amines which was implemented on pyrimidinones[114].

Hence, we attempted to design and develop the synthesis of novel purines bearing a combination of these moieties and to investigate the reactivity of such intermediates. The Traube synthesis was chosen to prepare the 2-substituted hypoxanthine from 5,6-diaminopyrimidinone as previously described[113]. We

reasoned that since regioselective Mitsunobu alkylations at the *N*-9 position of hypoxanthines had also been reported[115], subsequent conversion of the 6-oxo into a suitable leaving group X could lead to the synthesis of potentially valuable diaminopurine precursors of CDK inhibitors like Purvalanol A (see Scheme 3.1 below).

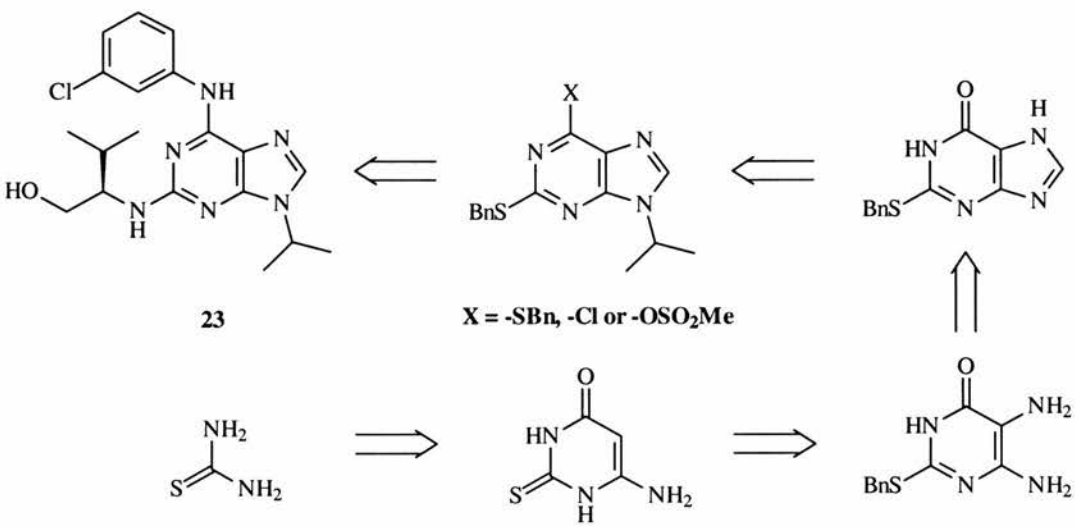

Scheme 3.1 Retrosynthesis of Purvalanol **23** from substituted 2-benzylsulfanylpurines via the Traube synthesis

3.2 *Results and discussion*

3.2.1 Traube synthesis of 2-benzylsulfanylhypoxanthine

When thiourea was treated with ethyl cyanoacetate in alkaline medium, followed by acidification with concentrated hydrochloric acid[116], the 6-aminopyrimidinone **24** was obtained in near quantitative yield as a colourless powder (see Scheme

3.2) and fully characterised. Interestingly, the IR spectrum indicates that the thiopyrimidinone tautomer is predominant in the solid state as an intense $\nu_{C=S}$ at 1185cm^{-1} was observed while no ν_{S-H} stretching was visible in the characteristic 2600-2550cm^{-1} region. The ESI$^-$ mass spectrum displays not only the molecular ion at m/z = 142 for [M-1]$^-$ but also the dimer at m/z = 285 and the trimer at m/z = 428. Crystals of thiopyrimidinone **24** suitable for XRD studies were obtained by recrystallisation of the crude powder from water and the crystal structure confirmed the results from the IR spectrum. An extensive network of hydrogen-bonding between the water and pyrimidinone molecules favors the formation of the structure: Figure 3.1 shows one type of H-bond between the oxygen atom O(7) of water to the N(3) hydrogen of an adjacent thiopyrimidinone molecule with a distance of 1.851(2) Å.

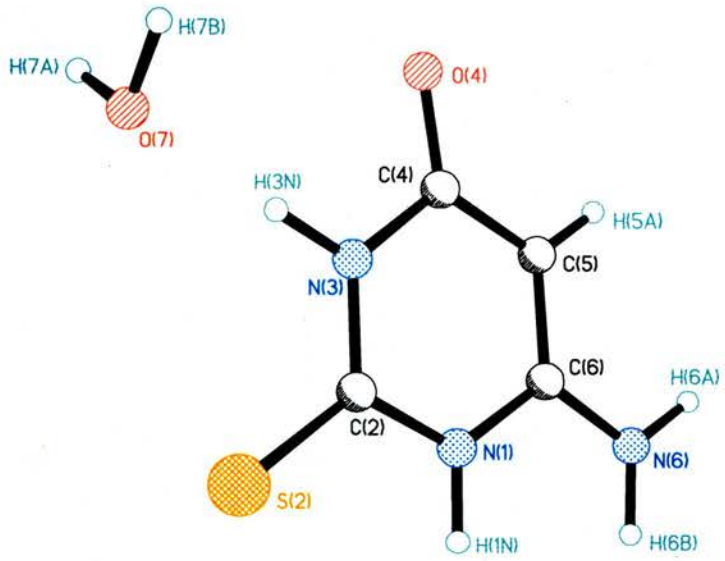

Figure 3.1 Crystal structure of thiopyrimidinone **24**

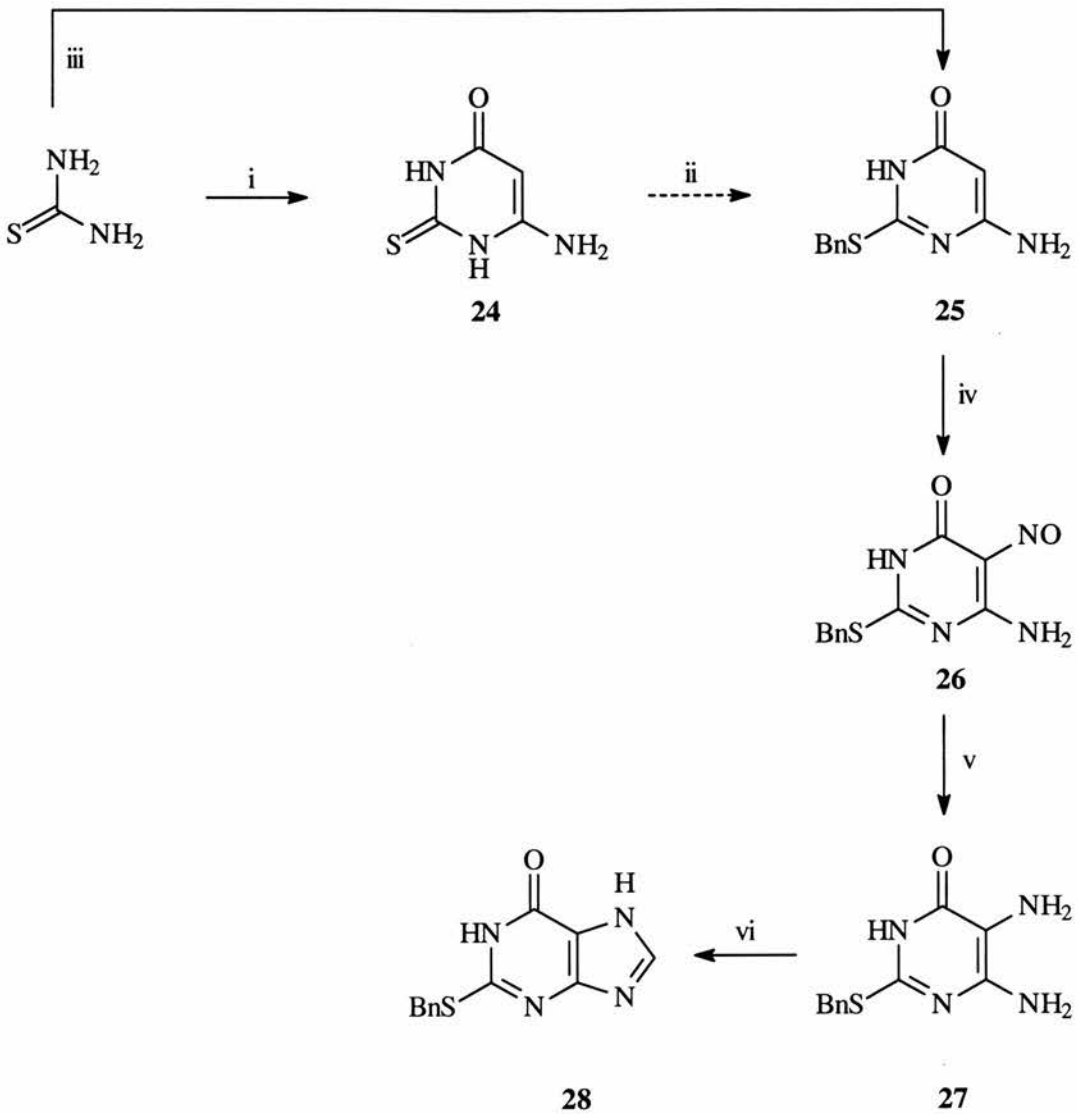

Conditions: i) ethyl cyanoacetate, EtONa, EtOH, Δ, then HCl (98%) ii) NaOH, EtOH, Δ, then BnCl, Δ iii) ethyl cyanoacetate, EtONa, EtOH, Δ, then BnCl (98%) iv) $NaOH_{(aq)}$, $NaNO_2$ then AcOH (92%) v) $Na_2S_2O_4$(aq), MeOH (97%) vi) $HC(OEt)_3$, DMF then HCl (92%)

Scheme 3.2 Traube synthesis of 2-benzylsulfanylhypoxanthine **28**

	24
Bond length	
N(1)-C(2)	1.3605(19)
N(1)-C(6)	1.378(2)
C(2)-N(3)	1.3514(19)
C(2)-S(2)	1.6731(15)
C(4)-O(4)	1.2594(18)
C(5)-C(6)	1.382(2)
C(6)-N(6)	1.340(2)
Bond angle	
C(2)-N(1)-C(6)	123.55(13)
C(2)-N(1)-H(1N)	116.5(13)
N(3)-C(2)-N(1)	116.09(13)
C(2)-N(3)-C(4)	124.51(13)
O(4)-C(4)-C(5)	125.26(14)
N(3)-C(4)-C(5)	117.28(13)
N(6)-C(6)-C(5)	124.21(14)

Table 3.1 Selected bond lengths (Å) and angles (º) for pyrimidinone **24**

Since the introduction of benzyl on the 2-thioxo group requires deprotonation prior to nucleophilic displacement on benzyl chloride, we opted for a one-pot cyclisation-benzylation in a sodium ethanoate solution, thus avoiding the isolation of 2-thiopyrimidinone **24**. The sodium salt of pyrimidinone **24** resulting from the cyclisation between ethyl cyanoacetate and thiourea was found to react at room temperature with benzyl chloride in very high yield. The crude oily solid obtained after evaporation of the solvent was easily purified by trituration with acetone and filtration on a sintered funnel. The precipitated

sodium chloride by-product was washed out with water while the excess benzyl chloride was removed by thorough washing with ether and acetone to finally retrieve analytically pure 2-benzylsulfanylsulfanylpurine **25**. Recrystallisation from ethanol afforded suitable crystals for XRD studies (Figure 3.2, Table 3.2). An intermolecular hydrogen bond occurs in the solid state between the hydrogen atom H(3A) of the 6-amino group of one molecule and the oxygen donor O(4) of an adjacent 6-aminopyrimidinone at a distance of 1.915(5) Å.

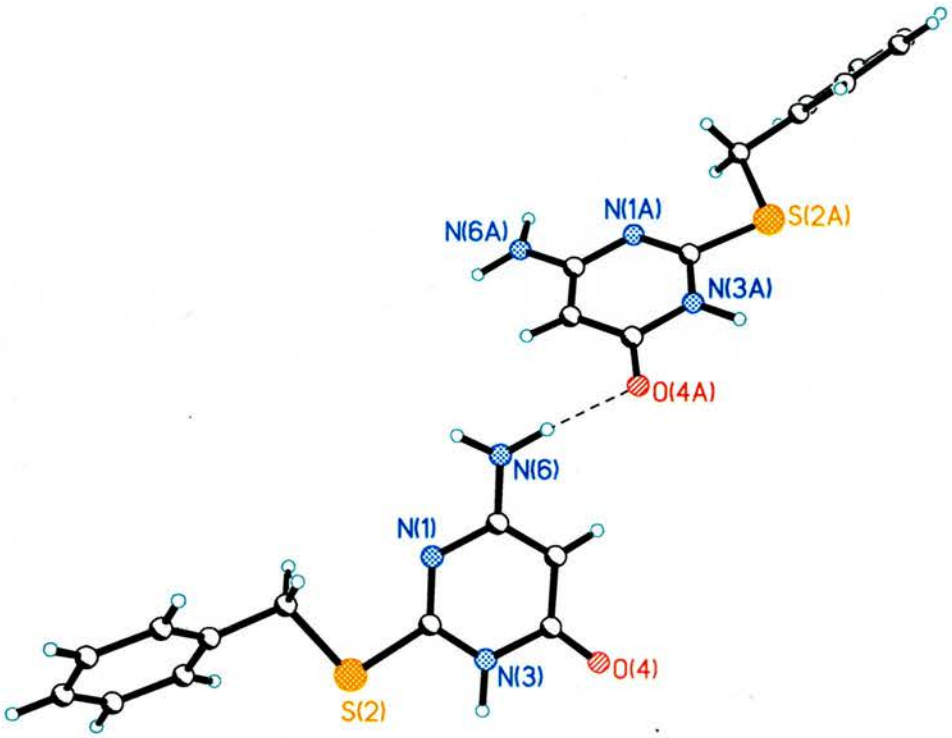

Figure 3.2 Crystal structure of 2-benzylsulfanylpyrimidinone **25**

	25
Bond length	
N(1)-C(2)	1.303(2)
N(1)-C(6)	1.379(2)
C(2)-N(3)	1.359(2)
C(2)-S(2)	1.7503(17)
C(4)-O(4)	1.267(2)
C(5)-C(6)	1.389(2)
C(6)-N(6)	1.338(2)
Bond angle	
C(2)-N(1)-C(6)	116.08(14)
N(3)-C(2)-S(2)	114.92(12)
O(4)-C(4)-C(5)	126.15(15)
C(8)-C(7)-S(2)	108.84(12)
C(6)-N(6)-H(6B)	116.6(16)
O(4)-C(4)-N(3)	118.03(15)

Table 3.2 Selected bond lengths (Å) and angles (º) for pyrimidinone **25**

The C-5 nitrosation of the 2-benzylsulfanylpyrimidinone **25** proceeded smoothly in 92% yield, by adding concentrated acetic acid very slowly to a solution of pyrimidinone **25**, sodium hydroxide and sodium nitrite in water. A colourless precipitate formed almost instantly after the addition of the first drops of acid and this turned progressively into an intensively blue coloured solid. We found that a very slow addition of the acid is definitely crucial to obtain the 5-nitrosopyrimidinone **26** in decent purity. Earlier attempts with a more rapid addition of the acid resulted in a pale purple precipitate that contained little amounts of the desired product along with several unidentified side-products.

Nevertheless, if the acid is slowly added at a rate of 2-3 drops per second through an addition funnel, the reaction produces a deep blue solid that can be purified by filtration and extensive washings with water, ether and acetone to afford the desired compound **26** as a deep blue solid in 92% yield. Full characterisation by NMR, IR, MS and elemental analysis confirmed the identity of the product. Interestingly, the ^{1}H spectrum displays two proton environments for the 6-amino group as two broad singlets at δ 9.18 and δ 11.25 ppm were noticed. We believed at first that this was caused by intermolecular hydrogen-bonding of one hydrogen of the 6-amino moiety with the oxygen atom of the neighbouring 5-nitroso. Fortunately, suitable crystals for crystallographic studies were obtained by recrystallisation from ethanol/water 9:1 (Figure 3.3). An intramolecular hydrogen-bond was indeed seen between the oxygen atom (O5) of the nitroso group and one hydrogen H(6A) of the 6-amino at a distance of 1.90(3) Å.

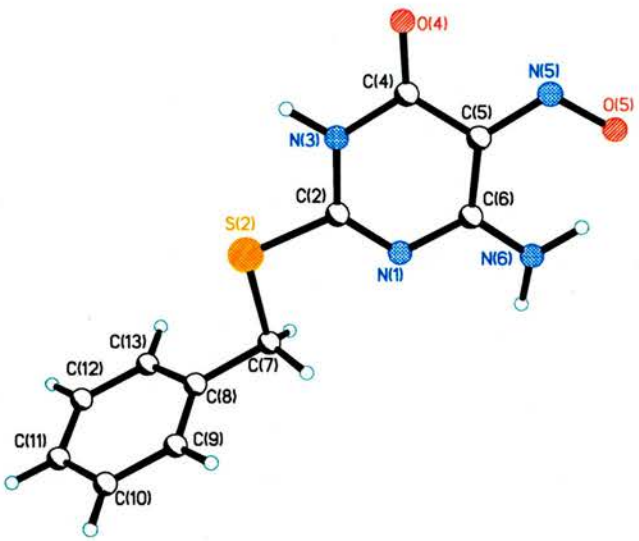

Figure 3.3 Crystal structure of 5-nitrosopyrimidinone **26**

However, a more complex assembly can be seen on Figure 3.4 which displays a dimeric arrangement of two pyrimidinone molecules through hydrogen-bonding between the oxygen atoms O(4) and O(4A) and the nitrogen protons H(3NA) and H(3N) at a distance of 1.824(5) Å. This centrosymmetric arrangement by hydrogen bonding is well known in biological systems as it constitutes the basis of the structure of DNA: its nucleic acids are connected by sets of specific hydrogen bonds between the cytosine (C)-guanine (G), adenine (A)-thymine(T) base pairs, as seen on Figure 3.5. Finally, a second type of hydrogen bond was observed between the hydrogen atom N(6A) and the oxygen O(4) of a third pyrimidinone molecule with a distance of 2.37(2) Å.

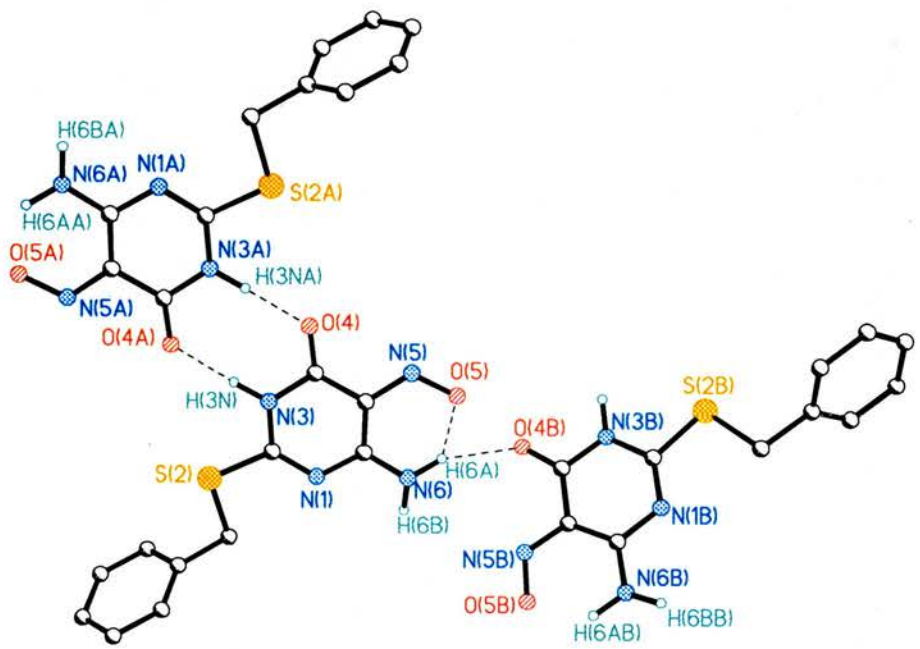

Figure 3.4 Arrangement by H-bonding interactions of 5-nitrosopyrimidinone **26**

	26
Bond length	
N(1)-C(2)	1.303(3)
N(1)-C(6)	1.374(3)
C(2)-N(3)	1.360(3)
C(2)-S(2)	1.743(2)
C(6)-N(6)	1.318(3)
Bond angle	
C(2)-N(1)-C(6)	116.9(2)
N(3)-C(2)-S(2)	113.38(18)
C(6)-N(6)-H(6B)	118.3(17)
O(4)-C(4)-N(3)	119.1(2)

Table 3.3 Selected bond lengths (Å) and angles (º) for pyrimidinone **26**

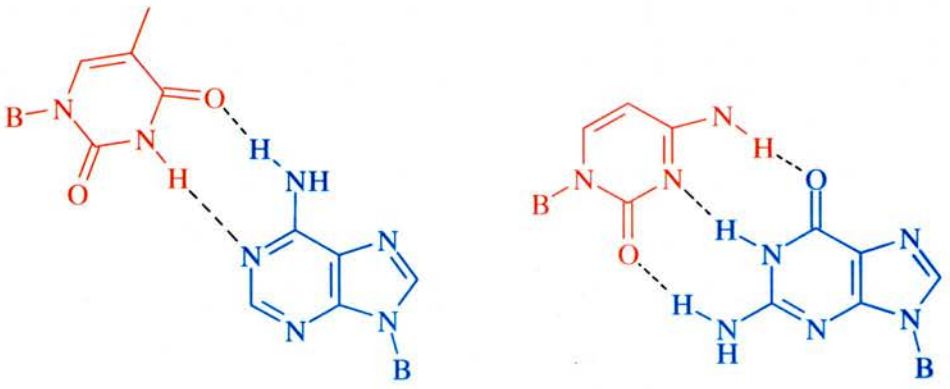

Adenine/thymine pairing

Guanine/Cytosine pairing

(B = 2-deoxyribose backbone)

Figure 3.5 Arrangement of H-bonding interactions of the DNA pairs AT and GC (H-bonds displayed as black dotted lines)

Reduction of the nitroso function of **26** with aqueous sodium dithionite in methanol readily afforded the 5,6-diaminopyrimidinone **27** required for the Traube reaction. The initial deep blue mixture gradually turned into a green mixture upon dropwise addition of the reducing solution. Filtration then thorough washings with water, acetone and ether afforded the diaminopyrimidinone **27** in 97% yield and full characterisation confirmed the purity of the product. The ESI$^-$ mass spectrum displays the molecular ion at *m/z* 247 thus $[M-1]^-$ while the results from the elemental analysis all lie within the ±0.4% limit for all elements. The melting point was also comparable to the reported value.

Treating the diaminopyrimidinone **27** with excess triethyl orthoformate and hydrochloric acid in DMF afforded 2-benzylsulfanylhypoxanthine **28** in good yield at room temperature, the product was precipitated as a yellow solid upon pouring of the dark solution on crushed ice, and isolated by filtration. Purification by washing with water then recrystallisation from absolute ethanol afforded the 2-benzylsulfanylhypoxanthine **28** as pale yellow needles. The data from the NMR, MS and IR spectra were consistent with the published data for this compound. XRD studies of the crystals afforded the structure shown in Figure 3.6. Due to the centrosymmetric packing through H-bonding between the oxygen O(6) and the hydrogen H(7N) of one hypoxanthine and the hydrogen H(7NB) and oxygen O(6B) of an adjacent molecule at a distance of 1.765(2) Å, the predominant tautomer of hypoxanthine **28** seems to be the 7*H* form rather than the 9*H* isomer as seen in Figure 3.6.

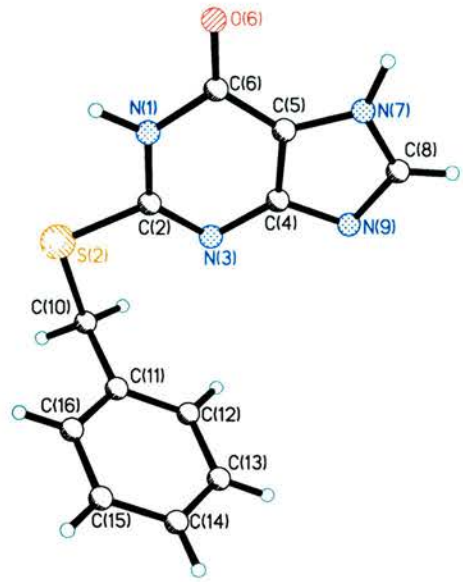

Figure 3.6 Crystal structure of hypoxanthine **28**

	28
Bond length	
N(1)-C(2)	1.381(2)
N(1)-C(6)	1.379(2)
C(2)-N(3)	1.304(2)
C(2)-S(2)	1.7580(19)
C(4)-C(5)	1.385(2)
N(7)-C(8)	1.349(2)
Bond angle	
C(2)-N(1)-C(6)	123.94(15)
N(3)-C(2)-S(2)	121.14(14)
C(2)-S(2)-C(10)	100.74(9)
N(9)-C(8)-N(7)	113.82(17)
N(7)-C(5)-C(4)	106.81(15)
O(6)-C(6)-C(5)	126.69(17)

Table 3.4 Selected bond lengths (Å) and angles (º) for hypoxanthine **28**

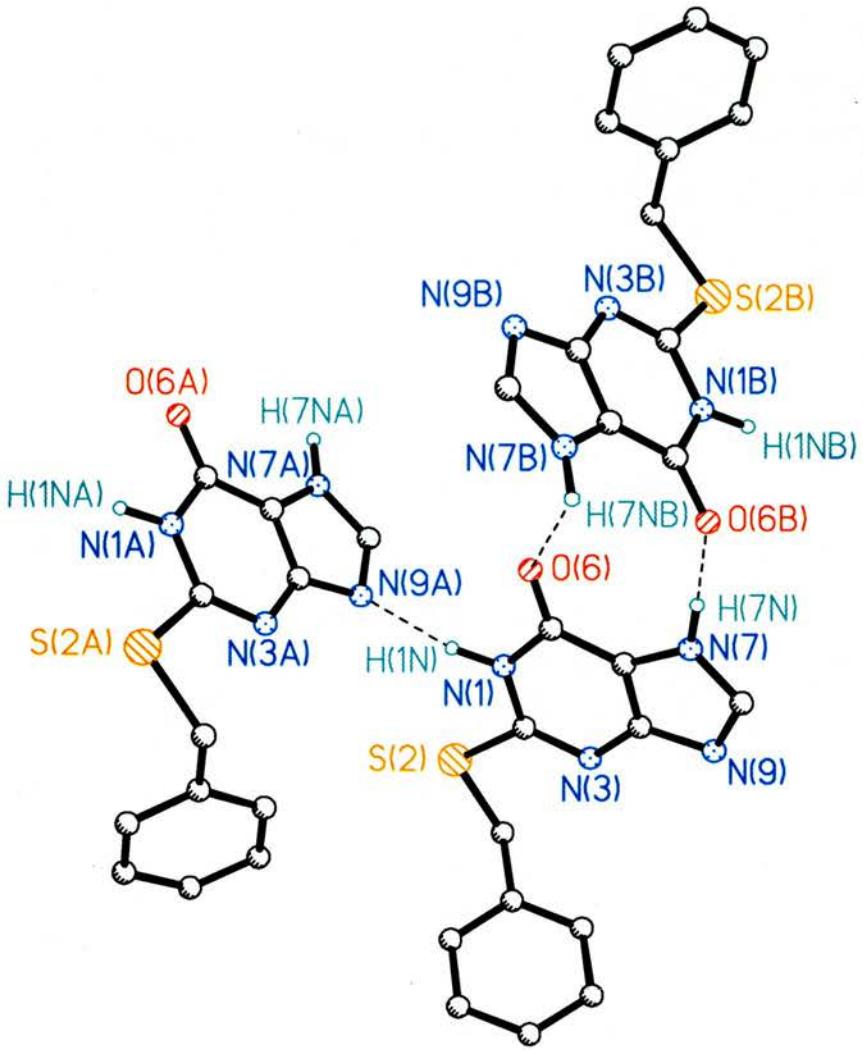

Figure 3.7 Hypoxanthine **28** showing hydrogen bonding between H(7) and O(6)

3.2.2 Attempted synthesis of purin-6-yl methanesulfonates

Direct conversion of hypoxanthine **28** into the purin-6-yl methanesulfonate ester with methanesulfonyl chloride in the presence of triethylamine[117] was not successful, even if the NMR, MS and elemental analysis data of the isolated crystalline solid fitted perfectly with the proposed structure **29c**. Reaction with *m*-chloroaniline resulted in the cleavage of the methanesulfonyl group, yielding a product that was characterised as the hypoxanthine precursor **28** (see scheme 3 below). Single crystal diffraction studies confirmed the structure as being the *N*-9-sulfonyl derivative **29a**. A suitable protecting group was thus necessary for further functionalisation of the 6-oxo moiety. The tritylation proceeded smoothly and only the 9-trityl derivative **29b** was isolated in 61% yield after flash column chromatography as crystalline needles suitable for XRD studies which confirmed the regioselectivity of the reaction.

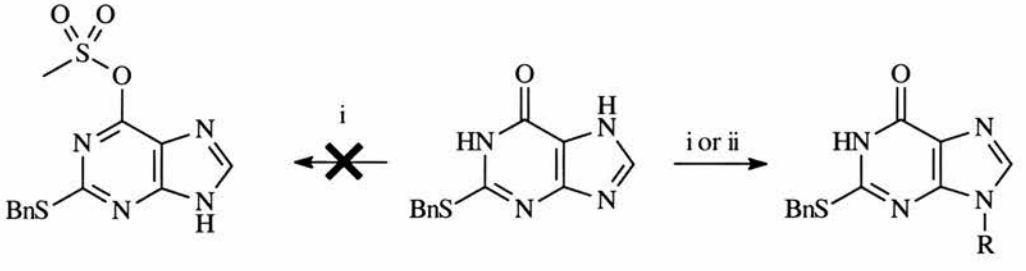

29c **28** **29a** (R = -SO_2Me) **29b** (R = -CPh_3)

Conditions: i) $MeSO_2Cl$, NEt_3, DCM, 0°C to r.t. (62%) ii) Ph_3CCl, NEt_3, DCM, 0°C to r.t. (61%)

Scheme 3.3 Synthesis of *N*-9 derivatives of hypoxanthine **28**

The crystal structures of N-9 substituted purines **29a** and **29b** are displayed in Figures 3.8 and 3.9. As for the former pyrimidinones **25** and **28**, the amide part of the molecule (-HN-C=O) favours the pairing arrangement through H-bonding interactions between the carbonyl oxygen of one molecule and the amide proton of the adjacent hypoxanthine with distances of 1.806(6) and 1.76 Å for respectively *N*-9 methanesulfonylpurine **29a** and the *N*-9 tritylpurine **29b**.

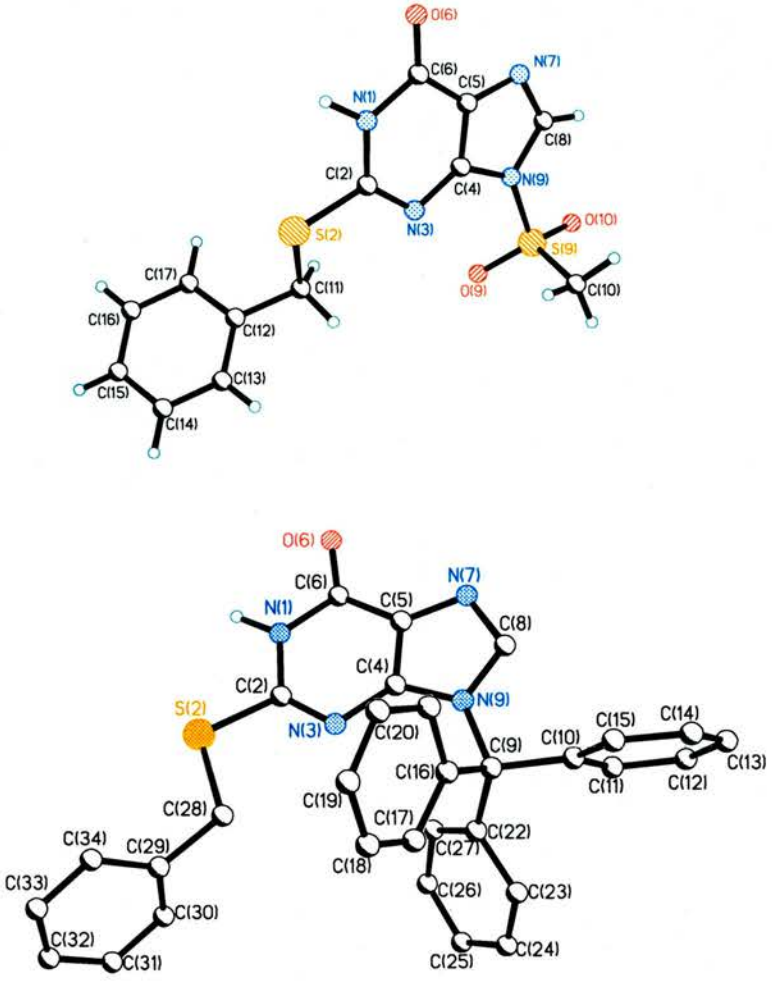

Figure 3.8 Crystal structure of *N*-9 methanesulfonylhypoxanthine **29a** and *N*-9 tritylhypoxanthine **29b**

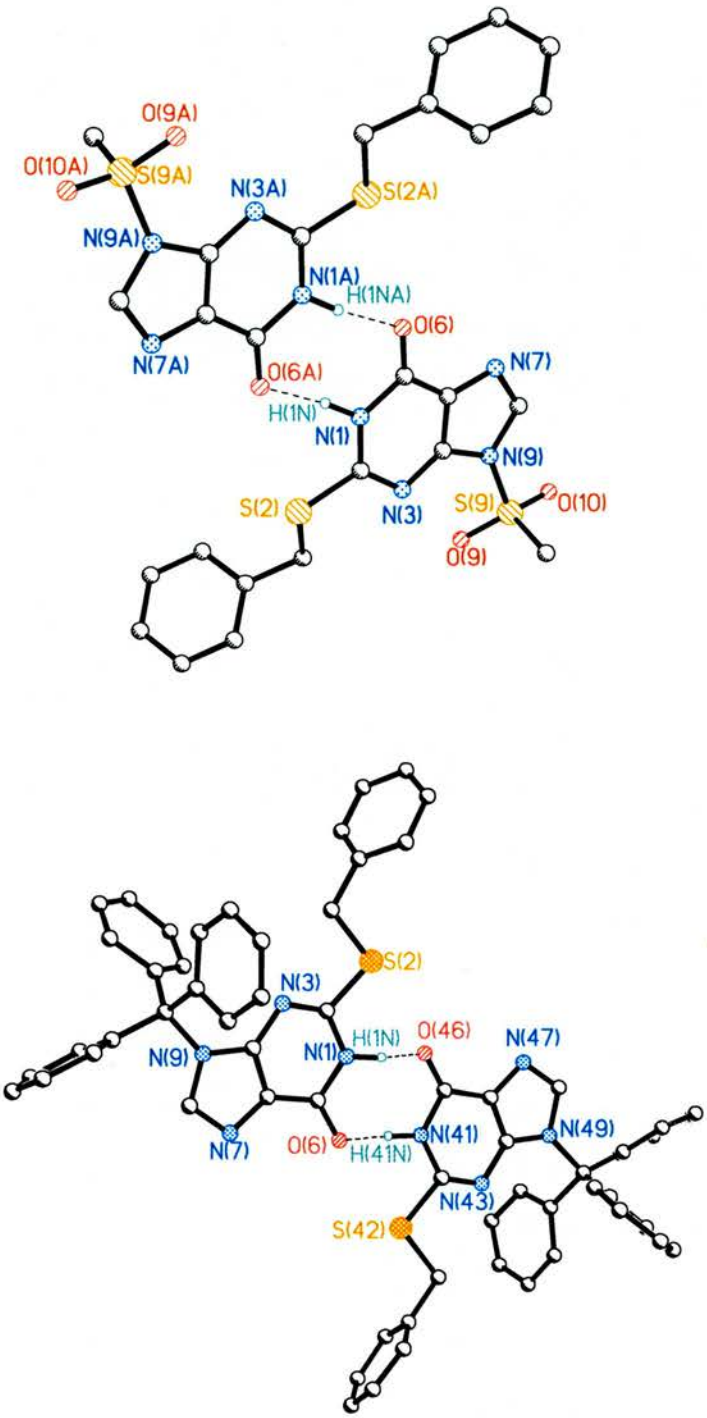

Figure 3.9 Similar dimer arrangements by amide H-bonding of hypoxanthines **29a** and **29b**

	29a	29b
Bond length		
N(1)-C(2)	1.366(3)	1.38(2)
N(1)-C(6)	1.394(3)	1.38(2)
C(2)-N(3)	1.314(3)	1.27(2)
C(2)-S(2)	1.749(3)	1.78(2)
C(4)-C(5)	1.378(4)	1.36(2)
N(7)-C(8)	1.313(4)	1.34(2)
Bond angle		
C(2)-N(1)-C(6)	125.2(2)	121.5(17)
N(1)-C(2)-S(2)	114.31(19)	112.6(14)
N(9)-C(4)-C(5)	104.4(2)	102.7(18)
N(7)-C(5)-C(4)	112.4(2)	115.8(19)
N(7)-C(5)-C(6)	129.7(2)	129(2)
C(4)-N(9)-C(8)	106.1(2)	108.8(17)

Table 3.5 Selected bond lengths (Å) and angles (º) for hypoxanthines **29a** and **29b**

In contrast to alkylation, sulfonylation of substituted hypoxanthines is known to occur frequently at oxygen rather than nitrogen[117]. It was thus assumed that treatment of hypoxanthine **29b** with methanesulfonyl chloride and triethylamine in dichloromethane would result in the desired *O*-mesyl compound that would act as a leaving group in nucleophilic substitutions. This approach was not successful with our *N*-9-tritylhypoxanthine **29b**. We assume that the *N*-

methanesulfonyl product **30b** was obtained instead in good yield as reacting it with *m*-chloroaniline in refluxing THF[114] yielded the **29b** precursor. Characterisation of purine **30b** by NMR was consistent with the introduction at the N-1 or O-6 but could not confirm the regioselectivity of the reaction, however the MS spectrum did not display neither the molecular ion nor peaks assignable to molecular fragments of **30b**. All attempts to obtain XRD quality single crystals were unsuccessful. The preparation and reactivity of the *O*-tosyl analogue of **29b** with *m*-chloroaniline was not investigated.

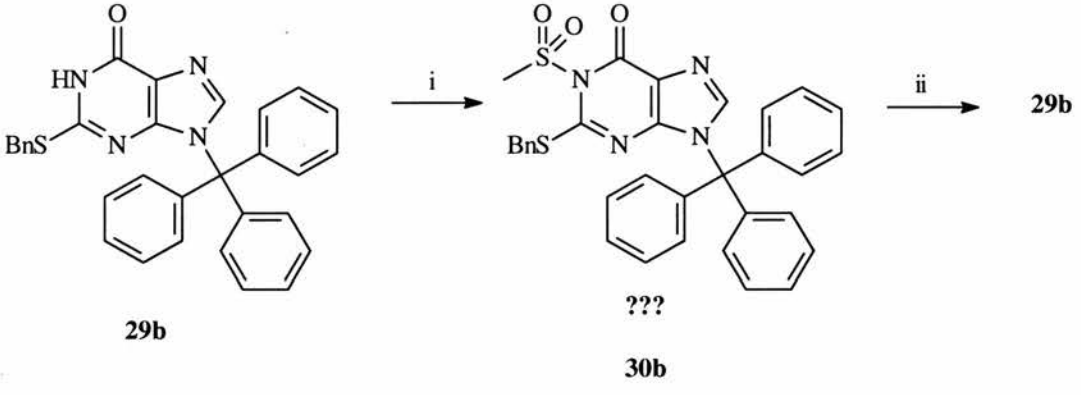

Conditions: i) $MeSO_2Cl$, NEt_3, DCM, 0°C to r.t. (98%) ii) *m*-chloroaniline, NEt_3, t-butanol, Δ

Scheme 3.4 Attempted synthesis of 6-*O*-methanesulfonyl derivative of 9-tritylhypoxanthine **29b**

Mitsunobu alkylation of hypoxanthines often occurs at *O*-6 rather than *N*-9 however we attempted a literature procedure[115] for a selective *N*-9 alkylation of hypoxanthine **28** (Scheme 3.5) in order to prepare the 2,6-diaminopurine precursor **31a**. The reaction proceeded to near completion according to TLC but the product was shown to be contaminated by the hydrazine by-product. As recrystallisations from several solvents failed to provide an analytically pure sample, the intermediate was used in the sulfonation without further purification. The elemental analysis, IR and MS spectra fitted with the possible regioisomers **31a** and **31b**. The regioselectivity of this synthetic sequence could not be determined by NMR but single crystal crystallography enabled the assignment of compound **31b**. Thus as anticipated, alkylation occurred at O-6 rather than N-9 so no further work was carried out.

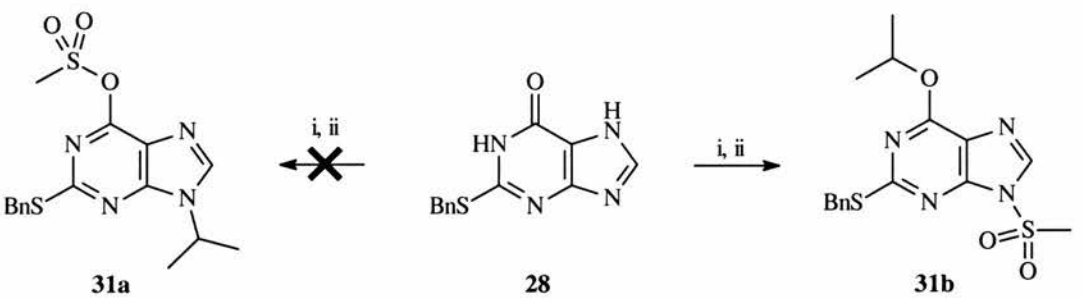

Conditions: i) Bu_3P, *i*-PrOH, THF, 0°C then DIAD, 2 days at r.t.
ii) $MeSO_2Cl$, NEt_3, DCM, 0°C to r.t. (16% over 2 steps)

Scheme 3.5 Attempted synthesis 9-isopropyl-6-*O*-mesylpurine **31a**

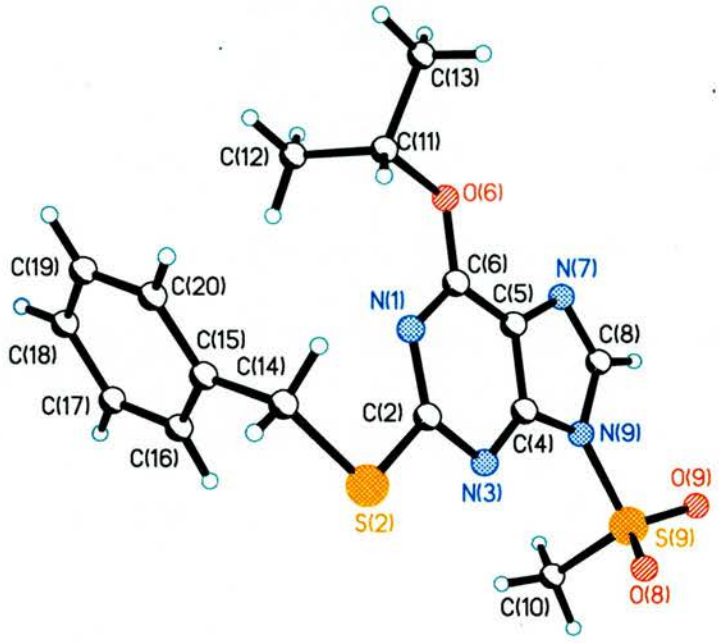

Figure 3.10 Crystal structure of purine **30b**

	30b
Bond length	
N(1)-C(2)	1.336(4)
C(6)-O(6)	1.326(4)
O(6)-C(11)	1.476(4)
S(2)-C(14)	1.805(4)
C(4)-N(9)	1.387(4)
N(7)-C(8)	1.298(4)
Bond angle	
C(2)-N(1)-C(6)	118.0(3)
N(3)-C(2)-S(2)	112.5(3)
C(6)-O(6)-C(11)	118.5(3)
C(8)-N(9)-S(9)	125.1(2)

Table 3.6 Selected bond lengths (Å) and angles (º) for hypoxanthine **30b**

3.2.3 Synthesis of Purvalanol A from 2-benzylsulfanyl-6-chloropurine

Chlorination of hypoxanthine **28** under anhydrous conditions[118] gave the novel 6-chloropurine **32** as crystalline needles following purification by chromatography in 89% yield (see Figure 3.11). The N(9) hydrogen of one molecule interacts by hydrogen bonding with the nitrogen N(7A) of an adjacent purine at a distance of 1.844(15) Å.

Reacting 6-chloropurine **32** under Mitsunobu conditions[119] with isopropanol and DEAD-Ph_3P only produced 20% of the desired *N*-9 substituted product **33a** that was contaminated with the hydrazine side-product **33b**, as shown in Scheme 3.6 below.

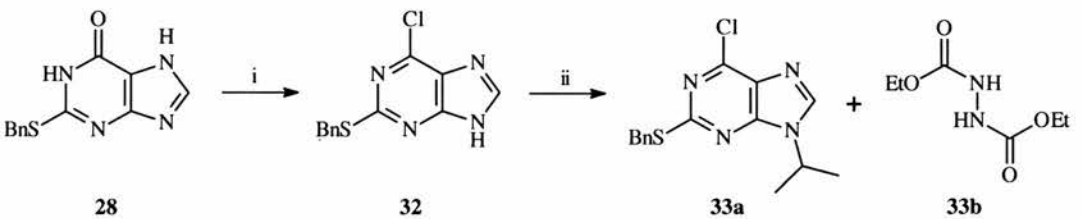

28 **32** **33a** **33b**

Conditions: i) $POCl_3$, DMA, NEt_4Cl, MeCN, 120°C (89%) ii) Ph_3P, THF, -10°C then DEAD, -10°C to r.t. (20%)

Scheme 3.6 Chlorination and Mitsunobu alkylation of purine **28**

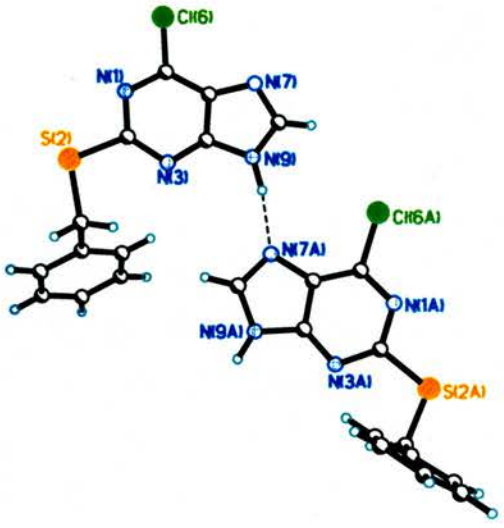

Figure 3.11 Crystal structure of purine **32**

	32
Bond length	
N(1)-C(2)	1.363(6)
C(6)-Cl(6)	1.732(4)
S(2)-C(2)	1.747(5)
C(13)-C(14)	1.483(6)
C(4)-N(9)	1.387(5)
N(7)-C(8)	1.319(5)
Bond angle	
C(2)-N(1)-C(6)	117.0(4)
N(1)-C(2)-S(2)	111.8(4)
C(6)-C(5)-N(7)	135.0(4)
N(3)-C(2)-N(1)	127.0(4)

Table 3.7 Selected bond lengths (Å) and angles (º) for 6-chloropurine **32**

However, a regioselective alkylation was successfully implemented with the DIAD-Ph_3P system in THF at -50ºC as analytically pure *N*-9-isopropylpurine **33a** was isolated as the only product after flash column chromatography in 69% yield and fully characterised.

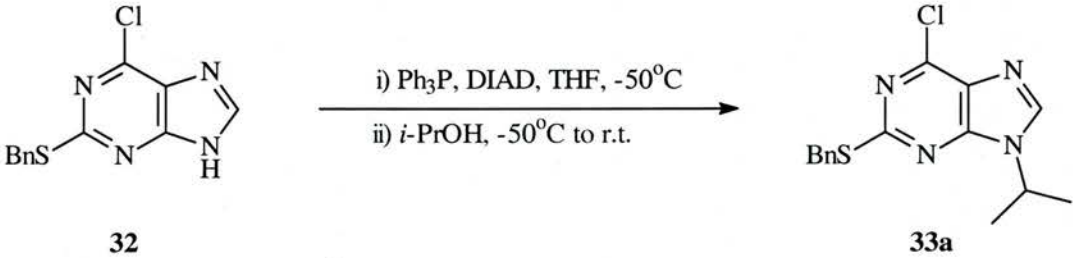

32 **33a**

Scheme 3.7 Regioselective Mitsunobu alkylation of purine **32**

HMBC NMR studies confirmed the regioselectivity of this alkylation since a $^{3}J(^{1}H\text{-}^{13}C)$ correlation was detected between the purine H-8 (δ 8.30) and the tertiary carbon of the *N*-9 isopropyl group (δ 49.9). Besides, more $^{3}J(^{1}H\text{-}^{13}C)$ correlations were seen between the tertiary isopropyl hydrogen –C<u>H</u>Me$_2$ (δ 4.73) and the C-4 (δ 153.9) and C-8 (δ 145.0) purine carbons. Recrystallisation from hexane provided single crystals as colourless plates suitable for crystallography. Figure 3.12 displays the crystal structure of 9-isopropylpurine **33a** and highlights the π-stacking of the purine rings.

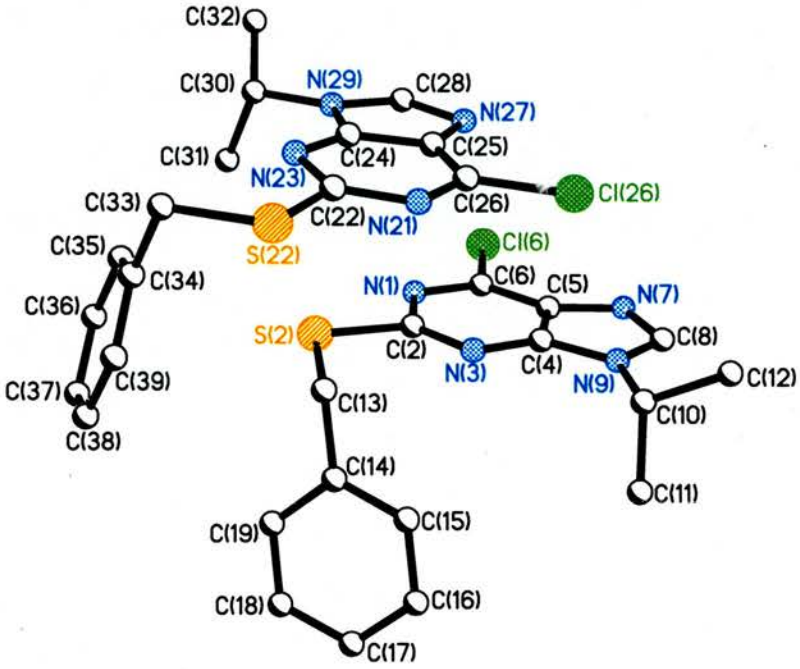

Figure 3.12 Crystal structure of purine **33a**

	33a
Bond length	
N(1)-C(6)	1.327(4)
C(6)-Cl(6)	1.736(3)
N(9)-C(10)	1.476(3)
S(2)-C(13)	1.819(3)
C(4)-C(5)	1.403(4)
C(2)-S(2)	1.762(3)
Bond angle	
C(6)-N(1)-C(2)	116.3(2)
N(1)-C(2)-S(2)	111.2(2)
N(9)-C(4)-C(5)	105.6(2)
C(12)-C(10)-C(11)	112.1(3)
C(2)-S(2)-C(13)	102.46(14)

Table 3.8 Selected bond lengths (Å) and angles (º) for purine **33a**

Complete oxidation with *m*-chloroperbenzoic of the 2-benzylsulfanylpurine **32** into the corresponding sulfone occurred at room temperature in dichloromethane in the presence of magnesium sulphate[112]. Suckling *et al* reported the formation of 2-oxopurine under these conditions[113] and recommended the use of dimethyldioxirane (DDO) as the best oxidising agent for 2-benzylsulfanylpurines. No 2-oxopurine was detected in our case and our procedure yielded the desired 2-sulfonylpurine as the main product. The reaction mixture was evaporated into a colourless powder that was used without further purification in the next reaction. Heating the sulfone in THF at 120ºC with R-valinol did not result in the nucleophilic displacement of the sulfonyl moiety by the amino alcohol as anticipated. Instead the corresponding 6-amino-2-

sulfonylpurine **34** was obtained and characterised by mass spectrometry (*m/z* 376.1437 thus $[M+H]^+$). This result was slightly unexpected as it had been reported that the benzylsulfanyl group reacted at room temperature with amines: no reaction occurred at room temperature in our hands or on gentle heating (45°C), so it was necessary to reflux the reaction mixture.

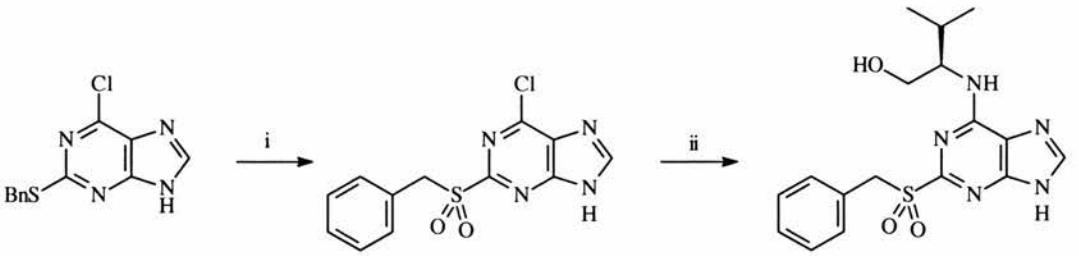

32 **34**

Conditions: i) $MgSO_4$, *m*-CPBA, DCM (100%) ii) R-valinol, THF, 120°C (44%)

Scheme 3.8 Unusual reactivity of purine **32**

It was thus necessary to introduce the aniline of Purvalanol A at the 6-position of purine **33a** prior to the oxidative cleavage of the benzylsulfanyl moiety with R-valinol at the 2-position. The traditionally used base catalysed conditions with aryl amines in the presence of triethylamine in refluxing ethanol[25] failed in our hands to yield the 6-anilinopurine (even in a sealed tube, conditions which failed for 2,6-dihalogenopurines in the previous Chapter). We discovered that the reaction proceeded to completion in the presence of small amounts of concentrated hydrochloric acid after 24 hours in refluxing *t*-butanol or *n*-butanol at ambient pressure. Purine **35** was isolated after neutralisation with triethylamine, extraction of the reaction mixture with dichloromethane then flash

column chromatography in 98% yield (see scheme 3.8). We believe that protonation at the N-1 position of the purine with the acid catalyst enhances the reactivity of the C-6 electrophilic carbon[120]. Nucleophilic substitution with the aniline then elimination of the catalyst (hydrochloric acid) enables the regain of aromaticity to generate the hydrochloride salt of purine **35**. In contrast, the base catalysed nucleophilic substitution with trimethylamine is known to generate a trimethylpurin-6-ylammonium chloride intermediate[121,122] that further reacts with primary and secondary aliphatic or aromatic amines as shown in Scheme 3.9.

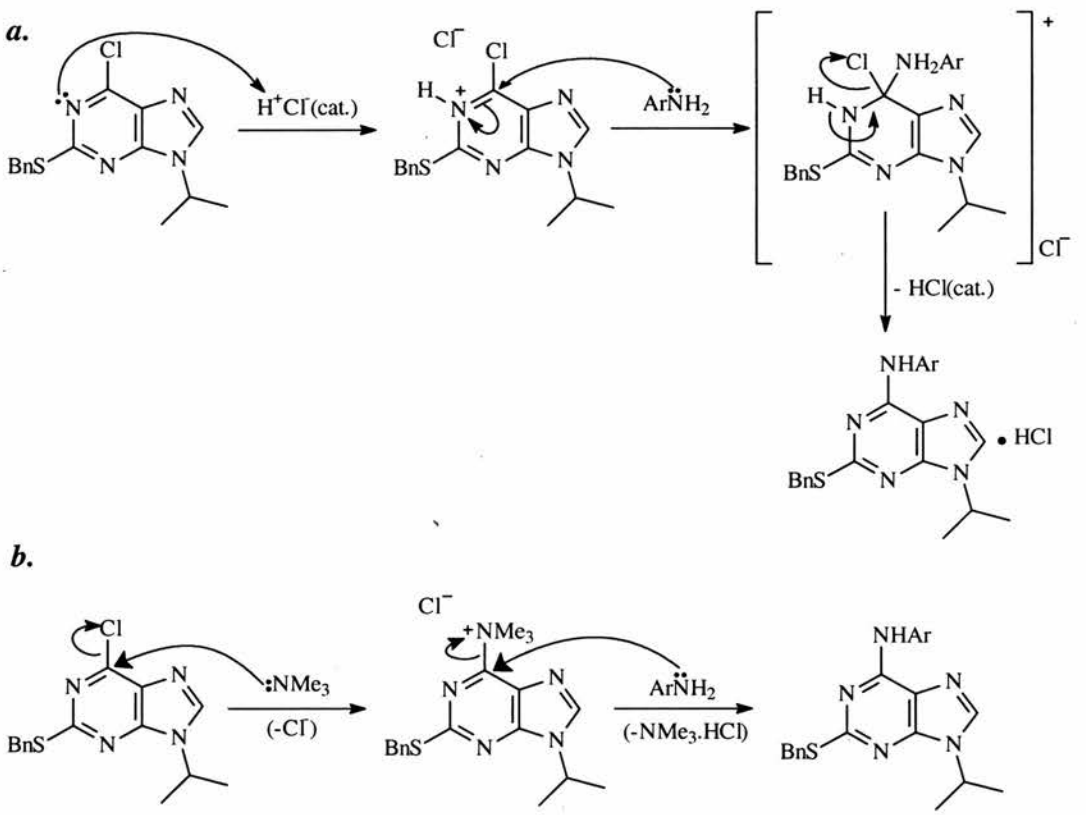

Scheme 3.9 ***a.*** Proposed mechanism for the acid catalysed S_NA_R

b. Reported mechanism for the base catalysed S_NA_R

Oxidation of the 2-benzylsulfanyl group with *m*-chloroperbenzoic was completed as previously and yielded the purine intermediate **36** in quantitative yield following flash column chromatography on silica gel. Unlike the 6-benzylsulfonylpurine series of page 81, we did not experience any problem of decomposition, confirming the lack of reactivity of the 2-benzylsulfonyl moiety with respect to the 6-chloride and the results obtained in Scheme 3.6 page 129. The ESI^+ mass spectrum displays the molecular ion at *m/z* 442.1114 thus $[M+H]^+$ while the IR spectrum features a sharp absorption at $3568cm^{-1}$ for the ν_{N-H} stretching and very intense $\nu_{S=O}$ signals at 1297 and $1131cm^{-1}$ for the sulfone group.

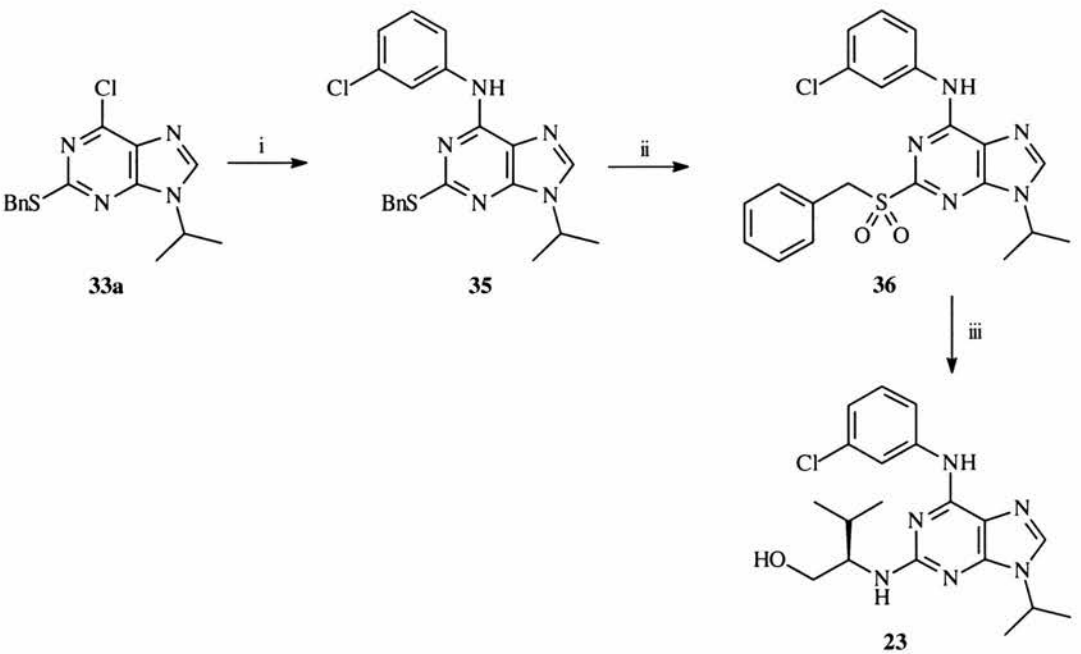

33a **35** **36** **23**

Conditions: i) *m*-chloroaniline, *n*-BuOH, cat.HCl, 120°C (98%) ii) MgSO4, *m*-CPBA, DCM (100%) iii) R-valinol, $EtN(Pr^i)_2$, *n*-BuOH, 160°C, sealed Parr bomb, 86%

Scheme 3.10 Synthesis of Purvalanol A **23** from the novel template **33a**

Finally, nucleophilic substitution with (*D*)-valinol was successful in a sealed Parr bomb at 160°C in *n*-butanol in the presence of *N,N,N*-diisopropylethylamine (Hunig's base) and Purvalanol A **23** was isolated following flash column chromatography in 86% yield. It was reported that the use of the benzylsulfonyl moiety as a leaving group is sometimes difficult in liquid phase synthesis due to the tricky separation of the benzylsulfinic acid side-product from the aminopurines but we did not experience such a problem. Given that the displacement with *m*-chloroaniline of 6-chloro-2-fluoropurine was reported by Schultz *et al* to occur only in a sealed tube at 140°C in *n*-butanol at a 56% yield, and that the displacement of 2-chloro, 2-iodo or even 2-fluoropurine with aliphatic amines are often incomplete, these results were particularly satisfactory.

3.3 ***Conclusions***

2-Benzylsulfanylhypoxanthine **28** has been easily prepared from thiourea and ethyl cyanoacetate over 5 steps in 80% yield using the well known Traube purine synthesis. All steps require little purification and the products are simply isolated by filtration and washings in near analytical purity so the preparation of this compound in multi-gram quantities is straightforward. X-Ray crystallography studies for most intermediates highlighted several sets of hydrogen bonding interactions occurring in the solid state for these pyrimidinones, some similar to the dimer arrangements of the DNA bases.

Attempts to functionalise the 6-oxy group into the *O*-methanesulfonyl leaving group were unsuccessful as substitution occurred at the *N*-9 position of hypoxanthine **28**. Protection with trityl chloride afforded the *N*-9 tritylpurine **29b** exclusively but reaction with methanesulfonyl chloride in the presence of triethylamine produced an unknown compound **30b**, which generated the hypoxanthine precursor **28** upon reaction with *m*-chloroaniline. Although the crystal structure could not be obtained we believe that sulfonylation occurred at the *N*-1 rather than at the normally favoured *O*-1 position. Another attempt to synthesise the desired diaminopurine template **31a** by Mitsunobu alkylation of **28** then sulfonylation afforded the 6-isopropoxy-9-methanesulfonylpurine **31b** instead.

Chlorination of hypoxanthine **28** was successful in completely anhydrous conditions and afforded the novel 6-chloropurine **32**, which could be alkylated at the *N*-9 position with the DIAD-Ph_3P-Pr^iOH system at -50°C to afford the 9-isopropylpurine **33a**. The regioselectivity was confirmed by HMBC NMR and XRD studies. Although purine **33a** was totally unreactive with *m*-chloroaniline in the traditional base catalysed S_NA_R conditions, we found that the reaction proceeded to completion with catalytic amounts of concentrated hydrochloric acid and have formulated a hypothetical mechanism to rationalise this result. Oxidative cleavage of the 2-benzylsulfanyl group with *m*-chloroperbenzoic acid then *R*-valinol was a high yielding sequence and afforded a potent diaminopurine CDK inhibitor, Purvalanol A **23**. To conclude, the reactivity of the novel 6-

chloro-2-benzylsulfanylpurine **33a** compares very favourably to dihalogenopurines and might represent a potentially useful template for the preparation of diaminopurines.

3.4 *Experimental*

6-Amino-2-thioxo-3*H*-4-pyrimidinone **24**

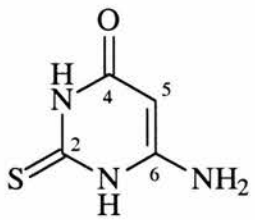

To ethanol (50mL), stirred under nitrogen at 0°C, was added sodium metal (1.52g, 66mmol) portionwise with evolution of hydrogen gas. When complete dissolution resumed, thiourea (4.56g, 60mmol) was added at room temperature, followed by ethyl cyanoacetate (6.40mL, 60mmol) and the mixture was refluxed with stirring for 24 hours. The resulting solution was concentrated into a yellow solid that was dissolved in water (50mL). Addition of concentrated hydrochloric acid afforded the desired pyrimidinone **4** as colourless needles (8.40g, 98%); mp=295°C (lit.[116] mp=295°C); ^{1}H NMR (300MHz, d_6-dmso) δ_H 4.68 (s, 1H, H5), 6.37 (broad s, 2H, N*H*$_2$), 11.52 (broad s, 1H, N*H*), 11.63 (broad s, 1H, N*H*); ^{13}C NMR (75.5MHz, d_6-dmso) δ_C 78.5 (C5), 154.7 (C6), 162.0 (C4), 174.9 (C2); MS (ESI$^+$): *m/z* 142 [M-H]$^-$, $C_4H_4N_3OS$ requires 142.0075; IR (KBr disc, cm^{-1}): 3428s, 3325s, 3206s, 3092s, 2965s, 2905s, 1629vs, 1596s, 1546vs, 1439s, 1298s, 1246m, 1185s,

1071m, 999w, 924m, 830m, 791s, 686w, 613m, 575m, 525m; Microanalytical data found: C: 33.72 H: 3.79 N: 29.87 S: 22.07, expected for $C_4H_5N_3OS$ C: 33.56 H: 3.52 N: 29.35 S: 22.40; Crystals suitable for X-Ray crystallography were obtained by recrystallisation from ethanol/water 1:1.

6-Amino-2-benzylsulfanyl-3*H*-4-pyrimidinone **25**

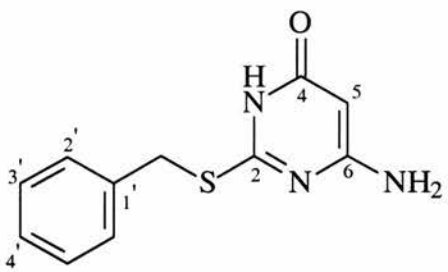

To ethanol (200mL), stirred under nitrogen in a dry ice cooling bath, was added sodium metal (6.08g, 0.24mol) portionwise with evolution of hydrogen gas. When complete dissolution resumed, thiourea (18.24g, 0.24mol) was added at room temperature, followed by diethyl cyanoacetate (25.6mL, 0.24mol) and the resulting mixture was refluxed with stirring for 24 hours. Benzyl chloride (42mL, 0.72mol) was added after cooling the reaction mixture and stirring was continued overnight under nitrogen. The solvent was removed under vacuum to result in a yellowish oily solid. Trituration with acetone (150mL) afforded a colourless solid that was filtered off, washed thoroughly with water, diethyl ether and acetone and dried extensively on the vacuum line to afford the 2-benzylsulfanypyrimidinone **25** (54.80g, 98%) as a colourless powder; mp=297°C (lit.[113] mp=297°C); ^{1}H NMR (300MHz, d_6-dmso) δ_H 4.32 (s, 2H, PhC*H*$_2$S-), 4.96 (s, 1H, H5), 6.59 (broad s, 2H, N*H*$_2$), 7.19-7.32 (m, 3H, aromatics *Ph*CH$_2$S-), 7.40-7.43 (m, 2H, aromatics

PhCH_2S-), 11.50 (very broad, N*H*); ^{13}C NMR (75.5MHz, d_6-dmso) δ_C 33.6 (PhC*H*$_2$S-), 81.7 (C5), 127.5 (Ph C4'), 128.7 (Ph C2'), 129.5 (Ph C3'), 138.3 (Ph C1'), 162.6 (C2), 163.9 (C4), 164.9 (C6); MS (CI^+): *m/z* 234 $[M-H]^-$, $C_{11}H_{11}N_3OS$ requires 233.06228; IR (KBr disc, cm^{-1}): 3449vs, 3295m, 3152s, 3052m, 2692m, 2830m, 1637vs, 1600vs, 1542vs, 1495s, 1443s, 1304s, 1253m, 1219s, 1089m, 1071m, 1013m, 981s, 921m, 867m, 818m, 771w, 714m, 694m, 605w, 591m, 565m, 528m; Microanalytical data found: C: 56.50 H: 4.68 N: 17.94 S: 13.66, expected for $C_{11}H_{11}N_3OS$ C: 56.63 H: 4.75 N: 18.01 S: 13.74; Crystals suitable for X-Ray crystallography were obtained by recrystallisation from MeOH.

6-Amino-2-benzylsulfanyl-5-nitroso-3*H*-4-pyrimidinone **26**

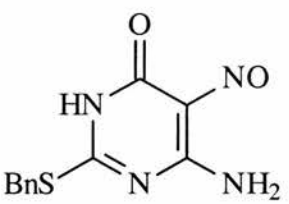

To a mixture of pyrimidinone **25** (55.92g, 0.24mol) in water (700mL) was added sodium hydroxide (13.24g, 0.33mol). After one hour of stirring, sodium nitrite (20.33g, 0.29mol) in water (100mL) was added to result in a partial yellowish solution. Acetic acid (100mL) was added dropwise over one hour to result in a dark blue foamy mixture. Stirring was continued for 3 days. The dark blue precipitate was filtered off, washed thoroughly with water, diethyl ether and acetone to afford after drying the 5-nitrosopyrimidinone **26** as a intensively blue powder (57.85g, 92%); mp=183°C (lit.[113] mp=185-187°C); ^{1}H (300 MHz, d_6-

dmso) δ_H 4.40 (s, 2H, PhC*H*$_2$S-), 7.22-7.33 (m, 3H, aromatics *Ph*CH$_2$S-), 7.46-7.48 (m, 2H, aromatics *Ph*CH$_2$S-), 9.18 (broad s, 1H, N*H*), 11.25 (broad s, 1H, N*H*), 12.72 (broad s, 1H, -CO-N*H*-); ^{13}C (75.4 MHz, d_6-dmso) δ_C 34.1 (Ph*C*H$_2$S-), 127.9 (Ph C2'), 128.9 (Ph C3'), 129.7 (Ph C4'), 137.2 (Ph C1'), 143.4 (C5), 147.1 (C6), 161.6 (C4), 167.5 (C2); MS (ESI$^-$): *m/z* 261 [M-H]$^-$, $C_{11}H_{10}N_4O_2S$ requires 262.05244; IR (KBr disc, cm^{-1}) 3449m, 3305m, 3156m, 3031m, 2914m, 1682vs, 1616vs, 1546vs, 1495vs, 1454vs, 1354m, 1304s, 1256s, 1217s, 1173s, 1126m, 1072m, 1028m, 968m, 917w, 817w, 787m, 695s, 565w, 537w; Microanalytical data found: C: 50.09 H: 4.05 N: 21.48 S: 11.95, expected for $C_{11}H_{10}N_4O_2S$ C: 50.37 H: 3.84 N: 21.36 S: 12.22; Crystals suitable for X-Ray crystallography were obtained by recrystallisation from MeOH/EtOH/water 1:1:1.

5,6-Diamino-2-benzylsulfanyl-3*H*-pyrimidin-4-one **27**

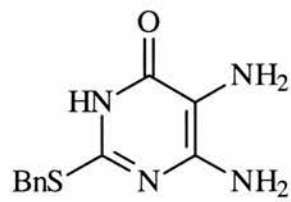

To a stirred suspension of 5-nitrosopyrimidinone **26** (23.66g, 90.3mmol) in methanol (200mL) was added a solution of sodium dithionite (99.68g, 519.2mmol) in water (200mL) with a gradual colour change from dark blue to pale green. Overnight stirring resulted in a greeny foamy mixture. The precipitated was filtered off, washed with water, acetone and ether to afford after drying the 5,6-diaminopyrimidinone **27** (21.72g, 97%) as a off-white powder, mp

185°C (lit.[113] 185-187°C); ^{1}H (300 MHz, d_6-dmso) δ_H (300 MHz, d_6-dmso, 25°C) 4.28 (s, 2H, PhCH_2S-), 5.81 (broad s, 2H, NH_2), 7.19-7.30 (m, 3H, aromatics), 7.38-7.42 (m, 2H, aromatics); ^{13}C (75.4 MHz, d_6-dmso) δ_C (75.4 MHz, d_6-dmso, 25°C); MS (ESI$^-$): *m/z* 247 [M-H]$^-$, $C_{11}H_{12}N_4OS$ requires 248.07318; IR (KBr disc, cm^{-1}) 3464s, 3353s, 2770s, 1626vs, 1497s, 1466s, 1427s, 1354s, 1275s, 1225s, 1194m, 1072w, 1028w, 1003w, 960s, 923m, 866m, 810w, 783w, 760s, 746m, 718s, 699m, 627m, 591w, 547m; Microanalytical data found: C: 53.55 H: 4.50 N: 22.97 S: 13.20, expected for $C_{11}H_{12}N_4OS$ C: 53.21 H: 4.87 N: 22.56 S: 12.91.

2-Benzylsulfanyl-7*H*-purin-6-one **28**

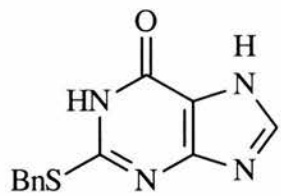

To a stirred suspension of 5,6-diaminopyrimidinone **27** (59.52g, 0.24mol) in N,N-dimethylformamide (100mL) was added under a nitrogen atmosphere triethyl orthoformate (350mL, 2mol) and concentrated hydrochloric acid (10mL). Stirring of the resulting dark red solution under nitrogen was continued for 2 days. The yellowish precipitate was filtered off, washed with water and recrystallised from ethanol to yield after drying the 2-substituted hypoxanthine **28** as colourless needles (56.97g, 92%), mp = 260°C (lit.[113] 263-265°C); R_f 0.14 [DCM/MeOH 95:5]; ^{1}H (300 MHz, d_6-dmso) δ_H (300 MHz, d_6-dmso) δ_H 4.43 (s, 2H, PhCH_2S-), 7.21-7.32 (m, 3H, aromatics), 7.42-7.45 (s, 2H, aromatics), 8.05 (broad s, 1H,

H8), 12.50 (broad s, 1H, NH); ^{13}C (75.4 MHz, d_6-dmso) δ_C 33.9 (s, $PhCH_2S$-), 115.1 (s, purine C5), 127.3 (s, Ph C4'), 128.4 (s, Ph C2'), 129.1 (s, Ph C3'), 136.8 (s, Ph C1'), 139.1 (s, purine C8), 151.4 (s, purine C4), 154.9 (s, purine C2), 156.5 (s, purine C6); MS (ESI^-): *m/z* 257 $[M-H]^-$, $C_{12}H_{10}N_4OS$ requires 258.05753; IR (KBr disc, cm^{-1}) 3104s, 2890m, 284m, 1682vs, 1572s, 1536m, 1514m, 1494m, 1452s, 1386m, 1359s, 1266w, 1225s, 1153m, 1116m, 1071w, 1027w, 959m, 912w, 858w, 818w, 785m, 775w, 762w, 696s, 670w, 614w, 565w, 536w; Microanalytical data found: C: 55.69 H: 3.72 N: 21.56 S: 12.13, expected for $C_{12}H_{10}N_4OS$ C: 55.80 H: 3.90 N: 21.69 S: 12.41. Crystals suitable for X-Ray crystallography were obtained by recrystallisation from acetone.

2-Benzylsulfanyl-9-methanesulfonyl-hypoxanthine **29a**

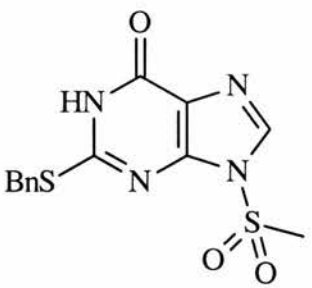

To a mixture of hypoxanthine **28** (1g, 3.86mmol) and DMAP (30mg, 0.23mmol) in DCM (40mL) was added triethylamine (6.4mL, 45.8mmol) at 0C under a nitrogen atmosphere. Methanesulfonyl chloride (0.45mL, 5.70mmol) was added dropwise and stirring under nitrogen was continued overnight at room temperature. The colourless precipitate was filtered off and washed once with cold DCM, then the filtrate was evaporated to full dryness into a yellow solid that was purified by flash column chromatography on silica gel using 2% MeOH in

DCM to afford the 9-methanesulfonylhypoxanthine **29a** as colourless needles (807mg, 62%), decomposition at 200°C; R_f 0.32 [DCM/MeOH 95:5]; ^1H (300 MHz, d_6-dmso) δ_H 3.74 (s, 3H, $-SO_2CH_3$), 4.47 (s, 2H, $PhCH_2S-$), 7.21-7.34 (m, 3H, Ph aromatics), 7.47-7.52 (m, 2H, Ph aromatics), 8.24 (s, 1H, hypoxanthine H8); ^{13}C (75.4 MHz, d_6-dmso) δ_C 34.5 ($PhCH_2S-$), 42.6 ($-SO_2CH_3$), 118.8 (hypoxanthine C5), 127.8 (Ph C2'), 128.9 (Ph C3'), 129.5 (Ph C4'), 137.1 (hypoxanthine C8), 137.3 (Ph C1'), 147.2 (hypoxanthine C6), 156.8 (hypoxanthine C4), 159.6 (hypoxanthine C2); MS (EI): *m/z* 337.0433 $[M]^+$, $C_{13}H_{12}N_4O_3S_2$ requires 337.0429; IR (KBr disc, cm^{-1}) 3102m, 3012m, 2931m, 2912m, 1702vs, 1542m, 1467w, 1375s, 1323m, 1262w, 1227m, 1183s, 1154m, 968w, 873w, 790w, 763m, 697w, 671m, 627w, 580w, 545m, 513w; Microanalytical data found: C: 46.52 H: 3.60 N: 16.38 S: 19.25, expected for $C_{13}H_{12}N_4O_3S_2$ C: 46.42 H: 3.60 N: 16.66 S: 19.06. Crystals suitable for X-Ray crystallography were obtained by recrystallisation from acetone.

2-Benzylsulfanyl-9-trityl-hypoxanthine **29b**

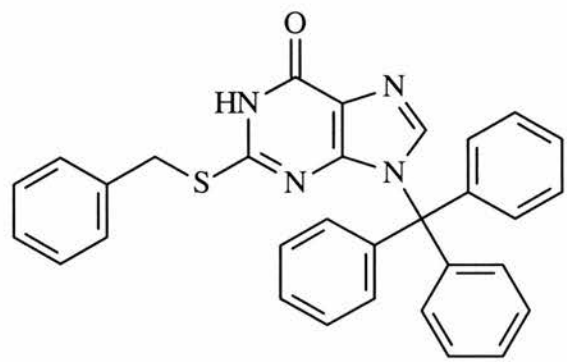

To a vigorously stirred suspension of hypoxanthine **28** (5g, 19.5mmol) in anhydrous dichloromethane (50mL) was added triethylamine (4.6mL, 29mmol)

under nitrogen. Following cooling to 0°C, a solution of trityl chloride (8g, 29mmol) in anhydrous dichloromethane (50mL) was added dropwise. Stirring under nitrogen was continued for 24 hours at room temperature and the reaction was monitored by TLC. The solvent volume was reduced in vacuum to a few mL and purification of the crude reaction mixture by flash column chromatography on silica gel with 2.5% methanol in dichloromethane yielded the expected 9-tritylhypoxanthine **28b** as colourless crystalline needles (5.95g, 61%), mp = 268°C (lit., 267-270°C); R_f 0.61 [DCM/MeOH 95:5]; ^{1}H (300 MHz, d_6-dmso) δ_H 3.45 (s, 2H, PhCH_2S-), 6.82-7.25 (m, 20H, trityl and benzyl aromatics), 7.56 (s, 1H, hypoxanthine H8), 12.44 (broad s, 1H, amide NH); ^{13}C (75.4 MHz, d_6-dmso) δ_C 33.6 ((Ph*C*H$_2$S-), 74.8 (N*C*Ph$_3$), 121.8 (C5), 126.2 (C2'), 126.9 (C6'), 127.0 (C7'), 127.4 (C3'), 127.8 (C4'), 128.9 (C8'), 135.2 (C1'), 139.2 (C8), 140.2 (C5'), 149.4 (C6), 154.8 (C4), 158.6 (C2); MS (ESI$^+$): *m/z* 501.1744 $[M+H]^+$, $C_{31}H_{24}N_4OS$ requires 501.1744; IR (KBr disc, cm^{-1}) 3053m, 3029m, 3002m, 2868m, 2840m, 1679vs, 1599m, 1561s, 1541s, 1494s, 1467m, 1443s, 1407w, 1349s, 1316m, 1244m, 1205vs, 1159m, 1144m, 1070w, 1036w, 1001w, 954w, 907w, 872m, 785w, 776w, 764m, 751s, 700vs, 681m, 670m, 649m, 609m, 563w, 553m, 505w; Microanalytical data found: C: 74.52 H: 5.25 N: 11.30 S: 6.89, expected for $C_{31}H_{24}N_4OS$ C: 74.38 H: 4.83 N: 11.19 S: 6.40. Crystals suitable for X-Ray crystallography were obtained by recrystallisation from layering a DCM solution with hexane.

2-Benzylsulfanyl-6-isopropoxy-9-mesyl-hypoxanthine **31b**

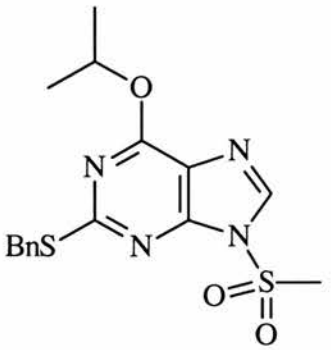

To a mixture of hypoxanthine **28** (2.5g, 9.8mmol) in THF (50mL) was added under a nitrogen atmosphere isopropanol (1.5mL, 19.5mmol) and tributylphosphine (4.9mL, 19.5mmol). Following cooling to -10°C, a solution of DIAD (3.9mL, 19.5mmol) in THF (50mL) was added dropwise at the same temperature, then the resulting red solution was stirred at 0°C for 3 hours, then at room temperature for 2 days under nitrogen. Evaporation under vaccum of the solvent afforded a reddish oil that was purified by flash chromatography on silica gel using 1-2.5% MeOH in DCM to afford a colourless solid that was triturated with hexane to remove the tributylphosphine oxide by-product. Washing of the precipitate with more hexane then drying afforded the alkylated hypoxanthine (R_f = 0.60 [DCM/MeOH 95:5], MS (ESI^+) *m/z* 301.1116 $[M+1]^+$, $C_{15}H_{16}N_4OS$ requires 301.1118). Triethylamine (2.8mL) was added to a solution of the alkylated hypoxanthine (500mg, 1.67mmol) and DMAP (13mg, 0.10mmol) in DCM (20mL) at room temperature under a nitrogen atmosphere. A solution of methanesulfonyl chloride (0.2mL, 2.45mmol) in DCM (20mL) was added dropwise at 0°C under nitrogen and stirring was continued for 24 hours. The triethylamine hydrochloride precipitate was filtered off and washed with cold DCM then the filtrate was evaporated to dryness into a colourless foam that was

purified by flash column chromatography on silica gel using 0.5% MeOH in DCM to afford the 6-isopropoxy-9-mesylpurine **31b** as crystalline plates (598mg, 16%); mp = 120°C; R_f 0.24 [DCM]; ^{1}H (300 MHz, d_6-dmso) δ_H 1.36 (d, $^3J_{H\text{-}H}$ = 6.61Hz, 6H, purine -CH(CH_3)$_2$), 3.36 (s, 3H, CH_3SO_2-), 4.36 (s, 2H, PhCH_2S-), 5.52 (s, $^3J_{H\text{-}H}$ = 6.61Hz, 1H, purine -C*H*(CH_3)$_2$), 7.13-7.26 (m, 3H, aromatics *Ph*CH_2S-), 7.38-7.42 (m, 2H, aromatics *Ph*CH_2S-), 8.03 (s, 1H, purine H8); ^{13}C (75.4 MHz, d_6-dmso) δ_C 21.8 (s, purine -CH(CH_3)$_2$), 35.9 (s, PhCH_2S-), 42.3 (s, CH_3SO_2-), 71.6 (s, purine -*C*H(CH_3)$_2$), 119.4 (s, purine C5), 127.2 (s, Ph C4'), 128.5 (s, purine C2'), 128.7 (s, purine C3'), 137.2 (s, Ph C1'), 137.4 (s, purine C8), 151.3 (s, purine C2), 160.12 (s, purine C2), 167.5 (s, purine C6); MS (ESI$^+$): *m/z* 379.0896 $[M+H]^+$, $C_{16}H_{18}N_4O_3S_2$ requires 379.0893; IR (KBr disc, cm^{-1}) 3102m, 3012m, 2931m, 2551m, 1625m, 1578vs, 1498wm, 1423s, 1373vs, 1318s, 1213s, 1177vs, 1145vs, 1103s, 966m, 908m, 861m, 832m, 799m, 789m, 774m, 702m, 654m, 626m, 572w, 551s, 515m; Microanalytical data found: C: 50.74 H: 4.85 N: 14.52 S: 16.68, expected for $C_{16}H_{18}N_4O_3S_2$ C: 50.78 H: 4.80 N: 14.81 S: 16.91. Crystals suitable for X-Ray crystallography were obtained by crystallisation from $CDCl_3$.

2-Benzylsulfanyl-6-chloropurine **32**

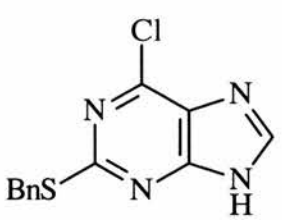

To thoroughly dried hypoxanthine **28** (500mg, 1.93mmol) and tetraethylammonium chloride (530mg, 3.20mmol) was added anhydrous acetonitrile (5mL) then DMA (0.25mL, 1.37mmol) under a nitrogen atmosphere. Phosphorus oxychloride (1mL, 11.9mmol) was added dropwise under nitrogen and the reaction mixture was then refluxed for 30 minutes at 120°C under nitrogen, to result in a orangish solution. Following cooling, pouring on to crushed ice (50mL), then partitition with DCM (3x35mL), the organics were dried over potassium carbonate and the solvent volume was reduced to about 10mL. Addition of hexane precipitated the 6-chloropurine **32** as a pale yellow solid (427mg, 89%); mp = 154°C; R_f 0.29 [DCM/MeOH 95:5]; ^{1}H (300 MHz, d_6-dmso) δ_H 4.49 (s, PhCH_2S-), 7.26-7.38 (m, 3H, aromatics *Ph*CH_2S-), 7.50-7.52 (s, aromatics *Ph*CH_2S-), 8.59 (s, purine H8); ^{13}C (75.4 MHz, d_6-dmso) δ_C 35.1 (s, Ph*C*H_2S-), 114.7 (s, purine C5), 127.5 (s, Ph C4'), 128.8 (s, Ph C2'), 129.4 (s, Ph C3'), 137.8 (s, purince C1'), 145.7 (s, purine C8), 155.9 (s, purine C4), 161.8 (s, purine C6), 163.5 (s, purine C2); MS (ESI$^-$): *m/z* 276.0158 [M-H]$^-$, $C_{12}H_9N_4SCl$ requires 275.0158; IR (KBr disc, cm^{-1})3067m, 3024m, 2964m, 2917m, 2768m, 2658m, 2543m, 1612s, 1557s, 1480w, 1454w, 1410w, 1376m, 1356vs, 1292m, 1262vs, 1216s, 1168m, 1155m, 1096s, 1072s, 1017s, 951m, 865m, 855s, 800s, 763m, 698m, 686w, 677w, 637m, 622w, 589w, 565w, 549w; Microanalytical data found: C: 52.75 H: 3.79 N: 20.12 S: 11.46, expected for $C_{12}H_9N_4SCl$ C: 52.17 H: 3.29 N: 20.29 S: 11.58. Crystals suitable for X-Ray crystallography were obtained by recrystallisation from DCM/hexane.

2-Benzylsulfanyl-6-chloro-9-isopropylpurine **33a**

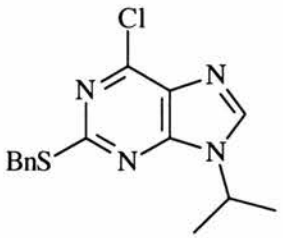

To thoroughly dried 6-chloropurine **32** (400mg, 1.45mmol) and triphenylphosphine (420mg, 1.6mmol) in a flame-dried round-bottomed Schlenk flask was added anhydrous THF (10mL) and the resulting solution was cooled to -50°C. DIAD (0.33mL, 1.6mmol) was added dropwise under nitrogen at the same temperature with stirring continued for 15 minutes then isopropanol (0.12mL, 1.6mmol) was added dropwise to the yellow mixture at -50°C. The resulting solution was gradually warmed to room temperature and stirred for 3 days under nitrogen. Following evaporation to full dryness the oily residue was purified by flash column chromatography on silica gel using petroleum ether 40-60°C then 1:1 EtOAc/Petroleum ether to afford the 9-isopropylpurine **33a** as a pale yellow solid (320mg, 69%); mp = 76-78°C; R_f 0.38 [EtOAc/hexane 2:1]; ^{1}H (300 MHz, MeOD) δ_H 1.47 (d, $^3J_{H\text{-}H}$ = 6.66Hz, 6H, purine CH(C*H*$_3$)$_2$), 4.28 (s, 2H, PhC*H*$_2$S-), 4.73 (septet, $^3J_{H\text{-}H}$ = 6.66Hz, 1H, purine C*H*(CH$_3$)$_2$), 7.00-7.13 (m, 3H, aromatics *Ph*CH$_2$S-), 7.29-7.31 (m, 2H, aromatics *Ph*CH$_2$S-), 8.30 (s, 1H, purine H8); ^{13}C (75.4 MHz, MeOD) δ_C 22.8 (s, purine CH(*C*H$_3$)$_2$), 37.1 (s, Ph*C*H$_2$S-), 50.2 (s, purine *C*H(CH$_3$)$_2$), 128.6 (s, Ph C4'), 129.8 (s, Ph C2'), 129.9 (s, purine C5), 130.4 (s, Ph C2'), 139.2 (s, Ph C1'), 145.4 (s, purine C8), 151.3 (s, purine C6), 153.9 (s, purine C4), 166.5 (s, purine C2); MS (ESI$^+$): *m/z* 341.0602 [M+Na]$^+$, $C_{15}H_{15}N_4SClNa$ requires 341.0604; IR (KBr disc, cm^{-1}) 3106m,

3083m, 3050m, 3026m, 3022m, 2975m, 2925m, 2864m, 1780w, 1733w, 1693w, 1588vs, 1546vs, 1495vs, 1495s, 1457s, 1410s, 1359vs, 1240s, 1211s, 1186s, 1156s, 1132s, 1104s, 1081m, 1025m, 958s, 895wm, 868s, 772s, 703m, 648s, 622s, 570m, 565m; Microanalytical data found: C: 56.97 H: 4.28 N: 17.53 S: 10.60, expected for $C_{12}H_9N_4SCl$ C: 56.59 H: 4.75 N: 17.61 S: 10.05. Crystals suitable for X-Ray crystallography were obtained by recrystallisation from hexane.

(*R*)-2-(2-benzylsulfonyl-9*H*-purin-6-ylamino)-3-methyl-butan-1-ol **34**

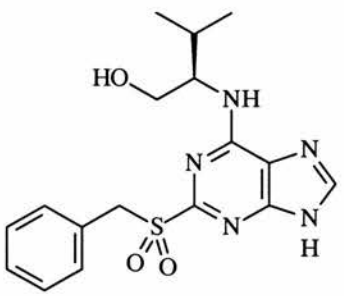

A mixture of *m*-chloroperbenzoic acid (284mg, 1.15mmol) and magnesium sulphate (400mg,) in DCM (5mL) was stirred overnight under nitrogen. Following filtration of the precipitate and washing with DCM (50mL), the filtrate was evaporated to full dryness into a pale yellow solid (MS (ESI$^-$) *m/z* 307 [M-1]$^-$, $C_{12}H_8N_4O_2SCl$ requires 307.00565). The crude 2-benzylsulfonylpurine was dissolved in anhydrous THF (10mL) then (*D*)-valinol (223mg, 2.16mml) was added and the resulting solution was refluxed overnight at 90°C under nitrogen and monitored by TLC. Evaporation to full dryness afforded a yellow solid that was purified by flash column chromatography on silica gel using 2-10% MeOH in DCM to afford the 6-aminopurine 34 as a colourless solid (80mg, 44%); mp =

176°C; R_f 0.36 [DCM/MeOH 95:5]; ^{1}H (300 MHz, MeOD) δ_H 0.95 (2xd, $^3J_{H\text{-}H}$ = 6.91Hz, 2x3H, valinol $(CH_3)_2CH$-), 2.00 (o, $^3J_{H\text{-}H}$ = 6.67 Hz, 1H, valinol $(CH_3)_2CH$-), 3.21 (q, $^3J_{H\text{-}H}$ = 1.54 Hz, 1H, valinol $HOCH_2CHNH$-), 3.70 (m, 2H, valinol $HOCH_2CH$-), 4.28 (dd, $^3J_{H\text{-}H}$ = 11.00 Hz and $^3J_{H\text{-}H}$ = 6.14 Hz ,1H, valinol $HOCH_2$-), 4.70 (d, $^3J_{H\text{-}H}$ = 4.86 Hz, 1H, valinol $HNCH$-), 4.83 (s, 2H, $PhCH_2SO_2$-), 7.10-7.13 (m, 3H, aromatics $PhCH_2SO_2$-), 7.19-7.22 (m, 2H, aromatics $PhCH_2SO_2$-), 8.11 (s, 1H, purine H8); ^{13}C (75.4 MHz, MeOD) δ_C 19.2 (s, valinol CH_3CH), 20.5 (s, valinol CH_3CH), 30.9 (s, -$CHMe_2$), 59.1 (s, $PhCH_2SO_2$-), 59.6 (s, valinol $HNCH$-), 63.7 (s, valinol $HOCH_2$-), 129.5 (s, purine C5), 130.1 (s, Ph C4'), 131.5 (s, Ph C2'), 132.7 (s, Ph C3'), 135.9, Ph C1'), 146.7 (s, purine C8), 154.3 (s, purine C6), 156.9 (s, purine C4), 159.8 (s, purine C2); MS (ESI^+): *m/z* 376.1437 $[M+H]^+$, $C_{17}H_{22}N_5O_3S$ requires 376.1443; IR (KBr disc, cm^{-1}) 3504m, 3292m, 3066m, 3034m, 2964s, 2921s, 2874m, 2811m, 1871w, 1623vs, 1586vs, 1460m, 1409s, 1370m, 1314vs, 1284vs, 1253s, 1200m, 1174m, 1152m, 1112s, 1074m, 965m, 870m, 802w, 791w, 777w, 752m, 716w, 697s, 671m, 697s, 631m, 589w, 577w, 559w, 512s; Microanalytical data found: C: 54.93 H: 5.10 N: 19.29 S: 8.13, expected for $C_{17}H_{21}N_5O_3S$ C: 54.38 H: 5.64 N: 18.66 S: 8.52.

2-Benzylsulfanyl-6-(3-chlorophenylamino)-9-isopropylpurine **35**

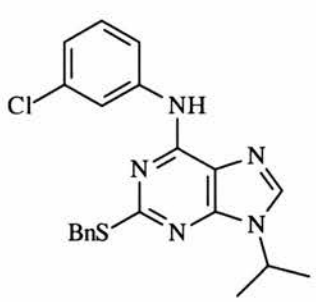

To a mixture of 6-chloropurine **33a** (250mg, 0.79mmol) in *n*-butanol (10mL) was added *m*-chloroaniline (0.12mL, 1.18mmol) then concentrated hydrochloric acid (2 drops) and the solution was stirred at 120°C for 24 hours. Following cooling of the resulting mixture and evaporation to full dryness into a dark oil, flash column chromatography on silica gel using petroleum ether 40-60°C then EtOAc/petroleum ether 1:1 afforded the 6-anilinopurine 35 as a pale yellow foam (316mg, 98%); R_f 0.19 [EtOAc/petroleum ether 40-60°C 1:1]; ^{1}H (300 MHz, d_6-dmso) δ_H 1.52 (d, $^3J_{H\text{-}H}$ = 6.66Hz, 6H, purine CH(C*H*$_3$)$_2$), 4.42 (s, 2H, PhCH_2S-), 4.76 (s, $^3J_{H\text{-}H}$ = 6.66Hz, 1H, purine C*H*(CH$_3$)$_2$), 7.04 (ddd, $^3J_{H\text{-}H}$ = 3.07Hz, $^3J_{H\text{-}H}$ = 2.05Hz, $^3J_{H\text{-}H}$ = 1.02Hz, 1H, aniline H_b), 7.15-7.34 (m, 4H, aromatics *Ph*CH_2S- and aniline H_d), 7.38-7.45 (m, 2H, aromatics PhCH_2S-), 7.81 (dd, $^3J_{H\text{-}H}$ = 7.68Hz and $^3J_{H\text{-}H}$ = 3.07Hz, aniline H_e), 8.16 (dd, 1H, $^3J_{H\text{-}H}$ = 4.10Hz and $^3J_{H\text{-}H}$ = 2.05Hz, aniline H_c), 8.32 (s, 1H, purine *H*8), 10.18 (s, 1H, aniline N*H*); ^{13}C (75.4 MHz, d_6-dmso) δ_C 22.4 (s, valinol (*C*H$_3$)$_2$CH), 35.0 (s, -*C*HMe$_2$), 47.2 (s, Ph*C*H$_2$S-), 118.4 (s, aniline C_b), 118.7 (s, purine C5), 120.5 (s, aniline C_f), 123.6 (s, aniline C_d), 127.4 (s, Ph *C*2'), 128.8 (s, Ph C3'), 129.4 (s, Ph C4'), 130.2 (s, aniline C_c), 134.9 (s, aniline C_e), 137.9 (s, purine *C*8), 138.3 (s, Ph C1'), 141.4 (s, aniline C_a), 150.7 (s, purine C4), 151.5 (s, purine C6), 164.9 (s, purine C2); MS (ESI$^+$): *m/z* 410.1221 [M+H]$^+$, $C_{21}H_{21}N_5SCl$ requires 410.1206; IR (KBr disc, cm^{-1}) 3321m, 3213m, 3112m, 3062m, 3029m, 2978s, 2933m, 1709s, 1616vs, 1575vs, 1532s, 1456vs, 1372s, 1325s, 1286s, 1268s, 1223m, 1197m, 1164m, 1132m, 1098m, 1077m, 1029s, 996m, 948m, 917m, 898w, 812m, 788s, 698s, 661m, 638m, 610m,

580, 564w, 542w, 513w; Microanalytical data found: C: 62.09 H: 5.74 N: 17.42 S: 7.52, expected for $C_{21}H_{20}N_5SCl$ C: 61.53 H: 4.92 N: 17.08 S: 7.82.

2-Benzylsulfonyl-6-(3-chlorophenylamino)-9-isopropylpurine **36**

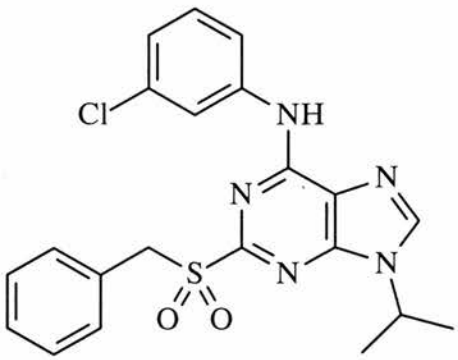

To a stirred mixture of magnesium sulphate (1.136g, 9.47mmol) and *m*-chloroperbenzoic acid (760mg, 3.08mmol) in anhydrous DCM was added a solution of 2-benzylsulfanylpurine **35** (420mg, 1.03mmol) in DCM (10mL) dropwise. Overnight stirring was continued overnight, then the precipitate was filtered off, washed thoroughly with DCM. The combined organics were evaporated to full dryness into a colourless solid that was purified by flash column chromatography on silica gel using EtOAc/petroleum ether 40-60C 1:1 at first to elute the *m*-chlorobenzoic acid then with EtOAc/pet.ether 3:1 to afford the 2-benzylsulfonylpurine **36** as a colourless foam (450mg, 99%); mp = 234°C; ^{1}H (300 MHz, d_6-dmso) δ_H 1.53 (d, $^3J_{H\text{-}H}$ = 6.66 Hz, 6H, purine CH(C*H*$_3$)$_2$), 4.74 (s, 2H, PhC*H*$_2$SO$_2$-), 4.89 (s, $^3J_{H\text{-}H}$ = 6.66Hz, 1H, purine C*H*(CH$_3$)$_2$), 7.05 (ddd, $^3J_{H\text{-}H}$ = 7.94Hz, $^3J_{H\text{-}H}$ = 1.79Hz, $^3J_{H\text{-}H}$ = 0.77Hz, 1H, aniline H_b), 7.19-7.23 (m, 4H, aromatics *Ph*CH$_2$SO$_2$- and aniline H_d), 7.27-7.33 (m, 2H, aromatics *Ph*CH$_2$SO$_2$-), 7.61 (ddd, $^3J_{H\text{-}H}$ = 8.19Hz and $^3J_{H\text{-}H}$ = 2.05Hz and $^3J_{H\text{-}H}$ = 0.77Hz, aniline H_e), 7.87 (t, 1H, $^3J_{H\text{-}H}$ = 2.05Hz, aniline H_e), 7.98 (s, 1H, purine *H*8), 8.14 (s, 1H, aniline N*H*); ^{13}C (75.4 MHz, d_6-dmso) δ_C 23.3 (s, valinol (*C*H$_3$)$_2$CH), 48.2 (s, -*C*HMe$_2$), 58.2 (s, PhC*H*$_2$SO$_2$-), 118.8 (s, aniline C_b), 120.8 (s, aniline C_f), 121.8

(s, aniline C_d), 121.9 (s, purine C5), 124.6 (s, Ph C_c), 127.6 (s, Ph C1'), 129.1 (s, Ph C3'), 130.6 (s, Ph *C*2'), 131.7 (s, Ph *C*4'), 135.1 (s, aniline C_e), 139.4 (s, aniline C_a), 141.3 (s, purine *C*8), 147.8 (s, purine C6), 151.9 (s, purine C4), 158.5 (s, purine C2); MS (ESI^+): *m/z* 442.1114 $[M+H]^+$, $C_{21}H_{21}N_5O_2SCl$ requires 442.1104; IR (KBr disc, cm^{-1}) 3568m, 3342m, 3215m, 3096w, 3030w, 2987w, 2931w, 1646s, 1618m, 1600m, 1571vs, 1479vs, 1456m, 1421m, 1363m, 1334m, 1297vs, 1224s, 1205m, 1172m, 1131s, 1104m, 1028m, 995m, 872m, 792m, 779m, 713s, 693s, 682m, 637s, 584m, 528s, 521m; Microanalytical data found: C: 58.31 H: 4.13 N: 16.30 S: 7.86, expected for $C_{21}H_{20}N_5O_2SCl$ C: 57.07 H: 4.56 N: 15.85 S: 7.26.

2-(1*R*-Isopropyl-2-hydroxyethylamino)-6-(3-chlorophenylamino)-9-isopropylpurine **23** (Purvalanol A)

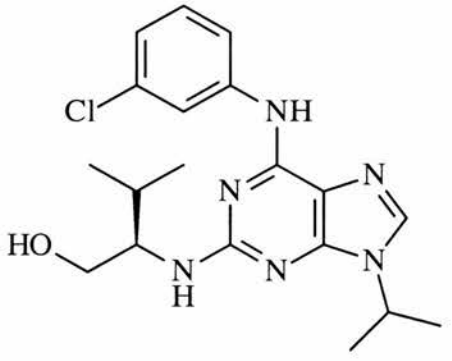

To a solution of 2-iodopurine **22** (170mg, 0.41mmol) in *n*-butanol (10mL) was added Hunig's base (0.5mL, 90mmol) and *R*-valinol (500mg, 4.9mmol). The resulting solution was heated at 160C in a Parr bomb for 24 hours. Following cooling down and evaporation to full dryness, the resulting oil was purified by flash chromatography on silica gel using 1-5% MeOH in DCM to afford

Purvalanol A as a colourless solid (137mg, 86%); R_f 0.20 [DCM/MeOH 95:5]; ^{1}H NMR (270 MHz, $CDCl_3$) δ_H 1.01 (d, $^3J(^1H\text{-}^1H)$ = 6.68 Hz, 6H, valinol $CH(CH_3)_2$), 1.47 (d, $^3J(^1H\text{-}^1H)$ = 6.70 Hz, 6H, purine $CH(CH_3)_2$), 1.97 (m, $^3J(^1H\text{-}^1H)$ = 6.70 Hz, 1H, valinol $CH(CH_3)_2$), 3.60-3.71 (m, 1H, valinol $NHCHCH_2OH$), 3.80-4.01 (m, 2H, valinol $NHCHCH_2OH$), 4.50 (sept, $^3J(^1H\text{-}^1H)$ = 6.70 Hz, 1H, purine $CH(CH_3)_2$), 5.16 (d, $^3J(^1H\text{-}^1H)$ = 7.94 Hz, 1H, valinol $NHCHCH_2OH$), 6.92 (d, $^3J(^1H\text{-}^1H)$ = 7.92 Hz, 1H, aniline C_d), 7.13 (t, $^3J(^1H\text{-}^1H)$ = 8.16 Hz, 1H, aniline C_c), 7.41 (d, $^3J(^1H\text{-}^1H)$ = 8.16 Hz, 1H, aniline C_b), 7.70 (t, $^3J(^1H\text{-}^1H)$ = 1.76 Hz, 1H, aniline C_f), 7.97 (s, 1H, purine H8), 8.47 (broad s, 1H, aniline NH); ^{13}C NMR (67. 9 MHz, $CDCl_3$) δ_C 19.1 (s, valinol $CH(CH_3)_2$), 19.5 (s, valinol $CH(CH_3)_2$, 23.2 (s, purine $CH(CH_3)_2$), 46.6 (s, purine $CH(CH_3)_2$), 30.0 (s, valinol $Me_2CHCHNH$), 59.5 (s, valinol $NHCHCH_2OH$), 64.7 (s, valinol $HOCH_2CHNH$), 114.5 (s, purine C5), 117.8 (s, aniline C_b), 119.8 (s, aniline C_f), 122.5 (s, aniline C_d), 131.3 (s, aniline C_c), 134.3 (s, aniline C_e), 135.1 (s, purine C8), 140.8 (s, aniline C_a), 150.9 (s, purine C4), 152.0 (s, purine C6), 159.8 (s, purine C2); MS (ESI^+): *m/z* 389.1863 $[M+1]^+$, IR (KBr disc, cm^{-1}): 3326m, 3232m, 3114m, 2960s, 2930s, 2873m, 1634s, 1575vs, 1480s, 1422m, 1362m, 1336m, 1031m, 1248m, 1172w, 1132m, 1080m, 1028m, 871w, 777m, 698w, 640m, 529w; $C_{19}H_{26}ClN_6O$ requires 389.1857; Microanalytical data found C: 59.03 H: 6.28 N: 22.69, expected for $C_{19}H_{25}ClN_6O$ C: 58.54 H: 6.61 N: 21.58.

CHAPTER 4: SYNTHESIS OF NOVEL DIAMINOPURINES

4.1 *Introduction*

As explained in Chapter One, we felt it was worth synthesising diaminopurines bearing modified analogues of Purvalanol A with sulfonamide substituents and phosphorus containing valinol side-chains to investigate the effects of these substitutions on CDK inhibition. Reduction of *R*-valine would allow the preparation of *R*-valinol as seen in scheme 4.1. Phosphorylation is known to occur on both nitrogen and oxygen, so regioselective *O*-phosphorylation required the use of a suitable amino protecting group.

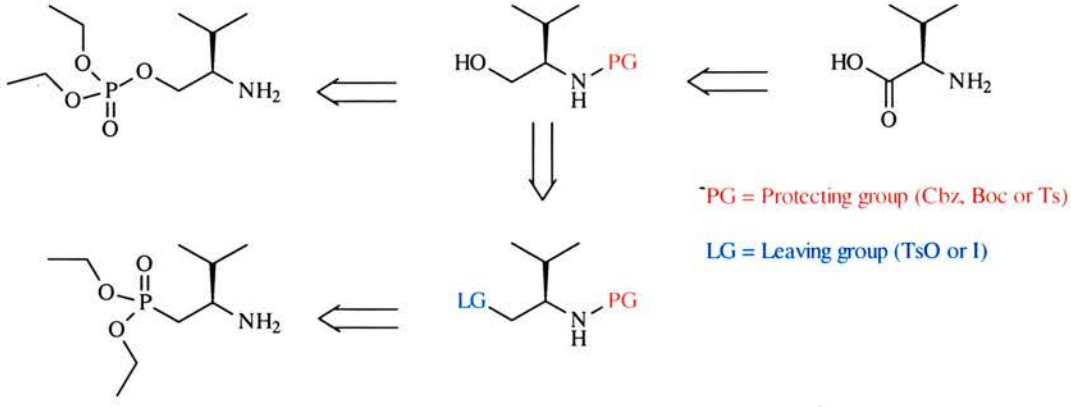

Scheme 4.1 Retrosynthesis for the required phosphorus containing valinol analogues

Potentially suitable groups were the benzyloxycarbonyl (Cbz or Z), Tosyl (Ts) and *tert*-butoxycarbonyl (*t*-Boc or Boc) moieties[123,124]. We also wanted to attempt the synthesis of *R*-(2-amino-3-methyl-butyl)-phosphonic esters using an analogous strategy by converting the alcohol function of protected valinol into a suitable leaving group that would drive the formation of a C-P bond by reaction with a phosphorus nucleophile.

The synthesis of 4-aminobenzenesulfonamides traditionally relies on the electrophilic substitution of protected anilines with chlorosulfonic acid[125], reaction with an amine and cleavage of the acetamide under acidic or basic conditions[123,124] (see Scheme 4.2 below).

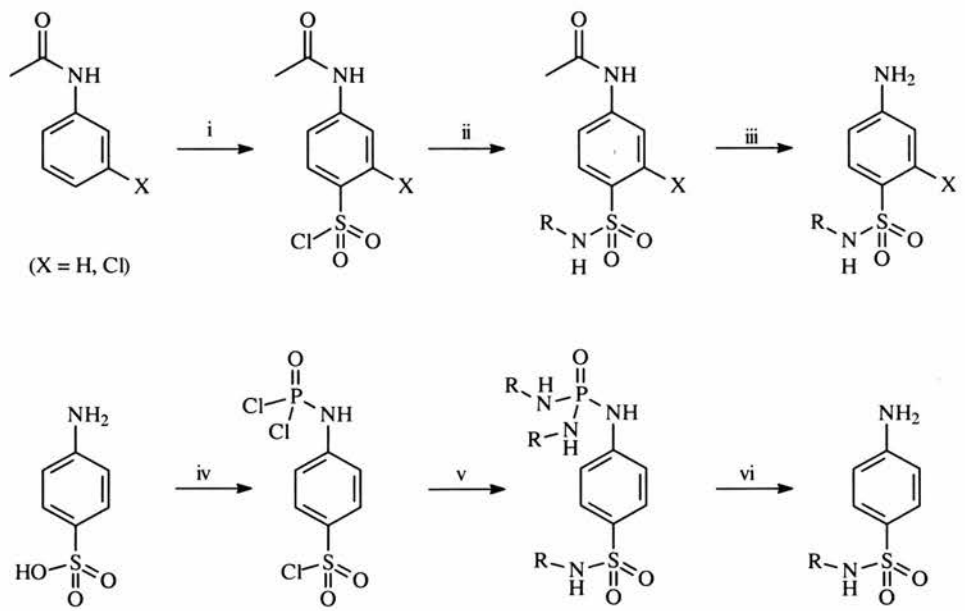

Conditions: i) $ClSO_3H$, Δ ii) RNH_2,MeCN, Δ iii) NaOH, Δ iv) PCl_5, Δ

v) RNH_2, H_2O, Δ vi) H_3O^+, Δ then NaOH

Scheme 4.2 Reported synthesis of 4-aminobenzene sulfonamides

Alternatively, reaction of sulfanilic acid with phosphorus pentachloride affords *N*-phenyl phosphoramamidic dichloride analogue following quenching with water[80] and the corresponding 4-aminobenzenesulfonamide following treatment with an amine, hydrolysis with aqueous hydrochloric acid then sodium hydroxide.

Finally, reaction of these valinol and aniline substituents with the purine template **33a** of the previous Chapter, would allow the synthesis of novel sulfur and phosphorus containing analogues of Purvalanol A **23**.

4.2 *Results and discussion*

4.2.1 Synthesis of phosphorus containing analogues of *R*-valinol

R-valinol was prepared by literature procedures[126-129]. X-Ray crystallography confirmed the chirality of the product as shown below in Figure 4.1 and reveals an assembly by hydrogen bondings between the amino hydrogen H(1B) of valinol and the oxygen atom O(3A) of the adjacent molecule and between the nitrogen N1(B) and the hydrogen H(3O) at distances of 2.094(4) Å and 1.792(3) Å respectively.

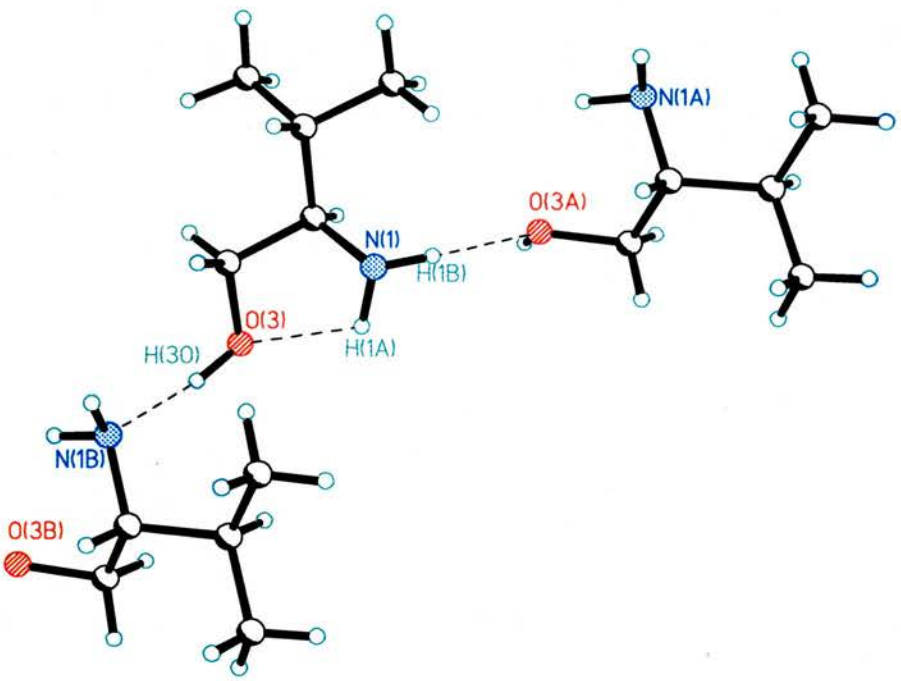

Figure 4.1 Crystal structure of *R*-valinol **38**

	38
Bond length	
N(1)-C(2)	1.4770(14)
C(2)-C(4)	1.5336(15)
C(3)-O(3)	1.4203(14)
C(4)-C(5)	1.5285(18)
Bond angle	
N(1)-C(2)-C(4)	111.03(8)
O(3)-C(3)-C(2)	110.43(9)
C(6)-C(4)-C(5)	109.22(11)
C(5)-C(4)-C(2)	111.50(9)

Table 4.1 Selected bond lengths (Å) and angles (º) for *R*-valinol **38**

Tosylation[130] of the amino alcohol **38** with *p*-toluenesulfonyl chloride in anhydrous pyridine at -10ºC gave the *bis*-tosyl valinol **39.** Precipitation by dropwise addition of hexane afforded the protected valinol **39** as colourless crystals suitable for XRD studies. The structure shown in Figure 4.2 displays the π-stacking occurring in the solid state between the phenyl rings of both tosyl groups. The IR spectrum displays two very strong ν_{so} vibrations for the sulfonamide at 1361 and 1180cm^{-1}. Figure 4.3 highlights the crystal packing of three molecules by hydrogen bonding between the amide hydrogen of one molecule with the sulfonamide oxygen of an adjacent *bis*-tosyl valinol at a distance of 2.035(11) Å.

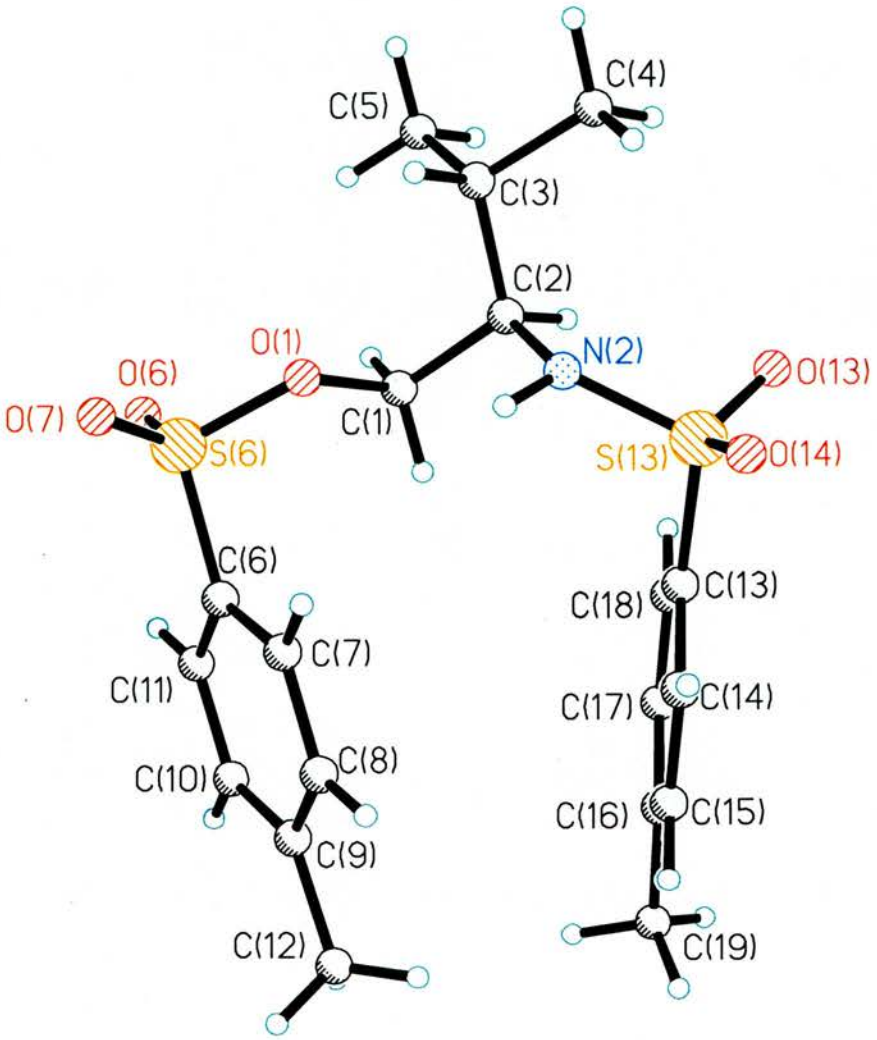

Figure 4.2 Crystal structure of *bis*-tosyl *R*-valinol **39**

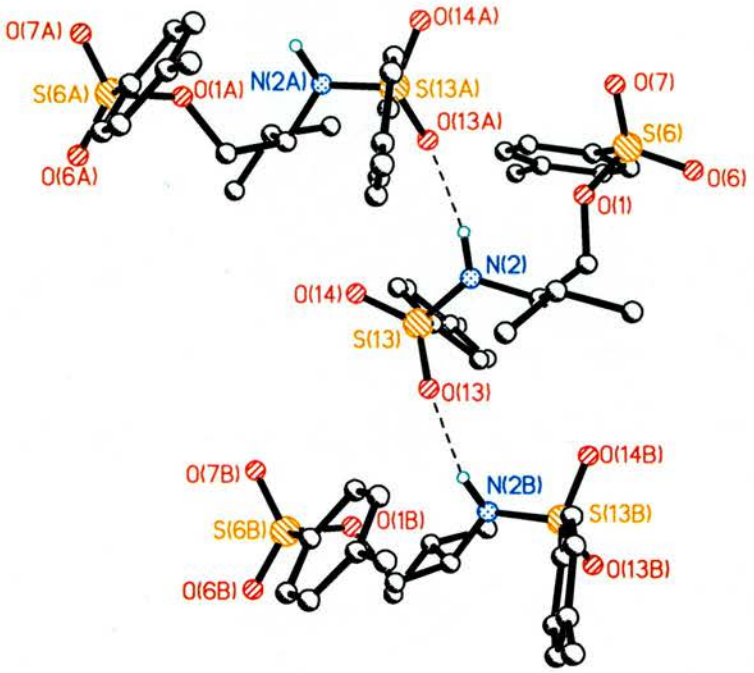

Figure 4.3 Crystal structure of *bis*-tosyl *R*-valinol **39**

	39
Bond length	
O(1)-S(6)	1.5722(18)
N(2)-S(13)	1.613(2)
C(9)-C(12)	1.503(4)
S(13)-O(13)	1.4489(18)
Bond angle	
O(1)-C(1)-C(2)	105.61(19)
C(1)-C(2)-C(3)	114.1(2)
O(7)-S(6)-O(1)	104.00(11)
O(14)-S(13)-C(13)	107.37(11)

Table 4.2 Selected bond lengths (Å) and angles (º)

for *bis*-tosyl-*R*-valinol **39**

The *O*-tosyl group of *bis*-tosyl valinol **39** was totally unreactive with 5 equivalents of lithium or sodium diethyl phosphate[131] after several days at reflux in anhydrous THF under a nitrogen atmosphere. The phosphate salts were prepared in situ by adding butyl lithium[132] or sodium hydride[133] to a solution of freshly distilled diethyl phosphite ($HP(O)(OEt)_2$) in anhydrous THF. It was decided to convert the *O*-tosyl group into an iodide and attempt an Arbuzov reaction[134] with triethyl phosphate. Unfortunately, no reaction occurred when heating the *bis*-tosyl valinol **39** with a large excess of potassium iodide in refluxing DMF. This was an unexpected result as this strategy is often used to convert alcohols to alkyl iodides.

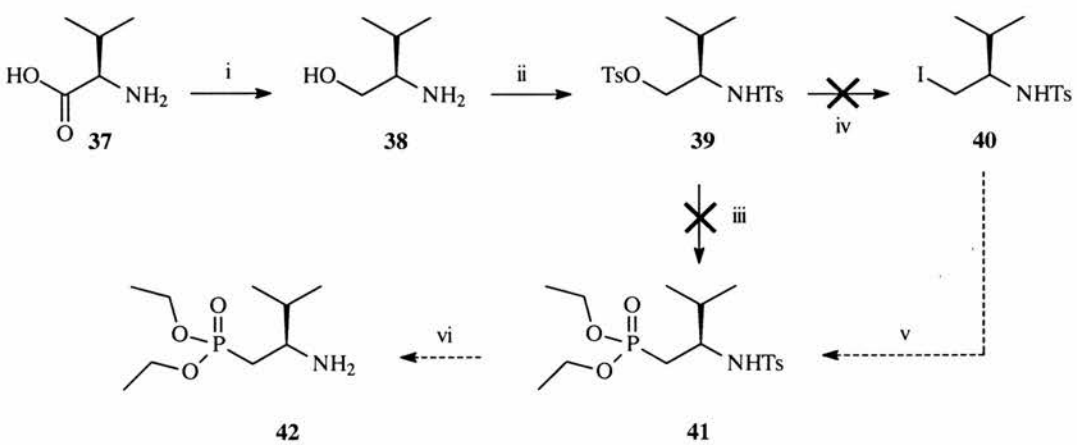

Conditions: i) $LiAlH_4$, THF, Δ, 98% ii) 2TsCl, Pyridine, -10°C to r.t., 99% iii) $5LiPO(OEt)_2$ or $5NaPO(OEt)_2$, THF, Δ iv) KI, DMF, Δ, several days v) $P(OEt)_3$, Δ vi) $Na\text{-}NH_{3(l)}$

Scheme 4.3 Attempted synthesis of *R*-(2-amino-3-methyl-butyl) phosphonic acid diethyl ester **42**

The strained aziridines have been reported to react with various nucleophiles under mild to moderate conditions[135,136]. As the reaction of *bis*-tosyl valinol **39** with lithium/sodium diethyl phosphate failed, it was tempting to generate a *N*-tosylaziridine and test its reactivity with lithium diethylphosphate as seen below in Scheme 4.4. The mechanism of aziridine formation involves deprotonation of the acidic sulfonamide hydrogen by sodium hydride followed by intramolecular nucleophilic attack on the electrophilic carbon bearing the tosylate group. Reaction of the aziridine with a phosphorus nucleophile such as lithium or sodium diethyl phosphate can lead in theory to the formation of alkyl phosphonic esters **41a** and **41b**.

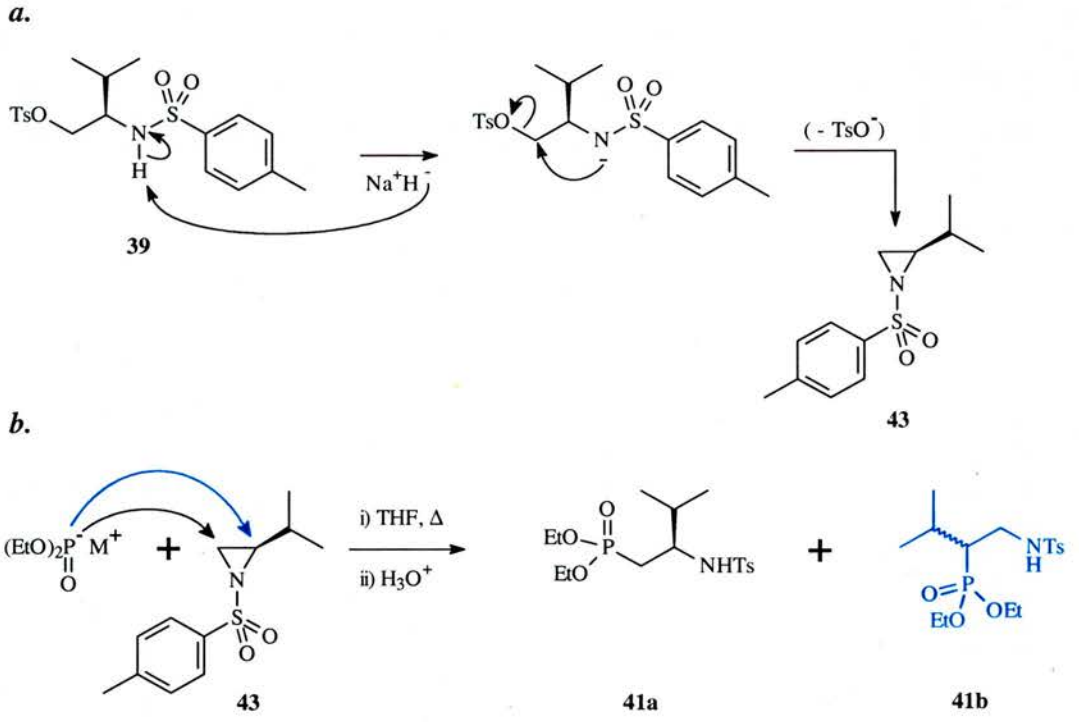

Scheme 4.4 ***a)*** Mechanism of formation for aziridine **43**

b) Possible phosphonic ester regioisomers

Reaction of *bis*-tosyl valinol **39** with sodium hydride in anhydrous THF under a nitrogen atmosphere was an almost instant clean reaction at room temperature that afforded the *N*-tosylaziridine **43** in very high yield. The reaction mixture was evaporated to dryness and the product was dissolved in DCM. The insoluble colourless solid (NaOTs) was filtered off and thoroughly washed with cold DCM and the combined organics were concentrated to a few mL. Crystallisation by dropwise addition of hexane afforded colourless crystalline needles suitable for XRD studies. The ^{1}H NMR clearly showed that only one tosyl group was present, as there was only one methyl group at δ 2.37 ppm while the ESI^{+} mass spectrum shows the molecular ion at *m/z* 262.0871 hence $[M+Na]^{+}$.

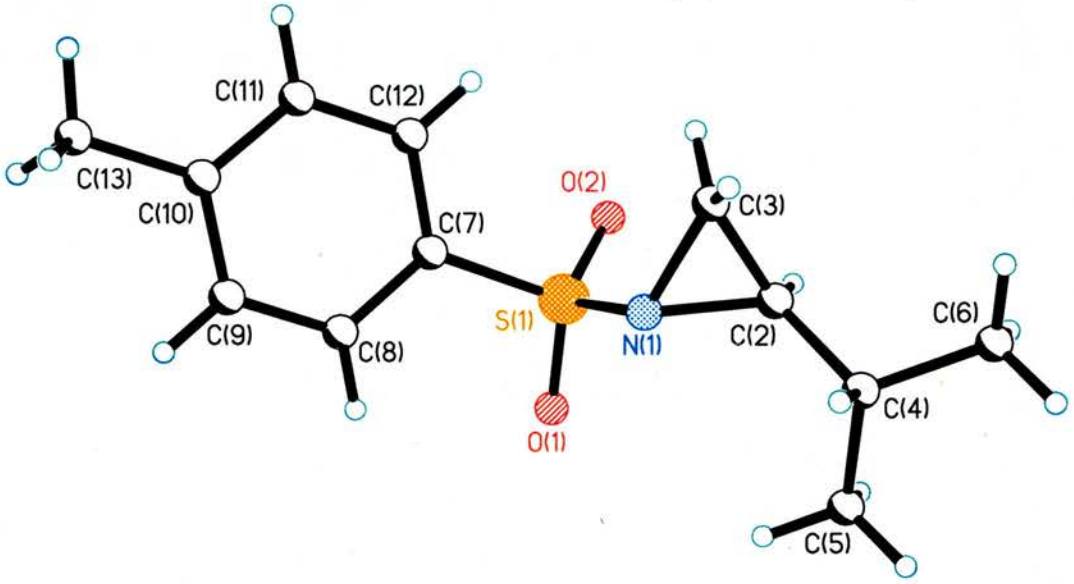

Figure 4.4 Crystal structure of *N*-tosylaziridine **43**

	43
Bond length	
S(1)-O(2)	1.4433(14)
S(1)-C(7)	1.757(2)
C(2)-C(4)	1.505(3)
C(8)-C(9)	1.387(3)
C(10)-C(13)	1.507(3)
Bond angle	
N(1)-S(1)-C(7)	101.72(8)
C(2)-N(1)-C(3)	59.48(11)
C(3)-N(1)-S(1)	116.33(12)
C(3)-C(2)-N(1)	60.47(12)
C(3)-C(2)-C(4)	124.37(16)
O C(5)-C(4)-C(6)	111.64(16)

Table 4.3 Selected bond lengths (Å) and angles (º) for *N*-tosylaziridine **43**

Reaction of aziridine **43** with lithium diethyl phosphate, formed *in situ* by treating a solution of diethyl phosphite in THF with *n*-butyl lithium, afforded after overnight stirring at room temperature and quenching with aqueous hydrochloric acid a 1:1 mixture of starting phosphite (δ 7.4ppm) and of an alkyl phosphonic ester (δ 28.9ppm) according to ^{31}P NMR and ESI$^+$ mass spectrometry (molecular ion at *m/z* 400.1318 hence $[M+Na]^+$). The reaction mixture was evaporated to full dryness and partitioned between water and ethyl acetate. The organics still contained a little of phosphite according to ^{31}P NMR but an attempt to purify the oily residue by distillation under vaccum resulted in the decomposition of the product. Indeed, neither the main fraction (bp

220°C/760mmHg) nor the undistilled residue seemed to contain any trace of the phosphate product according to ^{31}P NMR. We have not been able to investigate further but it is anticipated that refluxing the mixture with a slight excess of lithium diethyl phosphate (1.5 equivalent at most) could drive the reaction to completion and that the desired product could be isolated in better purity. It is interesting that only one regioisomer (δ 28.9 ppm) was detected by ^{31}P NMR, and we anticipate that the desired product **41a** is the favoured isomer due to the steric hindrance of the isopropyl group at the other eletrophilic carbon of the aziridine ring (see Scheme 4.4).

Protection of the amino group of *R*-valinol **38** with di-*tert*-butyl dicarbonate according to the procedure of Tarbell *et al.*[137] afforded the Boc-analogue **44** in 88% yield. Phosphorylation using iodine and triethyl phosphite[138,139] in anhydrous DCM at 0°C yielded several products according to ^{31}P NMR, the major product was the starting phosphite at δ 7.16ppm while the phosphorylated valinol at δ 0.17ppm was only a minor product of the mixture. As lowering or increasing the temperature of the reaction did not seem to influence the composition of the mixture according to ^{31}P NMR, it was decided to react the Boc-valinol **44** with diethyl chlorophosphate[140] (diethyl phosphochloridate) in the presence of an acid scavenger, in this instance triethylamine. The reaction did not occur at 0°C or at room temperature so it was necessary to reflux the reaction mixture in THF for several days, with the gradual precipitation of triethylamine hydrochloride as the reaction proceeded. ^{31}P NMR in the reaction solvent using a

$CDCl_3$ insert was used to monitor the extent of completion. Filtration of the precipitate then partition between DCM and aqueous sodium bicarbonate followed by evaporation to dryness afforded the desired *O*-phosphorylated valinol **45** as a colourless oil. An attempt to purify the product by distillation under vacuum was unsuccessful as the fraction still contained some phosphorus containing species.

It was decided to use this material without further purification. The next step involved acidic cleavage[141] of the Boc group in DCM / TFA 95:5 as reported in the literature. The reaction was incomplete after 2 days at room temperature as NMR showed there was mostly unreacted starting material. Slight heating (40°C) resulted after 2 hours in the cleavage of both the phosphoryloxy and the Boc moieties, so this strategy was not suitable for the preparation of *O*-phosphorylated valinols.

Protection of the amino function of valinol **38** with ZOSu (*N*-(benzyloxycarbonyloxy)-succinimide[142,143]) occurred almost instantly in ethyl acetate and the desired Z-valinol 47 was recovered after a basic work-up in 92% yield. The analytical data was consistent with the structure of the product. This particular protecting group seemed at first more suitable for this scheme, as its cleavage involves conditions that are compatible with the phosphoryloxy group[123,124]. However, phosphorylation using diethyl phosphochloridate and triethylamine in refluxing THF afforded very little product after 7 days according

to ^{31}P NMR. A slight improvement was achieved by replacing triethylamine with Hunig's base (*N,N,N*-diisopropylethyamine) as the product was isolated after aqueous work-up in 17% yield. The purity of the product was not improved after distillation under vacuum and no analytically pure sample of phosphorylated valinol **48** could be obtained. It was very surprising to us that the alcohol group of protected valinols **44** and **47** reacted only partially with this highly reactive phosphochloridate. Future attempts might involve the formation of the alkoxy anion by reaction with sodium hydride prior to the addition of the phosphochloridate.

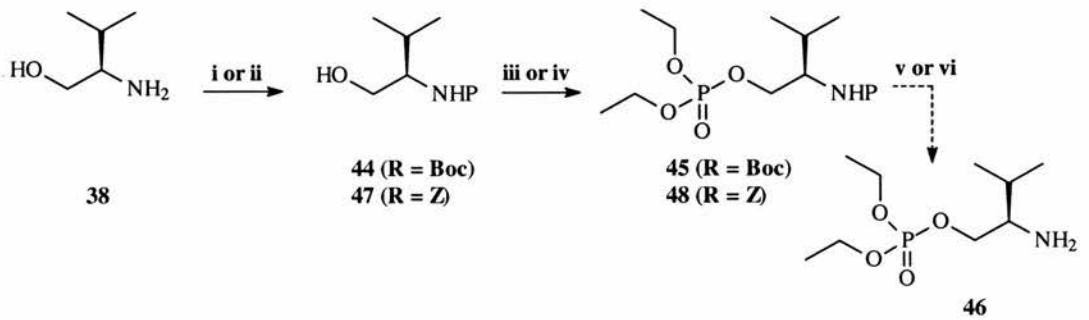

38

44 (R = Boc)
47 (R = Z)

45 (R = Boc)
48 (R = Z)

46

Conditions: i) $(Me_3COC(O))_2O$, DCM, 88% ii) ZOSu, EtOAc, 92% iii) $ClPO(OEt)_2$, NEt_3, THF, Δ iv) $P(OEt)_3$, I_2, DCM, several days v) DCM/TFA vi) H_2/Pd(C)

Scheme 4.5 Attempted synthesis of phosphoryloxyvalinol **46**

4.2.2 Synthesis of 4-aminobenzenesulfonamide derivatives

The synthesis of novel sulfonamide containing purine CDK was the initial goal of the project but the required 4-aminobenzenesulfonamides were not commercially available, hence we had to rely on the available literature procedures as described

in the following section. Sulfanilic acid **49** reacts with phosphorus pentachloride[80] as described in Scheme 4.6. Both the amine and oxygen lone pairs undergo nucleophilic attack on the phosphorus, then elimination of 2 molecules of hydrochloric acid and a molecule of phosphorus oxychloride affords the *N*-phenyl phosphoramimidic dichloride product **50a** following evaporation of the volatile phosphoryl chloride. Quenching with water gives the *N*-phenyl phosphoramamidic dichloride compound **50b**. Characterisation by high resolution EI mass spectrometry confirmed the identity of the product, displaying *m/z* 306.8789 hence $[M]^+$ while the microanalytical data were ±0.3% off the theoretical values. The IR spectrum shows a strong $\nu_{P=O}$ at 1261cm^{-1} and two very strong ν_{S-Cl} characteristic of the sulfonyl chloride group at 1367 and 1174cm^{-1}. The product is very insoluble in most solvents and decomposes in DMSO so no decent quality NMR could be obtained.

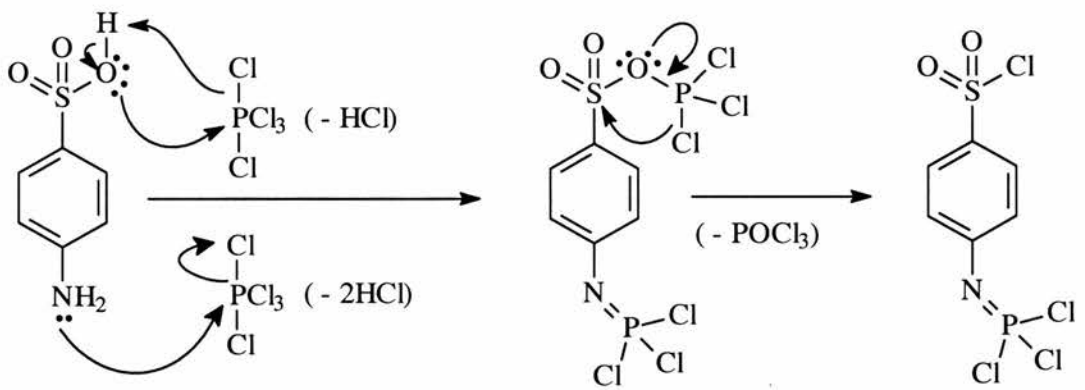

49 **50a**

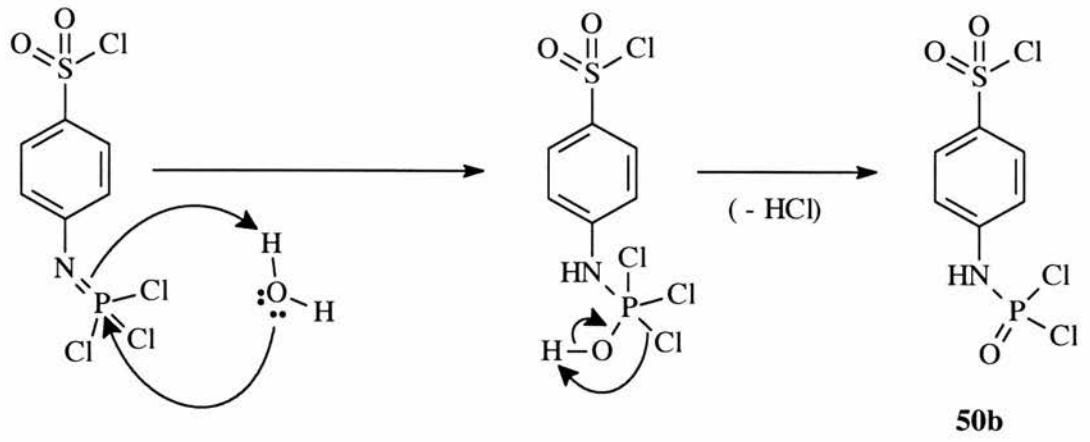

Scheme 4.6 Mechanism of formation for *N*-phenyl phosphoramamidic dichloride compound **50b**

Reacting phenylsulfonyl chloride with concentrated ammonia in refluxing THF was straightforward but the 4-aminobenzene sulfonamide **51a** was isolated in only 17% yield following reflux in 5M HCl, pH adjustment to 7-8 and recrystallisation of the residue from water. According to the literature[80], reflux in acidic conditions is necessary to hydrolyse the *N*-phenylphosphorodiamidic acid intermediate (see Scheme 4.7 below). Reaction with methylamine using the same methodology afforded the corresponding sulfonamide **51b** in only 7% yield but failed with 2-aminopyridine (Method A in Experimental section).

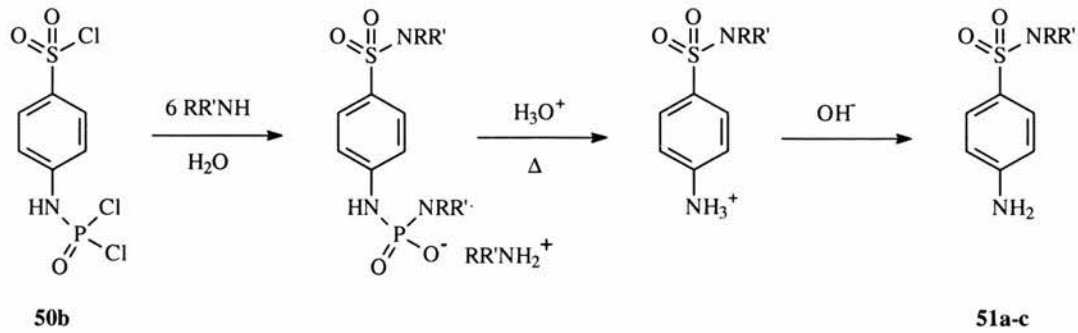

50b **51a-c**

Scheme 4.7 Reaction sequence for sulfonamides **51a-b**

Though the desired 4-aminobenzenesulfonamides **51a-c** were obtained through the above synthetic route, the yields were very low so it was decided to attempt their synthesis from protected aniline by reaction with chlorosulfonic acid, treatment with an amine and deprotection of the 4-amino group. The protection of aniline **52a** and 3-chloroaniline **52b** with acetic anhydride[144,145] was near quantitative and afforded the *N*-phenylacetamides **53a** and **53b**. Full characterisation by NMR, MS, IR and microanalysis was consistent with their structures.

The first attempts to introduce the chlorosulfonyl group by electrophilic substitution of these protected anilines with chlorosulfonic acid were unsuccessful as the original paper[146] indicated completion of the reaction after several hours of stirring of room temperature in chloroform. According to TLC and NMR, the resulting mixtures contained mostly the starting materials but there was evidence that the products **54a** and **54b** were present. Overnight stirring at 60°C (20 hours in total) with 3.3 equivalents of chlorosulfonic acid and careful quenching on crushed ice afforded the required phenyl sulfonyl chlorides **54a** and

54b as pale pink solids in 60 and 61% yield respectively. Analytically pure samples were obtained by recrystallisation from toluene and THF.

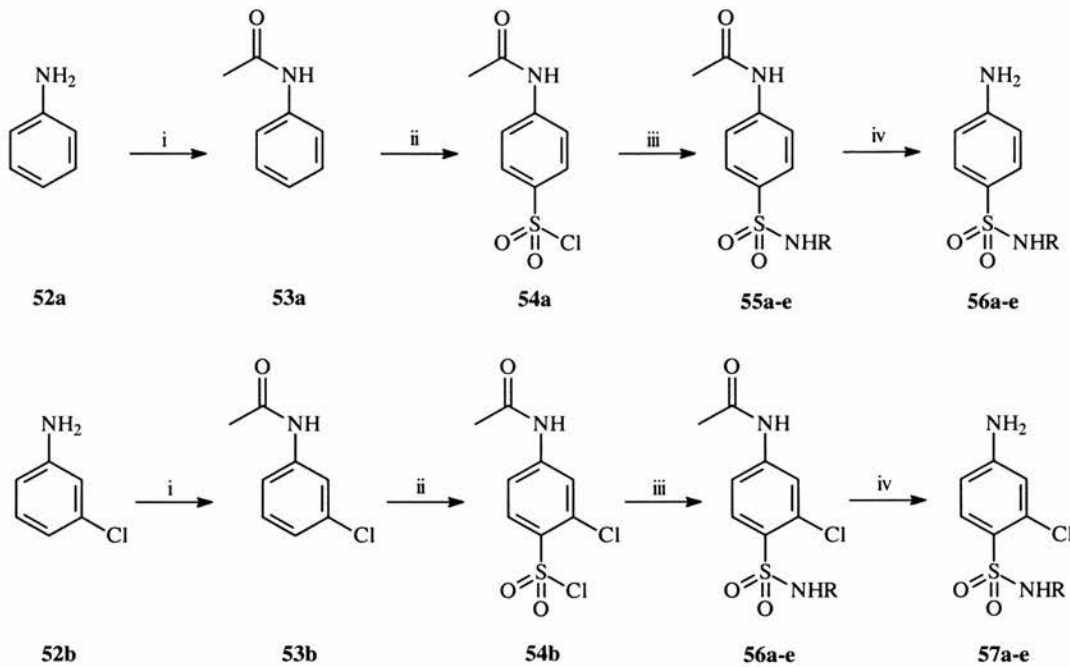

Conditions: i) $(MeCO)_2O$, MeCN ii) $ClSO_3H$, 60°C iii) 3-4 eq. RNH_2, MeCN, Δ (amine a = NH_3, b = H_2NMe, c = $H_2N(CH_2)_2OH$, d = 2-aminopyridine, e = 2-aminopyrimidine) iv) NaOH, Δ, then pH adjustment to 7-8

Scheme 4.8 Synthesis of benzene sulfonamides from anilines

Reaction with aliphatic amines generally proceeded in good yields (Method B in Experimental section). The hydrolysis of the acetyl protecting group was successful in 5M aqueous sodium hydroxide[123,147] and afforded the desired products **51a-b** and **57b-c** following pH adjustment to 7-8. The product purity for all compounds was satisfying after a single recrystallisation from water as suggested in the literature for similar sulfonamides. Table 4.4 summarises some

physical properties of the final 4-aminobenzene sulfonamides **51a-b** and **57b-c** and highlights that the slightly longer route involving the *N*-acetylated anilines is more efficient that the chlorination of sulfanilic acid.

Sulfonamide	X	R	mp (°C), (litt. (°C))	Method	Yield (%)	ν_{SO-N} (cm^{-1})	ν_{N-H} (cm^{-1})
51a	H	H	161	A	17	1295	3459
			(163)	B	35	1159	3389
51b	H	Me	110	A	7	1293	3466
			(108)	B	42	1150	3473
57b	Cl	Me	167	B	54	1302	3405
			(164-166)			1150	3389
57c	Cl	$(CH_2)_2OH$	120	B	67	1310	3405
						1160	3374

Table 4.4 Selected physical properties for sulfonamides **51a-b** and **57b-c**

(see page 176 for general formula)

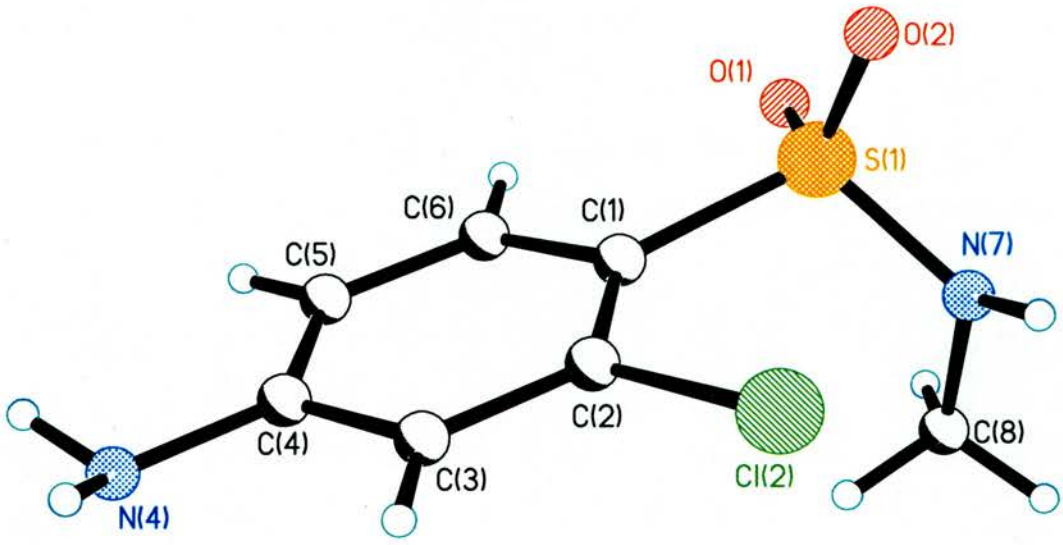

Figure 4.5 Crystal structure of sulfonamide **57b**

	57b
Bond length	
S(1)-O(1)	1.4315(12)
S(1)-N(7)	1.6042(14)
C(2)-Cl(2)	1.7420(15)
C(5)-C(6)	1.382(2)
N(7)-C(8)	1.458(2)
Bond angle	
O(1)-S(1)-N(7)	108.53(7)
O(2)-S(1)-N(7)	105.99(7)
C(6)-C(1)-S(1)	118.27(11)
C(2)-C(1)-S(1)	123.87(12)
O(1)-S(1)-C(1)	105.76(7)
C(6)-C(1)-C(2)	117.80(13)

Table 4.5 Selected bond lengths (Å) and angles (º) for sulfonamide **57b**

Aromatic amines (2-aminopyridine, 2-aminopyrimidine) appeared much less reactive towards the phenyl sulfonyl chlorides **54a** and **54b** and the reaction yields were very low, below 5%, even with 5-8 equivalents of the aromatic amine. We believe that these results can be rationalised as a consequence of the lack of nucleophilicity due to the delocalisation of the nitrogen lone pair in these electron deficient aromatic systems. Reacting the 2-amino groups with a strong base like *n*-butyl lithium could produce the corresponding lithium amides[148]. Those species are known to be very reactive towards electrophilic species[149] like sulfonyl chlorides **54a** and **54b**.

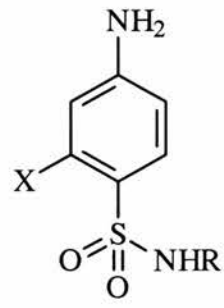

4.2.3 Synthesis of sulfonamide containing analogues of Purvalanol A

As presented in the previous Chapter, 6-chloro-2-benzylsulfanyl-9-isopropylpurine **33a** is a valuable intermediate for the preparation of 2,6-diaminopurines. However, it was anticipated that the reaction of the 6-chloride with the deactivated anilines bearing an electron-withdrawing sulfonamide group might be less successful than with *m*-chloroaniline. The reaction of 6-chloropurine **33a** with both anilines **51b** and **57b** was very clean and complete as no starting material was detected by TLC after 24 hours (*t*-butanol at 120°C in the presence of a couple of drops of concentrated hydrochloric acid). This result

demonstrates how reactive the C-Cl bond is in the presence of catalytic amounts of acid, although it can be argued that the traditionally used basic conditions might be driving the reaction to completion by scavenging the generated hydrogen chloride. Nevertheless, we have never managed to displace the 6-chloride of a purine with an aromatic amine as previously suggested. The ESI+ mass spectrum of **58a** and **58b** displays respectively the $[M+H]^+$ at *m/z* 491.1302 and the $[M+H]^+$ at *m/z* 525.0933. Complete peak assignment of the ^1H and ^{13}C NMR was possible by compiling the data from the Pendant, HMBC and HSQC NMR experiments.

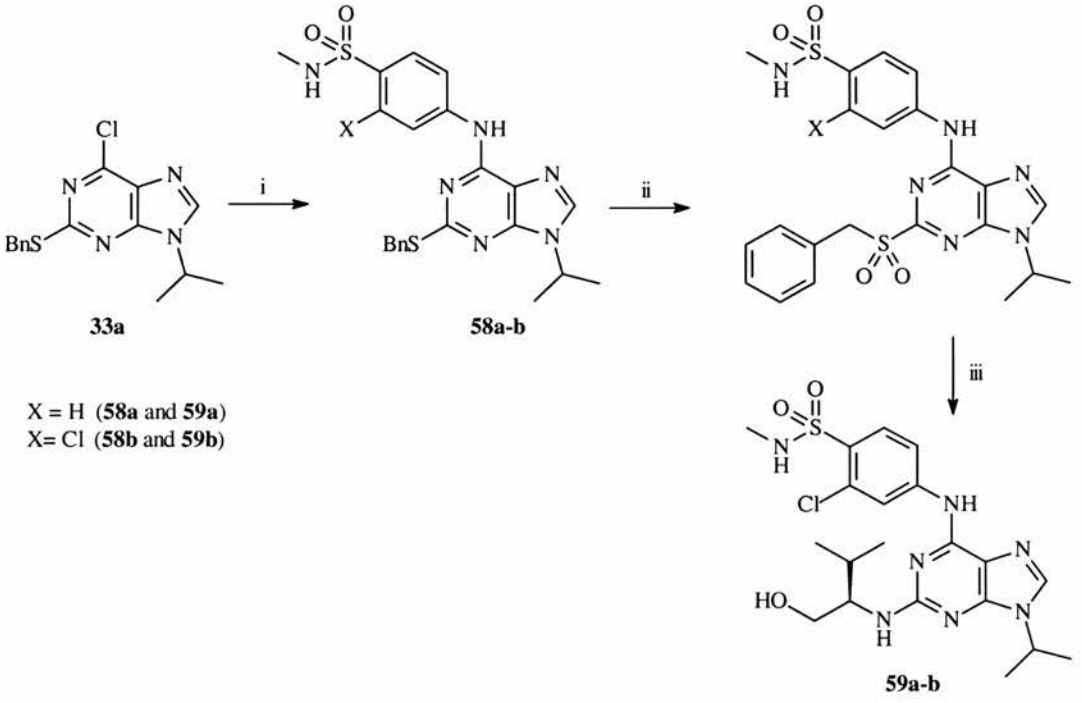

Conditions: i) aniline, $H^+_{(cat.)}$, *t*-BuOH, Δ ii) *m*-CPBA, $MgSO_4$, DCM iii) 10 eq. *R*-valinol, Hunig's base, BuOH, 160°C, sealed Parr bomb

Scheme 4.9 Synthesis of novel diaminopurines **59a-b** from the novel template **33a**

The oxidation of the 2-benzylsulfanyl into the corresponding sulfone was straightforward and complete as before using anhydrous conditions with the *m*-CPBA-MgSO4 combination in DCM. The insoluble inorganics were filtered off and washed with DCM. The filtrate was concentrated into the 2-benzylsulfonyl analogues of **58a-b** and the *m*-chlorobenzoic acid by-product. Mass spectrometry confirmed the presence of both products.

Displacement of the 2-benzylsulfonyl group with R-valinol was successful and the reaction afforded the novel diaminopurines **59a-b** in 70 and 75% yield respectively. Full characterisation was possible as analytical purity could be obtained following purification of the reaction mixture by flash chromatography on silica gel using a 1,2,3,4 then 5% MeOH in DCM. A slightly apolar by-product (ΔRf = 0.09 with 5% MeOH in DCM) was present in the product fractions if the mixture was eluted with 5% MeOH in DCM.

4.3 *Conclusions*

Our attempts to synthesise phosphorus containing R-valinol side-chains have unfortunately been unsuccessful. First of all, *O*-phosphorylation of Z- and Boc-*D*-valinol with both the $P(OEt)_3/I_2$ and $ClPO(OEt)_2/NEt_3$ systems produced complex mixtures of several phosphorus containing products that could not be

separated by distillation under vacuum. This is surprising as *O*-phosphorylation commonly occurs at room temperature with these reagents.

Our strategy based on the displacement of the tosyl leaving group with lithium phosphate was also unsuccessful, so we opted for the ring-opening of *N*-tosylaziridine with the same phosphorus nucleophile. Although the reaction produced an alkyl phosphonic ester according to ^{31}P NMR, it was not possible to obtain an analytically pure sample of this novel compound as decomposition is thought to have occurred during the attempted distillation. Further work is required to develop this method.

4-aminobenzene sulfonamides have been prepared according to modified literature procedures. Although the overall yields are very poor, the starting materials are affordable and the intermediates are easily prepared and purified. These deactivated anilines react well with the diaminopurine precursor **33a** in the presence of catalytic amounts of hydrochloric acid. Oxidative cleavage to afford the Purvalanol A analogues **59a-b** can be implemented by oxidising the 2-sulfanyl group with *m*-CPBA/$MgSO_4$ then reacting the sulfone in a sealed Parr bomb with R-valinol in the presence of Hunig's base.

To conclude, we have achieved the total synthesis of a highly efficient diaminopurine precursor, 6-chloro-2-benzylsulfanyl-9-isopropylpurine 33a that can be used for the preparation of diaminopurine CDK inhibitors.

4.4 *Experimental*

R-2-amino-3-methyl-butan-1-ol (R-valinol) **38**

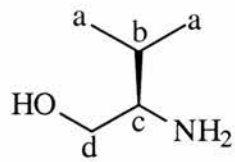

To a stirred mixture of lithium aluminium hydride (9.75g, 0.26mmol) in THF (500mL) was added at 0°C under a nitrogen atmosphere *R*-valine (15g, 0.13mmol) portionwise. Stirring at the same temperature was continued for 30 minutes, then at room temperature for 2 hours. Following reflux for 48 hours under nitrogen, the greyish mixture was cooled to 0°C and quenched by dropwise addition of water (9.75mL), aqueous 15% sodium hydroxide (14.6mL) then water (9.75mL) then left to stir overnight at room temperature. The resulting near colourless solid was filtered off, thoroughly washed with diethyl ether and the combined organics were dried over magnesium sulfate then evaporated to dryness into a colourless oil. Distillation under reduced pressure afforded *R*-valinol as a colourless oil that crystallises upon cooling below 0°C (12.95g, 98%), mp 36°C, lit.[126] 39-40°C); ^{1}H (300 MHz, d_6-dmso) δ_H 0.89-0.90 (2d, $^{3}J_{H\text{-}H}$ = 6.91 Hz, 2x3H, valinol H_a), 1.61 (m, $^{3}J_{H\text{-}H}$ = 6.91 Hz, 1H, valinol H_b), 2.46 (m, 1H, valinol H_c), 3.21 (dd, $^{3}J_{H\text{-}H}$ = 10.24Hz, $^{3}J_{H\text{-}H}$ = 7.68Hz, 1H, valinol H_d), 3.21 (dd, $^{3}J_{H\text{-}H}$ = 10.50Hz, $^{3}J_{H\text{-}H}$ = 4.86Hz, 1H, valinol H_d); ^{13}C (75.4 MHz, d_6-dmso) δ_C 18.0 (s, valinol C_a) 19.9 (s, valinol C_a), 30.4 (s, valinol C_b), 58.2 (s, valinol C_c), 64.8 (s, valinol C_d); MS (CI^+): *m/z* 104.1 $[M+H]^+$, $C_5H_{14}N_5NO$ requires 104.1; IR (KBr

disc, cm^{-1}) 3347s, 3241s, 2950s, 2865s, 1620s, 1571s, 1465s, 1383s, 1319m, 1287m, 1241m, 1142w, 1113w, 1064s, 1014m, 972m, 954w, 926w, 876w, 830w, 791w, 709w, 645w; Microanalytical data found: C: 58.36 H: 12.49 N: 13.62, expected for $C_5H_{13}NO$ C: 58.21 H: 12.70 N: 13.58.

R-Toluene-4-sulfonic acid 3-methyl-2-(toluene-4-sulfonylamino)-butyl ester **39**

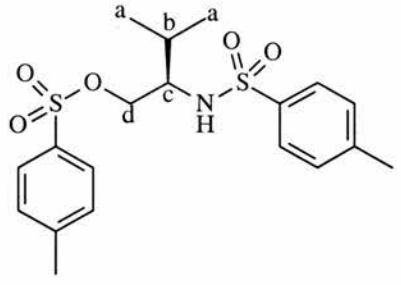

To a stirred solution of *p*-toluenesulfonyl chloride (3.91g, 20.4mmol) in dry pyridine (20mL) was added at -10°C under a nitrogen atmosphere *R*-valinol (1g, 9.71mmol) with almost dissolution and change to a bright yellow solution. Stirring at the same temperature under nitrogen was continued for 1 hour then at room temperature for 3 days. The volatiles were removed in vaccum and the yellowish oily solid was partitioned between DCM (100mL) and hydrochloric acid (3x30mL). The organics were further washed with aqueous saturated sodium bicarbonate, water then dried over potassium carbonate. Evaporation to full dryness afforded *bis*-tosyl valinol **39** as a colourless oil that solidifies on standing (3.95g, 99%); mp 114°C, litt.[130] 109-110°C; Rf 0.13 [EtOAc/hexane 4:1]; ^1H (300 MHz, $CDCl_3$) δ_H 0.66-0.69 (2d, $^3J_{H\text{-}H}$ = 6.91 Hz, 2x3H, valinol H_a), 1.77 (m, $^3J_{H\text{-}H}$ = 6.91 Hz, 1H, valinol H_b), 2.46 (m, 1H, valinol H_c), 2.35 (s, 3H, toluene CH_3), 2.39 (s, 3H, toluene CH_3), 3.07 (m, 1H, valinol H_c), 3.72 (dd, $^3J_{H\text{-}H}$ = 10.24Hz,

$^3J_{H\text{-}H}$ = 5.12Hz, 1H, valinol H_d), 3.93 (dd, $^3J_{H\text{-}H}$ = 10.24Hz, $^3J_{H\text{-}H}$ = 3.84Hz, 1H, valinol H_d), 4.77 (d, $^3J_{H\text{-}H}$ = 8.96Hz, 1H, NH), 7.19 (d, 2H, toluene aromatics), 7.27 (d, 2H, toluene aromatics), 7.61 (d, 2H, toluene aromatics), 7.64 (d, 2H toluene aromatics); ^{13}C (75.4 MHz, $CDCl_3$) δ_C 18.2 (s, valinol C_a) 19.3 (s, valinol C_a), 21.1 (s, toluene CH_3), 21.9 (s, toluene CH_3), 29.3 (s, valinol C_b), 58.0 (s, valinol C_c), 69.7 (s, valinol C_d), 127.5 (s, toluene *C*H), 128.4 (s, toluene *C*H), 130.1 (s, toluene *C*H), 130.4 (s, toluene *C*H), 132.6 (s, toluene CCH_3), 137.8 (s, toluene CCH_3), 144.0 (s, toluene CSO_2), 145.6 (s, toluene CSO_2); MS (ESI$^+$): *m/z* 434.1062 $[M+Na]^+$, $C_{19}H_{25}NO_5SNa$ requires 434.1072; IR (KBr disc, cm^{-1}) 3277s, 3038w, 2970m, 2931m, 2878m, 1926w, 1600m, 1498w, 1463m, 1444s, 1361vs, 1323s, 1292m, 1195s, 1180vs, 1160vs, 1092s, 1050m, 1021m, 985s, 964s, 951s, 896s, 847s, 814s, 789m, 706w, 669s, 636m, 628m, 572m, 550s, 532s; Microanalytical data found: C: 55.86 H: 5.98 N: 3.69 S: 15.87, expected for $C_{19}H_{25}NO_5S_2$ C: 55.45 H: 6.12 N: 3.40 S: 15.58.

S-2-Isopropyl-1-(toluene-4-sulfonyl)-aziridine **43**

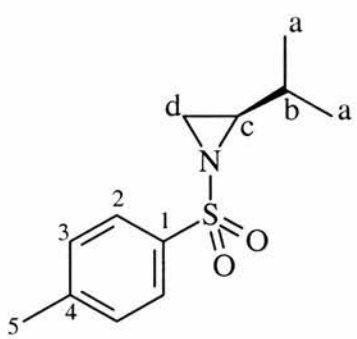

To a stirred solution of *bis*-tosyl-*R*-valinol **39** (2.5g, 6mmol) in anhydrous THF (40mL) was added under nitrogen sodium hydride (268mg, 60% w/w suspension

in mineral oil, 6.7mmol) to result in a yellowish mixture with vigorous evolution of hydrogen. Vigorous stirring was continued overnight under nitrogen, and the resulting near colourless mixture was evaporated to dryness into a white foam. DCM (50mL) was added and most of the solid dissolved, filtration then washing of the insoluble sodium tosylate with cold DCM afforded a colourless filtrate that was concentrated in vacuum to a few mL. Dropwise addition of hexane (5mL) afforded aziridine **43** as colourless crystalline neddles (1.4g, 96%); Rf 0.36 [EtOAc/hexane 4:1]; ^{1}H (300 MHz, $CDCl_3$) δ_H 0.72-0.82 (2d, $^{3}J_{H\text{-}H}$ = 6.91 Hz, 2x3H, isopropyl H_a), 1.33 (octet, $^{3}J_{H\text{-}H}$ = 6.91 Hz, 1H, isopropyl H_b), 2.03 (d, $^{3}J_{H\text{-}H}$ = 4.68 Hz, 1H, aziridine H_d), 2.37 (s, 3H, tosyl CH_3), 2.44 (dd, $^{3}J_{H\text{-}H}$ = 4.61 Hz and $^{3}J_{H\text{-}H}$ = 7.42 Hz, 1H, aziridine H_c), 2.54 (d, $^{3}J_{H\text{-}H}$ = 6.91Hz, $^{3}J_{H\text{-}H}$ = 5.12Hz, 1H, valinol H_d), 7.26 (dt, $^{3}J_{H\text{-}H}$ = 8.54 Hz and $^{3}J_{H\text{-}H}$ = 0.51 Hz, 2H, tosyl aromatics), 7.76 (dt, $^{3}J_{H\text{-}H}$ = 8.54 Hz and $^{3}J_{H\text{-}H}$ = 1.80 Hz, 2H, tosyl aromatics); ^{13}C (75.4 MHz, $CDCl_3$) δ_C 18.9 (s, isopropyl C_a), 19.1 (s, isopropyl C_a), 21.7 (s, toluene CH_3), 21.9 (s, toluene C_5), 29.7 (s, aziridine C_d), 30.3 (s, isopropyl C_b), 46.3 (s, aziridine C_c), 128.1 (s, tosyl C_2), 129.9 (s, tosyl C_3), 135.1 (s, tosyl C_1), 144.4 (s, tosyl C_4); MS (ESI^+): *m/z* 262.0871 $[M+Na]^+$, $C_{12}H_{17}NO_2SNa$ requires 262.0878; IR (KBr disc, cm^{-1}) 3052m, 2966s, 2927m, 2892m, 2867m, 1921w, 1596m, 1495w, 1459m, 1401w, 1384w, 1369w, 1320s, 1307s, 1290m, 1233m, 1199m, 1160vs, 1129m, 1092s, 1047w, 1020w, 977m, 963w, 938s, 889s, 836s, 814s, 781w, 729vs, 702m, 663s, 570s, 560s; Microanalytical data found: C: 59.78 H: 7.69 N: 5.12 S: 15.87, expected for $C_{12}H_{17}NO_2S$ C: 60.22 H: 7.16 N: 5.85 S: 15.42.

R-(1-Hydroxymethyl-2-methyl-propyl)-carbamic acid tert-butyl ester **44**

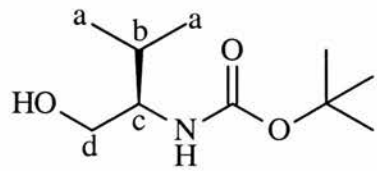

To a stirred solution of *R*-valinol **38** (1g, 9.71mmol) in anhydrous DCM (20mL) was added under nitrogen di-*tert*-butyl dicarbonate (2.22g, 10.2mmol) at 0°C to result in a cloudy mixture almost instantly. Vigorous stirring was continued overnight under nitrogen, and the resulting near colourless suspension was partitioned between DCM and saturated aqueous bicarbonate. The organics were further washed with water, dried over sodium sulfate and evaporated to dryness into *N*-Boc valinol **44** as a colourless oil (1.74g, 88%); ^{1}H (300 MHz, $CDCl_3$) δ_H 0.86-0.89 (2d, $^{3}J_{H\text{-}H}$ = 6.66 Hz, 2x3H, isopropyl H_a), 1.38 (s, 9H, C(CH_3)$_3$), 1.77 (octet, $^{3}J_{H\text{-}H}$ = 6.66 Hz, 1H, isopropyl H_b), 3.35 (broad s, 1H, O*H*), 3.52 (dd, $^{3}J_{H\text{-}H}$ = 6.14Hz and $^{3}J_{H\text{-}H}$ = 10.75Hz, 1H, valinol H_d), 3.61 (dd, $^{3}J_{H\text{-}H}$ = 11.01Hz and $^{3}J_{H\text{-}H}$ = 3.58Hz, 1H, valinol H_d); ^{13}C (75.4 MHz, $CDCl_3$) δ_C 18.9 (s, isopropyl C_a), 19.9 (s, isopropyl C_a), 28.8 (s, C(CH_3)$_3$), 29.7 (s, isopropyl C_b), 58.4 (s, C_c), 64.4 (s, C_d), 79.8 (s, C(CH$_3$)$_3$), 157.2 (s, C=O); MS (ESI$^+$): *m/z* 204.1595 [M+H]$^+$, $C_{10}H_{21}NO_3$ requires 204.1594; IR (KBr plates, cm^{-1}) 3392vs, 2965vs, 2929s, 2872s, 1713s, 1683s, 1535s, 1505s, 1468s, 1450s, 1390m, 1367m, 1312m, 1252m, 1173m, 1117m, 1074m, 1046m, 1025m, 982m, 901w, 864w, 781w; Microanalytical data found: C: 59.78 H: 11.52 N: 6.16, expected for $C_{10}H_{21}NO_3$ C: 59.09 H: 10.41 N: 6.89.

R-(1-Hydroxymethyl-2-methyl-propyl)-carbamic acid tert-butyl ester **45**

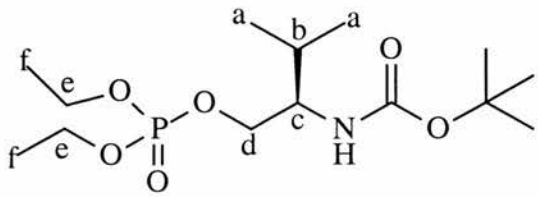

To a solution of *N*-Boc-*R*-valinol **44** (1.5g, 7.4mmol) in anhydrous THF (50mL) was added under nitrogen at room temperature triethylamine (10.3mL, 74mmol) followed by a solution of diethyl phosphorochloridate (1.2mL, 8.1mmol) in THF (50mL). Reflux and vigorous stirring of the solution was continued for 4 days under nitrogen and was followed by ^{31}P NMR in the reaction solvent using $CDCl_3$-inserts. Following cooling to room temperature, the triethylamine hydrochloride precipitate was filtered off and the filtrate was concentrated into a colourless oil that was partitioned between EtOAc (50mL) and water (2x30mL). The organics were dried over magnesium sulfate and evaporated to dryness to afford the phosphorylated valinol **45** a colourless oil (1.37g, 55%); ^{1}H (300 MHz, $CDCl_3$) δ_H 0.68-0.70 (2d, $^{3}J_{H\text{-}H}$ = 6.91 Hz, 2x3H, isopropyl H_a), 0.80 (s, 9H, $C(CH_3)_3$), 0.89 (triplet, $^{3}J_{H\text{-}H}$ = 7.17 Hz, 6H, phosphate H_f), 1.04 (octet, 1H, isopropyl H_b), 2.19 (m, 4H, phosphate H_e), 3.34 (m, 1H, valinol H_d), 3.76 (m, 1H, valinol H_d); ^{13}C (75.4 MHz, $CDCl_3$) δ_C 19.2 (s, isopropyl C_a), 19.9 (s, isopropyl C_a), 28.1 (s, $C(CH_3)_3$), 29.2 (s, isopropyl C_b), 53.7 (s, valinol C_c), 64.4 (d, $^{3}J_{P\text{-}C}$ = 2.76 Hz, C_d), 66.2 (d, $^{3}J_{P\text{-}C}$ = 2.76 Hz, phosphate C_e), 79.8 (s, $C(CH_3)_3$), 157.2 (s, C=O); ^{31}P (121.5 MHz, $CDCl_3$) δ_P 0.17; MS (ESI^+): *m/z* 362.1711 $[M+Na]^+$, $C_{14}H_{30}NO_6NaP$ requires 362.1708; IR (KBr plates, cm^{-1}) 2980vs, 2936vs, 2872s,

1713s, 1699m, 1652w, 1538m, 1471m, 1393m, 1368m, 1251s, 1168s, 1034vs, 897w, 818w.

2-(*N*-benzyloxycarbonyl-amino)-3-methyl-butan-1-ol **47**

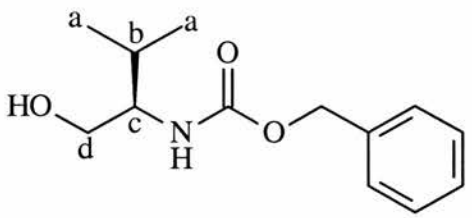

To a solution of *R*-valinol **38** (2g, 19.4mmol) in ethyl acetate (50mL) was added under nitrogen at room temperature a solution of *N*-(benzyloxycarbonyloxy)-succinimide (5.62, 95%, 21.4mmol) in ethyl acetate (10mL) dropwise over 10 minutes with gradual thickening of the reaction mixture. Stirring was continued for 3 days and the resulting pale yellowish solution was washed with saturated sodium bicarbonate and water, then dried over magnesium sulfate and evaporated to full dryness to yield the *N*-Cbz-valinol **47** as a colourless oil (4.23g, 92%); ^{1}H (270 MHz, $CDCl_3$) δ_H 0.89-0.91 (2d, $^{3}J_{H\text{-}H}$ = 7.16 Hz, 2x3H, isopropyl H_a), 1.82 (octet, $^{3}J_{H\text{-}H}$ = 6.94 Hz, 1H, isopropyl H_b), 3.58 (m, 1H, valinol O*H*), 3.63 (m, 2H, valinol H_d), 4.96 (d, 1H, N*H*), 5.08 (s, 2H, PhCH_2O), 7.32-7.37 (m, 5H, aromatics *Ph*CH_2O); ^{13}C (75.4 MHz, $CDCl_3$) δ_C 18.9 (s, isopropyl C_a), 19.9 (s, isopropyl C_a), 29.6 (s, isopropyl C_b), 58.9 (s, valinol C_c), 64.2 (s, valinol C_d), 67.3 (s, Ph*C*H_2O), 128.5 (s, aromatic *C*H), 128.6 (s, aromatic *C*H), 129.0 (s, aromatic *C*H), 136.8 (s, aromatic *C*CH_2O), 157.5 (s, C=O); MS (EI): *m/z* 237.1362 $[M]^+$, $C_{13}H_{19}NO_3$ requires 237.1359; IR (KBr plates, cm^{-1}) 3419vs, 3067s, 3035s, 2962s, 2872s, 1956w, 1814s, 1790s, 1695s, 1587m, 1539s, 1506s, 1471s, 1456s,

1258m, 1048m, 825w, 775m, 740s, 697s; Microanalytical data found: C: 66.03 H: 8.92 N: 6.29, expected for $C_{13}H_{19}NO_3$ C: 65.80 H: 8.07 N: 5.90.

[1-(Diethoxy-phosphoryloxymethyl)-2-methyl-propyl]-

carbamic acid benzyl ester **48**

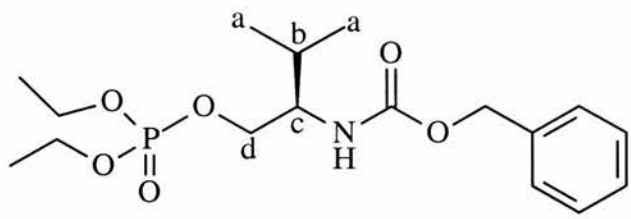

To a solution of *N*-Cbz-*R*-valinol **47** (6g, 25.32mmol) in anhydrous THF (50mL) was added under nitrogen at room temperature *N,N,N*-diisopropylethylamine (10.5mL, 60.25mmol) followed by diethyl phosphorochloridate (7.7mL, 50.63mmol) dropwise over 10 minutes. Stirring at 90°C under nitrogen was continued for 3 days under nitrogen and was followed by ^{31}P NMR in the reaction solvent using $CDCl_3$-inserts. Following cooling to room temperature, the triethylamine hydrochloride precipitate was filtered off and the filtrate was concentrated into a colourless oil that was partitioned between EtOAc (50mL) and water (2x30mL). The organics were dried over magnesium sulfate and evaporated to dryness to afford the phosphorylated valinol **48** a colourless oil (1.60, 17%); ^1H (300 MHz, $CDCl_3$) δ_H 0.90 (d, $^3J_{H\text{-}H}$ = 6.66 Hz, 6H, isopropyl H_a), 1.06 (octet, 1H, isopropyl H_b), 1.30 (t, $^3J_{H\text{-}H}$ = 7.43 Hz, phosphate CH_3CH_2O-), 1.84 (s, $^3J_{H\text{-}H}$ = 6.66 Hz, 1H, $CH(CH_3)_3$), 3.58 (m, 1H, valinol H_c), 3.96-4.20 (m, 6H, phosphate OCH_2CH_3 and valinol H_d), 5.00 (d, $^3J_{H\text{-}H}$ = 4.61 Hz, 1H, valinol N*H*), 7.24 (m, 5H, aromatic Cbz); ^{13}C (75.4 MHz, $CDCl_3$) δ_C 11.9 (s,

phosphate CH_3CH_2O-), 19.4 (s, valinol C_a), 29.8 (s, valinol C_b), 41.7 (s, -OCH_2Ph), 53.1 (s, valinol C_c). 62.5 (d, $^3J_{P\text{-}C}$ = 6.08 Hz, valinol C_d), 63.5 (d, $^3J_{P\text{-}C}$ = 6.08 Hz, phosphate C_e), 127.8 (s, Ph C_2), 128.3 (s, Ph C_4), 128.6 (s, Ph C_3), 136.9 (s, Ph C_1), 158.9 (s, C=O); ^{31}P (121.5 MHz, $CDCl_3$) δ_P -0.17; MS (ESI^+): *m/z* 396.1560 $[M+Na]^+$, $C_{17}H_{28}NO_6NaP$ requires 396.1552; IR (KBr plates, cm^{-1}) 3345s, 3033m, 2964s, 2874m, 2672w, 2510w, 1717s, 1586m, 1538s, 1498s, 1455m, 1393m, 1370m, 1266vs, 1164m, 1037vs, 945s, 774m, 737m, 699m, 509m.

N-(p-chlorosulfonylphenyl)phosphoramidic trichloride **50b**

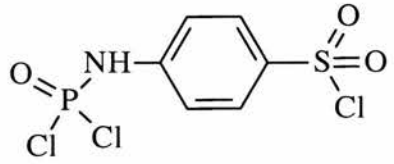

To sulfanilic acid (g, mmol) was added phosphorus pentachloride (59.38g, mmol) with vigorous shaking for 2 minutes. After the slightly exothermic reaction resumed, heating with stirring was continued for 6 hours to result in a yellowish mixture. The volatiles were removed under vacuum to retrieve a colourless solid. Water (500mL) was added in one portion and following stirring for 1 hour, the precipitate was filtered off and thoroughly dried under vaccum at 40°C to afford phenylsulfonyl chloride **50b** as a colourless powder (g, 86% yield); mp 158°C, litt.[80] 155°C; MS (EI): *m/z* 306.8789 $[M]^+$, $C_6H_5NO_3PS$ requires 306.8788; IR (KBr plates, cm^{-1}) 3201m, 3109m, 2931w, 2853w, 1592s, 1497s, 1468s, 1367vs, 1297s, 1261vs, 1197s, 1174vs, 1088s, 942s, 840s, 712w,

695w, 595vs; Microanalytical data found: C: 23.56 H: 1.31 N: 4.44, expected for $C_{13}H_{19}NO_3$ C: 65.36 H: 1.63 N: 4.54.

4-aminobenzene sulfonamide **51a** (Method A)

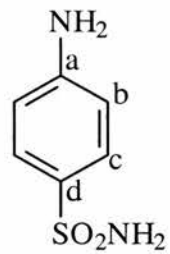

To a stirred mixture of phenylsulfonyl chloride **50b** (3g, 9.72mmol) in anhydrous THF (50mL) was added under nitrogen aqueous concentrated ammonia (2.70mL, 58.72mmol) dropwise over 5 minutes, then stirring under nitrogen was continued overnight at 90°C. Evaporation to dryness afforded an oily solid that was refluxed in 5M HCl (100mL) for 6 hours, cooled down then carefully neutralised to pH 7 by dropwise addition of sodium hydroxide (about 25g). The water was removed under vaccum to yield a colourless residue. Recrystallisation from boiling water afforded sulfonamide **51a** as a colourless solid (0.28g, 17%); mp 165°C, litt.[150] 163°C; ^{1}H (300 MHz, d_6-dmso) δ_H 7.20 (d, $^3J_{H\text{-}H}$ = 7.29 Hz, 1H, aromatic H_b), 7.64 (d, $^3J_{H\text{-}H}$ = 7.29 Hz, 2H, aromatic H_c); ^{13}C (75.4 MHz, d_6-dmso) δ_C 121.8 (s, aromatic C_b), 127.4 (s, aromatic C_c), 134.0 (s, aromatic C_a), 146.8 (s, aromatic C_d); MS (ESI$^+$): *m/z* 194.9 $[M+Na]^+$, $C_6H_8N_2O_2SNa$ requires 195.0; IR (KBr disc, cm^{-1}) 3459m, 3389m, 3345m, 3243w, 1624m, 1597vs, 1500m, 1459w, 1432w, 1403w, 1295s, 1175m, 1159s, 1095s, 1079m, 1000w, 847m, 826s, 686m, 695m,

551s; Microanalytical data found: C: 41.45 H: 4.89 N: 14.30, expected for $C_6H_8N_2O_2S$ C: 41.85 H: 4.68 N: 16.27.

4-aminobenzene sulfonamide **51b** (Method A)

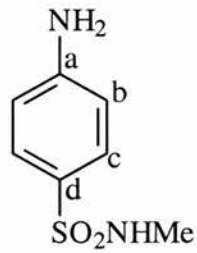

To a stirred mixture of phenylsulfonyl chloride **50b** (3g, 9.72mmol) in anhydrous THF (50mL) was added under nitrogen a solution of methylammonium chloride (6.56g, 97mmol) in saturated aqueous sodium bicarbonate (25mL) and reflux was continued for 5 hours. The solvent was removed and 5M HCl (50mL) was added to the residue, stirring at reflux for 8 hours, prior to careful neutralisation to pH 7 by dropwise addition of sodium hydroxide. The water was removed under vaccum to yield a colourless residue. Recrystallisation from boiling water afforded sulfonamide **51b** as a colourless solid (126mg, 7%); mp 111°C, litt.[151] 108°C; ^{1}H (300 MHz, d_6-dmso) δ_H 2.38 (s, 3H, -SO_2NHCH_3), 5.98 (s, 2H, -NH_2), 6.68 (d, $^3J_{H\text{-}H}$ = 8.71 Hz, 1H, aromatic H_b), 6.98 (s, 1H, -SO_2NHCH_3), 745 (d, $^3J_{H\text{-}H}$ = 8.71 Hz, 2H, aromatic H_c); ^{13}C (75.4 MHz, d_6-dmso) δ_C 29.0 (s, -SO_2NHCH_3), 113.0 (s, aromatic C_b), 124.5 (s, aromatic C_d), 152.8 (s, aromatic C_a); MS (ESI$^+$): *m/z* 209.00 $[M+Na]^+$, $C_7H_{10}N_2O_2SNa$ requires 209.03; IR (KBr disc, cm^{-1}) 3466m, 3373m, 3307m, 3243m, 2979w, 2931w, 1628s, 1597vs,

1503s, 1466w, 1438w, 1405w, 1293vs, 1187w, 1150vs, 1093s, 1071m, 1010w, 848m, 828s, 680s, 635m, 555s; Microanalytical data found: C: 45.92 H: 5.10 N: 16.90, expected for $C_7H_{10}N_2O_2S$ C: 45.15 H: 5.42 N: 15.05.

N-phenylacetamide **53a**

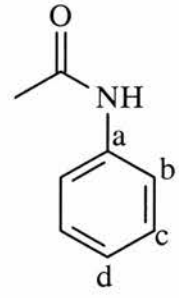

To aniline (10mL, 0.10mol) in anhydrous acetonitrile (40mL) was added under nitrogen acetic anhydride (11.4mL, 0.12mol) dropwise over 5 minutes, then stirring under nitrogen was continued overnight. Evaporation to dryness afforded an oily solid that was triturated with water (100mL) then filtered off, washed with water (500mL) then dried under vaccum at 60°C to yield acetamide 53a as a off-tan solid (12.39g, 84%); mp 116°C, litt.[152] 117-118°C; Rf 0.24 [EtOAc/hexane 1:1]; ^{1}H (300 MHz, $CDCl_3$) δ_H 2.03 (s, 3H, CH_3CO), 6.99 (t, $^3J_{H\text{-}H}$ = 7.42 Hz, 1H, aromatic H_d), 7.18 (t, $^3J_{H\text{-}H}$ = 7.42 Hz, 2H, aromatic H_c), 7.42 (d, $^3J_{H\text{-}H}$ = 8.71 Hz, 2H, aromatic H_b), 8.35 (broad s, 1H, N*H*); ^{13}C (75.4 MHz, $CDCl_3$) δ_C 24.7 (s, methyl CH_3CO), 120.7 (s, aromatic C_b), 124.7 (s, aromatic C_d), 129.3 (s, aromatic C_c), 138.5 (s, aromatic C_a), 169.7 (s, amide *C*=O; MS (ESI$^+$): *m/z* 157.6 $[M+Na]^+$, C_8H_9NONa requires 158.06; IR (KBr disc, cm^{-1}) 3295s, 3195m, 3137m, 3060m, 3022m, 2858w, 2802w, 1951w, 1664vs, 1599vs, 1559s, 1539s, 1501s, 1490s, 1435s, 1369s, 1323s, 1264s, 1180w, 1160w, 1081w, 1041m,

1013m, 998w, 962m, 907m, 849w, 839w, 753vs, 694vs, 664m, 603w; Microanalytical data found: C: 70.80 H: 6.89 N: 10.46, expected for C_8H_9NO C: 71.09 H: 6.71 N: 10.36.

N-(3-chlorophenyl)acetamide **53b**

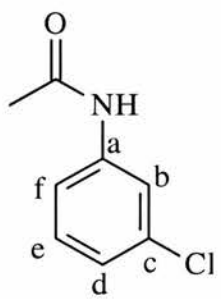

To 3-chloroaniline (50mLmL, 0.47mol) in anhydrous acetonitrile (150mL) was added under nitrogen acetic anhydride (50mL, 0.70mol) dropwise over 15 minutes, then stirring under nitrogen was continued overnight. Evaporation to dryness afforded an oily solid that was triturated with water (500mL) then filtered off, washed with water (500mL), recrystallised from cyclohexane then dried under vaccum at 60°C to afford the N-acetamide **53b** as a colourless crystalline powder (77.97g, 98%); mp 79°C, litt.[153] 78°C; Rf 0.43 [EtOAc/hexane 1:1]; ^{1}H (300 MHz, $CDCl_3$) δ_H 2.08 (s, 3H, CH_3CO), 6.97 (t, $^3J_{H\text{-}H}$ = 7.94 Hz, 1H, aromatic H_d), 7.10 (t, $^3J_{H\text{-}H}$ = 7.94 Hz, 1H, aromatic H_e), 7.25 (t, $^3J_{H\text{-}H}$ = 8.19 Hz, 1H, aromatic H_f), 7.57 (t, $^3J_{H\text{-}H}$ = 1.79 Hz, 1H, aromatic H_b), 8.50 (broad s, 1H, N*H*); ^{13}C (75.4 MHz, $CDCl_3$) δ_C 24.8 (s, methyl CH_3CO), 118.5 (s, aromatic C_f), 120.7 (s, aromatic C_b), 124.7 (s, aromatic C_c), 130.3 (s, aromatic C_e), 134.8 (s, aromatic C_c), 139.6 (s, aromatic C_a), 169.8 (s, amide *C*=O; MS (ESI$^+$): *m/z* 192.5 $[M+Na]^+$, $C_8H_8ClNONa$ requires 192.0; IR (KBr disc, cm^{-1}) 3299m, 3257m,

3187m, 3121m, 3078m, 1672vs, 1594vs, 1542vs, 1474s, 1420s, 1369m, 1330m, 1310m, 1280s, 1260s, 1229m, 1164w, 1091w, 1074w, 1038w, 1012w, 998w, 962w, 902w, 870m, 784s, 753m, 704m, 681m, 608m, 532w, 523w; Microanalytical data found: C: 57.02 H: 4.61 N: 8.13, expected for C_8H_8ClNO C: 56.65 H: 4.75 N: 8.26.

4-Acetylamino-benzenesulfonyl chloride **54a**

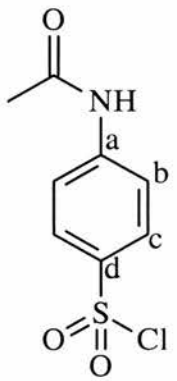

To chlorosulfonic acid (20mL, 200mmol) was added under nitrogen acetamide **53a** (8.4, 62.2mmol) portionwise at 0°C, then stirring under nitrogen was continued for 1 hour at romm temperature. Stirring at 60°C was continued under nitrogen for 20 hours. Following cooling to room temperature, the resulting thick mixture was poured carefully on crushed ice (400mL) to precipitate a pink oil that was partitioned with DCM (2x100mL). The organics were dried over sodium bicarbonate then evaporated to dryness to afford a near colourless solid. Recrystallisation from toluene afforded pure phenylsulfonyl chloride 54a as very pale pink needles (8.82g, 60%); mp 146°C, litt.[154] 149°C; ^{1}H (300 MHz, $CDCl_3$) δ_H 2.19 (s, 3H, CH_3CO), 7.72 (dt, $^3J_{H\text{-}H}$ = 9.73 Hz and $^3J_{H\text{-}H}$ = 2.56 Hz, 2H, aromatic H_c), 7.89 (dt, $^3J_{H\text{-}H}$ = 9.73 Hz and $^3J_{H\text{-}H}$ = 2.56 Hz, 2H, aromatic H_d),

7.96 (broad s, 1H, N*H*); ^{13}C (75.4 MHz, $CDCl_3$) δ_C 25.2 (s, methyl CH_3CO), 119.8 (s, aromatic C_b), 129.0 (s, aromatic C_c), 138.9 (s, aromatic C_a), 144.7 (s, aromatic C_d), 168.2 (s, amide *C*=O; MS (EI^+): *m/z* 233 $[M]^+$, $C_8H_8ClNO_3SNa$ requires 232.99; IR (KBr disc, cm^{-1}) 3305m, 3265m, 3189m, 3112m, 3043m, 1681s, 1606m, 1585vs, 1538vs, 1494s, 1407s, 1371s, 1316m, 1265s, 1189m, 1169vs, 1083m, 1037w, 1009w, 839m, 723w, 707m, 631m, 607w, 565s, 535m; Microanalytical data found: C: 41.22 H: 3.53 N: 5.93, expected for $C_8H_8ClNO_3S$ C: 41.12 H: 3.45 N: 5.99.

4-Acetylamino-2-chloro-benzenesulfonyl chloride **54b**

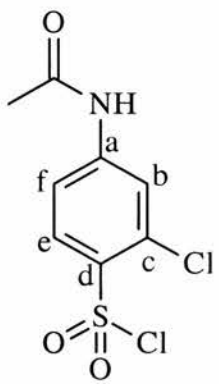

To chlorosulfonic acid (30mL, 300mmol) stirred at 0°C under nitrogen was added 3-chlorophenylacetamide 53b (8.5g, 0.05mol) then stirring under nitrogen was continued for 1 hour at the same temperature. Stirring at was continued for 22 hours under nitrogen. Following cooling to room temperature and careful pouring on to crushed ice (500mL), the oily precipitate was partitioned with DCM (2x150mL), and the organics were dried over sodium bicarbonate and evaporated to dryness into a pinkish solid. Recrystallisation from THF afforded the desired phenylsulfonyl chloride 54b as near colourless needles (8.20g, 61%); mp 125°C,

litt.[155] 120-126°C; Rf 0.38 [EtOAc/hexane 2:1]; ^{1}H (270 MHz, $CDCl_3$) δ_H 2.22 (s, 3H, CH_3CO), 7.54 (dd, $^3J_{H\text{-}H}$ = 8.83 Hz and $^3J_{H\text{-}H}$ = 1.97 Hz, 1H, aromatic H_f), 7.93 (broad s, 1H, N*H*), 7.97 (d, $^3J_{H\text{-}H}$ = 1.97 Hz, 1H, aromatic H_b), 8.01 (d, $^3J_{H\text{-}H}$ = 8.83 Hz, 1H, aromatic H_e); ^{13}C (75.4 MHz, $CDCl_3$) δ_C 25.2 (s, methyl CH_3CO), 117.3 (s, aromatic C_f), 122.6 (s, aromatic C_b), 132.0 (s, aromatic C_e), 134.4 (s, aromatic C_d), 135.8 (s, aromatic C_c), 145.3 (s, aromatic C_a), 170.0 (s, amide *C*=O; MS (CI^+): *m/z* 268 $[M+H]^+$, $C_8H_7Cl_2NO_3S$ requires 266.95; IR (KBr disc, cm^{-1}) 3323m, 3285m, 3193m, 3103m, 3023m, 1702s, 1609m, 1596vs, 1527vs, 1499s, 1435m, 1403s, 1389s, 1325m, 1321m, 1232s, 1178m, 1173vs, 1033m, 1031w, 1000w, 856m, 712w, 709m, 626m, 515m; Microanalytical data found: C: 35.91 H: 2.67 N: 5.63, expected for $C_8H_7Cl_2NO_3S$ C: 35.84 H: 2.63 N: 5.22.

Preparation of sulfonamides **55a-d** and **56a-b** from *p*-(*N*-acetylamino)-phenylsulfonyl chlorides **54a-b** (Method B):

To a stirred solution of the phenylsulfonyl chloride **54a-b** (30mmol) in anhydrous acetonitrile (100mL) was added the amine (90-120mmol / 3-4 equivalents) dropwise/portionwise under a nitrogen atmosphere at room temperature, then reflux of the reaction mixture was continued for 24 hours under nitrogen. Following evaporation to full dryness, 5M NaOH (100mL) was added to the residues **55a-d/56a-b** and the resulting mixtures were refluxed for 12-24 hours and the reaction followed by TLC using 5-10% MeOH in DCM. When the

reaction was complete, the solution was evaporated to 10mL, and the pH was adjusted to 7-8 by dropwise addition of concentrated hydrochloric acid. The precipitate was filtered off and recrystallised when necessary from water.

4-(*N*-acetylamino)-N-methyl-benzene sulfonanide **55a**

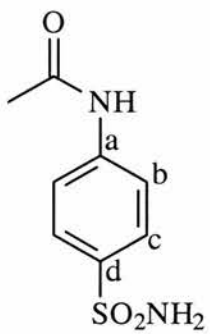

Colourless powder (0.73g, 67%); mp 220°C, litt.[156] 218-219°C; ^{1}H (270 MHz, d_6-dmso) δ_H 2.14 (s, 3H, C*H*$_3$CO), 7.31 (s, 2H, -SO$_2$N*H*$_2$), 7.77 (dd, $^{3}J_{H\text{-}H}$ = 9.47 Hz and $^{3}J_{H\text{-}H}$ = 3.33 Hz, 2H, aromatic H_b), , 7.83 (dd, $^{3}J_{H\text{-}H}$ = 9.47 Hz and $^{3}J_{H\text{-}H}$ = 3.33 Hz, 2H, aromatic H_c), 10.36 (broad s, 1H, N*H*); ^{13}C (75.4 MHz, d_6-dmso) δ_C 24.4 (s, methyl *C*H$_3$CO), 118.8 (s, aromatic C_b), 127.0 (s, aromatic C_c), 138.4 (s, aromatic C_d), 142.5 (s, aromatic C_a), 169.4 (s, amide *C*=O); MS (ESI$^-$): *m/z* 213.05 [M-H]$^-$, $C_8H_{10}N_2O_3S$ requires 213.03; IR (KBr disc, cm^{-1}) 3353s, 3299s, 3260s, 3107m, 3037m, 2927w, 2850w, 2783w, 1671vs, 1595vs, 1530vs, 1401s, 1375m, 1298vs, 1268m, 1160vs, 1096m, 1018w, 972w, 909m, 858m, 830s, 743m, 716m, 695m, 634m, 621m, 600m, 546m, 539m, 519w; Microanalytical data found: C: 45.01 H: 4.96 N: 12.54, expected for $C_8H_{10}N_2O_3S$ C: 44.85 H: 4.71 N: 13.08.

4-(*N*-acetylamino)-N-methyl-benzene sulfonanide **55b**

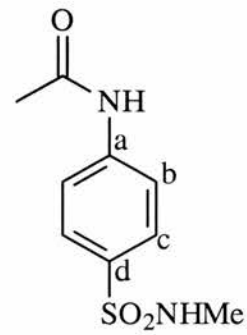

Colourless needles (2.24g, 78%); mp 198°C, litt.[157] 185°C; ^{1}H (300 MHz, $CDCl_3$) δ_H 2.06 (s, 3H, CH_3CO), 2.36 (s, 3H, -SO_2NHCH_3), 7.67 (dt, $^{3}J_{H\text{-}H}$ = 8.97 Hz and $^{3}J_{H\text{-}H}$ = 2.05 Hz, 2H, aromatic H_b), 7.74 (dt, $^{3}J_{H\text{-}H}$ = 8.71 Hz and $^{3}J_{H\text{-}H}$ = 2.30 Hz, 2H, aromatic H_c), 10.37 (broad s, <1H, N*H*); ^{13}C (75.4 MHz, $CDCl_3$) δ_C 24.3 (s, methyl CH_3CO), 28.9 (s, methyl -SO_2NHCH_3), 119.1 (s, aromatic C_b), 128.1 (s, aromatic C_c), 133.1 (s, aromatic C_a), 143.0 (s, aromatic C_d), 169.7 (s, amide *C*=O); MS (ESI$^-$): *m/z* 227.06 [M-H]$^{\cdot}$, $C_9H_{11}N_2O_3S$ requires 227.05; IR (KBr disc, cm^{-1}) 3323m, 3272m, 3166s, 2983m, 2924m, 2877m, 2845m, 2806m, 1684s, 1591s, 1536s, 1499m, 1460m, 1402m, 1380m, 1323vs, 126s, 1189w, 1157vs, 1093s, 1068s, 1027w, 1002w, 964w, 865w, 850m, 836s, 819s, 794s, 697s, 794s, 697s, 633m, 613s, 597m, 563m, 554s, 508m; Microanalytical data found: C: 48.20 H: 5.69 N: 13.45, expected for $C_9H_{12}N_2O_3S$ C: 47.36 H: 5.30 N: 12.28.

N-[4-(2-Hydroxy-ethylsulfamoyl)-phenyl]-acetamide **55c**

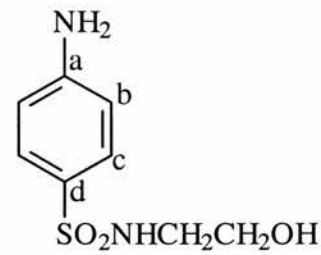

Red oil (3.70g, 95%); ^{1}H (300 MHz, d_6-dmso) δ_H 2.06 (s, 3H, C*H*$_3$CO), 2.49 (broad s, <1H, O*H*), 2.74 (t, $^{3}J_{H\text{-}H}$ = 6.40 Hz, 2H, -NHC*H*$_2$CH$_2$OH), 2.97 (broad s, <1H, N*H*), 3.35 (t, $^{3}J_{H\text{-}H}$ = 6.40 Hz, 2H, -NHCH$_2$C*H*$_2$OH), 7.69 (dd, $^{3}J_{H\text{-}H}$ = 6.91 Hz and $^{3}J_{H\text{-}H}$ = 2.30 Hz, 2H, aromatic H_b), 7.76 (dd, $^{3}J_{H\text{-}H}$ = 8.96 Hz and $^{3}J_{H\text{-}H}$ = 2.30 Hz, 2H, aromatic H_c), 10.35 (broad s, <1H, N*H*COMe); ^{13}C (75.4 MHz, $CDCl_3$) δ_C 24.5 (s, methyl *C*H$_3$CO), 45.4 (s, -NH*C*H$_2$CH$_2$OH), 54.00 (s, -NHCH$_2$*C*H$_2$OH), 118.9 (s, aromatic C_b), 128.0 (s, aromatic C_c), 134.5 (s, aromatic C_a), 143.0 (s, aromatic C_d), 169.3 (s, amide *C*=O); MS (ESI$^-$): *m/z* 257.04 [M-H]$^-$, $C_{10}H_{13}N_2O_4S$ requires 257.06; Microanalytical data found: C: 47.30 H: 4.98 N: 11.23, expected for $C_{10}H_{14}N_2O_4S$ C: 46.50 H: 5.46 N: 10.85.

N-[4-(2-Hydroxy-ethylsulfamoyl)-phenyl]-acetamide **55d**

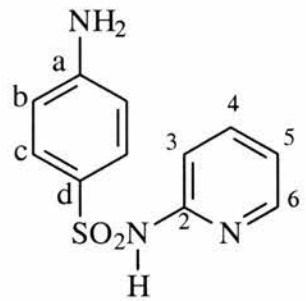

Tan plates (970mg, 26%); mp 223°C; ^{1}H (300 MHz, d_6-dmso) δ_H 2.04 (s, 3H, CH_3CO), 6.83 (td, $^{3}J_{H\text{-}H}$ = 5.63 Hz and $^{3}J_{H\text{-}H}$ = 2.02 Hz, 1H, pyridine H_5), 7.13 (d, $^{3}J_{H\text{-}H}$ = 9.47 Hz, 1H, pyridine H_3), 7.70 (dd and m, $^{3}J_{H\text{-}H}$ = 6.91 Hz and $^{3}J_{H\text{-}H}$ = 2.05 Hz, 3H, aromatics H_b and pyridine H_3), 7.78 (dd, $^{3}J_{H\text{-}H}$ = 6.91 Hz and $^{3}J_{H\text{-}H}$ = 2.05 Hz, 2H, aromatics H_c), 10.28 (broad s, <1H, N*H*), 11.80 (broad s, <1H, N*H*); ^{13}C (75.4 MHz, d_6-dmso) δ_C 24.4 (s, methyl CH_3CO), 113.8 (s, pyridine C_3), 116.1 (s, pyridine H_5), 118.8 (s, aromatic C_b), 128.1 (s, aromatic C_c), 135.7 (s, aromatic C_d), 140.5 (s, pyridine H_4), 142.9 (s, aromatic C_a), 144.1 (s, pyridine H_6), 153.3 (s, aromatic C_b), 169.4 (s, amide C=O); MS (ESI$^-$): *m/z* 290.04 [M-H]$^-$, $C_{13}H_{12}N_3O_3S$ requires 290.05; IR (KBr disc, cm^{-1}) 3445s, 3379s, 3314s, 3164s, 3067m, 3028m, 2963m, 2917m, 1695m, 1629vs, 1559s, 1540s, 1488s, 1443vs, 1404m, 1385m, 1320m, 1268m, 1142m, 1085m, 1035w, 991m, 958m, 853m, 834m, 772s, 739m, 636m, 624m, 570m, 521m; Microanalytical data found: C: 54.30 H: 4.19 N: 13.12, expected for $C_{13}H_{13}N_3O_3S$ C: 53.60 H: 4.50 N: 14.42.

N-(3-Chloro-4-methylsulfamoyl-phenyl)-acetamide **56b**

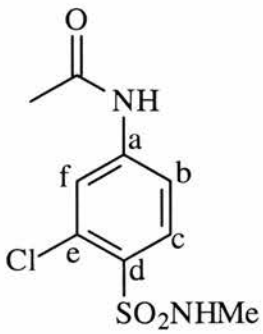

Tan needles (7.2g, 90%); mp 268°C; ^{1}H (300 MHz, d_6-dmso) δ_H 2.09 (s, 3H, CH_3CO), 2.41 (s, 3H, -SO_2NHCH_3), 7.68 (dd, $^{3}J_{H\text{-}H}$ = 8.71 Hz and $^{3}J_{H\text{-}H}$ = 2.05 Hz, 1H, aromatic H_b), 7.83 (d, $^{3}J_{H\text{-}H}$ = 8.71 Hz, 1H, aromatic H_c), 7.91 (broad s, <1H, N*H*COMe), 8.03 (d, $^{3}J_{H\text{-}H}$ = 2.05 Hz, 1H, aromatics H_f), 10.80 (broad s, <1H, N*H*Me); ^{13}C (75.4 MHz, d_6-dmso) δ_C 24.5 (s, methyl CH_3CO), 28.7 (s, methyl CH_3NH), 117.1 (s, aromatic C_b), 120.8 (s, aromatic C_c), 130.3 (s, aromatic C_e), 131.4 (s, aromatic C_a), 132.12 (s, aromatic C_a), 144.2 (s, aromatic C_f), 169.8 (s, amide *C*=O); MS (ESI$^-$): *m/z* 260.99 [M-H]$^-$, $C_9H_{10}ClN_2O_3S$ requires 261.01; IR (KBr disc, cm^{-1}) 3335s, 3301s, 3176m, 3102m, 3043m, 2992m, 2954m, 2769w, 1694s, 1683s, 1589vs, 1529vs, 1470m, 1426w, 1400s, 1382vs, 1321vs, 1249s, 1158vs, 1114s, 1072m, 1033m, 1009m, 953w, 889w, 866m, 854w, 832w, 748w, 717w, 701w, 675m, 625s, 586m, 554w, 537w, 508w; Microanalytical data found: C: 41.65 H: 3.45 N: 10.68, expected for C9H11ClN2O3S C: 41.30 H: 3.85 N: 10.70.

N-*4*-Amino-2-chloro-N-methyl-benzenesulfonamide **57b**

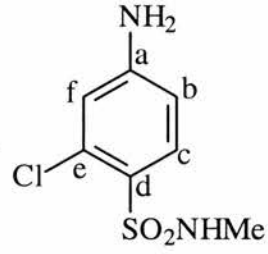

Tan needles (4.12g, 69%); mp 159°C, litt.[158] 164-166°C; ^{1}H (300 MHz, d_6-dmso) δ_H 2.35 (s, 3H, C*H*$_3$CO), 6.21 (broad s, 2H, N*H*$_2$), 6.53 (dd, $^{3}J_{H\text{-}H}$ = 8.71 Hz and $^{3}J_{H\text{-}H}$ = 2.05 Hz, 1H, aromatic H_b), 6.66 (d, $^{3}J_{H\text{-}H}$ = 2.05 Hz, 1H, aromatic H_f), 7.10 (broad s, <1H, N*H*Me), 7.53 (d, $^{3}J_{H\text{-}H}$ = 8.71 Hz, 1H, aromatics H_c); ^{13}C (75.4 MHz, d_6-dmso) δ_C 28.7 (s, methyl *C*H$_3$CO), 111.3 (s, aromatic C_b), 114.9 (s, aromatic C_f), 121.4 (s, aromatic C_e), 132.1 (s, aromatic C_d), 133.0 (s, aromatic C_c), 153.9 (s, aromatic C_a); MS (ESI$^+$): *m/z* 242.97 $[M+Na]^+$, $C_7H_9ClN_2O_2SNa$ requires 242.99; IR (KBr disc, cm^{-1}) 3405s, 3389s, 3236s, 3171s, 2959m, 2920m, 2817m, 1655s, 1597s, 1561m, 1479m, 1428m, 1302s, 1263m, 1242m, 1150s, 1111s, 1083s, 1031m, 912w, 860m, 82s, 669s, 597m, 547s, 520m; Microanalytical data found: C: 38.23 H: 4.02 N: 11.68, expected for $C_7H_9ClN_2O_2S$ C: 38.10 H: 4.11 N: 12.69. Suitable crystals for XRD studies were obtained by layering a DCM solution with hexane.

N-4-Amino-2-chloro-N-(2-hydroxy-ethyl)-benzenesulfonamide **57c**

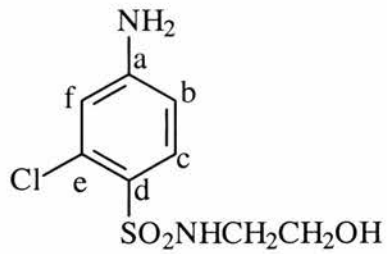

Orangish solid (2.5g, 71%); mp 198°C; ^{1}H (300 MHz, d_6-dmso) δ_H 2.83 (dd, $^{3}J_{H\text{-}H}$ = 12.55 Hz and $^{3}J_{H\text{-}H}$ = 6.14 Hz, 2H, -$SO_2NHCH_2CH_2OH$), 3.42 (dd, $^{3}J_{H\text{-}H}$ = 12.03 Hz and $^{3}J_{H\text{-}H}$ = 6.40 Hz, 2H, -$SO_2NHCH_2CH_2OH$), 4.77 (t, $^{3}J_{H\text{-}H}$ = 5.38, 1H, -$SO_2NHCH_2CH_2OH$), 6.19 (s, ^{2}H, NH_2), 6.60 (dd, $^{3}J_{H\text{-}H}$ = 8.71 Hz and $^{3}J_{H\text{-}H}$ = 2.30 Hz, aromatic H_b), 6.75 (d, $^{3}J_{H\text{-}H}$ = 2.05 Hz, 1H, aromatic H_f), 7.16 (t, $^{3}J_{H\text{-}H}$ = 5.89 Hz, 1H, -$SO_2NHCH_2CH_2OH$), 7.63 (d, $^{3}J_{H\text{-}H}$ = 8.71 Hz, 1H, aromatic H_c); ^{13}C (75.4 MHz, d_6-dmso) δ_C 45.1 (s, -$SO_2NHCH_2CH_2OH$), 60.1 (s, -$SO_2NHCH_2CH_2OH$), 111.4 (s, aromatic C_b), 115.0 (s, aromatic C_f), 122.7 (s, aromatic C_e), 132.2 (s, aromatic C_d), 132.7 (s, aromatic C_c), 153.8 (s, aromatic C_a); MS (ESI$^-$): *m/z* 249.0 [M-H]$^-$, $C_8H_{10}ClN_2O_3S$ requires 249.01; IR (KBr disc, cm^{-1}) 3405s, 3374s, 3341s, 3254m, 3116m, 3082m, 2965w, 2911w, 2895w, 2856w, 1643m, 1597w, 1565m, 1475w, 1455m, 1426m, 1391m, 1351w, 1323s, 1310s, 1242s, 1207m, 1160vs, 1158vs, 1122m, 1101m, 1085w, 1068s, 1058m, 1033m, 933w, 907w, 878m, 854w, 824w, 815m, 736s, 698m, 665m, 599m, 551sm 523w; Microanalytical data found: C: 38.89 H: 4.23 N: 11.56, expected for $C_8H_{11}ClN_2O_3S$ C: 38.33 H: 4.42 N: 11.17.

4-(2-benzylsulfanyl-9-isopropyl-9*H*-purin-6-ylamino)-*N*-methyl-benzenesulfonamide **58a**

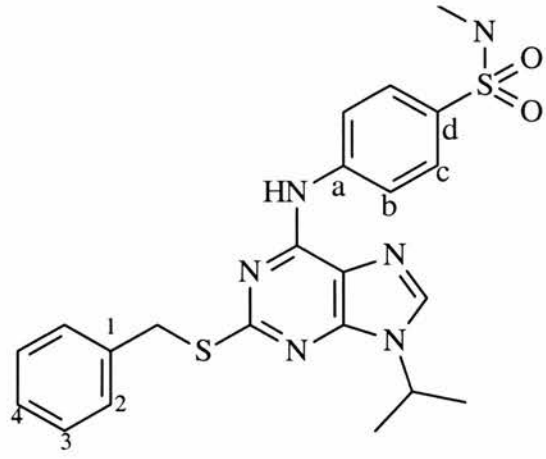

To a stirred mixture of 6-chloropurine **33a** (250mg, 0.78mmol) in *t*-butanol (10mL) was added aniline **51b** (219mg, 1.18mmol) followed by concentrated hydrochloric acid (2 drops) under nitrogen. The resulting mixture was stirred at 120°C for 24 hours under nitrogen and was evaporated to full dryness into a yellow solid. Flash chromatography on silica gel using2:1 EtOAc/Petroleum ether 40-60°C afforded 6-anilinopurine as a orangish oil (352mg, 97%); Rf 0.16 [EtOAc/hexane 2:1]; ^{1}H (300 MHz, d_6-dmso) δ_H 1.53 (d, $^{3}J_{H\text{-}H}$ = 6.66 Hz, 6H, -CH(CH_3)$_2$), 2.38 (d, $^{3}J_{H\text{-}H}$ = 5.12 Hz, 3H, -SO_2NHCH_3), 4.43 (s, 2H, PhCH_2S), 4.78 (s, $^{3}J_{H\text{-}H}$ = 6.66 Hz, 1H, CH(CH$_3$)$_2$), 7.20-7.33 (m, 3H, aromatic Ph H_2), 7.41 (d, $^{3}J_{H\text{-}H}$ = 7.94, 2H, aromatic H_3 and H_4), 7.65 (d, $^{3}J_{H\text{-}H}$ = 8.96 Hz, 2H, aniline H_b), 8.08 (d, $^{3}J_{H\text{-}H}$ = 8.96 Hz, 2H, aromatic H_c), 8.35 (s, 1H, purine H8), 10.37 (broad s, 1H, -NH); ^{13}C (75.4 MHz, d_6-dmso) δ_C 22.4 (s, CH(*C*H$_3$)$_2$), 29.0 (s, -NH*C*H$_3$), 34.9 (s, Ph*C*H$_2$S-), 47.2 (s, *C*H(CH$_3$)$_2$), 118.5 (s, purine C_5), 120.5 (s, aromatic aniline C_b), 127.3 (s, aromatic Ph C_2), 127.8 (s, aromatic aniline C_c), 128.7 (s, aromatic Ph C_4), 129.2 (s, aromatic Ph C_4), 132.6 (s, aromatic aniline

C_d), 138.6 (s, aromatic Ph C_1), 139.9 (s, purine C_8), 143.5 (s, aromatic aniline C_a), 150.7 (s, purine C_6), 151.3 (s, purine C_4), 162.8 (s, purine C_2); MS (ESI^+): *m/z* 491.1302 $[M+H]^+$, $C_{22}H_{24}N_6O_2S_2Na$ requires 491.1300; IR (KBr disc, cm^{-1}) 3323s, 3239s, 3245w, 3121w, 3101w, 3069w, 3012w, 2977w, 2932m, 1654m, 1609s, 1574vs, 1481w, 1479s, 1403m, 1392m, 1348s, 1215w, 1165w, 1147m, 1130w, 1157m, 1039w, 1012w, 931w, 841w, 821w, 788w, 692wm, 674w, 650w, 631w, 614w, 589w, 543w; Microanalytical data found: C: 56.74 H: 4.51 N: 17.82 S: 13.03, expected for $C_{22}H_{24}N_6O_2S_2$ C: 56.51 H: 4.96 N: 17.97 S: 13.71.

4-(2-benzylsulfanyl-9-isopropyl-9*H*-purin-6-ylamino)-2-chloro-*N*-methyl-benzenesulfonamide **58b**

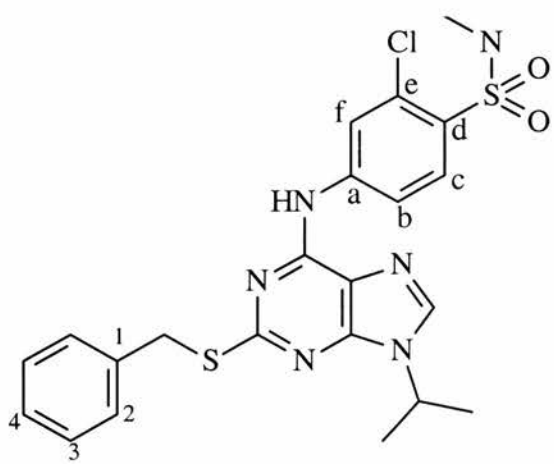

To a stirred mixture of 6-chloropurine **33a** (250mg, 0.78mmol) in *t*-butanol (10mL) was added aniline **57b** (260mg, 1.18mmol) followed by concentrated hydrochloric acid (2 drops) under nitrogen. The resulting mixture was stirred at 120°C for 24 hours under nitrogen and was evaporated to full dryness into a yellow solid. Flash chromatography on silica gel using 2:1 EtOAc/Petroleum ether 40-60°C afforded 6-anilinopurine as a orangish oil (352mg, 97%); Rf 0.16

[EtOAc/hexane 2:1]; ^{1}H (300 MHz, $CDCl_3$) δ_H 1.53 (d, $^{3}J_{H\text{-}H}$ = 6.91 Hz, 6H, -$CH(CH_3)_2$), 2.42 (d, $^{3}J_{H\text{-}H}$ = 4.86 Hz, 3H, -SO_2NHCH_3), 4.45 (s, 2H, $PhCH_2S$), 4.76 (s, $^{3}J_{H\text{-}H}$ = 6.66 Hz, 1H, $CH(CH_3)_2$), 7.20-7.33 (m, 2H, aromatic Ph H_3), 7.43 (d, $^{3}J_{H\text{-}H}$ = 6.91 Hz, 2H, aromatic H_2), 7.51 (dd. $^{3}J_{H\text{-}H}$ = 9.73 Hz and $^{3}J_{H\text{-}H}$ = 4.86 Hz, 1H, H_4), 7.81 (d, $^{3}J_{H\text{-}H}$ = 8.96 Hz, 1H, aniline H_c), 7.99 (d, $^{3}J_{H\text{-}H}$ = 8.96 Hz, H, aromatic H_b), 8.40 (2s, 2x1H, purine H8 and -N*H*); ^{13}C (75.4 MHz, $CDCl_3$) δ_C 22.4 (s, $CH(CH_3)_2$), 28.8 (s, -$NHCH_3$), 35.0 (s, $PhCH_2S$-), 47.3 (s, $CH(CH_3)_2$), 118.3 (s, purine C_5), 118.7 (s, aromatic aniline C_b), 122.2 (s, aromatic aniline C_f), 127.3 (s, aromatic Ph C_2), 128.7 (s, aromatic Ph C_4), 129.2 (s, aromatic Ph C_3), 129.6 (s, aromatic aniline C_d), 131.2 (s, aromatic aniline C_e), 131.7 (s, aromatic aniline C_c), 138.4 (s, aromatic Ph C_1), 140.3 (s, purine C_8), 144.6 (s, aromatic aniline C_a), 150.9 (s, purine C_6), 151.0 (s, purine C_4), 162.8 (s, purine C_2); MS (ESI^+): *m/z* 525.0933 $[M+Na]^+$, $C_{22}H_{23}ClN_6O_2S_2Na$ requires 525.0910; IR (KBr disc, cm^{-1}) 3307m, 3221m, 3201w, 3134w, 3119w, 3081w, 3028w, 2975w, 2934w, 1642m, 1604m, 1563s, 1495w, 1479s, 1410m, 1382m, 1328s, 1235m, 1195w, 1161m, 1131w, 1114w, 1069w, 1033m, 1018m, 949w, 916w, 871w, 833w, 819w, 788w, 716m, 695wm, 680w, 640w, 635w, 608w, 574w, 558w; Microanalytical data found: C: 52.42 H: 4.95 N: 16.59 S: 13.95, expected for $C_{22}H_{23}ClN_6O_2S_2$ C: 52.53 H: 4.61 N: 16.71 S: 12.75.

4-[2-(1-hydroxymethyl-2-methyl-propylamino)-9-isopropyl-9*H*-purin-6-ylamino]-*N*-methyl-benzenesulfonamide **59a**

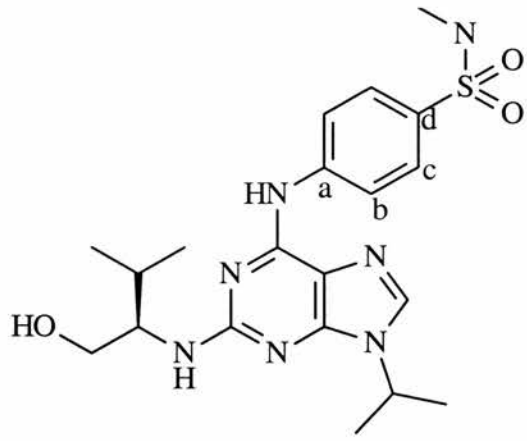

To a stirred mixture of *m*-CPBA (176mg, 70% w/w with water, 1.29mmol) and magnesium sulfate (485mg) in DCM (10mL) was added under nitrogen a solution of 6-anilinopurine **58a** (200mg, 0.43mmol) in DCM (5mL) and stirring was continued overnight. The mixture was filtered off and the precipitate washed thoroughly with DCM. The combined organics were concentrated in vaccum into the sulfone analogue of purine **58a** which was characterised by ESI^+ mass spectrometry (*m/z* 491.1299 thus $[M+Na]^+$). The residue was dissolved in *t*-butanol (10mL) then Hunig's base (0.5mL) followed by *R*-valinol (500mg, 4.85mmol) were added. The resulting solution was stirred at 160°C for 48 hours in a Parr bomb, cooled down and evaporated to full dryness into a yellow oil. Flash chromatography on silica gel using 1-5% MeOH in DCM afforded the desired 2,6-diaminopurine 59a as a orangish oil (135mg, 70%); Rf 0.19 [DCM/MeOH 95:5]; ^1H (300 MHz, $CDCl_3$) δ_H 0.94-0.95 (2d, $^3J_{H-H}$ = 6.66 Hz, 2x3H, valinol -CH(C*H*$_3$)$_2$), 1.44 (2d, $^3J_{H-H}$ = 6.66 Hz, 2x3H, purine -CH(C*H*$_3$)$_2$), 1.93 (s, $^3J_{H-H}$ = 6.66 Hz, 2x3H, valinol -C*H*$(CH_3)_2$), 2.54 (d, , $^3J_{H-H}$ = 6.66 Hz,

2x3H, sulfonamide -NH(CH_3)), 3.70 (m, 1H, valinol NHCHCH_2OH), 3.89 (m, 2H, valinol NHCHCH_2OH), 4.45 (s, $^3J_{H\text{-}H}$ = 6.66 Hz, 1H, purine CH(CH_3)$_2$), 5.11 (d, $^3J_{H\text{-}H}$ = 7.94 Hz, 1H, valinol NHCHCH$_2$OH), 5.38 (dd, 1H, $^3J_{H\text{-}H}$ = 10.75 Hz and $^3J_{H\text{-}H}$ = 5.38 Hz, 1H, valinol NHCHCH$_2$OH), 7.51 (s, 1H, aniline NH), 7.64 (d, $^3J_{H\text{-}H}$ = 8.71, 2H, aromatic aniline H_b), 7.82 (d, $^3J_{H\text{-}H}$ = 8.71 Hz, 2H, aromatic aniline H_c), 8.53 (s, 1H, purine H8); ^{13}C (75.4 MHz, $CDCl_3$) δ_C 19.4-19.9 (2d, valinol CH(CH_3)$_2$), 22.8 (s, valinol CH(CH$_3$)$_2$), 29.6-30.4 (2d, purine CH(CH_3)$_2$), 47.1 (s, sulfonamide -NHCH_3), 59.8 (s, valinol NHCHCH_2OH), 65.1 (s, valinol NHCHCH_2OH), 115.3 (s, purine C_5), 119.4 (s, aromatic aniline C_b), 128.6 (s, aromatic aniline C_c), 131.6 (s, aromatic aniline C_d), 135.6 (s, purine C_8), 144.0 (s, aromatic aniline C_a), 151.6 (s, purine C_6), 151.9 (s, purine C_4), 160.0 (s, purine C_2); MS (ESI$^-$): *m/z* 446.1972 [M-H]$^-$, $C_{20}H_{28}N_7O_3S$ requires 446.1974; IR (KBr plates, cm^{-1}) 3342s, 3121m, 2964w, 2929s, 2871m, 1701m, 1629s, 1577s, 1497s, 1466s, 1407m, 1370m, 1322m, 1257m, 1158s, 1095m, 1066m, 1034m, 912w, 837m, 788w, 731m, 638m, 561m; Microanalytical data found: C: 54.26 H: 6.98 N: 22.85 S: 7.65, expected for $C_{20}H_{28}N_7O_3S$ C: 53.67 H: 6.53 N: 21.91 S: 7.16.

2-chloro-4-[2-(1-hydroxymethyl-2-methyl-propylamino)-9-isopropyl-9*H*-purin-6-ylamino]-*N*-methyl-benzenesulfonamide **59b**

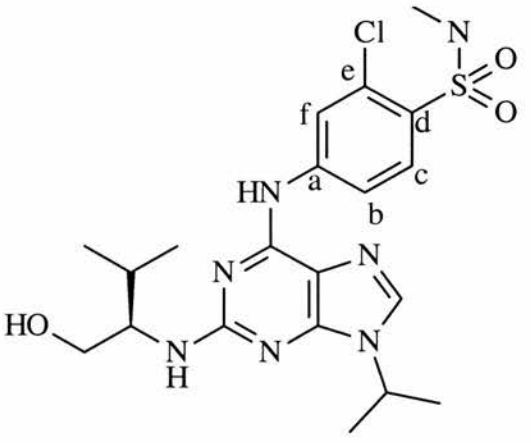

To a stirred mixture of *m*-CPBA (150mg, 70% w/w with water, 0.60mmol) and magnesium sulfate (226mg) in DCM (10mL) was added under nitrogen a solution of 6-anilinopurine **58b** (100mg, 0.20mmol) in DCM (5mL) and stirring was continued overnight. The mixture was filtered off and the precipitate washed thoroughly with DCM. The combined organics were concentrated in vaccum into the sulfone analogue of purine **58b** which was characterised by ESI^+ mass spectrometry (*m/z* 557.0808 thus $[M+Na]^+$). The residue was dissolved in *t*-butanol (5mL) then Hunig's base (0.25mL) followed by *R*-valinol (206mg, 2mmol) were added. The resulting solution was stirred at 160°C for 48 hours in a Parr bomb, cooled down and evaporated to full dryness into a orangish oil. Flash chromatography on silica gel using 1-5% MeOH in DCM afforded the desired 2,6-diaminopurine 59a as a orangish oil (72mg, 75%); Rf 0.23 [DCM/MeOH 95:5]; ^1H (300 MHz, $CDCl_3$) δ_H 0.98-0.99 (2d, $^3J_{H\text{-}H}$ = 6.66 Hz, 2x3H, valinol – $CH(CH_3)_2$), 1.53 (2d, $^3J_{H\text{-}H}$ = 6.66 Hz, 2x3H, purine $CH(CH_3)_2$), 1.97 (s, $^3J_{H\text{-}H}$ = 6.61 Hz, 2x3H, valinol $CH(CH_3)_2$), 2.38 (d, $^3J_{H\text{-}H}$ = 5.12 Hz, 3H, sulfonamide

N*H*(CH_3)), 3.74 (m, 1H, valinol NHC*H*CH_2OH), 3.89 (m, 2H, valinol NHCHC*H*$_2$OH), 4.78 (s, $^3J_{H\text{-}H}$ = 6.66 Hz, 1H, purine C*H*(CH_3)$_2$), 5.23 (d, $^3J_{H\text{-}H}$ = 7.64 Hz, 1H, valinol N*H*CHCH_2OH), 5.40 (dd, $^3J_{H\text{-}H}$ = 9.97 Hz and $^3J_{H\text{-}H}$ = 5.64 Hz, 1H, valinol NHCHCH_2O*H*), 7.67 (d, $^3J_{H\text{-}H}$ = 8.91 Hz, 1H, aniline H_c), 7.92 (d, $^3J_{H\text{-}H}$ = 8.96 Hz, H, aromatic H_b), 8.36 (2s, 2x1H, purine H8 and -N*H*); ^{13}C (75.4 MHz, $CDCl_3$) δ_C 19.2-19.7 (2d, valinol CH(*C*H3)$_2$), 22.6 (s, valinol *C*H(*C*H3)$_2$), 28.9 (s, -NH*C*H_3), 29.8-30.1 (2d, purine *C*H(*C*H3)$_2$), 47.5 (s, purine *C*H(CH_3)$_2$), 60.0 (s, valinol NH*C*HCH_2OH), 66.2 (s, valinol NHCH*C*H_2OH), 118.6 (s, aromatic aniline C_b), 123.6 (s, aromatic aniline C_f), 129.7 (s, aromatic aniline C_d), 131.5 (s, aromatic aniline C_e), 132.1 (s, aromatic aniline C_c), 141.2 (s, purine C_8), 147.3 (s, aromatic aniline C_a), 150.3 (s, purine C_6), 150.9 (s, purine C_4), 162.2 (s, purine C_2); MS (ESI$^+$): *m/z* 504.1558 $[M+Na]^+$, $C_{20}H_{28}ClN_7O_3SNa$ requires 504.1561; IR (KBr plates, cm^{-1}) 3356s, 3136m, 2944w, 2939w, 2867w, 1687m, 1634s, 1564s, 1502s, 1500s, 1429m, 1289m, 1249m, 1159w, 1086m, 1057w, 1029w, 891w, 819m, 698m, 547w; Microanalytical data found: C: 50.96 H: 5.61 N: 20.94, expected for $C_{20}H_{28}ClN_7O_3S$ C: 49.84 H: 5.86 N: 20.34.

REFERENCES

1 H. Busch, *Molecular biology of cancer*, Chapter 1, Academic Press, 1974

2 R. Doerg, *Textbook of organic, medicinal and pharmaceutical chemistry*, Chapter 8: Antineoplastic agents, 1982

3 G. Jouen, *Chem.Br.*, 2001, **37**, 6, 36-38

4 M. Murphy, *Chem.Ind.(London)*, 2001, **24**, 783

5 World Health Organization database, *www.dep.iarc.fr/globocam/globocam.html*

6 American Cancer Society, *www.immuneinstitute.com/statistics.htm*

7 R. Stevenson, *Chem.Br.*, 2001, **37**, 24-25

8 A. Murray, *Chem.Biol.*, 1994, **1**, 191-195

9 D. Hung *et al*, *Chem.Biol.*, 1996, **3**, 623-639

10 W. Wells, *Chem.Biol.*, 1997, **4**, 631-632

11 N. Pavletich, *J.Mol.Biol.*, 1999, **287**, 821-828

12 D.Morgan, *Annu.Rev.Cell Dev.Biol.*, 1997, **13**: 261-291

13 H. De Bondt *et al*, *Nature*, 1993, **363**, 595-602

14 H Kobayashi, E Stewart, R Poon, JP Adamczewski, J Gannon, and T Hunt, *Mol.Biol.Cell*, 1992, **3**: 1279-1294

15 E.M. Lees and E. Harlow, *Mol.Cell Biol.*, 1993, **13,** 1194-1201

16 T.M. Sielecki, J.F. Boylan, P.A. Benfield, and G.L. Trainor, *J.Med.Chem.*, 2000, **43**, 1-18

17 C.J. Sherr, *Science*, 1996, **274**, 1672-1677

18 V Leclerc, JP Tassan, PH O'Farrell, EA Nigg, and P Leopold, *Mol.Biol.Cell,* 1996, **7**, 505-513

19 C. Koch and K. Nasmyth, *Curr.Opin.Cell Biol.*, 1994, **6**, 451-459

20 Brookhaven Protein Data Bank, *www.pdb.org*

21 A.A. Russo, P.D. Jeffrey and N.P. Pavletich , *Nature Struct. Biol.*, 1996, **3**: 696-700

22 M. Knockaert, P. Greengard and L. Meijer, *Trends Pharmacol. Sci.*, 2002, **23**, 417-425

23 P. Imbach, H.G. Capraro, P. Furet, H. Mett, T. Meyer and J. Zimmermann, *Bioorg. Med.Chem. Lett.*, 1999, **9**, 91-96

24 Y.T. Chang, N.S. Gray, G.R. Rosania, D.P. Sutherlin, S. Kwon, T.C. Norman, R. Sarohia, M. Leost, L. Meijer and P.G. Schultz, *Chem.Biol.*, 1999, **6**, 361-375

25 M.Legraverend, P.Tunnah, M. Noble, P.Ducrot, O.Ludwig, D.. Grierson, M. Leost, L. Meijer, and J. Endicott, *J.Med.Chem.*, 2000, **43**, 1282-1292

26 M. Otyepka, V. Krystof, L. Havlicek, V. Siglerova, M. Strnad, and J. Koca, *J.Med.Chem.*, 2000, **43**, 2506-2513

27 P. Ducrot, M. Legraverend, and D.S. Grierson, *J.Med.Chem.*, 2000, **43**, 4098-4108

28 T. Honma, K. Hayashi, T. Aoyama, N. Hashimoto, T. Machida, K. Fukasawa, T. Iwama, C. Ikeura, M. Ikuta, I. Suzuki-Takahashi, Y. Iwasawa, T. Hayama, S Nishimura, and H. Morishima, *J.Med.Chem.*, 2001, **44**, 4615-4627

29 T. Honma, T. Yoshizumi, N. Hashimoto, K.Hayashi, N.Kawanishi, K.Fukasawa, T.Takaki, C.Ikeura, M.Ikuta, I.Suzuki-Takahashi, T.Hayama, S.Nishimura, and H.Orishima, *J.Med.Chem.*, 2001, **44**, 4628-4640

30 H. N.Bramson, J. Corona, S.T. Davis, S.H. Dickerson, M.Edelstein, S.V. Frye, R.T. Gampe, Jr., P.A. Harris, A.Hassell, W.D. Holmes, R.N. Hunter, K.E. Lackey, B. Lovejoy, M.J. Luzzio, V. Montana, W.J. Rocque, D. Rusnak, L. Shewchuk, J.M. Veal, D.H. Walker, and L. F. Kuyper, *J.Med.Chem.*, 2001, **44**, 4339-4358

31 T. Annie, T. Fong, L.K. Shawver, L. Sun, C. Tang, H. App, T.J. Powell, Y.H. Kim, R. Schreck, X. Wang, W. Risau, A. Ullrich, K.P. Hirth, and G. McMahon, *Cancer Res.*, 1999, **59**, 99-106

32 P. Singh and R. Kumar, *J.Enzyme Inhib.*, 1998, **13**, 125-134

33 G.W. Rewcastle, B.D. Palmer, A.J. Bridges, H.D. Hollis-Showalter, L. Sun, J. Nelson, A. McMichael, A.J. Kraker, D.W. Fry, and W.A. Denny, *J.Med.Chem.*, 1996, **39**, 918-928

34 A. Furusaki, N. Hashiba, T. Matsumoto, A. Hirano, Y. Iwai, and S. Omura, *Bull.Chem.Soc.Jpn.,* 1982, **55**, 3681-3685

35 L. Meijer, *Trends Cell Biol.*, 1996, **6**, 393-397

36 *Drugs and Market Development*, 1997, May 1, 89-100

37 F. O. Ranelleti, R. Ricci, L. M. Larocca, N. Maggiano, A. Capelli, G. Scamibia, P. Benedett-Panici, S. Mancuso, C. Rumi, M. Piantelli, *Int.J.Cancer,* 1992, **50**, 486-492

38 *NCI PDG Clinical Trial Search*, November 1997

39 *PCT Int. Appl.* WO 97 16447 A 970509

40 W.F. de Azevedo Jr., H.-J.Mueller-Dieckmann, U. Schulze-Gahmen, P.J. Worland, E. Sausville, and S.-H. Kim, *Proc.Natl.Acad.Sci. USA*, 1996, **93**, 2735-2740

41 D. Zaharevitz, C. Kunick, C. Schultz, L. Meijer, M. Leost, R. Gussio, A. Senderowicz, T. Lahusen, and E. Sausville, *Am.Assoc. Cancer Res.*, 1999, Apr 10-14

42 C. Schultz, A. Link, M. Leost, D. W. Zaharevitz, R. Gussio, E.A. Sausville, L. Meijer, and C. Kunick, *J.Med.Chem.*, 1999, **42**, 2909-2919

43 J. Vesely, L. Havlicek, M. Strnad, J. J. Blow, A. Donella-Deana, D. E. Letha, J. Kato, L. Dutivaud, O. Lucrero, and L. Meier, *Eur.J.Biochem.*, 1997, **224**, 771-786

44 N. Glab, B. Labidi, L. Qin, C. Trehin, C. Bergounioux and L. Meijer, *FEBS Lett.*, 1994, **353**, 207-211

45 S.R. Schow, R.L. Mackman, C.L. Blum, E.Brooks, A.G. Horsma, A.Joly, S.S. Kerwar, G.Lee, D.Shiffman, M.G. Nelson *et al.*, *Bioorg.Med.Chem.Lett.*, 1997, **7**, 2697-2702

46 B. Schutte, L. Nieland, M. van Engeland, M.E.R. Henfling, L. Meijer and F.C.S. Ramaekers, *Exp.Cell Res.*, 1997, **236**, 4-15

47 M. Legraverend, O. Ludwig, E. Bisagni, S. Leclerc and L. Meijer, *Bioorg.Med.Chem.Lett.*, 1998, **8**, 793-798

48 *216th ACS National Meeting*, Boston, MA, August 23-27 1998

49 M.J. Luzzio, N. Bramson, S. Dickerson, S.V. Frye, P. Harris, A. M. Hassell, W. Holmes, R. Hunter, L. Kuyper, K. Lackey, B. Lovejoy, V. Montana, W. Rocque, L. Shewchuk, J. Veal, D. Walker, *Am. Assoc. Cancer Res.*, 1999, Apr 10-14

50 *PCT Int. Appl.* WO 9915500 A1 99401

51 D.A. Nugiel, A.M. Etzkorn, A. Vidwans, P.A. Benfield, M. Boisclair, C.R. Burton, S. Cox, P.M. Czerniak, D. Doleniak, and S.P. Seitz, *J.Med.Chem.*, 2001, **44**, 1334-1336

52 P. Furet, T. Meyer, A. Strauss, S. Raccuglia and J.M. Rondeau,*Bioorg.Med.Chem.Lett.*, 2002, **12**, 221-224

53 D.A. Nugiel, A. Vidwans, A.M. Etzkorn, K.A. Rossi, P.A. Benfield, C.R. Burton, S. Cox, D. Doleniak and S.P. Seitz, *J.Med.Chem.*, 2002, **45**, 5224-5232

54 R.N. Misra, D.B. Rawlins, H.Y. Xiao, W. Shan, I. Bursuker, K.A. Kellar, J.G. Mulheron, J.S. Sack, J.S. Tokarski, S.D. Kimball, and K.R. Webster, *Bioorg.Med.Chem.Lett.*, 2003, **13**, 2405-2408

55 Y. Mettey, M. Gompel, V. Thomas, M. Garnier, M. Leost, I. Ceballos-Picot, M. Noble, J. Endicott, J.M. Vierfond, and L. Meijer, *J.Med.Chem.*, 2003, **46**, 222-236

56 M.A. Ortega, M.E. Montoya, B. Zarranz, A. Jaso, I. Aldana, S. Leclerc, L. Meijer, and A.Monge, *Bioorg.Med.Chem.Lett.*, 2002, **10**, 2177-2184

57 G.Patrick, *An introduction to medicinal chemistry*, Oxford University Press, 1995

58 D.Taddei, *"From the test tube to the chemist's", The discovery and development process of a new prescription*, , Knoll Pharmaceuticals, BASF Pharma UK, 2000

59 F.D.King, *Medicinal Chemistry: Principles and Practice*Wiley Press, 1995

60 C.H. Oh, S.C. Lee, K.S. Lee, K.S. Woo, C.Y. Hong, B.S. Yang, D.J. Baek, J.H. Cho, *Arch Pharm (Weinheim)*, 1999, **332**,187-190.

61 M. Legraverend, O. Ludwig, E. Bisagni, S. Leclerc, L. Meijer, N. Giocanti, R. Sadri and V. Favaudon' *Bioorg.Med.Chem.*, 1999, **7**, 1281-1293

62 R.Silvermann, The Organic Chemistry of Drug Design and Drug Action, Academic Press, 1992, 352-397

63 L. Havlicek, J. Hanu, J. Vesel, S. Leclerc, L. Meijer, G. Shaw, and M. Strnad, *J.Med.Chem.*, 1997, **40**, 408-412

64 T. Naumann and H. Matter, *J.Med.Chem.*, 2002, **45**, 2366-2378

65 P.J. Goodford, *J.Med.Chem.*, 1985, **28**, 849-857

66 R.C. Wade, K.J. Clark, and P.J. Goodford' *J.Med.Chem.*, 1993, **36**, 140-156

67 R.D. Cramer III, D.E. Patterson, J.D. Bunce, *J.Am.Chem.Soc.*, 1988, **110**, 5959-5967

68 M. Clark, R. D. Cramer III, D. M. Jones, D. E. Patterson, and P. E. Simeroth' *Tetrahedron Comput.Methodol.*, 1990, **3**, 47-59

69 G. Klebe, U. Abraham, T. Mietzner, *J.Med.Chem.*, 1994, **37**, 4130-4146

70 M. Bohm, J. Sturzebecher, G. Klebe, *J.Med.Chem.*, 1999, **42**, 458-477

71 W. Kubinyi, *3D-QSAR in Drug Design: Theory, Methods and Applications*, Ed.ESCOM, LEIDEN (NL), 1993

72 T.G.Davies, D.J.Pratt, J.A.Endicott, L.N.Johnson and M.E.N.Noble, *Pharmacol.Therapeutics,* 2002, **93**, 125-133

73 N.S. Gray, S. Kwon, and P.G. Schultz, *Tet.Lett.*, 1997, **38**, 1161-1164

74 M. Legraverend, H. Boumchita, and E.Bisagni, *Synthesis*, 1990, 587-590

75 J.Joule and F.Mills, *Heterocyclic Chemistry*, 4th edition, Blackwell Science, 2000, 465-467

76 V. Brun, M. Legraverend, and D.S. Grierson, *Tet. Lett.*, 2001, **42**, 8161-6164

77 V. Brun, M. Legraverend, and D.S. Grierson, *Tet. Lett.*, 2001, **42**, 8165-6167

78 V. Brun, M. Legraverend, and D.S. Grierson, *Tet. Lett.*, 2001, **42**, 8169-6171

79 W.B. Smith and O.C. Ho, *J.Org.Chem.*, 1990, **55**, 2543-2545

80 T.I. Bieber and B. Kane, *J.Org.Chem.*, 1956, **21**, 1198-1999

81 L.B. Townsend and R.S. Tipson, *Nucleic Acid Chemistry*, Wiley-Interscience, 1978

82 J.D. Westover, G.R. Revankar, R.K. Robins, R.D. Madsen, J.R. Ogden et al., *J.Med.Chem.*, 1981, **24**, 941-946

83 E.W. van Tilburg, P.A.M. van der Klein, J.F.D. Kuenzel, M. de Groote, C. Stannek, A. Lorenzen, and P. Jzerman, *J.Med.Chem.*, 2001, **44**, 18; 2966-2975

84 Z.S. Shi, B.H. Yang, and Y.L. Wu, *Tetrahedron*, 2002, **58**, 3287 - 3296

85 V.P. Palle, E.O. Elzein, S.A. Gothe, Z. Li, Z. Gao, S. Meyer, B. Blackburn, and J.A. Zablocki, *Bioorg.Med.Chem.Lett.*, 2002, **12**, 20, 2935 - 2940.

86 M.J. Morris and B. Uznanski, *Can.J.Chem.*, 1981, **59**, 2601-2606

87 J.F. Gerster, J.W. Jones, and R.K. Robins, *J.Org.Chem.*, 1963, **28**, 945-948

88 J.A. Montgomery, S.D. Clayton, and A.T. Shortnacy, *J.Heterocyclic.Chem.*, 1979, **16**, 157-160

89 M.J. Robins, and B. Uznanski, *Can.J.Chem.*, 1981, **59**, 2608-2611

90 A.F. Cook, and R.T. Barlett, *J.Org.Chem.*, 1980, **45**, 4020-4025

91 D.H. Williams and I. Fleming, *Spectroscopic Methods in Organic Chemistry*, Fifth Edition, McGraw-Hill, London, 1995

92 W. Saenger, *Principles of Nucleic Acid Structure*, Springer-Verlag, New York, 1982

93 A.R. Katritzky and R. Taylor, *Adv.Heterocycl.Chem.*, 1990, **47**, 1

94 A. Matsuda, M. Shinozaki, T. Yamaguchi, H. Homma, R. Nomoto, T. Miyasaka, K. Watanabe and T. Abiru, *J.Med.Chem.*, 1992, **35**, 241-252

95 V. Nair and S.G. Richardson, *Synthesis*, 1982, 670-672

96 V. Nair and D.A. Young, *J.Org.Chem.*, 1985, **50**, 406-408

97 R.P. Panzica, R.J. Rousseau, R.K. Robins and L.B. Townsend, *J.Am.Chem.Soc.*, 94, 4708-4714

98 J.L. Abad, B.L. Gaffney and R.A. Jones, *J.Org.Chem.*, 1999, **64**, 6575-6582.

99 R.K. Robins, E.F. Godefroi, E.C. Taylor, L.R. Lewis and A. Jackson, *J.Chem.Soc.*, 1961, **83**, 2574-2579

100 L.R. Lewis, F.H. Schneider and R.K. Robins, *J.Org.Chem.*, 1961, **26**, 3837.

101 K. Kato, H. Hayakawa, H. Tanaka, H. Kumamoto, S. Shindoh and T. Miyasaka, *J.Org.Chem.*, 1997, **62**, 6833-6841

102 H. Kumamoto, H. Tanaka, R. Tsukioka, Y. Ishida, A. Nakamura, S. Kimura, H. Hayakawa, K. Kato and T. Miyasaka, *J.Org.Chem.*, 1999, **64**, 7773-7780

103 M.A. Thius and J.K. Kawakami, *Synth.Commun.*, 1992, **22**, 1461; M.A. Thius, *Tetrahedron*, 1995, **51**, 6605

104 J. Tesse, *Bull.Soc Chim.Fr.*, 1973, 787-793; C. Glacet, J. Brocard, *Bull.Soc.Chim.Fr.*, 1969, 4133-4135

105 J. Wang, C. Zhang, Z. Qu, Y.Hou, B. Chen and P. Wu, *J.Chem.Res.*, 1994, 294-295

106 O. Mitsunobu, *Synthesis*, 1981, **1**, 1-28

107 A. Toyota, N. Katagiri, and C. Kaneko, *Heterocycles*, 1993, **36**, 1625-1630

108 R. Dembinski, *Eur.J.Org.Chem.*, 2004, **13**, 2763-2772

109 Y. Rew and M. Goodman, *J.Org.Chem.*, 2002, **67**, 8820-8826

110 M.F. Malley, J.Z. Gougoutas, *J.Org.Chem.*, 1996, **61**, 7955-7958

111 V.Brun, M.Legraverend and D.S.Grierson, *Tetrahedron*, 2002, **58**, 7911-7923

112 V.Brun, M.Legraverend and D.S.Grierson, *Tetrahedron*, 2002, **58**, 7911-7923

113 C.L.Gibson, S. La Rosa and C.J.Suckling, *Org.Biomol.Chem.*, 2003, **1**, 1909-1918

114 M.Y.Chu-Moyer, W.E.Ballinger, D.A.Beebe, .Berger, J.B.Coutcher, W.W.Day, J.Li, B.L.Mylari, P.J.Oates and R.M.Weekly, *J.Med.Chem.*, 2002, **45**, 511-528

115 B.Zacharie, L.Gagnon, G.Attardo, T.P.Conolly, Y.St-Denis, and C.L.Penney, *J.Med.Chem*, 1997, **40**, 2883-2894

116 B.Masjost, P.Ballmer, E.Borroi, G.Zurcher, F.K.Winkler, R.Jakob-Roetne and F.Diederich, *Chem.Eur.Journal,* 2000, **6**, 971-982

117 H.P.Daskalov, M.Sekine and T.Hata, *Bull.Chem.Soc.Jpn.*, 1981, **54**, 3076-3083

118 M.Morris and B.Uznanski, *Can.J.Chem.*, 1981, **59**, 2601-2606

119 A.Toyota, N.Katagiri, and C.Kaneko, *Heterocycles*, 1983, **36**, 7, 1625-1630

120 K.Banks, *J.Am.Chem.Soc.*, 1944, **66**, 1127-1130

121 N.K.Lembicz, S.Grant, W.Clegg, R.J.Griffin, S.L.Health and B.T.Holding, *J.Chem.Soc.Perkin Trans.I*, 1997, 185-186

122 M.Ashwell, C.Bleasdale, B.T.Golding andI.K.O'Neill, *J.Chem.Soc., Chem.Comm.*, 1990, 955

123 T.W.Greene, *Protective Groups in Organic Synthesis*, Wiley-Interscience, 1981

124 P.J. Kocienski, *Protecting Groups*, Thieme-Verlag, Stuttgart-New York, 1994

125 J.Rosevean and J.F.K.Wilshire, *Aust.J.Chem.*, 1982, **35**, 1727-1732

126 H.Gershan and R.Rodin, *J.Med.Chem.*, 1965, **8**, 864-866

127 D.A.Quagliato, P.M.Andrae and E.M.Matclan, *J.Org.Chem.*, 2000, **65**, 5037-5042

128 J.Granander, R.Scott and G.Hilmersson, *Tetrahedron*, 2002, **58**, 4797-4725

129 Personal reference, M. Weston, *Organon Research*, Scotland, UK

130 M.E.Duggan and O.S.Karanewski, *Tetrahedron Lett.*, 1983, **24**, 2935-2938

131 P.Puyau and J.J. de Macedo, Phosphorus, *Sulfur Silicon Relat.Elem.*, 1997, **129**, 13-46

132 D.Redmore, *J.Org.Chem.*, 1970, **35**, 4114-4117

133 O.E.O.Hormi, E.O.Pajunen, A.K.C.Avall and P.Pennanen, *Synth.Comm.*, 1990, **20**, 1865-1867

134 E.S.Chaumann and M.Moeller, *Chem.Ber.*, 1988, **121**, 707-708; U.Maitra and P.Babu, *Steroids*, 2003, **68**, 459-464

135 J.L.Vicario, D.Badia and L.Carillo, *J.Org.Chem.*, 2001, **66**, 5801-5807

136 D.Tanner, *Angew.Chem.Int.Ed.Engl.*, 1994, **33**, 559

137 B.M.Pope, Y.Yamamoto and D.S.Tarbell, *Org.Synth.Coll. Vol.VI*, 1988, 418

138 A.T.Koppisch and C.D.Poulter, *J.Org.Chem.*, 2002, **67**, 5416-5418

139 T.Gefflaut, M.Lemaire, M.L.Valentin and J.Bolte, *J.Org.Chem.*, 1997, **62**, 5920-5922

140 Y.Kozawa and M.Mori, *J.Org.Chem.*, 2003, **68**, 8068-8074

141 N.Sakai and Y.Ohfume, *J.Am.Chem.Soc.*, 1992, **144**, 998-1010

142 J.P.Mazaleyrat, K.Wright, A.Gaucher, M.Wakselman, S.Oancea, F.Formaggio, C.Toniolo, V.Setnicka, J.Kapitan and T.A.Keiderling, *Tetrahedron Asymm.*, 2003, **14**, 1879-1893

143 E.K.Dziadulewicz, T.J.Ritchie, A.Hallett, C.R.Snell, J.W.Davies, R.Wrigglesworth, A.R.Dunstan, G.C.Bloomfield, G.S.Drake, P.McIntyre, M.C.Brown *et al.*, *J.Med.Chem.*, 2002, **45**, 2160-2172

144 R.Boothe, C.Dial, R.Conaway, R.M.Pagni, G.W.Kabalka, Tetrahedron Lett., 1986, **27**, 2207-2210

145 A.M.Granados and P.de Rossi, *J.Org.Chem.,* 2001, **66**, 1548-1552

146 M.Ludwig, O.Pytela, K.Kalfus and M.Vecera, *Collect.Czech.Chem.Comm.*, 1984, **49**, 1182-1192

147 R.Adams., P.H.Long and A.J.Johanson, *J.Am.Chem.Soc.*, 1939, **61**, 2342-2349

148 Z.Li, J.Huang, T.Yao, Y.Qian and M.Leng, *J.Organomet.Chem.*, 2000, **598**, 339-347

149 F.Slotta, *Chem.Ber.*, 1930, 678-675

150 M.Manousek et *al.*, *Collect.Czech.Chem.Comm.,* 1968, **33**, 4000-4003

151 L.Fedorov *et al.*, *J.Organomet.Chem.*, 1972, **40**, 251-262

152 H.Buechi, *Pharm.Acta Helv.*, 1974, **49**, 102-103

153 Fourneau, Trefouel and Wancolle, *Bull.Soc.Chim.Fr.*, 1930, **47**, 749

154 C.Bridges *et al.*, *Biochem.J.*, 1695, **96**, 829

155 L.English *et al.*, *J.Am.Chem.Soc.*, 1946, **68**, 453-457

156 R.Stolle, H.J.Niclas and L.Zolch, *Pharmazie*, 1982, **37**, 702-705

157 Lespagnol *et al.*, *Bull.Soc.Chim.Fr.*, 1960, 493

158 S.Petrow, *J.Pharm.Pharmacol.*, 1960, **12**, 705

APPENDIX: SINGLE CRYSTAL X-RAY DATA

Details of collections and refinements for:	***Local ID number:***
o 2-amino-6-hydroxy-9-(*tris*-*O*-acetyl-β,D-ribofuranosyl)purine **8**	dtdw4
o 2-amino-6-chloro-9-(*tris*-*O*-acetyl-β,D-ribofuranosyl)purine **9**	hmdt1
o 6-chloro-2-iodo-9-(*tris*-*O*-acetyl-β,D-ribofuranosyl)purine **10**	dtdw6
o 6-chloro-9*H*-purine monohydrate **13**	dtdw3
o 6-chloro-9-(tetrahydro-pyran-2-yl)-9*H*-purine **14**	dtdw5
o 6-chloro-2-iodo-9-(tetrahydro-pyran-2-yl)-9H-purine **16**	dtdw1
o 6-chloro-2-iodo-9*H*-purine **11**	dtdw10
o 6-benzylsulfanyl-2-iodo-9-isopropylpurine **20**	dtdw24
o 6-amino-2-thioxo-3*H*-4-pyrimidinone **24**	dtdw11
o 6-amino-2-benzylsulfanyl-3*H*-4-pyrimidinone **25**	dtdw12
o 6-amino-2-benzylsulfanyl-5-nitroso-3*H*-4-pyrimidinone **26**	dtdw14
o 2-benzylsulfanyl-7*H*-purin-6-one **28**	dtdw16

- 2-benzylsulfanyl-9-methanesulfonyl-hypoxanthine **29a** dtdw13
- 2-benzylsulfanyl-9-trityl-hypoxanthine **29b** dtdw15
- 2-benzylsulfanyl-6-isopropoxy-9-mesyl-hypoxanthine **31b** dtdw17
- 2-benzylsulfanyl-6-chloropurine **32** dtdw19
- 2-benzylsulfanyl-6-chloro-9-isopropylpurine **33a** dtdw26
- *R*-2-amino-3-methyl-butan-1-ol **38** dtdw18
- *R*-Toluene-4-sulfonic acid 3-methyl-2-(toluene-4-sulfonylamino)-butyl ester **39** dtdw22
- *S*-2-Isopropyl-1-(toluene-4-sulfonyl)-aziridine **43** dtdw23
- *N-4*-Amino-2-chloro-N-methyl-benzenesulfonamide **57b** dtdw21

Crystal data and structure refinement for **8** dtdw4.

Identification code	dtdw4	
Empirical formula	C17 H23 N5 O9	
Formula weight	441.40	
Temperature	125(2) K	
Wavelength	0.71073 Å	
Crystal system	Orthorhombic	
Space group	P2(1)2(1)2(1)	
Unit cell dimensions	a = 10.967(3) Å	α= 90°.
	b = 12.913(3) Å	β= 90°.
	c = 14.322(4) Å	γ = 90°.
Volume	2028.3(9) $Å^3$	
Z	4	
Density (calculated)	1.445 Mg/m^3	
Absorption coefficient	0.118 mm^{-1}	
F(000)	928	
Crystal size	.15 x .1 x .1 mm^3	
Theta range for data collection	2.12 to 23.32°.	
Index ranges	-12<=h<=12, -14<=k<=13, -13<=l<=15	
Reflections collected	8822	
Independent reflections	2876 [R(int) = 0.2605]	
Completeness to theta = 23.32°	98.6 %	
Absorption correction	MULTISCAN	
Max. and min. transmission	1.00000 and 0.861656	
Refinement method	Full-matrix least-squares on F^2	
Data / restraints / parameters	2876 / 0 / 285	
Goodness-of-fit on F^2	0.786	
Final R indices [I>2sigma(I)]	R1 = 0.0677, wR2 = 0.0991	
R indices (all data)	R1 = 0.1976, wR2 = 0.1389	
Absolute structure parameter	0(3)	
Largest diff. peak and hole	0.252 and -0.289 $e.Å^{-3}$	

Crystal data and structure refinement for **9** hmdt1

Identification code	hmdt1	
Empirical formula	C16 H18 Cl N5 O7	
Formula weight	427.80	
Temperature	125(2) K	
Wavelength	0.71073 Å	
Crystal system	Monoclinic	
Space group	C2	
Unit cell dimensions	a = 21.599(7) Å	α= 90°.
	b = 7.695(2) Å	β= 121.216(4)°.
	c = 13.386(4) Å	γ = 90°.
Volume	1902.6(10) $Å^3$	
Z	4	
Density (calculated)	1.493 Mg/m^3	
Absorption coefficient	0.252 mm^{-1}	
F(000)	888	
Crystal size	0.3 x 0.3 x 0.2 mm^3	
Theta range for data collection	1.78 to 23.28°.	
Index ranges	-23<=h<=23, -8<=k<=7, -14<=l<=14	
Reflections collected	4067	
Independent reflections	2326 [R(int) = 0.0187]	
Completeness to theta = 23.28°	98.8 %	
Absorption correction	Multiscan	
Max. and min. transmission	1.00000 and 0.702910	
Refinement method	Full-matrix least-squares on F^2	
Data / restraints / parameters	2326 / 3 / 273	
Goodness-of-fit on F^2	1.042	
Final R indices [I>2sigma(I)]	R1 = 0.0321, wR2 = 0.0794	
R indices (all data)	R1 = 0.0332, wR2 = 0.0803	
Absolute structure parameter	0.05(6)	
Largest diff. peak and hole	0.201 and -0.212 $e.Å^{-3}$	

Crystal data and structure refinement for **10** dtdw6

Identification code	dtdw6	
Empirical formula	C16 H16 Cl I N4 O7	
Formula weight	538.68	
Temperature	125(2) K	
Wavelength	0.71073 Å	
Crystal system	Orthorhombic	
Space group	P2(1)2(1)2(1)	
Unit cell dimensions	a = 9.227(2) Å	α= 90°.
	b = 11.661(3) Å	β= 90°.
	c = 18.817(4) Å	γ = 90°.
Volume	2024.6(8) $Å^3$	
Z	4	
Density (calculated)	1.767 Mg/m^3	
Absorption coefficient	1.760 mm^{-1}	
F(000)	1064	
Crystal size	.1 x .03 x .03 mm^3	
Theta range for data collection	2.05 to 23.28°.	
Index ranges	-10<=h<=9, -5<=k<=12, -20<=l<=20	
Reflections collected	7972	
Independent reflections	2798 [R(int) = 0.1271]	
Completeness to theta = 23.28°	97.0 %	
Absorption correction	MULTISCAN	
Max. and min. transmission	1.00000 and 0.802583	
Refinement method	Full-matrix least-squares on F^2	
Data / restraints / parameters	2798 / 0 / 220	
Goodness-of-fit on F^2	0.938	
Final R indices [I>2sigma(I)]	R1 = 0.0619, wR2 = 0.0992	
R indices (all data)	R1 = 0.1097, wR2 = 0.1103	
Absolute structure parameter	0.00	
Largest diff. peak and hole	2.628 and -0.664 $e.Å^{-3}$	

Crystal data and structure refinement for **13** dtdw3

Identification code	dtdw3	
Empirical formula	C5 H5 Cl N4 O	
Formula weight	172.58	
Temperature	125(2) K	
Wavelength	0.71073 Å	
Crystal system	Triclinic	
Space group	P-1	
Unit cell dimensions	a = 7.8757(18) Å	α= 83.428(4)°.
	b = 8.4609(19) Å	β= 82.374(4)°.
	c = 10.502(2) Å	γ = 76.546(4)°.
Volume	672.0(3) $Å^3$	
Z	4	
Density (calculated)	1.706 Mg/m^3	
Absorption coefficient	0.506 mm^{-1}	
F(000)	352	
Crystal size	.1 x .1 x .1 mm^3	
Theta range for data collection	2.48 to 23.26°.	
Index ranges	-8<=h<=8, -9<=k<=9, -11<=l<=9	
Reflections collected	3354	
Independent reflections	1875 [R(int) = 0.0497]	
Completeness to theta = 23.26°	96.5 %	
Absorption correction	MULTISCAN	
Max. and min. transmission	1.00000 and 0.961823	
Refinement method	Full-matrix least-squares on F^2	
Data / restraints / parameters	1875 / 6 / 224	
Goodness-of-fit on F^2	0.948	
Final R indices [I>2sigma(I)]	R1 = 0.0343, wR2 = 0.0726	
R indices (all data)	R1 = 0.0531, wR2 = 0.0774	
Extinction coefficient	0.0009(11)	
Largest diff. peak and hole	0.293 and -0.260 $e.Å^{-3}$	

Crystal data and structure refinement for **14** dtdw5

Identification code	dtdw5	
Empirical formula	C10 H11 Cl N4 O	
Formula weight	238.68	
Temperature	293(2) K	
Wavelength	0.71073 Å	
Crystal system	Monoclinic	
Space group	P2(1)/n	
Unit cell dimensions	a = 11.478(5) Å	α= 90°.
	b = 4.5766(16) Å	β= 97.701(18)°.
	c = 21.703(10) Å	γ = 90°.
Volume	1129.8(8) $Å^3$	
Z	4	
Density (calculated)	1.403 Mg/m^3	
Absorption coefficient	0.322 mm^{-1}	
F(000)	496	
Crystal size	.15 x .05 x .05 mm^3	
Theta range for data collection	3.15 to 24.71°.	
Index ranges	-13<=h<=13, -4<=k<=5, -17<=l<=25	
Reflections collected	4027	
Independent reflections	1737 [R(int) = 0.0555]	
Completeness to theta = 24.71°	89.6 %	
Absorption correction	Multiscan	
Max. and min. transmission	1.00000 and 0.4395	
Refinement method	Full-matrix least-squares on F^2	
Data / restraints / parameters	1737 / 0 / 146	
Goodness-of-fit on F^2	0.874	
Final R indices [I>2sigma(I)]	R1 = 0.0524, wR2 = 0.0928	
R indices (all data)	R1 = 0.1587, wR2 = 0.1188	
Extinction coefficient	0.0023(12)	
Largest diff. peak and hole	0.146 and -0.198 $e.Å^{-3}$	

Crystal data and structure refinement for **16** dtdw1

Identification code	dtdw1	
Empirical formula	C10 H10 Cl I N4 O	
Formula weight	364.57	
Temperature	125(2) K	
Wavelength	0.71073 Å	
Crystal system	Monoclinic	
Space group	P2(1)/c	
Unit cell dimensions	a = 4.8021(10) Å	α= 90°.
	b = 11.860(2) Å	β= 95.098(4)°.
	c = 21.790(4) Å	γ = 90°.
Volume	1236.1(4) $Å^3$	
Z	4	
Density (calculated)	1.959 Mg/m^3	
Absorption coefficient	2.796 mm^{-1}	
F(000)	704	
Crystal size	.1 x .1 x .18 mm^3	
Theta range for data collection	1.88 to 23.27°.	
Index ranges	-5<=h<=5, -12<=k<=13, -24<=l<=21	
Reflections collected	5159	
Independent reflections	1726 [R(int) = 0.0444]	
Completeness to theta = 23.27°	96.7 %	
Absorption correction	SADABS	
Max. and min. transmission	1.00000 and 0.694487	
Refinement method	Full-matrix least-squares on F^2	
Data / restraints / parameters	1726 / 0 / 155	
Goodness-of-fit on F^2	1.025	
Final R indices [I>2sigma(I)]	R1 = 0.0279, wR2 = 0.0624	
R indices (all data)	R1 = 0.0329, wR2 = 0.0645	
Extinction coefficient	0.0010(4)	
Largest diff. peak and hole	0.767 and -0.392 $e.Å^{-3}$	

Crystal data and structure refinement for **11** dtdw10

Identification code	dtdw10	
Empirical formula	C5 H4 Cl I N4 O	
Formula weight	298.47	
Temperature	125(2) K	
Wavelength	0.71073 Å	
Crystal system	Monoclinic	
Space group	P2(1)/c	
Unit cell dimensions	a = 7.172(2) Å	α= 90°.
	b = 16.732(5) Å	β= 115.863(4)°.
	c = 7.577(2) Å	γ = 90°.
Volume	818.2(4) $Å^3$	
Z	4	
Density (calculated)	2.423 Mg/m^3	
Absorption coefficient	4.194 mm^{-1}	
F(000)	560	
Crystal size	0.2 x 0.2 x 0.08 mm^3	
Theta range for data collection	2.43 to 25.38°.	
Index ranges	-8<=h<=8, -20<=k<=20, -5<=l<=9	
Reflections collected	4704	
Independent reflections	1448 [R(int) = 0.0326]	
Completeness to theta = 25.38°	96.1 %	
Absorption correction	MULTISCAN	
Refinement method	Full-matrix least-squares on F^2	
Data / restraints / parameters	1448 / 3 / 122	
Goodness-of-fit on F^2	1.051	
Final R indices [I>2sigma(I)]	R1 = 0.0302, wR2 = 0.0727	
R indices (all data)	R1 = 0.0347, wR2 = 0.0753	
Extinction coefficient	0.0009(4)	
Largest diff. peak and hole	1.141 and -1.020 $e.Å^{-3}$	

Crystal data and structure refinement for **20** dtdw24.

Identification code	dtdw24	
Empirical formula	C15 H15 I N4 S	
Formula weight	410.27	
Temperature	93(2) K	
Wavelength	0.71073 Å	
Crystal system	Monoclinic	
Space group	P2(1)/n	
Unit cell dimensions	a = 9.1790(11) Å	α= 90°.
	b = 9.1771(14) Å	β= 98.809(2)°.
	c = 19.688(3) Å	γ = 90°.
Volume	1638.9(4) Å^3	
Z	4	
Density (calculated)	1.663 Mg/m^3	
Absorption coefficient	2.080 mm^{-1}	
F(000)	808	
Crystal size	0.1500 x 0.0500 x 0.0500 mm^3	
Theta range for data collection	2.33 to 25.35°.	
Index ranges	-11<=h<=8, -11<=k<=11, -23<=l<=15	
Reflections collected	12909	
Independent reflections	2764 [R(int) = 0.0279]	
Completeness to theta = 25.35°	92.3 %	
Absorption correction	Multiscan	
Max. and min. transmission	1.0000 and 0.8299	
Refinement method	Full-matrix least-squares on F^2	
Data / restraints / parameters	2764 / 0 / 193	
Goodness-of-fit on F^2	1.078	
Final R indices [I>2sigma(I)]	R1 = 0.0205, wR2 = 0.0452	
R indices (all data)	R1 = 0.0225, wR2 = 0.0463	
Largest diff. peak and hole	0.684 and -0.487 e.Å^{-3}	

Crystal data and structure refinement for **24** dtdw11

Identification code	dtdw11	
Empirical formula	C4 H7 N3 O2 S	
Formula weight	161.19	
Temperature	100(2) K	
Wavelength	0.71073 Å	
Crystal system	Monoclinic	
Space group	C2/c	
Unit cell dimensions	a = 14.913(5) Å	α= 90°.
	b = 7.487(2) Å	β= 113.834(6)°.
	c = 12.985(4) Å	γ = 90°.
Volume	1326.2(7) $Å^3$	
Z	8	
Density (calculated)	1.615 Mg/m^3	
Absorption coefficient	0.426 mm^{-1}	
F(000)	672	
Crystal size	0.2000 x 0.1000 x 0.1000 mm^3	
Theta range for data collection	3.24 to 26.36°.	
Index ranges	-18<=h<=12, -9<=k<=9, -14<=l<=16	
Reflections collected	4252	
Independent reflections	1232 [R(int) = 0.0155]	
Completeness to theta = 26.36°	90.5 %	
Absorption correction	MULTISCAN	
Max. and min. transmission	1.00000 and 0.8666	
Refinement method	Full-matrix least-squares on F^2	
Data / restraints / parameters	1232 / 6 / 115	
Goodness-of-fit on F^2	1.089	
Final R indices [I>2sigma(I)]	R1 = 0.0299, wR2 = 0.0709	
R indices (all data)	R1 = 0.0320, wR2 = 0.0728	
Largest diff. peak and hole	0.212 and -0.198 $e.Å^{-3}$	

Crystal data and structure refinement for **25** dtdw12.

Identification code	dtdw12	
Empirical formula	C11 H11 N3 O S	
Formula weight	233.29	
Temperature	100(2) K	
Wavelength	0.71073 Å	
Crystal system	Monoclinic	
Space group	P2(1)/c	
Unit cell dimensions	a = 10.652(3) Å	α= 90°.
	b = 7.897(2) Å	β= 102.664(6)°.
	c = 13.419(4) Å	γ = 90°.
Volume	1101.2(5) $Å^3$	
Z	4	
Density (calculated)	1.407 Mg/m^3	
Absorption coefficient	0.275 mm^{-1}	
F(000)	488	
Crystal size	0.2000 x 0.2000 x 0.0700 mm^3	
Theta range for data collection	3.11 to 26.35°.	
Index ranges	-13<=h<=12, -9<=k<=9, -16<=l<=15	
Reflections collected	7261	
Independent reflections	2098 [R(int) = 0.0189]	
Completeness to theta = 26.35°	93.0 %	
Absorption correction	Multiscan	
Max. and min. transmission	1.00000 and 0.5776	
Refinement method	Full-matrix least-squares on F^2	
Data / restraints / parameters	2098 / 3 / 157	
Goodness-of-fit on F^2	1.139	
Final R indices [I>2sigma(I)]	R1 = 0.0433, wR2 = 0.1060	
R indices (all data)	R1 = 0.0459, wR2 = 0.1099	
Largest diff. peak and hole	0.324 and -0.369 $e.Å^{-3}$	

Crystal data and structure refinement for **26** dtdw14.

Identification code	dtdw14	
Empirical formula	C11 H10 N4 O2 S	
Formula weight	262.29	
Temperature	125(2) K	
Wavelength	0.71073 Å	
Crystal system	Monoclinic	
Space group	P2(1)/n	
Unit cell dimensions	a = 9.677(3) Å	α= 90°.
	b = 10.564(3) Å	β= 110.840(5)°.
	c = 12.285(4) Å	γ = 90°.
Volume	1173.7(6) Å^3	
Z	4	
Density (calculated)	1.484 Mg/m^3	
Absorption coefficient	0.275 mm^{-1}	
F(000)	544	
Crystal size	.14 x .14 x .1 mm^3	
Theta range for data collection	2.32 to 25.36°.	
Index ranges	-11<=h<=11, -11<=k<=12, -14<=l<=12	
Reflections collected	5885	
Independent reflections	2090 [R(int) = 0.0500]	
Completeness to theta = 25.36°	96.8 %	
Absorption correction	MULTISCAN	
Max. and min. transmission	1.00000 and 0.772813	
Refinement method	Full-matrix least-squares on F^2	
Data / restraints / parameters	2090 / 3 / 176	
Goodness-of-fit on F^2	0.923	
Final R indices [I>2sigma(I)]	R1 = 0.0418, wR2 = 0.0842	
R indices (all data)	R1 = 0.0809, wR2 = 0.0972	
Extinction coefficient	0.0084(18)	
Largest diff. peak and hole	0.271 and -0.288 e.Å^{-3}	

Crystal data and structure refinement for **28** dtdw16.

Identification code	dtdw16	
Empirical formula	C12 H10 N4 O S	
Formula weight	258.30	
Temperature	125(2) K	
Wavelength	0.71073 Å	
Crystal system	Monoclinic	
Space group	P2(1)/c	
Unit cell dimensions	a = 20.596(5) Å	α= 90°.
	b = 4.7267(11) Å	β= 106.922(3)°.
	c = 13.090(3) Å	γ = 90°.
Volume	1219.2(5) $Å^3$	
Z	4	
Density (calculated)	1.407 Mg/m^3	
Absorption coefficient	0.258 mm^{-1}	
F(000)	536	
Crystal size	.1 x .1 x .02 mm^3	
Theta range for data collection	2.07 to 25.36°.	
Index ranges	-24<=h<=23, -5<=k<=5, -15<=l<=14	
Reflections collected	6822	
Independent reflections	2185 [R(int) = 0.0294]	
Completeness to theta = 25.36°	97.6 %	
Absorption correction	MULTISCAN	
Max. and min. transmission	1.00000 and 0.836739	
Refinement method	Full-matrix least-squares on F^2	
Data / restraints / parameters	2185 / 2 / 172	
Goodness-of-fit on F^2	1.048	
Final R indices [I>2sigma(I)]	R1 = 0.0352, wR2 = 0.0846	
R indices (all data)	R1 = 0.0482, wR2 = 0.0915	
Extinction coefficient	0.0050(15)	
Largest diff. peak and hole	0.196 and -0.245 $e.Å^{-3}$	

Crystal data and structure refinement for **29a** dtdw13

Identification code	dtdw13	
Empirical formula	C13 H12 N4 O3 S2	
Formula weight	336.39	
Temperature	125(2) K	
Wavelength	0.71073 Å	
Crystal system	Triclinic	
Space group	P-1	
Unit cell dimensions	a = 7.4495(15) Å	α= 90.270(4)°.
	b = 7.4665(15) Å	β= 102.866(3)°.
	c = 13.573(3) Å	γ = 95.404(4)°.
Volume	732.5(3) $Å^3$	
Z	2	
Density (calculated)	1.525 Mg/m^3	
Absorption coefficient	0.381 mm^{-1}	
F(000)	348	
Crystal size	.1 x .1 x .01 mm^3	
Theta range for data collection	1.54 to 25.34°.	
Index ranges	-8<=h<=8, -8<=k<=8, -16<=l<=15	
Reflections collected	4725	
Independent reflections	2628 [R(int) = 0.0211]	
Completeness to theta = 25.34°	98.5 %	
Absorption correction	MULTISCAN	
Max. and min. transmission	1.00000 and 0.865892	
Refinement method	Full-matrix least-squares on F^2	
Data / restraints / parameters	2628 / 1 / 204	
Goodness-of-fit on F^2	1.036	
Final R indices [I>2sigma(I)]	R1 = 0.0444, wR2 = 0.1135	
R indices (all data)	R1 = 0.0607, wR2 = 0.1219	
Largest diff. peak and hole	0.387 and -0.344 $e.Å^{-3}$	

Crystal data and structure refinement for **29b** dtdw15

Identification code	dtdw15	
Empirical formula	C32.50 H27 Cl3 N4 O S	
Formula weight	627.99	
Temperature	125(2) K	
Wavelength	0.71073 Å	
Crystal system	Monoclinic	
Space group	P2(1)/c	
Unit cell dimensions	a = 30.107(8) Å	α= 90°.
	b = 10.225(3) Å	β= 100.062(5)°.
	c = 19.879(5) Å	γ = 90°.
Volume	6026(3) $Å^3$	
Z	8	
Density (calculated)	1.384 Mg/m^3	
Absorption coefficient	0.407 mm^{-1}	
F(000)	2600	
Crystal size	.1 x .1 x .01 mm^3	
Theta range for data collection	2.06 to 25.30°.	
Index ranges	-34<=h<=36, -12<=k<=12, -23<=l<=23	
Reflections collected	34933	
Independent reflections	10895 [R(int) = 1.2167]	
Completeness to theta = 25.30°	99.3 %	
Absorption correction	MULTISCAN	
Max. and min. transmission	1.00000 and 0.590953	
Refinement method	Full-matrix least-squares on F^2	
Data / restraints / parameters	10895 / 0 / 374	
Goodness-of-fit on F^2	0.797	
Final R indices [I>2sigma(I)]	R1 = 0.1431, wR2 = 0.2264	
R indices (all data)	R1 = 0.5762, wR2 = 0.4137	
Extinction coefficient	0.0043(6)	
Largest diff. peak and hole	0.475 and -0.543 $e.Å^{-3}$	

Crystal data and structure refinement for **31b** dtdw17

Identification code	dtdw17	
Empirical formula	C17 H19 Cl3 N4 O3 S2	
Formula weight	497.83	
Temperature	125(2) K	
Wavelength	0.71073 Å	
Crystal system	Monoclinic	
Space group	P2(1)/c	
Unit cell dimensions	a = 10.4009(10) Å	α= 90°.
	b = 28.866(3) Å	β= 101.790(2)°.
	c = 14.8133(15) Å	γ = 90°.
Volume	4353.6(7) $Å^3$	
Z	8	
Density (calculated)	1.519 Mg/m^3	
Absorption coefficient	0.640 mm^{-1}	
F(000)	2048	
Crystal size	.16 x .1 x .1 mm^3	
Theta range for data collection	1.57 to 25.37°.	
Index ranges	-12<=h<=12, -30<=k<=34, -17<=l<=17	
Reflections collected	22684	
Independent reflections	7923 [R(int) = 0.0459]	
Completeness to theta = 25.37°	99.0 %	
Absorption correction	MULTISCAN	
Max. and min. transmission	1.00000 and 0.856255	
Refinement method	Full-matrix least-squares on F^2	
Data / restraints / parameters	7923 / 0 / 526	
Goodness-of-fit on F^2	1.011	
Final R indices [I>2sigma(I)]	R1 = 0.0505, wR2 = 0.1069	
R indices (all data)	R1 = 0.0980, wR2 = 0.1281	
Extinction coefficient	0.00022(15)	
Largest diff. peak and hole	0.375 and -0.466 $e.Å^{-3}$	

Crystal data and structure refinement for **32** dtdw19

Identification code	dtdw19	
Empirical formula	C12 H9 Cl N4 S	
Formula weight	276.74	
Temperature	125(2) K	
Wavelength	0.71073 Å	
Crystal system	Monoclinic	
Space group	P2(1)/c	
Unit cell dimensions	a = 12.845(5) Å	α= 90°.
	b = 9.781(4) Å	β= 105.341(9)°.
	c = 10.378(4) Å	γ = 90°.
Volume	1257.5(8) $Å^3$	
Z	4	
Density (calculated)	1.462 Mg/m^3	
Absorption coefficient	0.456 mm^{-1}	
F(000)	568	
Crystal size	.1 x .1 x .1 mm^3	
Theta range for data collection	1.64 to 25.37°.	
Index ranges	-15<=h<=15, -11<=k<=11, -10<=l<=12	
Reflections collected	7791	
Independent reflections	2251 [R(int) = 0.1518]	
Completeness to theta = 25.37°	97.1 %	
Absorption correction	Multiscan	
Max. and min. transmission	1.00000 and 0.637129	
Refinement method	Full-matrix least-squares on F^2	
Data / restraints / parameters	2251 / 1 / 167	
Goodness-of-fit on F^2	0.798	
Final R indices [I>2sigma(I)]	R1 = 0.0535, wR2 = 0.0887	
R indices (all data)	R1 = 0.1707, wR2 = 0.1121	
Largest diff. peak and hole	0.321 and -0.361 $e.Å^{-3}$	

Crystal data and structure refinement for **33a** dtdw26

Identification code	dtdw26	
Empirical formula	C15 H15 Cl N4 S	
Formula weight	318.82	
Temperature	93(2) K	
Wavelength	0.71073 Å	
Crystal system	Monoclinic	
Space group	P2(1)/c	
Unit cell dimensions	a = 8.676(3) Å	α= 90°.
	b = 15.695(4) Å	β= 92.295(6)°.
	c = 22.263(6) Å	γ = 90°.
Volume	3029.2(14) $Å^3$	
Z	8	
Density (calculated)	1.398 Mg/m^3	
Absorption coefficient	0.388 mm^{-1}	
F(000)	1328	
Crystal size	0.1000 x 0.1000 x 0.0100 mm^3	
Theta range for data collection	2.60 to 25.35°.	
Index ranges	-8<=h<=10, -18<=k<=18, -24<=l<=26	
Reflections collected	22748	
Independent reflections	5187 [R(int) = 0.0550]	
Completeness to theta = 25.35°	93.3 %	
Absorption correction	MULTISCAN	
Max. and min. transmission	1.0000 and 0.8315	
Refinement method	Full-matrix least-squares on F^2	
Data / restraints / parameters	5187 / 0 / 380	
Goodness-of-fit on F^2	1.130	
Final R indices [I>2sigma(I)]	R1 = 0.0552, wR2 = 0.1163	
R indices (all data)	R1 = 0.0711, wR2 = 0.1259	
Largest diff. peak and hole	0.503 and -0.294 $e.Å^{-3}$	

Crystal data and structure refinement for **38** dtdw18

Identification code	dtdw18	
Empirical formula	C5 H13 N O	
Formula weight	103.16	
Temperature	125(2) K	
Wavelength	0.71073 Å	
Crystal system	Orthorhombic	
Space group	P2(1)2(1)2(1)	
Unit cell dimensions	a = 4.8372(8) Å	α= 90°.
	b = 8.4947(15) Å	β= 90°.
	c = 15.660(3) Å	γ = 90°.
Volume	643.47(19) $Å^3$	
Z	4	
Density (calculated)	1.065 Mg/m^3	
Absorption coefficient	0.073 mm^{-1}	
F(000)	232	
Crystal size	.12 x .1 x .1 mm^3	
Theta range for data collection	2.60 to 25.35°.	
Index ranges	-5<=h<=5, -10<=k<=10, -18<=l<=17	
Reflections collected	3547	
Independent reflections	1129 [R(int) = 0.0142]	
Completeness to theta = 25.35°	96.5 %	
Absorption correction	Multiscan	
Max. and min. transmission	1.00000 and 0.896815	
Refinement method	Full-matrix least-squares on F^2	
Data / restraints / parameters	1129 / 3 / 79	
Goodness-of-fit on F^2	1.087	
Final R indices [I>2sigma(I)]	R1 = 0.0284, wR2 = 0.0781	
R indices (all data)	R1 = 0.0300, wR2 = 0.0792	
Absolute structure parameter	0.1(15)	
Extinction coefficient	0.025(8)	
Largest diff. peak and hole	0.147 and -0.111 $e.Å^{-3}$	

Crystal data and structure refinement for **39** dtdw22

Identification code	dtdw22	
Empirical formula	C19 H25 N O5 S2	
Formula weight	411.52	
Temperature	125(2) K	
Wavelength	0.71073 Å	
Crystal system	Orthorhombic	
Space group	P2(1)2(1)2(1)	
Unit cell dimensions	a = 9.594(2) Å	α= 90°.
	b = 10.742(3) Å	β= 90°.
	c = 19.745(5) Å	γ = 90°.
Volume	2034.8(9) $Å^3$	
Z	4	
Density (calculated)	1.343 Mg/m^3	
Absorption coefficient	0.291 mm^{-1}	
F(000)	872	
Crystal size	.1 x .1 x .1 mm^3	
Theta range for data collection	2.06 to 25.37°.	
Index ranges	-11<=h<=7, -12<=k<=12, -23<=l<=23	
Reflections collected	10412	
Independent reflections	3663 [R(int) = 0.0374]	
Completeness to theta = 25.37°	98.9 %	
Absorption correction	Multiscan	
Max. and min. transmission	1.00000 and 0.814997	
Refinement method	Full-matrix least-squares on F^2	
Data / restraints / parameters	3663 / 1 / 251	
Goodness-of-fit on F^2	0.879	
Final R indices [I>2sigma(I)]	R1 = 0.0358, wR2 = 0.0818	
R indices (all data)	R1 = 0.0450, wR2 = 0.0853	
Absolute structure parameter	0.00(7)	
Extinction coefficient	0.0030(8)	
Largest diff. peak and hole	0.456 and -0.302 $e.Å^{-3}$	

Crystal data and structure refinement for **43** dtdw23

Identification code	dtdw23	
Empirical formula	C12 H17 N O2 S	
Formula weight	239.33	
Temperature	93(2) K	
Wavelength	0.71073 Å	
Crystal system	Orthorhombic	
Space group	P2(1)2(1)2(1)	
Unit cell dimensions	a = 6.2664(11) Å	α= 90°.
	b = 13.656(3) Å	β= 90°.
	c = 14.193(4) Å	γ = 90°.
Volume	1214.5(5) $Å^3$	
Z	4	
Density (calculated)	1.309 Mg/m^3	
Absorption coefficient	0.252 mm^{-1}	
F(000)	512	
Crystal size	0.2500 x 0.1500 x 0.1000 mm^3	
Theta range for data collection	2.07 to 26.37°.	
Index ranges	-7<=h<=6, -16<=k<=15, -17<=l<=11	
Reflections collected	7698	
Independent reflections	2325 [R(int) = 0.0395]	
Completeness to theta = 26.37°	94.8 %	
Absorption correction	Multiscan	
Max. and min. transmission	1.0000 and 0.3862	
Refinement method	Full-matrix least-squares on F^2	
Data / restraints / parameters	2325 / 0 / 149	
Goodness-of-fit on F^2	0.535	
Final R indices [I>2sigma(I)]	R1 = 0.0304, wR2 = 0.0746	
R indices (all data)	R1 = 0.0389, wR2 = 0.0837	
Absolute structure parameter	0.02(7)	
Extinction coefficient	0.001(4)	
Largest diff. peak and hole	0.335 and -0.403 $e.Å^{-3}$	

Crystal data and structure refinement for **57b** dtdw21

Identification code	dtdw21	
Empirical formula	C7 H9 Cl N2 O2 S	
Formula weight	220.67	
Temperature	125(2) K	
Wavelength	0.71073 Å	
Crystal system	Monoclinic	
Space group	C2/c	
Unit cell dimensions	a = 19.729(3) Å	α= 90°.
	b = 5.9096(10) Å	β= 101.906(3)°.
	c = 15.990(3) Å	γ = 90°.
Volume	1824.1(5) Å^3	
Z	8	
Density (calculated)	1.607 Mg/m^3	
Absorption coefficient	0.614 mm^{-1}	
F(000)	912	
Crystal size	.16 x .1 x .01 mm^3	
Theta range for data collection	2.11 to 25.37°.	
Index ranges	-23<=h<=23, -7<=k<=7, -19<=l<=17	
Reflections collected	5334	
Independent reflections	1617 [R(int) = 0.0220]	
Completeness to theta = 25.37°	96.8 %	
Absorption correction	Multiscan	
Max. and min. transmission	1.00000 and 0.802533	
Refinement method	Full-matrix least-squares on F^2	
Data / restraints / parameters	1617 / 3 / 131	
Goodness-of-fit on F^2	1.032	
Final R indices [I>2sigma(I)]	R1 = 0.0229, wR2 = 0.0564	
R indices (all data)	R1 = 0.0283, wR2 = 0.0582	
Largest diff. peak and hole	0.251 and -0.261 e.Å^{-3}	